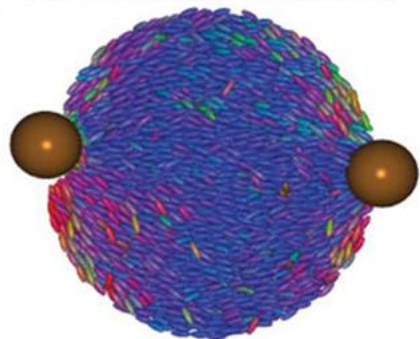
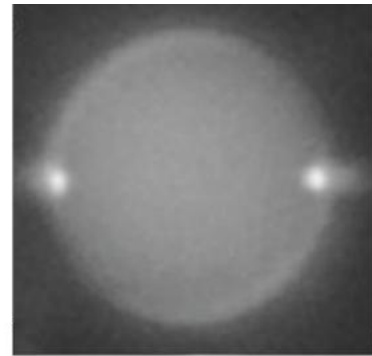
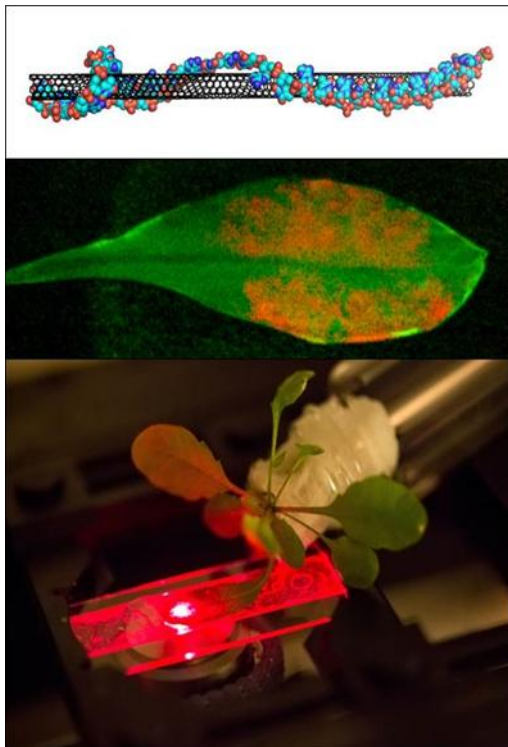
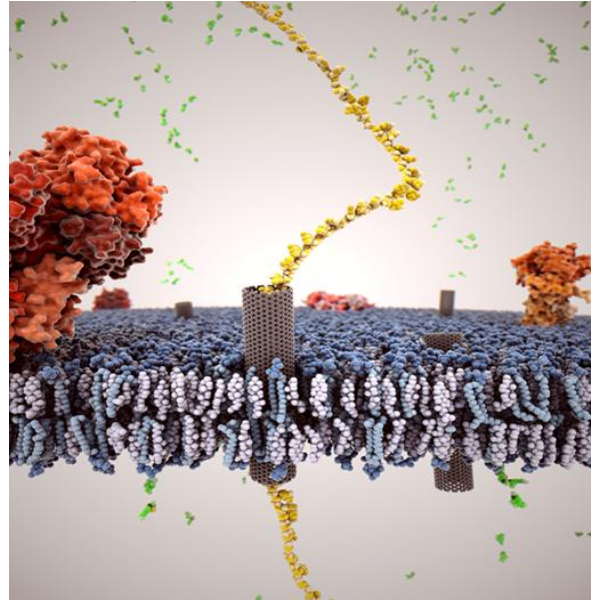
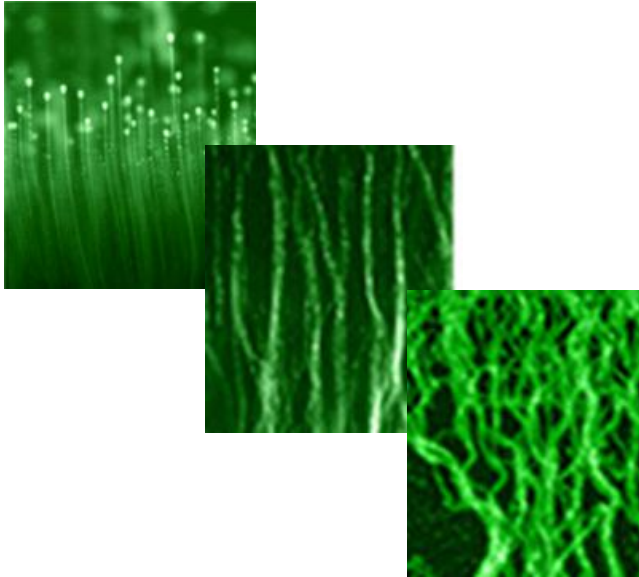


Biomolecular Materials

Principal Investigators' Meeting—2015

August 3–5, 2015

Hilton Washington DC North/Gaithersburg, Gaithersburg, MD



U.S. DEPARTMENT OF
ENERGY

Office of
Science

Office of Basic Energy Sciences
Materials Sciences and Engineering Division

On the Cover

- Top Left: Diversity of self-assembled structures formed by sticky colloidal particles: From left to right, an array of “mushrooms”, wavy colloidal “fur”, and dense fiber network. The features of the architectures were tuned by controlling the electric field and particle surface properties.
Courtesy: Igor Aronson, Argonne National Laboratory
- Top Right: Depiction of carbon nanotube (CNT) inserted into a cell membrane, with a single strand of DNA passing through the nanotube.
Courtesy: Adam M. Gardner/Aleksandr Noy, Lawrence Livermore National Laboratory
- Bottom Left: Nanobionic Leaf: DNA-coated carbon nanotubes (top) incorporated inside chloroplasts in the leaves of living plants (middle) boost plant photosynthesis. Leaves infiltrated with carbon nanotubes (orange) are imaged with a single particle microscope that monitors their near infrared fluorescence (bottom).
Courtesy: Michael Strano, Massachusetts Institute of Technology
- Bottom Right: Fluorescent image of adsorbed polystyrene particles on liquid crystal droplet (top) and simulation of particle adsorption (bottom); region of disorder within droplets coincides exactly with the particle positions
Courtesy: Juan de Pablo, University of Chicago

This document was produced under contract number DE-AC05-06OR23100 between the U.S. Department of Energy and Oak Ridge Associated Universities.

The research grants and contracts described in this document are supported by the U.S. DOE Office of Science, Office of Basic Energy Sciences, Materials Sciences and Engineering Division.

Foreword

This volume comprises the scientific content of the 2015 Biomolecular Materials Principal Investigators' Meeting sponsored by the Materials Sciences and Engineering (MSE) Division in the Office of Basic Energy Sciences (BES) of the U. S. Department of Energy (DOE). The meeting, held on August 3–5, 2015, at the Hilton Washington DC North/Gaithersburg in Gaithersburg, MD, is the sixth such meeting on this topic, and is one of several research theme-based Principal Investigators' Meetings conducted by BES. The meeting's focus is on research at the intersection of materials sciences and biology, and the agenda at this year's meeting is representative of many of the major scientific areas supported by the Biomolecular Materials program. In addition, this meeting will provide an opportunity to consider how this program may continue to evolve to support DOE's mission. As has been the case for other BES Principal Investigators' Meetings, previous meetings have been highly valued and cherished by the participants for the opportunity to see the entire research program, learn about the latest results/advances, develop new ideas, and forge new collaborations. The meeting will also help MSE in assessing the state of the program, identifying new research directions, and recognizing programmatic needs.

The Biomolecular Materials Core Research Activity (CRA) formally came into existence following the recommendations of a workshop sponsored by the Basic Energy Sciences Advisory Committee (BESAC) in 2002. In addition, recent BES workshops and The National Academies' reports have clearly identified mastering the capabilities of living systems as a Grand Challenge that could provide the knowledge base to discover, design, and synthesize new materials with totally new properties for next-generation energy technologies. To address these goals, the Biomolecular Materials program supports fundamental research in the discovery, design, and synthesis of functional materials and complex structures based on principles and concepts of biology. The major programmatic focus is on the design and scalable creation of robust energy-relevant materials and systems with collective behavior, which rival or exceed biology's extraordinary effectiveness for controlling matter, energy, and information.

I look forward to the active participation of the attendees at this meeting during the presentations, poster sessions, and other opportunities for discussion. I hope that the collective sharing of their ideas and new research results will bring fresh perspectives and insights for the continued development of this field and its value to DOE's mission, as has been the case at past BES Principal Investigators' Meetings. The advice and help of Meeting Chairs, James De Yoreo and Michael Strano, in organizing this meeting are deeply appreciated. My sincere thanks also go to Teresa Crockett in MSE and Linda Severs and her colleagues at the Oak Ridge Institute for Science and Education (ORISE) for their outstanding work in taking care of all the logistical aspects of the meeting.

Mike Markowitz
Program Manager, Biomolecular Materials
Materials Sciences and Engineering Division
Office of Basic Energy Sciences
U.S. Department of Energy

Agenda

**2015 Biomolecular Materials
Principal Investigators' Meeting Agenda**

Monday, August 3, 2015

- 7:15 – 8:15 **Breakfast**
- 8:15 – 8:30 *Introductory Remarks*
Meeting Chairs: **James De Yoreo** and **Michael Strano**
Pacific Northwest National Laboratory/Massachusetts Institute of Technology
- Session 1: Defining Sequence, Structure, and Function in Materials**
Chair: **James De Yoreo**, Pacific Northwest National Laboratory
- 8:30 – 9:05 **Peter Schultz**, Scripps Research Institute
Biotemplated Self-Assembly of Protein Superstructures
- 9:05 – 9:40 **Faik Akif Tezcan**, University of California, San Diego
Chemically Directed Self-Assembly of Protein Superstructures
- 9:40 – 10:15 **George Bachand**, Sandia National Laboratories
Active Assembly of Dynamic and Adaptable Materials: Active Protein Assemblies
- 10:15 – 10:40 **Break**
- 10:40 – 11:15 **Sanat Kumar**, Columbia University
DNA-Grafted Building Blocks Designed to Self-Assemble into Desired Nanostructures
- 11:15 – 11:55 **William L. Wilson**, University of Illinois at Urbana-Champaign, Harvard University
Directed Assembly of Bio-Inspired Supramolecular Materials for Energy Transport and Capture: Mesoscale Construction of Functional Materials in Hydrodynamic Flows
- 11:55 – 1:00 **Working Lunch/Poster Introductions**
- 1:00 – 2:30 **Poster Session 1**
- Division and Program Updates**
- 2:30 – 3:00 **Linda Horton**, Director of Materials Synthesis & Engineering
- 3:00 – 3:20 **Mike Markowitz**, Program Manager, Biomolecular Materials
- 3:20 – 3:40 **Roger French**, Case Western Reserve University
Upcoming BESAC Report - Challenges at the Frontiers of Matter and Energy: Transformative Opportunities for Discovery Science

- 3:40 – 4:00 **Break**
- Session 2: Active Assembly**
Chair: **Atul Parikh**, University of California, Davis
- 4:00 - 4:35 **Zvonimir Dogic**, Brandeis University
Hierarchical active matter: from extensile bundles to flowing gels, streaming liquid crystals and motile emulsions
- 4:35 – 5:10 **Joanna Aizenberg**, Harvard University
Harnessing Chemo-mechanical Energy Transduction to Create Systems that Selectively Catch and Release Biomolecules
- 5:10 – 5:45 **Cyrus Safinya**, University of California, Santa Barbara
Miniaturized Hybrid Materials Inspired by Nature
- 5:45 – 7:00 **Poster Session 1, continued**
- 7:00 – 8:30 **Dinner and Meeting Discussions**

Tuesday, August 4, 2015

- 7:00 – 8:00 **Breakfast**
- 8:00-8:15 **Anna Balazs**, University of Pittsburgh
MSE Council Workshop on Dissipative Assembly
- Session 3: Managing Heterogeneity and Defects**
Chair: **Anna Balazs**, University of Pittsburgh and **Sharon Glotzer**, University of Michigan
- 8:15 – 8:50 **Ned Seeman**, New York University
Self-Assembly and Self-Replication of Novel Materials from Particles with Specific Recognition
- 8:50 – 9:25 **Elisa Franco & Rebecca Schulman**, University of California, Riverside and Johns Hopkins University
Programmable Dynamic Self-Assembly of DNA Nanostructures
- 9:25- 10:00 **Nicholas Abbott**, University of Wisconsin
Bioinspired Hierarchical Design of Chiral Mesoscale Liquid Crystalline Assemblies
- 10:00 – 10:20 **Break**

Session 3, continued:

10:20 – 10:55 **Juan de Pablo**, Argonne National Laboratory/University of Chicago – Institute for Molecular Engineering
Solvent-assisted Non-equilibrium Directed Self-assembly of Complex Polymeric Materials

10:55 – 11:30 **Bogdan Dragnea**, Indiana University
Virus-enabled Biomaterials: Linking Biological Unit, Topology and Thermodynamics in Virus-like Particles

11:30 – 12:05 **Monica Olvera de la Cruz**, Northwestern University
Electrostatic Driven Self Assembly Design of Functional Nanostructures

12:05 – 1:05 **Working Lunch/Poster Introductions**

1:05 – 2:35 **Poster Session 2**

Session 4: Managing Interfacial Processes
Chair: **Lara Estroff**, Cornell University

2:35 – 3:10 **Christine Keating**, Pennsylvania State University
Enzyme-Controlled Mineralization in Biomimetic Microenvironments Formed by Aqueous Phase Separation and Lipid Vesicles

3:10 – 3:45 **Gordana Dukovic**, University of Colorado
Semiconductor Nanocrystals as Light Harvesters for Biomimetic Solar Fuel Generation

3:45 – 4:20 **Anand Jagota**, Lehigh University
Surface Mechanical Properties of Bio-Inspired Architectures

4:20 – 4:40 **Break**

4:40 – 5:15 **Todd Emrick**, University of Massachusetts
Experimental Realization of ‘Repair-and-Go’ Using Microencapsulation of Nanomaterials

5:15 – 5:50 **Sarah Heilshorn**, SLAC National Accelerator Laboratory
Self-healing and Self-regulating Bio-inspired Materials

5:50 – 7:00 **Poster Session 2, continued**

7:00 – 8:30 **Dinner/Meeting Discussions**

Wednesday, August 5, 2015

7:15 – 8:15 **Breakfast**

Session 5: Managing Energy Transfer

Chair: **Michael Strano**, Massachusetts Institute of Technology

8:15 – 8:50 **Ozgur Sahin**, Columbia University
Assembling Microorganisms into Energy Converting Materials

8:50 – 9:25 **Jennifer Cha**, University of Colorado
Rigid Biopolymer Nanocrystal Systems for Controlling Multicomponent Nanoparticle Assembly and Orientation in Thin Film Solar Cells

9:25 – 10:00 **Alfredo Alexander-Katz**, Massachusetts Institute of Technology
Biomimetic Templated Self-Assembly of Light Harvesting Nanostructures

10:00 – 10:35 **Samuel Stupp**, Northwestern University
Nanoengineering of Complex Materials

10:30 – 11:00 **Break**

11:00 – 12:00 *Open Discussion on Future Program Topics & Science-driven Tools Development, Concluding Comments*
James De Yoreo and Michael Strano, Meeting Chairs
Mike Markowitz, Program Manager, Biomolecular Materials

12:00 **Meeting Adjourns**

Table of Contents

Table of Contents

Foreword	i
Agenda	v
Table of Contents	xi
 Laboratory Projects	
<i>Dynamics of Active Self-Assembled Materials</i>	
Igor S. Aronson, Alexey Snezhko, and Andrey Sokolov	3
<i>Active Assembly of Dynamic and Adaptable Materials: Active Protein Assemblies</i>	
George D. Bachand, Erik Spoerke, Mark Stevens, and Darryl Sasaki	9
<i>Molecular Nanocomposites—Complex Nanocomposites Subtask</i>	
Paul G. Clem, Jeff Brinker, Bryan Kaehr, Hongyou Fan, Frank van Swol, and Stanley Chou	13
<i>Molecular Nanocomposites—Adaptive and Reconfigurable Nanocomposites Subtask</i>	
Paul G. Clem, Dale L. Huber, Darryl Y. Sasaki, Mark J. Stevens, Amalie L. Frischknecht, and Hongyou Fan	20
<i>Solvent Assisted Nonequilibrium Directed Self Assembly of Complex Polymeric Materials</i>	
Juan de Pablo, Matt Tirrell, Paul Nealey, and Wei Chen	25
<i>Self-Healing and Self-Regulating Bio-inspired Materials</i>	
Sarah Heilshorn, Seb Doniach, Nick Melosh, and Andy Spakowitz	31
<i>Bioinspired Materials</i>	
Surya Mallapragada, Mufit Akinc, David Vaknin, Marit Nilsen-Hamilton, Alex Travesset, Wenjie Wang, Ruslan Prozorov, Tanya Prozorov, and Dennis Bazylinski	36
<i>Directed Organization of Functional Materials at Inorganic-Macromolecular Interfaces</i>	
Aleksandr Noy, Jim De Yoreo, Tony Van Buuren, and Chun-Long Chen	41
<i>Early Career: Real-Time Studies of Nucleation, Growth and Development of Ferromagnetism in Individual Protein-Templated Magnetic Nanocrystals</i>	
Tanya Prozorov	47
<i>Active Assembly of Dynamic and Adaptable Materials: Artificial Microtubules</i>	
Erik D. Spoerke, George D. Bachand, Mark Stevens, and Darryl Sasaki	51

University Grant Projects

<i>Bioinspired Hierarchical Design of Chiral Mesoscale Liquid Crystalline Assemblies</i> Nicholas L. Abbott and Juan J. de Pablo	59
<i>Harnessing Chemo-mechanical Energy Transduction to Create Systems that Selectively Catch and Release Biomolecules</i> Joanna Aizenberg and Anna Balazs	64
<i>Biomimetic Templated Self-Assembly of Light Harvesting Nanostructures</i> Alfredo Alexander-Katz	69
<i>Design and Synthesis of Structurally Tailored and Engineered Macromolecular (STEM) Gels</i> Anna C. Balazs and Krzysztof Matyjaszewski	73
<i>Designing Dual-Functionalized Gels that Move, Morph and Self-Organize in Light</i> Anna C. Balazs	77
<i>Rigid Biopolymer Nanocrystal Systems for Controlling Multicomponent Nanoparticle Assembly and Orientation in Thin Film Solar Cells</i> Jennifer N. Cha	81
<i>Self-Assembly and Self-Replication of Novel Materials from Particles with Specific Recognition</i> P. Chaikin, N. Seeman, M. Weck, and D. Pine	87
<i>Hierarchical Active Matter: From Extensile Bundles to Flowing Gels, Streaming Liquid Crystals and Motile Emulsions</i> Zvonimir Dogic	91
<i>Virus-Enabled Biomaterials: Linking Biological Unit, Topology and Thermodynamics in Virus-Like Particles</i> Bogdan Dragnea	95
<i>Semiconductor Nanocrystals as Light Harvesters for Biomimetic Solar Fuel Generation</i> Gordana Dukovic	100
<i>Experimental Realization of ‘Repair-and-Go’ using Microencapsulation of Nanomaterials</i> Todd Emrick	105
<i>Controlling Structure Formation Pathways in Functional Bio-hybrid Nanomaterials</i> Lara A. Estroff and Ulrich Wiesner	110
<i>Material Lessons from Biology: Nano-to-Mesoscale Organization of Biominerals by Mollusk Shell Proteins</i> John Spencer Evans	114

<i>Dynamic Self-Assembly of DNA Nanotubes</i> Elisa Franco	119
<i>Long Range van der Waals-London Dispersion Interactions for Biomolecular and Inorganic Nanoscale Assembly: Duplex to Quadruplex DNA</i> R. H. French, N. F. Steinmetz, V. A. Parsegian, and W. Y. Ching	123
<i>A Hybrid Biological/Organic Photochemical Half-Cell for Generating H₂</i> John H. Golbeck and Donald A. Bryant	130
<i>Optical and Electro-optic Modulation of Biomimetically Functionalized Nanotubes</i> Padma Gopalan, David McGee, Francois Leonard, Bryan Wong, and Franz Himpfel	134
<i>Strong Autonomous Self-Healing Materials via Dynamic Chemical Interactions</i> Zhibin Guan	139
<i>Development of Smart, Responsive Communicating and Motile Microcapsules</i> Daniel A. Hammer and Daeyeon Lee	143
<i>Surface Mechanical Properties of Bioinspired Architectures</i> Anand Jagota and Chung-Yuen Hui	148
<i>Enzyme-Controlled Mineralization in Biomimetic Microenvironments Formed by Aqueous Phase Separation and Lipid Vesicles</i> C. D. Keating	153
<i>DNA-Grafted Building Blocks Designed to Self-Assemble into Desired Nanostructures</i> S. Kumar, V. Venkatasubramanian, and O. Gang	157
<i>Biomolecular Assembly Processes in the Design of Novel Functional Materials</i> Jeetain Mittal	162
<i>Biological and Biomimetic Low-Temperature Routes to Materials for Energy Applications</i> Daniel E. Morse	163
<i>Electrostatic Driven Self-Assembly Design of Functional Nanostructures</i> Monica Olvera de la Cruz and Michael J. Bedzyk	167
<i>Dynamic Self-Assembly: Constrained Phase and Mesoscale Dynamics in Lipid Membranes</i> Atul N. Parikh and Sunil K. Sinha	171
<i>Long Range van der Waals-London Dispersion Interactions for Biomolecular and Inorganic Nanoscale Assembly: Design and Anisotropy</i> V. A. Parsegian, W. Y. Ching, R. H. French, and N. F. Steinmetz	175

<i>Integrating Rhodopsins in H⁺-FETs for Bioinspired Energy Conversion</i> Marco Rolandi and Francois Baneyx	182
<i>Miniaturized Hybrid Materials Inspired by Nature</i> C. R. Safinya, Y. Li, and K. Ewert	186
<i>Assembling Microorganisms into Energy Converting Materials</i> Ozgur Sahin	191
<i>Exploration of Chemically Tailored, Hierarchically Patterned 3-D Biogenic and Biomimetic Structures for Control of Infrared Radiation</i> Kenneth H. Sandhage and Joseph W. Perry	196
<i>A Modular Architecture for Dynamic, Environmentally Adaptive DNA Nanostructures</i> Rebecca Schulman	198
<i>Biopolymers Containing Unnatural Amino Acids</i> Peter G. Schultz	202
<i>Fabrication and Assembly of Robust, Water-Soluble Molecular Interconnects via Encoded Hybridization</i> Timothy F. Scott	207
<i>Self-Assembly for Colloidal Crystallization and Biomimetic Structural Color</i> Michael J. Solomon and Sharon C. Glotzer	211
<i>Carbon Nanotubes for Solar Energy Harvesting in Plants</i> Michael S. Strano	213
<i>Nanoengineering of Complex Materials</i> Samuel I. Stupp	217
<i>Chemically Directed Self-Assembly of Protein Superstructures</i> F. Akif Tezcan	221
<i>Self-Assembly of Pi-Conjugated Peptides in Aqueous Environments Leading to Energy-Transporting Bioelectronic Nanostructures</i> John D. Tovar, Howard E. Katz, and Andrew L. Ferguson	226
<i>Dynamic Self-Assembly, Emergence, and Complexity</i> George M. Whitesides	230
<i>Directed Assembly of Bio-Inspired Supramolecular Materials for Energy Transport and Capture: Mesoscale Construction of Functional Materials in Hydrodynamic Flows</i> William L. Wilson, Charles Schroeder, A. L. Ferguson, and J. J. Cheng	236

Poster Listing	243
Author Index	251
Participant List	253

***LABORATORY
PROJECTS***

Dynamics of Active Self-Assembled Materials

PI: Igor S. Aronson, Co-Investigators: Alexey Snezhko, Andrey Sokolov

Mailing Address: Materials Science Division, Argonne National Laboratory, 9700 South Cass Avenue, Argonne, IL60439. E-mail: aronson@anl.gov

Program Scope

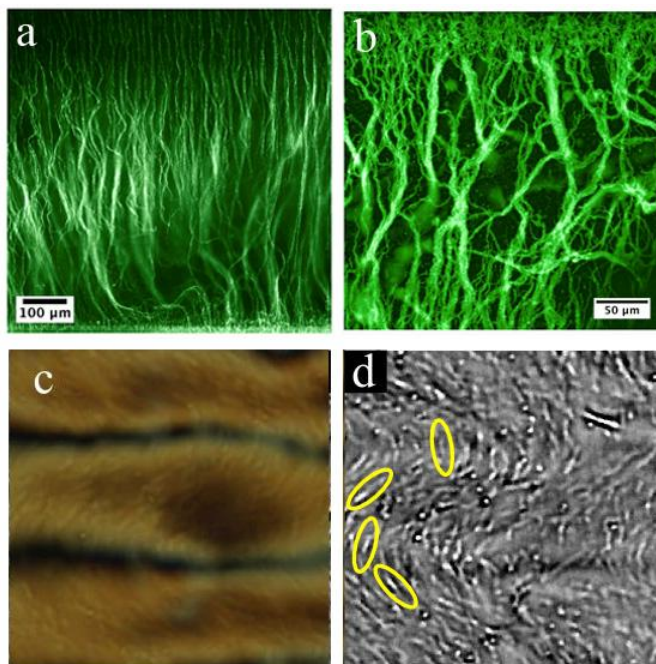
Self-assembly, a natural tendency of simple building blocks to organize into complex architectures, is a unique opportunity for materials science. The in-depth understanding of self-assembly paves the way for the design of tailored smart materials for emerging energy technologies, such as materials that can self-heal, regulate porosity, strength, water or air resistance, viscosity, or conductivity. However, self-assembled materials pose a formidable challenge: they are intrinsically complex, with often-hierarchical organization occurring on many nested length and time scales. Our approach is a combination of in-depth theoretical and experimental studies of the dynamics of active self-assembled material for the purpose of control, prediction, and design of novel bio-inspired materials for emerging energy applications.

In the past two years our program yielded discoveries of dynamically self-assembled tunable architectures including “sticky” colloidal particles and viscosity controls of dynamic assembly in ferromagnetic suspensions, and a new class of active matter - the living liquid crystals - a bio-mechanical system represented by a suspension of swimming bacteria in lyotropic liquid crystal. For all these systems we have developed theoretical understanding leading to prediction and control of the emergent self-assembled structures. In the next three years we will explore new approaches to synthesis and discovery of a broad class of self-assembled bio-inspired materials stemming from the advances of our program: functional 2D and 3D tunable colloidal structures built from elementary sub-units out of equilibrium, living liquid crystals with the controlled orientations of director, from chiral to homeotropic.

The project synergistically integrates theory, simulations, and experiments, and focuses on the fundamental issues at the forefront of contemporary materials science. On the theoretical side we consider a theory and large-scale molecular dynamics simulations, implemented on Graphic Processing Units (GPU), of active self-assembly in the systems of magnetic nano- and microparticles, swimming microorganisms, and a mesoscale description (phase field models) of self-organization in active bio-inspired materials. We actively use unique fabrication, characterization, and computational user facilities in Argonne National Laboratory: Center for Nanoscale Materials, Advance Photon Source, and Leadership Computing Facility via peer-reviewed users proposals.

Recent Progress

Self-assembled tunable colloidal networks. Surfaces decorated with dense arrays of microscopic fibers exhibit unique materials properties, including superhydrophobicity and ultra-low friction. Nature relies on “hairy” surfaces to protect blood capillary from wear and infections (endothelial glycocalyx). We conducted studies of self-assembled tunable networks of microscopic polymer fibers formed by sticky colloidal particles. Studies revealed a large variety of self-assembled networks, ranging from dense colloidal “fur” to highly interconnected gels, see Figure 1 a,b. The networks emerge via dynamic self-assembly



in the alternating electric field from a non-aqueous suspension of “sticky” polymeric colloidal particles with a controlled degree of polymerization. The resulting architectures can be further tuned by the frequency and amplitude of the electric field and surface properties of the particles. We demonstrated, by coating the fibers with a thin layer of SnO₂ using atomic layer deposition, that the networks can serve as templates for transparent conductor. These self-assembled tunable materials are promising candidates for large surface area electrodes in batteries and organic photovoltaic cells, as well as for microfluidic sensors and filters.

Figure 1. Top: Self-assembled structures formed by sticky epoxy particles [9]. a) Permanent self-assembled polymer brushes (hair) formed by the sticky particles with a high degree of polymerization; b) A network of bundled chains of sticky particles (gel); c) Living liquid crystal [10]. Emergence of a wavy periodic structure in liquid crystal with swimming bacteria observed by cross-polarized microscopy; d) A bright-field image of the living liquid crystal. Some bacteria are highlighted by yellow ellipsoids.

Active Liquid Crystalline Materials: Living Liquid Crystals. Many biological liquids (cytoplasm, mucus, DNA or polypeptide solutions) are anisotropic and exhibit a certain degree of liquid crystallinity. Anisotropy of the suspending liquid significantly affects the swimming dynamics of an individual bacterium and impacts their collective behavior. In turn, the activity (due to motility of bacteria) affects material and optical properties of the medium. Our studies have shown that living bacteria (*B. subtilis*) can be transferred to the non-toxic lyotropic (i.e. water-soluble) LC media (DSCG), and yield highly nontrivial interactions with the molecular ordering of the LC. First, due to strong anisotropy of the LC, individual bacteria tend to swim along the nematic direction. Second, swimming bacteria can perturb the orientational order of the

liquid crystal or even cause its local melting, making the nanometer-thick flagella optically visible and thus enabling liquid crystal nanoscopy (LCN). Third, self-organized textures emerge from the initial uniform LLC alignment with a characteristic length controlled by a balance between activity and anisotropic viscoelasticity of liquid crystal, see Figure 1 c,d. We have shown that bacteria can transport a cargo (a microscopic particle) along a predetermined trajectory defined by the direction of molecular orientation of the liquid crystal. LLC can lead to valuable biosensing applications and biomaterials design.

Future Plans

Self-assembly and particle transport in driven colloidal suspensions under in-plane excitations. This research direction is stemming from our successful study of dynamic self-assembly of magnetic colloids confined at the interfaces between non-miscible liquids or air and liquid. The primary goals of this research are (i) understanding of fundamental mechanisms governing active self-assembly in confined colloidal systems with long-ranged interactions; (ii) exploration of design concepts of broad class of active tunable self-assembled structures for soft robotics and particle transport at the interfaces. Our preliminary results obtained in a ferromagnetic colloidal suspension energized by a uniaxial in-plane magnetic field revealed new class of dynamically self-assembled architectures emerging in a certain range of the excitation parameters and ranging from pulsating clusters and particle-thick wires to arrays of self-propelling spinners rotating in either direction. The spinners are formed via spontaneous breaking of the uniaxial symmetry of the energizing field. All structures are reversible. Possible

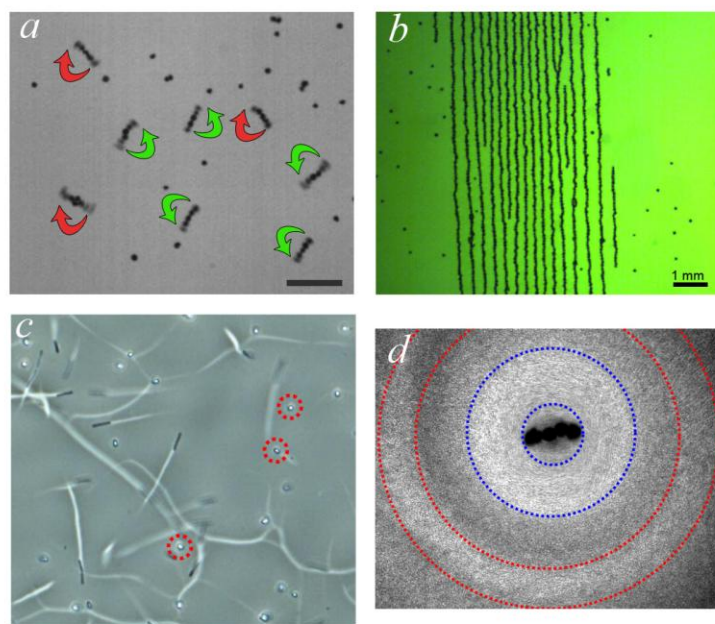


Figure 2. a) dynamically self- assembled spinners (short rotating chains) at a liquid interface. Spinners rotate in either direction (illustrated by arrows) with the frequency of the applied field. Scale bar is 1 mm; b) parallel arrays of particle-thick dynamic wires; c) Living bacteria in a thin glass cell with the homeotropically aligned liquid crystal. Swimming bacteria appear as dark short rods with bright traces. Some motile bacteria are oriented vertically and are trapped for a certain period of time (red dashed circles); d) Distribution of bacteria in the vicinity of a rotating microscopic particle in the suspending liquid. Motile bacteria are expelled by the hydrodynamic vortex created by the particle (area between blue dashed circles) due to shear-induced reorientation.

applications include design of reconfigurable wire networks for soft robotics and flexible electronics, or non-contact mixing at interfaces.

Material properties of living liquid crystals with controlled director orientations. A success of our proposed concept of living liquid crystal (LLC) motivated further exploration of material and optical properties of this unique biomechanical system. New studies will focus on LLC with chiral and homeotropic (perpendicular to the surface) director orientations. The main goals of this research are understanding interactions between biological and synthetic component of this material, and synthesis of biomechanical active materials with the unique mechanical and optical properties. Thus, in addition to LLC with planar alignment of the director, we will investigate of properties of LLC in (i) homeotropic and (ii) chiral cells. Our preliminary experiments revealed a number of striking phenomena. Rod-shaped swimming bacteria in a LC glass cell with the homeotropic alignment are found in two distinct dynamic states: (i) motile bacteria that swim parallel to the surface and (ii) vertically oriented spinning bacteria that are trapped by the elastic forces in LC, see Figure 2c. The number of trapped bacteria and frequency of the transitions between two states depends on the activity of bacteria (that can be controlled by the amount of dissolved oxygen in the LLC and temperature). Swimming bacteria in LLC in the homeotropic cell can also follow the tracks of other bacteria, forming long self-organized “trains”. We plan to investigate the effects of the applied shear stress on self-organization of LLC. A preliminary study shows that a hydrodynamic vortex created by a rotating particle expels motile bacteria from the center of the vortex, while immotile bacteria remain distributed homogeneously, see Figure 2d. We anticipate that our biomechanical system will provide the basis for devices with new functionalities, reconfigurable optical and rheological properties, sensitive to chemical agents or temperature.

Publications (which acknowledge DOE support- last two years)

1. G. Kokot, D. Piet, G.M. Whitesides, I. S. Aranson, A. Snezhko, “Emergence of reconfigurable wires and spinners via dynamic self-assembly”, *Scientific Reports (Nature)* **5**, 9528 (2015)
2. K.H. Nagai, Y. Sumino, R. Montagne, I.S. Aranson, H. Chate, “Collective motion of self-propelled particles with memory”, *Physical Review Letters* **114**, 168001 (2015)
3. J. Lober, F. Ziebert, I.S. Aranson, “Collisions of deformable cells lead to collective migration” *Scientific Reports (Nature)* **5**, 9172 (2015)

4. A. Sokolov, S. Zhou, O.D. Lavrentovich, I.S. Aranson,
“Individual behavior and pairwise interactions between microswimmers in anisotropic liquid”,
Physical Review E **91**, 013009 (2015)
5. M. Tournus, A. Kirshtein, L.V. Berlyand, I.S. Aranson,
“Flexibility of bacterial flagella in external shear results in complex swimming trajectories”,
Journal of the Royal Society Interface **12**, 20140904 (2015)
6. A. Kaiser, A. Sokolov, I.S. Aranson, H. Lowen,
“Mechanisms of Carrier Transport Induced by a Microswimmer Bath”,
IEEE Transactions on Nanobioscience **14**, 260 (2015)
7. A. Snezhko and I.S. Aranson,
“Velocity statistics of dynamic spinners in out-of-equilibrium magnetic suspensions”,
Soft Matter, DOI: 10.1039/C5SM01163A (2015)
8. P Scherpelz, K Padavić, A Murray, A Glatz, IS Aranson, K Levin,
“Generic equilibration dynamics of planar defects in trapped atomic superfluids”,
Physical Review A **91** (3), 033621 (2015)
9. A. Demortiere, A. Snezhko, M. Sapozhnikov, N. Becker, T. Proslie, I. Aranson,
“Self-assembled tunable networks of sticky colloidal particles”,
Nature Communications **5**, 3117 (2014)
10. S. Zhou, A. Sokolov, O.D. Lavrentovich, I.S. Aranson,
“Living liquid crystals” ,
Proceedings of National Academy of Sciences **111**, 1265 (2014)
11. A. Kaiser, A. Peshkov, A. Sokolov, B. ten Hagen, H. Lowen, I.S. Aranson,
“Transport powered by bacterial turbulence”,
Physical Review Letters **112**, 158101 (2014)
12. A. Dreher, I.S. Aranson, K. Kruse,
“Spiral actin-polymerization waves can generate amoeboidal cell crawling”,
New Journal of Physics **16**, 055007 (2014)
13. S. Ngo, A. Peshkov, I.S. Aranson, E. Bertin, F. Ginelli, H. Chate,
“Large-scale chaos and fluctuations in active nematics”,
Physical Review Letters **113**, 038302 (2014)
14. J. Lober, F. Ziebert, I.S. Aranson,
“Modeling crawling cell movement on soft engineered substrates”,
Soft Matter **10**, 1365 (2014)

15. F. Ziebert, I.S. Aranson,
“Modular approach for modeling cell motility”,
European Physical Journal-Special Topics **223**, 1265 (2014)
16. S. Tricard, R. F Shepherd, C. A Stan, Ph. W Snyder, R. Cademartiri, D. Zhu, I. S Aranson, E.
I Shakhnovich, G. M Whitesides,
“Mechanical Model of Globular Transition in Polymers”,
ChemPlusChem, **80**, 37-41 (2014)
17. P Scherpelz, K Padavić, A Rançon, A Glatz, IS Aranson, K Levin,
“Phase imprinting in equilibrating Fermi gases: the transience of vortex rings and other
defects”,
Physical Review Letters. **113**, 125301 (2014)
18. J. Martin, A. Snezhko,
“Driving self-assembly and emergent dynamics in colloidal suspensions by time dependent
magnetic fields”, Invited Review,
Reports on Progress in Physics **76**, 126601 (2013)
19. SD Ryan, A Sokolov, L Berlyand, IS Aranson,
“Correlation properties of collective motion in bacterial suspensions”,
New journal of Physics **15**, 105021 (2013)
20. DL Piet, AV Straube, A Snezhko, IS Aranson,
“Model of dynamic self-assembly in ferromagnetic suspensions at liquid interfaces”,
Physical Review E **88**, 033024 (2013)

Active Assembly of Dynamic and Adaptable Materials: Active Protein Assemblies

Principal Investigator: George D. Bachand

Co-Investigators: Erik Spoerke, Mark Stevens, and Darryl Sasaki

Mailing Address: Nanosystems Synthesis & Analysis Department, Sandia National Laboratories, PO Box 5800, MS 1303, Albuquerque, NM 87185

Email: gdbacha@sandia.gov

Program Scope

The *Active Assembly of Dynamic and Adaptable Materials* research program examines fundamental materials science issues at the intersection of biology, nanomaterials, and hybrid interfaces. The overall program goal is to understand how nature's biomolecular machines assemble non-equilibrium, multi-scale materials, and to apply these principles and components in hybrid or composite materials whose assembly and organization can be "self-directed" or autonomously responsive to stimuli. Research in this program is specifically focused on (1) the active assembly of hybrid nanomaterials based on motor protein-driven transport and assembly of cytoskeletal filaments, and (2) the design and exploration of "artificial microtubules" that mimic the dynamic, non-equilibrium behaviors of the natural filaments.

Many of unique behaviors found in living systems (e.g., active color change) are commonly associated with dynamic self-assembly (DSA) processes.¹ The interactions underpinning these dynamic processes depend strongly on the dissipation of energy, commonly through enzymatic reactions. Our program has focused one of the active transport systems found ubiquitously in eukaryotic cells, specifically microtubules (MTs) and their associated motor protein, kinesin. MTs are hollow filaments composed of $\alpha\beta$ tubulin dimers whose energy-dissipative assembly is used to push, pull, or rearrange the cell's cytoskeleton. MTs also serve as "train tracks" for the bidirectional transport of organelles by the motor proteins through the conversion of chemical energy into mechanical work. Living organisms use the concerted and dynamic interactions between motors and MTs for physiological processes ranging from chromosomal segregation at the cellular level to macroscopic color changing behaviors at the organismal level.² Thus, learning to exploit, mimic, and/or translate the role of these active proteins and emergent biological behaviors represents an opportunity to dramatically advance nanomaterials assembly.

Recent Progress

DSA of Lipid and Polymer Nanotube Networks

Membranous intracellular networks formed by the endoplasmic reticulum (ER) and Golgi apparatus play a critical role in the compartmentalization of eukaryotic cells, and are sites of important physiological processes such as protein synthesis. Transport and structural reorganization of these organelles by cytoskeletal motors enable the cell to adapt to and meet the changing physiological needs.^{3, 4} The structural (and functional) complexity of these organelles starkly contrasts the limited morphologies formed through self-assembly of lipids in aqueous media (i.e., micelles, liposomes, and bilayers). As a means to achieving more complex and dynamic lipid structures, we demonstrated the DSA of large-scale ($>10 \text{ } \mu\text{m}$) networks of interconnected lipid nanotube networks through the energy-dissipative transport by kinesin molecular machines.⁵ A valuable aspect of these lipid networks is their ability to "self-heal," similar to their biological analogs; new pathways are continuously being generated as failures

occur (i.e., branches collapse) in the larger network. The highly-parallel nature of this DSA process enables formation of networks on relatively short-time scales (e.g., minutes). We further demonstrated the ability of these networks to transport semiconductor nanocrystals (Qdots) based on one-dimensional or single-file, one-dimensional diffusion depending upon the concentration of nanocrystals on the nanotubes.⁵

As with lipids, amphiphilic block copolymers also self-assemble into a similar, limited range of morphologies. Block copolymer display physical behaviors analogous to lipids but with increased stability, and thus have been regarded as a more robust synthetic analog. The goal of our most recent work was to explore the DSA of polymer nanotube networks using biomolecular active

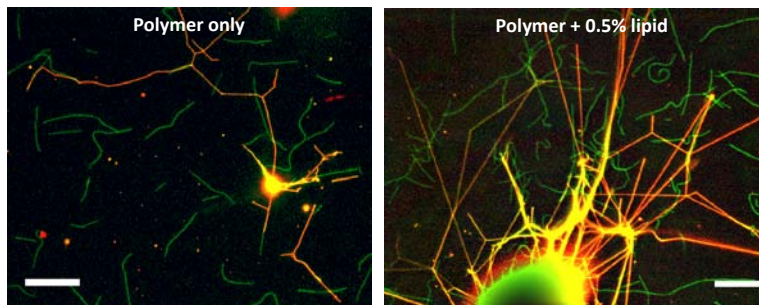


Fig. 1. DSA of polymer and polymer/lipid nanotubes (red) based on the work done by kinesin molecular machines and MT shuttles. Scale bar = 10 μ m

transport. We chose poly(ethylene oxide)-b-poly(butadiene) (PEO-PDB) as model diblock copolymer because it is one of the most widely studied vesicle-forming polymers, and many of the relevant physical properties of the resulting membranes are known. Our work demonstrated that the collective action of kinesin molecular machines produce sufficient forces and mechanical work to extract nanotubes from polymer vesicles (Fig. 1), forming networks with similar size and morphology to those generated from lipid vesicles.⁶ As anticipated, the resulting polymer networks persisted considerably longer than lipid networks, owing to the comparative stability of the polymer membranes. We further demonstrated that the use of polymer amphiphiles in these nanotube networks introduces anomalies in membrane-based transport that should be considered when designing soft, tubular highways for transport in biomimetic systems. Overall, this work demonstrates the ability to apply biomolecular machine-driven DSA to form morphologically complex block copolymer structures, substantially increasing the library of soft amphiphilic materials capable of forming large-scale nanotube networks.

DSA of Nanocomposite Rings

Several research groups have shown that the collective action of kinesin molecular machines acting on MT shuttles carrying “sticky” cargo (e.g., streptavidin-coated Qdots) can drive their DSA into ring structures.⁷ While hypothetical descriptions have been proposed, the exact mechanism underlying this DSA process has remained elusive primarily based on the inability to characterize the early initiation stages. To address this issue, we applied an active microfluidic deoxygenation device⁸ to characterize, in real-time, the DSA of nanocomposite rings immediately following the introduction of semiconductor nanocrystals. Our data confirm that three of the proposed mechanisms do in fact lead to the formation of MT rings. The first mechanism, pinning, occurs when MTs encounter a “dead” motor and the leading tip gets pinned. Continued transport and pushing by kinesin motors leads to a buckled morphology and formation of rings with generally small inner diameters. In contrast, large rings are formed by the second mechanism, strain-induced DSA, where collisions between MTs lead to the formation of oligomers in which twisted and kinked domain leads to frozen-in curvature. The

curved transport trajectory leads to head-tail interactions, forming an enclosed ring. The final mechanism, simultaneous collision, involves the collision of three or more MTs colliding simultaneously to form an enclosed polygon. Continued action by the kinesin motors induces remodeling of the polygon and the formation of an elliptical or circle ring morphology with diameters intermediate to those formed by pinning or strain-induced DSA.

Future Plans

Future work with the motor-driven DSA of lipid and polymer nanotube networks will concentrate on increasing the complexity of the system as a model for primitive, biomolecular communication networks. We will initially explore the behaviors of multi-vesicle networks including characterization of polymer/lipid network connectivity, nanotube junction morphology, and self-healing properties. In addition, the transport of semiconductor nanocrystals and other nanomaterials in the interstitial space of lipid/polymer nanotubes will be evaluated. Future work on the DSA of nanocomposite rings will focus on alternating MT composition in order to modulate ring morphology and enable multi-material nanocomposite rings.

Acknowledgment

This research was supported by the U.S. Department of Energy, Office of Basic Energy Sciences, Division of Materials Sciences and Engineering, Project KC0203010. Sandia National Laboratories is a multi-program laboratory managed and operated by Sandia Corporation, a wholly owned subsidiary of Lockheed Martin Corporation, for the U.S. Department of Energy's National Nuclear Security Administration under contract DE-AC04-94AL85000.

Abstract References

1. Fialkowski, M.; Bishop, K. J. M.; Klajn, R.; Smoukov, S. K.; Campbell, C. J.; Grzybowski, B. A. *Journal of Physical Chemistry B* **2006**, 110, (6), 2482-2496.
2. Goldstein, L. S. B.; Yang, Z. H. *Annual Review of Neuroscience* **2000**, 23, 39-71.
3. Wozniak, M. J.; Bola, B.; Brownhill, K.; Yang, Y. C.; Levakova, V.; Allan, V. J. *Journal of Cell Science* **2009**, 122, (12), 1979-1989.
4. Lippincottschwartz, J.; Cole, N. B.; Marotta, A.; Conrad, P. A.; Bloom, G. S. *Journal of Cell Biology* **1995**, 128, (3), 293-306.
5. Bouxsein, N. F.; Carroll-Portillo, A.; Bachand, M.; Sasaki, D. Y.; Bachand, G. D. *Langmuir* **2013**, 29, (9), 2992-2999.

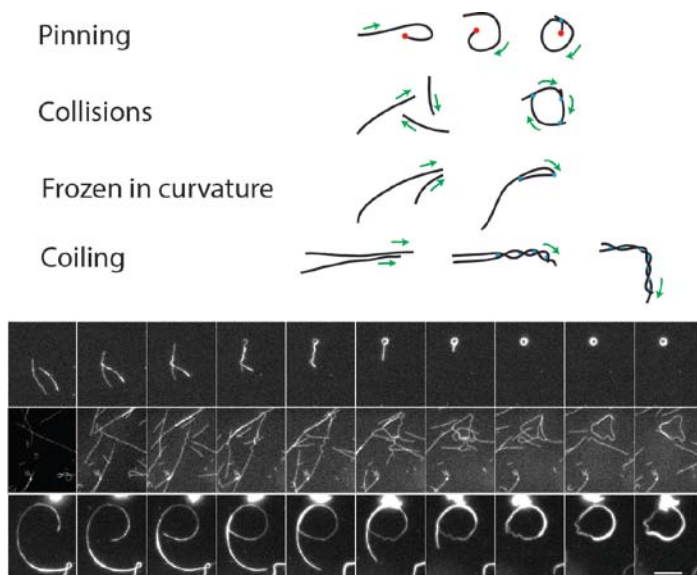


Fig. 2. (top) Schematic diagrams and **(bottom)** time-lapse fluorescent images of the different mechanisms of nanocomposite rings by the motor-driven DSA of MTs and semiconductor nanocrystals.

6. Paxton, W. F.; Boussein, N. F.; Henderson, I. M.; Gomez, A.; Bachand, G. D. *Nanoscale* **2015**, 7, (25), 10998-1004.
7. Liu, H. Q.; Spoerke, E. D.; Bachand, M.; Koch, S. J.; Bunker, B. C.; Bachand, G. D. *Advanced Materials* **2008**, 20, (23), 4476-4481.
8. Vandelinder, V.; Bachand, G. D. *Analytical Chemistry* **2014**, 86, (1), 721-8.

DOE-Sponsored Publications (2014-2015)

- Stevens, M.J. How shape affects microtubule and nanoparticle assembly. *Science* **2014**, 343, 981-982.
- Spoerke, E.D.; Connor, B.A.; Gough, D.V.; McKenzie, B.B.; Bachand, G.D. Microtubule-templated cadmium sulfide nanotube assemblies. *Particle & Particle Systems Characterization* **2014**, 31(8), 863-870 (cover).
- Cheng, S.; Stevens, M.J. Self-assembly of chiral tubules. *Soft Matter* **2014**, 10, 510-518.
- Ting, C.L.; Frischknecht, A.L.; Stevens, M.J.; Spoerke, E.D. Electrostatically tuned self-assembly of branched amphiphilic peptides. *Journal of Physical Chemistry B* **2014**, 118(29), 8624-8630.
- Vandelinder, V.; Bachand, G.D. Photodamage and the importance of photoprotection in biomolecular-powered device applications. *Analytical Chemistry* **2014**, 86(1), 721-728.
- Bachand, G.D.; Boussein, N.F.; VanDelinder, V.; Bachand, M. Biomolecular motors in nanoscale materials, devices, and systems. *Wiley Interdisciplinary Reviews: Nanomedicine and Nanobiotechnology* **2014**, 6, 163-177 (invited review).
- Gough, D.V.; Wheeler, J.S.; Spoerke, E.D. Supramolecular assembly of asymmetric self-neutralizing amphiphilic peptide wedges. *Langmuir* **2014**, 30(30), 9201-9209.
- Boussein, N.F.; Bachand, G.D. Divalent counter-ion regulation of microtubule stability, flexibility and motility. *Biomacromolecules* **2014**, 15(10), 3696-705
- Bachand, M.; Boussein, N.F.; Cheng, S.; von Hoyningen-Huene, S; Stevens, M.J.; Bachand, G.D. Directed self-assembly of 1D microtubule nano-arrays. *RSC Advances* **2014**, 4, 51641-54649.
- Momin, N.; Lee, S.; Gadok, A.K.; Busch, D.J.; Bachand, G.D.; Hayden, C.C.; Stachowiak, J.C.; Sasaki, D.Y. Designing lipids for selective partitioning into liquid ordered membrane domains. *Soft Matter* **2015**, 11, 3241-3250.
- Bachand, G.D.; Spoerke, E.D.; Stevens, M.J. (2015) Microtubule-based Nanomaterials: Borrowing from Nature's dynamic biopolymers. *Biotechnology and Bioengineering* **2015**, 112(6), 1065-1073 (invited review).
- Jones, B.H.; Martinez, A.M.; Wheeler, J.S.; Spoerke, E.D. Surfactant-induced assembly of enzymatically-stable peptide hydrogels. *Soft Matter* **2015**, 11(18), 3572-3580 (selected for "2015 Soft Matter Hot Papers").
- Paxton, W.F.; Boussein, N.F.; Henderson, I.M.; Bachand G.D. Dynamic assembly of polymer nanotube networks via kinesin powered microtubule filaments. *Nanoscale* **2015**, 7(25), 10998-11004.

Molecular Nanocomposites – Complex Nanocomposites Subtask

Principal Investigator: Paul G. Clem; Subtask Lead: Jeff Brinker; Co-PIs Bryan Kaehr, Hongyou Fan, Frank van Swol, Stanley Chou

Mailing Address: Sandia National Laboratories, Advanced Materials Lab, 1001 University Blvd, SE, Albuquerque, NM 87106

Program Scope

The goal of the Complex Nanocomposite task is the discovery and understanding of new chemically- and physically-based synthesis and assembly methodologies to construct and integrate complex porous and composite materials, which exhibit structure and function across multiple length scales. A significant aim is to establish processing-structure-property relationships for new nanocomposites prepared by self-assembly, directed assembly, and templating procedures pioneered by the team members through over a decade of DOE support. Emphasis is on construction of 2- and 3D nanocomposites with feature sizes and interfacial behaviors designed to allow energy conversion, transduction, or storage and/or enable

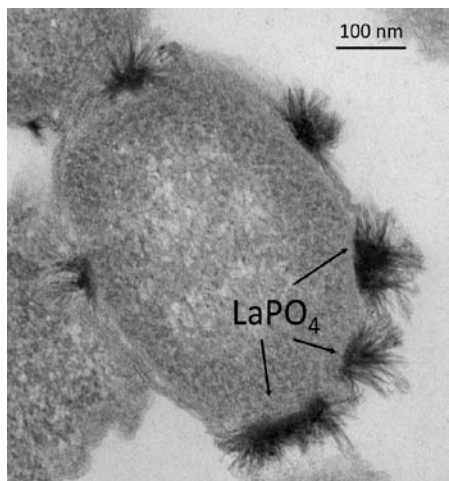


Fig. 1. LaPO₄ modified *E. coli* cell formed via rare earth oxide dephosphorylation of the bacterial cell wall.

development of life-like structure and functionality. An example of a complex nanocomposite is the rare earth phosphate modified *E. coli* cell shown in **Fig. 1**. This biotic/abiotic cell represents a new form of living material with retained viability and motility but altered phenotype, cellular interactions, and function. Overall, the idea of using the responsiveness of living, energy dissipating cells or organisms to program/direct the formation of synthetic materials is a representative theme of our program.

This project employs self-assembly, in particular evaporation-induced self-assembly and cell-directed assembly, in combination with top-down directed assembly procedures like bio-compatible multi-photon lithography, pressure-directed assembly, and atomic layer deposition to create model composite materials, which can be further chemically or physically ‘adjusted’ at the nm to μm scale.

Further we use and develop advanced *in situ* scattering and diffraction methodologies along with electron and probe microscopies to characterize the formation and structures of the complex composites and probe their collective properties deriving from hierarchical organization.

Recent Progress

Co-opting cellular shapes to generate functional particles - We have pioneered approaches where the biomolecular surfaces of cells—both inside and outside—can direct formation of conformal and self-limiting porous silica layers resulting in shape-preserved composite and inorganic materials.^{1,2} This process of silica bioreplication has the potential to impact diverse areas—from biocatalysis to material synthesis. Considering particle synthesis, overcoming viscous forces to produce complex, nonspherical shapes is particularly challenging; this is a problem that is continuously solved in nature by dynamic biological entities such as cells. For example, red blood cells (RBCs) can undergo dramatic and reversible shape transformations simply by minor perturbations of the cell membrane (**Fig. 2**). By capturing this biological

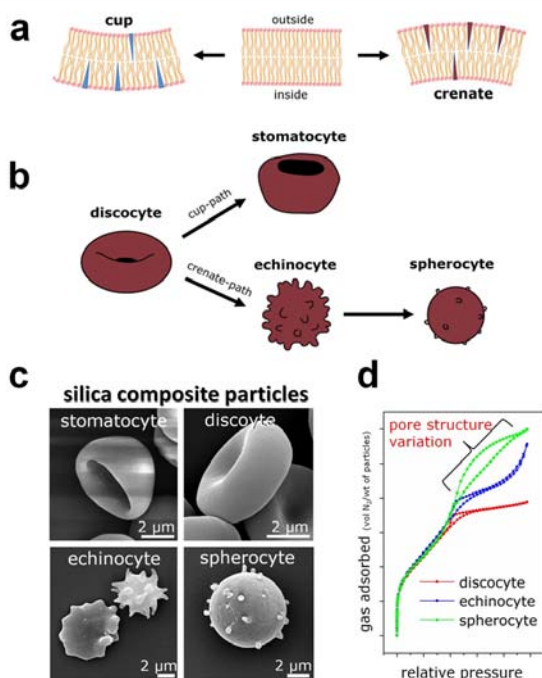


Fig. 2. Chemical agents preferentially inserting into the inner or outer leaflet of the cell membrane drive shape changes in erythrocytes, providing abilities to tune particle interactions and mesopore dimensions of silica

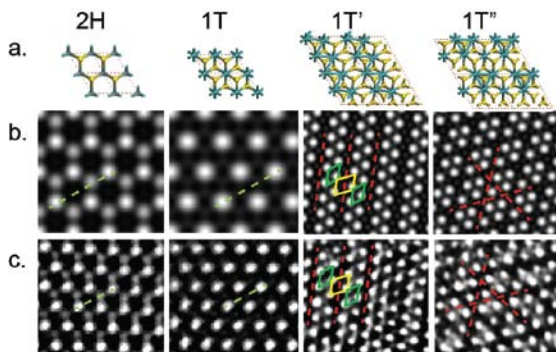


Fig. 3. Exfoliated MoS₂ as artificial, cellular membrane with embedded enzymatic function. Allotropic reconstruction of MoS₂ basal plane activates enzyme-like activities on the basal plane absent in natural MoS₂. This enables path for theory guided discovery of biomimetic components in next generation cells replicas and protocells. a. DFT predicted allotropic structures and basal plane phase change b. simulated HAADF TEM images of predicted phases. c. experimental verification by aberration corrected HAADF TEM.

fundamental building blocks facilitating theoretically guided experimentation and discovery of inorganic “cellular-components” of increased function and complexity.

Future Plans

Continue to investigate the mechanism of SCR - Our current hypothesis is that at its isoelectric point (pH~3) silicic acid molecules (similar to water) diffuse throughout the fixed cell, replace bound water at biomolecular interfaces, and are amphoterically catalyzed by proximal proteins

response in a silica cell replica (SCR), we can produce distinct libraries of non-spherical particles with tunable porosity that can be further transformed into metallic, semi-conductive and ferromagnetic particles and assemblies. This ability to use cellular responses as “structure directing agents” offers an unprecedented toolset to design colloidal-scale materials.

Inorganic materials mimicking natural enzymatic functions

– In conjunction with replication of cellular structure, we aim to recapitulate enzymatic function using modular synthetic components that could be incorporated into inorganic cellular mimics, e.g. protocells (see following discussion). To that end, we have pursued flexible, conformal two-dimensional components with enzymatic functions embedded in the basal plane that could be ‘molded’ onto the surface of SCR features via directed or non-covalent interactions. The principal model system pursued in the past year is the transition metal dichalcogenide family (MX₂), including MoS₂ and WS₂, which can be exfoliated into flexible 2D monolayers with scalable chemical synthesis to match the synthetic scale of SCRs.³ A significant obstacle however is that, for mechanically exfoliated MX₂, catalytic sites are confined to the sheet edges, thus impairing their efficacy as catalytic cell membranes. Another impediment is the overall need to better understand the energetics and catalytic efficiency of these materials, which is often confounded by synthetic variations, and different allotropic reconstructions resulting from phase changes. Using computationally guided experimentation, we established processing-structure-property relationships of MX₂ materials, elucidating a synthetic pathway to MX₂ monolayers with basal plane hydrogenase-like catalytic activity that we rationalized by DFT calculations (**Fig. 3**).⁴ The tools uncovered here are

and other membrane components to form a self-limiting, several nm-thick silica replica. We will test this hypothesis using quantitative calorimetric studies of cell/silica/water interactions complemented with molecular dynamics and *ab initio* calculations of a water/silicic acid/protein system (with L. Ciacchi, University of Bremen).

Optimize SCR procedures for retained biofunctionality - Activity of subclasses of enzymes will be evaluated in fixed cells, silicified cells, and silicified cells after varying stages of desilicification. Based on our model, we anticipate that gradual de-silicification should ‘thaw’ the system and allow recovery of biofunctionality as shown by preliminary results in **Fig. 4**. Importantly, we envision that by preserving the native molecularly crowded environment of the cell, which evolved to conduct biomolecular chemistry, we should be able to perform coupled chemical reactions using a partially desilicified cellular platform. Biofunction will also be assessed following environmental challenges (e.g., chemical, temperature) versus non-silicified controls.

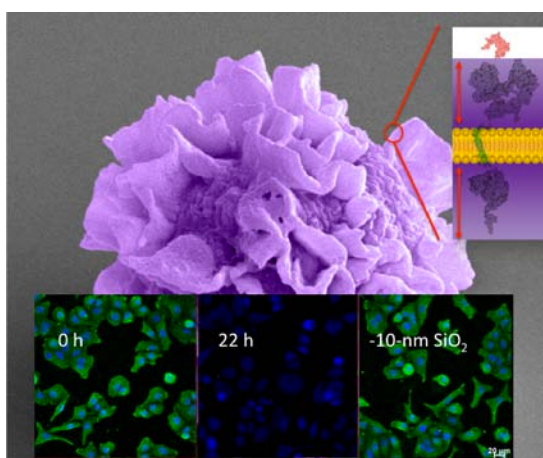


Fig. 4. Silica cell replica – lower inset shows antibody (green) binding to surface receptors before silicification (0 h), after 22 h of silicification, where receptors are obscured by silica (as depicted in upper inset), and after etching of ~10-nm of SiO₂, which re-reveals receptors and re-establishes antibody binding as in original cell.

Protocells as Platforms Dissipative Self-Assembly

(with Atul Parik, UC Davis) - protocells are artificial cells constructed of synthetic (abiotic) and natural (biotic) components and designed to perform some functions of real cells. However protocells could be more mechanically and chemically durable and much more chemically complex, incorporating synthetic optical, magnetic, catalytic, and electronic components. Furthermore protocells could be assembled into higher order structures analogous to tissues or organs potentially within vascularized networks to enable connectivity and flow of chemical energy and information. First generation protocells (*Nature Mater.* 2011) comprised mesoporous silica cores loaded with cargo and encapsulated within a synthetic cell membrane. As depicted in **Fig. 5** we have expanded its definition to include metallic or

silica cell replica cores, native cell membranes, 2D monolayer (e.g. MoS₂) or polymer/polymersome coatings, and molecular machines (valves). A key design feature is 3D compartmentalization. This enables the establishment of and operation within potential gradients (chemical, optical, mechanical, electrical etc), which is key to energy harvesting, storage and dissipation to perform desired functions. The modular nature of protocells will enable us to assemble completely new cell and tissue-like materials with artificial and as yet unknown functionalities. In particular we will focus on ‘intracellular’ biomimetic designs of the protocell. Natural cells are extremely crowded, where the 3D cytoskeletal network has evolved to organize proteins into local arrangements optimized for efficient of chemical reactions. We envision a new generation of protocells where the structured and compartmentalized interior recapitulates the natural scaffolding and crowdedness of the intracellular space, and the exterior supports the membrane on a 3D surface where the adhesion energy and local curvature stabilize the membrane and direct curvature dependent fluidity and phase behavior³ unachievable with liposomes and polymersomes.

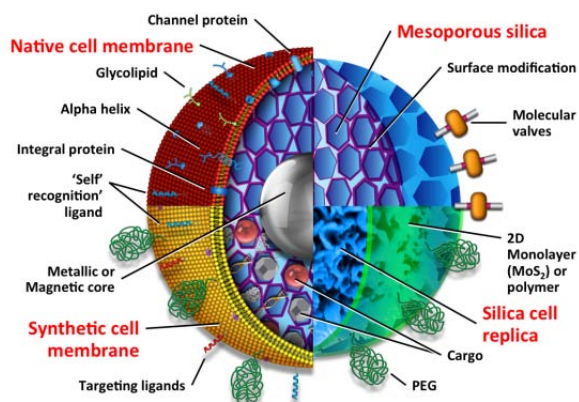


Fig. 5. Next generation protocells with variable metallic/silica/cell replica cores, native cell membranes, 2D monolayer (e.g. MoS₂) or polymer/polymersome coatings, and molecular machines (valves).

Exploration of Rare Earth Modified Bacteria

The dephosphorylation pathway, which is shared by all trivalent rare earth oxides, involves the irreversible formation of highly insoluble rare earth phosphates from any bioavailable phosphorous source. Questioning whether rare earth oxides (REO) would desphosphorylate bacterial cell membranes, we tested a library of REO nanoparticles against Gram negative *E. coli* and *S. enterica* and Gram positive *S. aureus* and found in all cases the formation of rare earth phosphates with needle or urchin-like structures (e.g **Fig. 1**) and retained function for exposure levels up to 100 µg/ml. These rare earth phosphate modified bacteria represent a new living

biotic/abiotic material/phenotype. Further, rare earth phosphates, e.g. LaPO₄, exhibit a unique combination of properties including insolubility, thermal stability, low toxicity, and high quantum yield.⁵ ‘Doping’ of other rare-earth ions (LaPO₄:Ln³⁺; Ln = Ce, Sm, Gd, Tb, Sr, etc) allows tuning of spectral emission over wide ranges due to specific 4f–5d and 4f–4f electronic transitions, which can yield intense and narrow emission,⁶ making rare earth phosphates of great interest as highly photostable luminescent chemical probes. Finally rare earth phosphates are catalytically active for reactions including, dehydration of 2-propanol, cracking/dehydrogenation of cumene, and isomerization of butane.⁷

References cited

- (1) Kaehr, B.; Townson, J. L.; Kalinich, R. M.; Awad, Y. H.; Swartzentruber, B. S.; Dunphy, D. R.; Brinker, C. J.: Cellular complexity captured in durable silica biocomposites. *Proc. Natl. Acad. Sci. U. S. A.* **2012**, *109*, 17336-17341.
- (2) Meyer, K. C.; Coker, E. N.; Bolintineanu, D. S.; Kaehr, B.: Mechanically Encoded Cellular Shapes for Synthesis of Anisotropic Mesoporous Particles. *J. Am. Chem. Soc.* **2014**, *136*, 13138-13141.
- (3) Chou, S. S.; Kaehr, B.; Kim, J.; Foley, B.; De, M.; Hopkins, P.; Huang, J.; Brinker, C. J.; Dravid, V. P.: Chemically Exfoliated MoS₂ as Near-Infrared Photothermal Agents. *Angew. Chem., Int. Ed.* **2013**, *52*, 4160-4164.
- (4) Chou, S. S.; Sai, N.; Lu, P.; Coker, E. N.; Liu, S.; Artyushkova, K.; Luk, T. S.; Kaehr, B.; Brinker, C. J.: Understanding catalysis in a multi-phasic, two dimensional transition metal dichalcogenide. *Nat Commun* **2015**, *Accepted*.
- (5) Schatzmann, M. T.; Mecartney, M. L.; Morgan, P. E. D.: Synthesis of monoclinic monazite, LaPO₄, by direct precipitation. *J. Mater. Chem.* **2009**, *19*, 5720-5722.
- (6) Panatarani, C.; Anggoro, D.; Joni, I. M.: Rare Earth Doped on LaPO₄ Nanocrystal. *International Conference on Physics and Its Applications (Icpap 2011)* **2012**, *1454*, 227-229.
- (7) Onoda, H.; Nariyai, H.; Moriwaki, A.; Maki, H.; Motooka, I.: Formation and catalytic characterization of various rare earth phosphates. *J. Mater. Chem.* **2002**, *12*, 1754-1760.

Publications

- (1) Brinker, C. J.; Clem, P. G.: Quartz on Silicon. *Science* 2013, 340, 818-819.
- (2) Chou, S. S.; Kaehr, B.; Kim, J.; Foley, B.; De, M.; Hopkins, P.; Huang, J.; Brinker, C. J.; Dravid, V. P.: Chemically Exfoliated MoS₂ as Near-Infrared Photothermal Agents. *Angew. Chem., Int. Ed.* 2013, 52, 4160-4164.
- (3) Kendall, E. L.; Ngassam, V. N.; Gilmore, S. F.; Brinker, C. J.; Parikh, A. N.: Lithographically Defined Macroscale Modulation of Lateral Fluidity and Phase Separation Realized via Patterned Nanoporous Silica-Supported Phospholipid Bilayers. *J. Am. Chem. Soc.* 2013, 135, 15718-15721.
- (4) Martin, K. E.; Tian, Y.; Busani, T.; Medforth, C. J.; Franco, R.; van Swol, F.; Shelnutz, J. A.: Charge Effects on the Structure and Composition of Porphyrin Binary Ionic Solids: ZnTPPS/SnTMePyP Nanomaterials. *Chem. Mater.* 2013, 25, 441-447.
- (5) Townson, J. L.; Lin, Y.-S.; Agola, J. O.; Carnes, E. C.; Leong, H. S.; Lewis, J. D.; Haynes, C. L.; Brinker, C. J.: Re-examining the Size/Charge Paradigm: Differing in Vivo Characteristics of Size- and Charge-Matched Mesoporous Silica Nanoparticles. *J. Am. Chem. Soc.* 2013, 135, 16030-16033.
- (6) Xiong, S.; Dunphy, D. R.; Wilkinson, D. C.; Jiang, Z.; Strzalka, J.; Wang, J.; Su, Y.; de Pablo, J. J.; Brinker, C. J.: Revealing the Interfacial Self-Assembly Pathway of Large-Scale, Highly-Ordered, Nanoparticle/Polymer Monolayer Arrays at an Air/Water Interface. *Nano Lett.* 2013, 13, 1041-1046.
- (7) Carmer, J.; van Swol, F.; Truskett, T. M.: Note: Position-dependent and pair diffusivity profiles from steady-state solutions of color reaction-counterdiffusion problems. *J. Chem. Phys.* 2014, 141, 046101.
- (8) Chen, G.; Liaw, S. S.; Li, B.; Xu, Y.; Dunwell, M.; Deng, S.; Fan, H.; Luo, H.: Microwave-assisted synthesis of hybrid Co_xNi_{1-x}(OH)₂ nanosheets: Tuning the composition for high performance supercapacitor. *J. Power Sources* 2014, 251, 338-343.
- (9) Durand, M.; Kraynik, A. M.; van Swol, F.; Käfer, J.; Quilliet, C.; Cox, S.; Ataei Talebi, S.; Graner, F.: Statistical mechanics of two-dimensional shuffled foams: Geometry-topology correlation in small or large disorder limits. *Phys. Rev. E* 2014, 89, 062309.
- (10) Fei, L.; Xu, Y.; Wu, X.; Chen, G.; Li, Y.; Li, B.; Deng, S.; Smirnov, S.; Fan, H.; Luo, H.: Instant gelation synthesis of 3D porous MoS₂@C nanocomposites for lithium ion batteries. *Nanoscale* 2014, 6, 3664-3669.
- (11) Fleharty, M. E.; van Swol, F.; Petsev, D. N.: Manipulating Semiconductor Colloidal Stability Through Doping. *Phys. Rev. Lett.* 2014, 113, 158302.
- (12) Fleharty, M. E.; van Swol, F.; Petsev, D. N.: The effect of surface charge regulation on conductivity in fluidic nanochannels. *J. Colloid Interface Sci.* 2014, 416, 105-111.
- (13) Foley, B. M.; Gorham, C. S.; Duda, J. C.; Cheaito, R.; Szejewski, C. J.; Constantin, C.; Kaehr, B.; Hopkins, P. E.: Protein Thermal Conductivity Measured in the Solid State Reveals Anharmonic Interactions of Vibrations in a Fractal Structure. *J. Phys. Chem. Lett.* 2014, 5, 1077-1082.
- (14) Fu, Y.; Li, B.; Jiang, Y.-B.; Dunphy, D. R.; Tsai, A.; Tam, S.-Y.; Fan, H.; Zhang, H.; Rogers, D.; Rempe, S.; Atanassov, P.; Cecchi, J. L.; Brinker, C. J.: Atomic Layer Deposition of L-Alanine Polypeptide. *J. Am. Chem. Soc.* 2014, 136, 15821-15824.

- (15) Li, B.; Smilgies, D.-M.; Price, A. D.; Huber, D. L.; Clem, P. G.; Fan, H.: Poly(N-isopropylacrylamide) Surfactant-Functionalized Responsive Silver Nanoparticles and Superlattices. *ACS Nano* 2014, 8, 4799-4804.
- (16) Li, B.; Wen, X.; Li, R.; Wang, Z.; Clem, P. G.; Fan, H.: Stress-induced phase transformation and optical coupling of silver nanoparticle superlattices into mechanically stable nanowires. *Nat Commun* 2014, 5.
- (17) Li, W.; Fan, H.; Li, J.: Deviatoric Stress-Driven Fusion of Nanoparticle Superlattices. *Nano Lett.* 2014, 14, 4951-4958.
- (18) Liu, S.; Li, B.; Fan, H.; Luk, T. S.; Sinclair, M. B.; Brener, I.: Investigation of Quantum Dot—Quantum Dot Coupling at High Hydrostatic Pressure. In *CLEO: 2014*; Optical Society of America: San Jose, California, 2014; pp FTh4C.3.
- (19) Meyer, K. C.; Coker, E. N.; Bolinteanu, D. S.; Kaehr, B.: Mechanically Encoded Cellular Shapes for Synthesis of Anisotropic Mesoporous Particles. *J. Am. Chem. Soc.* 2014, 136, 13138-13141.
- (20) Townson, J. L.; Lin, Y.-S.; Chou, S. S.; Awad, Y. H.; Coker, E. N.; Brinker, C. J.; Kaehr, B.: Synthetic fossilization of soft biological tissues and their shape-preserving transformation into silica or electron-conductive replicas. *Nat Commun* 2014, 5.
- (21) Wu, H.; Wang, Z.; Fan, H.: Stress-Induced Nanoparticle Crystallization. *J. Am. Chem. Soc.* 2014, 136, 7634-7636.
- (22) Zhong, Y.; Wang, J.; Zhang, R.; Wei, W.; Wang, H.; Lü, X.; Bai, F.; Wu, H.; Haddad, R.; Fan, H.: Morphology-Controlled Self-Assembly and Synthesis of Photocatalytic Nanocrystals. *Nano Lett.* 2014, 14, 7175-7179.
- (23) Zhong, Y.; Wang, Z.; Zhang, R.; Bai, F.; Wu, H.; Haddad, R.; Fan, H.: Interfacial Self-Assembly Driven Formation of Hierarchically Structured Nanocrystals with Photocatalytic Activity. *ACS Nano* 2014, 8, 827-833.
- (24) Carmer, J.; Jain, A.; Bollinger, J. A.; van Swol, F.; Truskett, T. M.: Tuning structure and mobility of solvation shells surrounding tracer additives. *J. Chem. Phys* 2015, 142, 124501.
- (25) Chou, S. S.; Huang, Y.-K.; Kim, J.; Kaehr, B.; Foley, B. M.; Lu, P.; Dykstra, C.; Hopkins, P. E.; Brinker, C. J.; Huang, J.; Dravid, V. P.: Controlling the Metal to Semiconductor Transition of MoS₂ and WS₂ in Solution. *J. Am. Chem. Soc.* 2015, 137, 1742-1745.
- (26) Chou, S. S.; Sai, N.; Lu, P.; Coker, E. N.; Liu, S.; Artyushkova, K.; Luk, T. S.; Kaehr, B.; Brinker, C. J.: Understanding catalysis in a multi-phasic, two dimensional transition metal dichalcogenide. *Nat Commun* 2015, Accepted.
- (27) Dunphy, D. R.; Sheth, P. H.; Garcia, F. L.; Brinker, C. J.: Enlarged Pore Size in Mesoporous Silica Films Templated by Pluronic F127: Use of Poloxamer Mixtures and Increased Template/SiO₂ Ratios in Materials Synthesized by Evaporation-Induced Self-Assembly. *Chem. Mater.* 2015, 27, 75-84.
- (28) Fleharty, M. E.; van Swol, F.; Petsev, D. N.: Charge regulation at semiconductor-electrolyte interfaces. *J. Colloid Interface Sci.* 2015, 449, 409-415.
- (29) Johnson, P. E.; Muttill, P.; MacKenzie, D.; Carnes, E. C.; Pelowitz, J.; Mara, N. A.; Mook, W. M.; Jett, S. D.; Dunphy, D. R.; Timmins, G. S.; Brinker, C. J.: Spray-Dried Multiscale Nano-biocomposites Containing Living Cells. *ACS Nano* 2015.

(30) Sun, J.; Jakobsson, E.; Wang, Y.; Brinker, C.: Nanoporous Silica-Based Protocells at Multiple Scales for Designs of Life and Nanomedicine. *Life* 2015, 5, 214.

Molecular Nanocomposites—Adaptive and Reconfigurable Nanocomposites Subtask

Principal Investigator: Paul G. Clem; Subtask Lead: Dale L. Huber; Co-investigators: Darryl Y. Sasaki, Mark J. Stevens, Amalie L. Frischknecht, and Hongyou Fan

Sandia National Laboratories, Albuquerque, NM and Livermore, CA

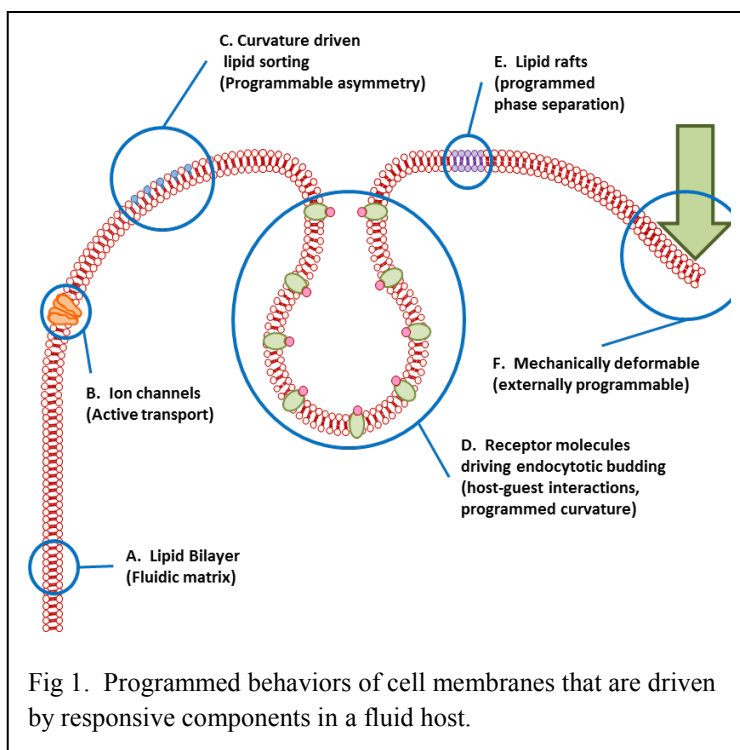
Program Scope

The goal of the Adaptive and Reconfigurable Nanocomposites subtask is to explore the basic science associated with the use of energy consuming, switchable, and responsive components to create programmable and reconfigurable nanocomposites. We take much of our inspiration for these functional hierarchical assemblies from biology, and can make an illustrative analogy with the programmable molecules and assemblies present in a cell membrane. The complex responsive behaviors of a cell are the result of a wide range of individual molecules present in a fluid matrix that allows them to maintain their own distinct responsive behaviors (see Fig 1).

To construct molecular nanocomposites that are truly adaptable and configurable, we must have two classes of building blocks. First are elements that can be programmed using energy sources such as heat, light, or magnetic fields, and the second set of building blocks are mobile hosts that allow components to reconfigure themselves in response to applied stimuli.

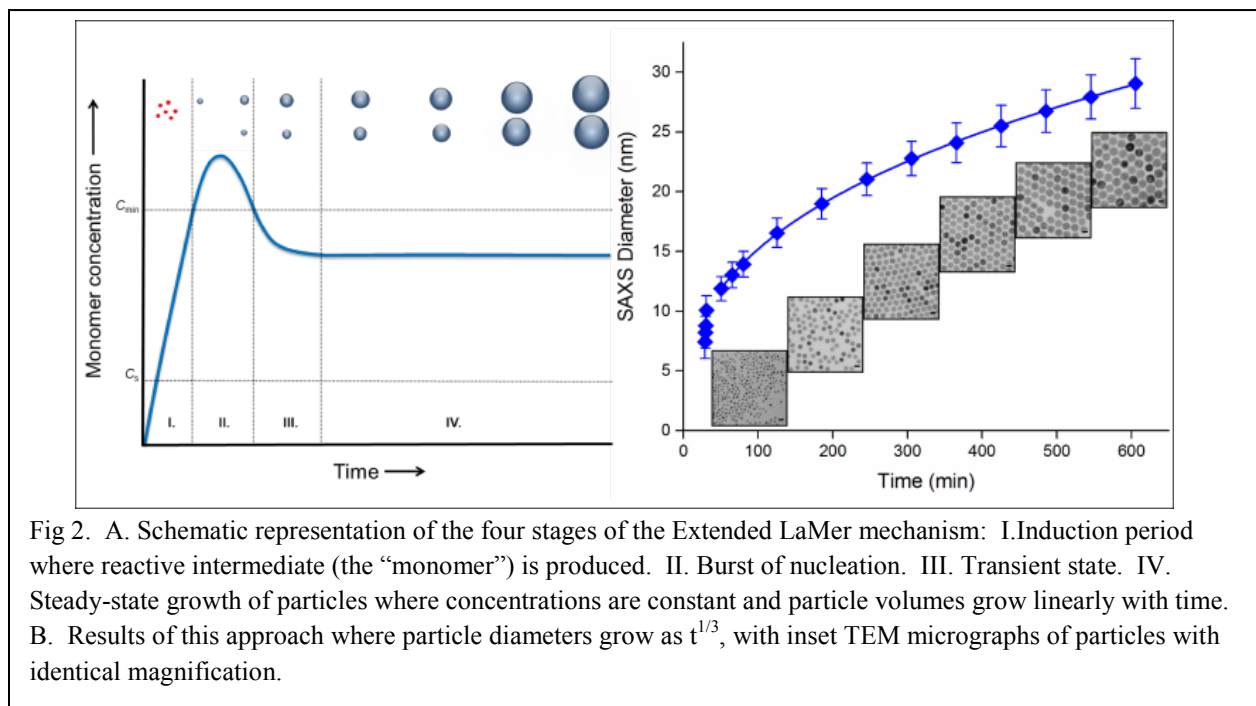
A significant amount of effort is geared towards new synthetic methods for making responsive materials. Biological systems are known for their extremely precise and reproducible syntheses. Exerting precise control over behaviors first requires precise control over the synthesis of the components.

While our inspiration is from nature, our systems are abiotic, and are purely synthetic. We take advantage of the full range of environments available to us including high temperature synthesis, and aim to create systems that are robust and useable over a wider range of conditions than biological systems.



Recent Progress

Biologically-informed nanoparticle synthesis. In many respects, the particles produced by magnetotactic bacteria are ideal materials, as they are perfect, single crystals and form stable mesoscopic structures. Catalytically active proteins allow them to form in water at near ambient temperatures, in a carefully controlled environment inside a magnetosome. In this controlled environment, these crystals are formed over the course of many hours, leading to the uniform product. In contrast we have found literature preparations of magnetic nanoparticles to be lacking in control and reproducibility. These reactions typically occur in tens of minutes, in an environment that is rapidly changing in temperature and reagent concentration. Instead of taking a truly biomimetic approach to their synthesis, we have taken a biologically informed approach that learns from the biological system but works in a dramatically different environment (see Fig. 2).



Our reactions occur in high temperature organic solvents, and in much more concentrated systems than are possible in biological synthesis. But we have learned from the biological approach and maintain a constant temperature and concentration, and have extended the length of the reaction to approximately ten hours. These controls mimic the constant environment of the magnetosome, and are designed to produce consistent single crystal materials with exquisite reproducibility. The result of this reaction is an ensemble of particles whose volume grows linearly with time (diameter grows as $t^{1/3}$ as in Fig 2b) while maintaining low size distributions.¹ With this heightened control we have demonstrated unprecedented reproducibility, with a coefficient of variation in particle size of only 4% batch-to-batch. This reaction approach also

allows early monitoring of the reaction to predict future sizes due to the steady state growth conditions. We have termed this new, general approach, the Extended LaMer mechanism.

Controlled phase behavior in mixed polymer monolayers.

Programmed phase separation is regularly used to drive behaviors in biological systems. We are investigating a unique approach to controlling phase behavior on surfaces. Building on previous work on phase separation in binary mixtures of polymers attached to surfaces², we have designed a ternary polymer brush that has rich phase behaviors. By simultaneous simulation and experiment, we are mapping the phase diagram of this system for the first time and have observed unique and useful phase behaviors (see Fig. 2 for examples)³. While this work is in a relatively early stage, we are investigating methods to make this phase behavior programmable and are exploring integrating these materials into our nanocomposite systems.

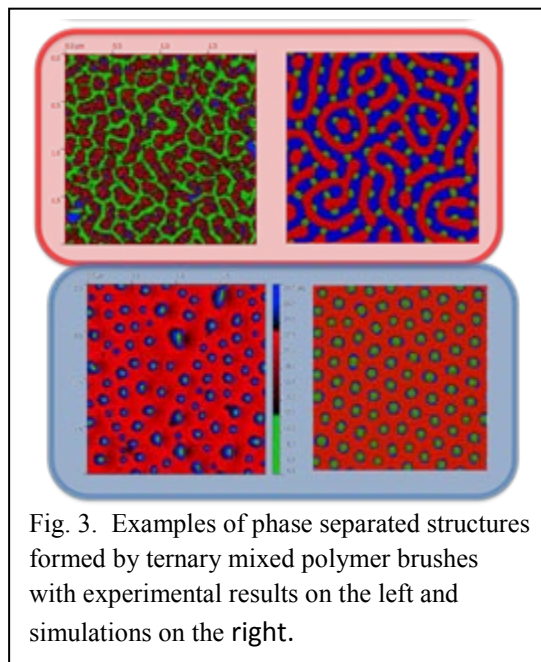


Fig. 3. Examples of phase separated structures formed by ternary mixed polymer brushes with experimental results on the left and simulations on the right.

Multi-component responsive constructs. We are deploying our responsive building blocks in increasingly complex motifs that mimic the sensitive control of cellular behaviors. For example, some lipids in biological structures are known to preferentially move to high curvature regions of membranes. We can mimic this behavior in an artificial system with 200 nm diameter hemispheres rising from an otherwise planar substrate. Artificial lipids have been designed that can be programmed to preferentially move to the high curvature regions of the substrate forming 200 nm domains on a 600 nm square lattice (Fig 4a).⁴

Responsive materials have also been deployed on nanoparticle systems to control the behavior of the nanoparticles. We have developed an alkyl chain functionalized oligo-NIPAM that has temperature responsive phase behavior that we have been investigating both experimentally and through simulation.⁵ These surfactant molecules can form stable coatings on particles without covalent bonding, which simplifies assembly. Coating nanoparticles with these responsive molecules imparts programmable behaviors to the particles yielding reversible changes in plasmon resonance when in solution, and systematic changes in spacing when in superlattices (Figs 4b and 4c).⁶

Future Plans

The project is evolving to create more complex assemblies and structures that can have multiple responsive behaviors. Significant effort has gone into synthesizing magnetic nanoparticles with consistent magnetic properties that will allow us to drive responsive behaviors with magnetic field in addition to temperature and host-guest interactions. Curvature driven sorting of

molecules is also being expanded to systems with programmed changes in curvature. In the medium term we will create appropriate combinations of responsive materials that will allow the multiple applications of force to mimic complex cellular functions like cell division.

Acknowledgements

This research was supported by the Division of Materials Science and Engineering in the Department of Energy Office of Basic Energy Sciences. Sandia National Laboratories is a multi-program laboratory managed and operated by Sandia Corporation, a wholly owned subsidiary of Lockheed Martin Corporation, for the U.S. Department of Energy's National Nuclear Security Administration under contract DE-AC04-94AL85000.

References

1. Vreeland, E. C.; Watt, J.; Schober, G. B.; Hance, B. G.; Austin, M. J.; Price, A. D.; Fellows, B. D.; Monson, T. C.; Hudak, N. S.; Maldonado-Camargo, L.; Bohorquez, A. C.; Rinaldi, C.; Huber, D. L., Enhanced Nanoparticle Size Control by Extending LaMer's Mechanism. In review.
2. Price, A. D.; Hur, S.-M.; Fredrickson, G. H.; Frischknecht, A. L.; Huber, D. L., Exploring Lateral Microphase Separation in Mixed Polymer Brushes by Experiment and Self-Consistent Field Theory Simulations. *Macromolecules* **2012**, *45* (1), 510-524.
3. Simocko, C. K.; Frischknecht, A. L.; Huber, D. L., Nanoscale Phase Separation in Ternary Polymer Brushes. Manuscript in preparation.
4. Ogunyankin, M. O.; Huber, D. L.; Sasaki, D. Y.; Longo, M. L., Nanoscale Patterning of Membrane-Bound Proteins Formed through Curvature-Induced Partitioning of Phase-Specific Receptor Lipids. *Langmuir* **2013**, *29* (20), 6109-6115.
5. Abbott, L. J.; Tucker, A. K.; Stevens, M. J., Single Chain Structure of a Poly(N-isopropylacrylamide) Surfactant in Water. *J. Phys. Chem. B* **2015**, *119* (9), 3837-3845.
6. Li, B.; Smilgies, D. M.; Price, A. D.; Huber, D. L.; Clem, P. G.; Fan, H., Poly(N-isopropylacrylamide) Surfactant-Functionalized Responsive Silver Nanoparticles and Superlattices. *ACS Nano* **2014**, *8* (5), 4799-804.

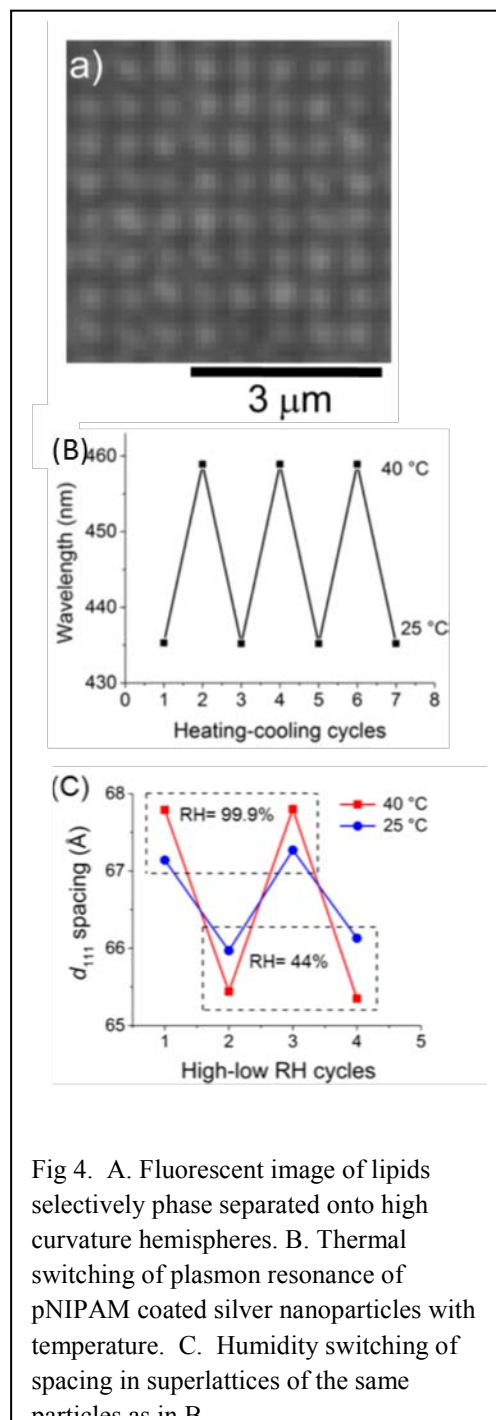


Fig 4. A. Fluorescent image of lipids selectively phase separated onto high curvature hemispheres. B. Thermal switching of plasmon resonance of pNIPAM coated silver nanoparticles with temperature. C. Humidity switching of spacing in superlattices of the same particles as in B.

Publications (2013-2015)

1. Hoppe, S. M.; Sasaki, D. Y.; Kinghorn, A. N.; Hattar, K., In-Situ Transmission Electron Microscopy of Liposomes in an Aqueous Environment. *Langmuir* **2013**, *29* (32), 9958-9961.
2. Monson, T. C.; Ma, Q.; Stevens, T. E.; Lavin, J. M.; Leger, J. L.; Klimov, P. V.; Huber, D. L., Implication of Ligand Choice on Surface Properties, Crystal Structure, and Magnetic Properties of Iron Nanoparticles. *Particle & Particle Systems Characterization* **2013**, *30* (3), 258-265.
3. Monson, T. C.; Rodriguez, M. A.; Leger, J. L.; Stevens, T. E.; Huber, D. L., A simple low-cost synthesis of brookite TiO₂ nanoparticles. *Journal of Materials Research* **2013**, *28* (3), 348-353.
4. Monson, T. C.; Venturini, E. L.; Petkov, V.; Ren, Y.; Lavin, J. M.; Huber, D. L., Large enhancements of magnetic anisotropy in oxide-free iron nanoparticles. *Journal of Magnetism and Magnetic Materials* **2013**, *331*, 156-161.
5. Ogunyankin, M. O.; Huber, D. L.; Sasaki, D. Y.; Longo, M. L., Nanoscale Patterning of Membrane-Bound Proteins Formed through Curvature-Induced Partitioning of Phase-Specific Receptor Lipids. *Langmuir* **2013**, *29* (20), 6109-6115.
6. Price, A. D.; Huber, D. L., Controlled polymer monolayer synthesis by radical transfer to surface immobilized transfer agents. *Polymer Chemistry* **2013**, *4* (5), 1565-1574.
7. Tucker, A. K.; Stevens, M. J., Study of the structure dependent behavior of polyelectrolyte in water. *J Chem Phys* **2013**, *139* (10), 104907.
8. Gilmore, S. F.; Sasaki, D. Y.; Parikh, A. N., Thermal Annealing Triggers Collapse of Biphasic Supported Lipid Bilayers into Multilayer Islands. *Langmuir* **2014**, *30* (17), 4962-4969.
9. Li, B.; Smilgies, D. M.; Price, A. D.; Huber, D. L.; Clem, P. G.; Fan, H., Poly(N-isopropylacrylamide) Surfactant-Functionalized Responsive Silver Nanoparticles and Superlattices. *ACS Nano* **2014**, *8* (5), 4799-804.
10. Abbott, L. J.; Tucker, A. K.; Stevens, M. J., Single Chain Structure of a Poly(N-isopropylacrylamide) Surfactant in Water. *J. Phys. Chem. B* **2015**, *119* (9), 3837-3845.

Solvent Assisted Non Equilibrium Directed Self Assembly of Complex Polymeric Materials

Juan de Pablo, Matt Tirrell, Paul Nealey, Wei Chen
Institute for Molecular Engineering, Argonne National Laboratory

Scope of Work: Our efforts at the Institute of Molecular Engineering at Argonne National Laboratory seek to understand at a fundamental level the solvent and charged-assisted assembly of polymeric materials into ordered functional materials. To that end, we combine synthesis, characterization, and modeling at multiple length scales, in a project that involves biopolymers, including polypeptides and DNA, as well as synthetic materials.

Recent Progress: Over the past year, our groups have made advances in two areas, namely charge-driven directed assembly and solvent-assisted directed assembly. Specifically, our groups at Argonne National Laboratory studied the self-assembly of polyelectrolytes based on naturally occurring peptide molecules, and the solvent-assisted directed assembly of synthetic charged block copolymers on nano-patterned substrates.

Polyelectrolyte complexes present new opportunities for self-assembled soft matter. Factors determining whether the phase of the complex is solid or liquid remain unclear. Naturally occurring ionic polypeptides enable examination of the effects of stereochemistry on complex formation. In our own research, we were able to demonstrate that chirality determines the state of polyelectrolyte complexes, formed from mixing dilute solutions of oppositely charged polypeptides, via a combination of electrostatic and hydrogen-bonding interactions. As illustrated in Figure 1, our groups showed that fluid complexes occur when at least one of the polypeptides in the mixture is racemic, which disrupts backbone hydrogen-bonding networks (Nature Communications, 6, 6052, 2014). In contrast, pairs of purely chiral polypeptides, of any sense, form compact, fibrillar solids with a β -sheet structure. Analogous behaviour occurs in micelles formed from polypeptide block copolymers with polyethylene oxide, where assembly into aggregates with either solid or fluid cores, and eventually into ordered phases at high concentrations, is possible. Overall, our results to date suggest that chirality is an exploitable tool for manipulating material properties in polyelectrolyte complexation.

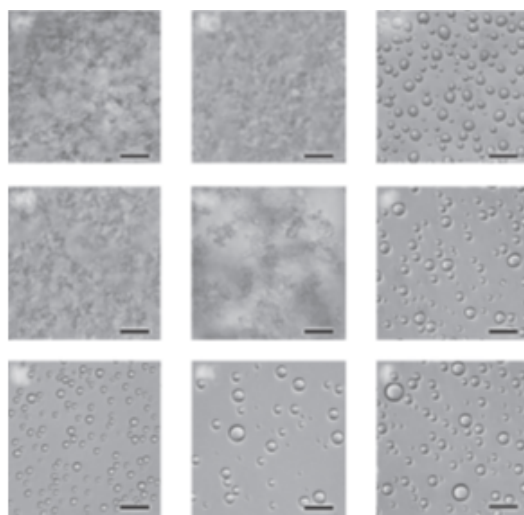


Figure 1 - Optical micrographs of polyelectrolyte complexes. Bright-field optical micrographs showing the liquid coacervates or solid precipitates resulting from the stoichiometric electrostatic complexation of L, D, or racemic (D,L) poly(lysine) with L, D or racemic (D,L) poly(glutamic acid) at a total residue concentration of 6 and 100mM NaCl. Complexes are formed from (a) pLK β pLE, (b) pDK β pLE, (c) p(D,L)K β pLE, (d) pLK β pDE, (e) pDK β pDE, (f) p(D,L)K β pDE, (g) pLK β p(D,L)E, (h) pDK β p(D,L)E, (i) p(D,L)K β p(D,L)E. Liquid coacervate droplets are only observed during complexation involving a racemic polymer. Scale bars, 25 μ m. (from Nat. Comm., 6, 6052, 2014).

Using a combination of experiments and simulations with atomistic models, our groups demonstrated that the polypeptide chirality not only determines the physical state of the resulting polyelectrolyte complexes (that is, liquid or solid), but also defines the strength of intermolecular interactions, and thus the material properties. Simulations of two interacting polypeptides in water, for example, showed that the homochiral poly(lysine) (pLK) and poly-(glutamic acid) (pLE) system rapidly forms a parallel β -sheet in the center of the peptides, which was fully formed after only a few hundred nanoseconds (see Figure 2). This structure remained stable throughout the duration of the simulation. The formation of a stable β -sheet structure allows the peptides to bind more tightly, reducing the centre of mass distance to about 0.2 nm. In contrast, a homochiral poly(lysine) and racemic poly-(glutamic acid) (p(D,L)E) system (Figure 2) formed a less compact structure with a center of mass distance varying between 0.3 and 0.9 nm. These peptides remained in mostly coil, bend and turn conformations, with only rapidly transient β -sheet formation observed for durations of less than 100 ns, and mostly in a region of the glutamic acid peptide where a sequence of three consecutive L amino acids was present. While electrostatic interactions act over long distances, the shorter-range nature of polar hydrogen-bonding forces, combined with steric packing and hydration, provide additional methods for controlling self-assembly.

In addition to chirality, by relying on a fundamental study of DNA-protein charged complexes, our groups were also able to identify additional features that arise in biological polymers such as DNA and that may be used for assembly of new synthetic materials. Specifically, we focused on the study of structure-properties in nucleosomes, which provide the basic unit of compaction in eukaryotic genomes, and on the mechanisms that dictate their position at specific locations along a DNA sequence. By relying on molecular models of DNA and proteins to elucidate various aspects of nucleosome positioning, we discovered that DNA's histone affinity is encoded in its sequence-dependent shape, including subtle deviations from the ideal straight B-DNA form and local variations of minor groove width (Physical Review Letters, 113,168101, 2014). Through high-precision simulations of the free energy of nucleosome complexes, we also demonstrated that, depending on DNA's intrinsic curvature, histone binding can be dominated by bending interactions or electrostatic interactions. The insights provided by our theoretical work suggest that by engineering curvature and charge into

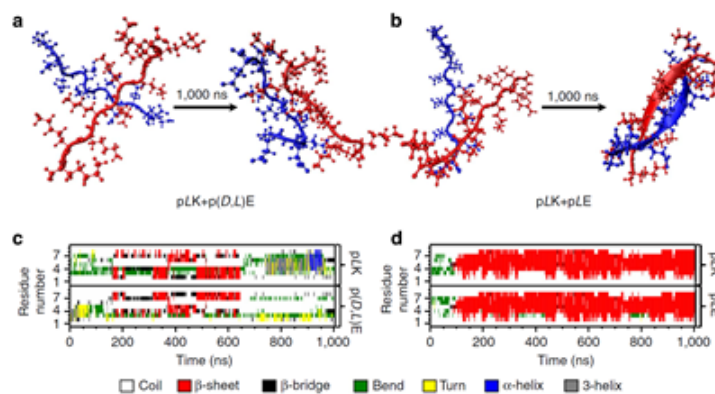


Figure 2 - MD simulations of polyelectrolyte complexes. Visualization and residue maps indicating polypeptide secondary structure from representative MD simulations for two pairs of poly(lysine) and poly(glutamic acid) peptides of ten segments. Polypeptides are initially equilibrated in a random coil conformation and then allowed to complex for 1,000 ns. (a) A representative simulation of homochiral pLK complexing with racemic p(D,L)E indicates preservation of a mostly random coil structure, as would be expected for liquid coacervates, while (b) homochiral polypeptides pLK with pLE shows the evolution of β -strand structure expected for a solid precipitate. Map of secondary structure as a function of time for (c) pLK+p(D,L)E and (d) pLK+pLE (from Nat. Comm., 6, 6052, 2014).

polymeric molecules, it might be possible to arrive at design rules for new classes of composite materials where macromolecules are induced to wrap around nanoscale inclusions in a programmable manner.

On the synthetic polymer front, our efforts have focused on precise control of morphology and orientation in charged, self-assembled materials for applications in energy storage, separations, and energy harvesting, to name a few. The challenge here is that connecting micro-structure and morphology to bulk transport properties, like ionic conductivity, in polymer electrolytes is a difficult proposition because it is difficult to achieve precise and accurate control of orientation of the ionic domains in polymer electrolyte films. Achieving such precise and accurate control of the morphology of polymer electrolyte is postulated for maximizing ionic conductivity and achieving anisotropic ion transport within these materials and could have broad application to a variety of electrochemical technologies such as miniaturized supercapacitors and capacitive electrodeionization for low energy water purification. As illustrated in Figure 3, in our work we have registered poly(styrene-*block*-2-vinyl pyridine) block copolymers (PSbP2VP) perpendicular to a substrate surface over large areas through the control of the interfacial energies and utilizing a versatile solvent vapor annealing technique. After block copolymer assembly, a simple chemical vapor deposition technique selectively converted the 2-vinyl pyridine block (2VP) to 2-vinyl n-methyl pyridinium groups (2VNMP⁺) – which are anion charge carriers. The prepared block copolymer electrolytes maintained their orientation and ordered nanostructure upon the selective introduction of ion moieties into the P2VP block and upon ion-exchange to other counterion forms (e.g., chloride for water treatment and hydroxide ions for alkaline electrochemical energy storage and conversion technologies). The prepared block copolymer electrolyte films demonstrated remarkably high chloride ion conductivities – over 40 mS cm⁻¹ at 20 °C. Straight line lamellae of block copolymer electrolytes was realized using chemoepitaxy and density multiplication on chemical patterns.

More generally, it is important to

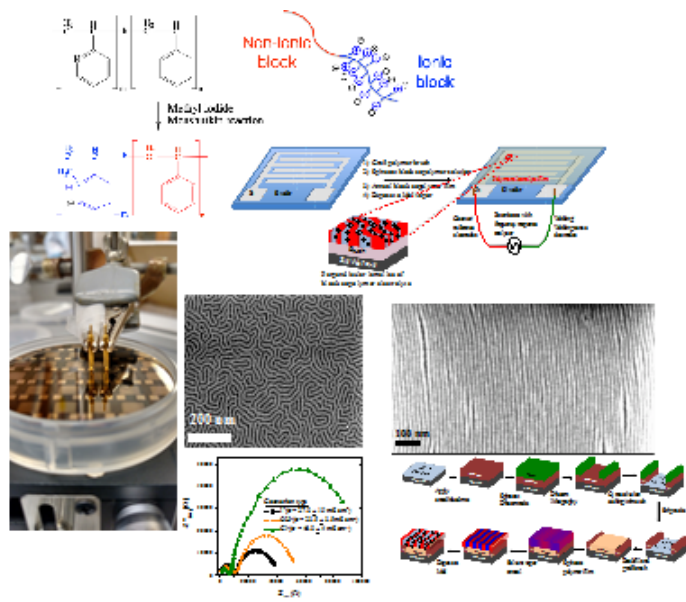


Figure 3 - Selected images from manuscript in preparation. At the top, the chemical structure of the block copolymer before and after introduction of ionic groups. Interdigitated electrode structures containing thin-film polymer electrolytes. Light colored domains in SEM images represent the ion-containing block while the dark colored domains represent polystyrene. The images represent phase-separated ionic domains from non-ionic domains. Both blocks in the block copolymer were registered perpendicular to the substrate surface. Nyquist plot was from electrochemical impedance spectroscopy performed on the block polymer electrolyte film in the iodide, chloride, and hydroxide ion forms. Finally, chemical patterns were used for the directed self-assembly of block copolymer electrolytes (lower right hand corner).

emphasize that the results described above could not have been realized without resorting to solvent-assisted assembly strategies. Indeed, solvent annealing is known to provide an effective means to control the self-assembly of block copolymer (BCP) thin films. Multiple effects, including swelling, shrinkage, and morphological transitions, act in concert to yield ordered or disordered structures. The current understanding of these processes, however, is limited; by relying on a theoretically informed coarse-grained model of block copolymers, depicted schematically in Figure 4, our groups developed a conceptual framework that permits prediction and rationalization of experimentally observed behaviors. Through proper selection of several process conditions, we were able to demonstrate that a narrow window of solvent pressures exists over which one can direct a BCP material to form well-ordered, defect-free structures (ACS Macro Letters, 4, 11, **2015**).

Future Plans: The effects we have identified in this project raise obvious follow-on questions about the effects of sequence distribution within globally achiral polymers or designed effects that can be created by tailoring sequences of chiral peptides, which we are now pursuing. While sequence specificity in biology controls the three-dimensional assembly of proteins, we propose that patterns of chirality could have significant implications for tailoring of material properties without otherwise altering the chemical composition of polypeptide-based materials. For instance, this type of control could be utilized to tailor the rheological response of bulk materials and formulate delivery systems with controlled water content. Furthermore, coupling this type of polar and electrostatically guided self-assembly with more complex molecular architectures, as in the block copolymer systems considered in our research, enables the creation of interesting classes of new materials with novel self-assembling structures, functionality and responsiveness. Note, too, that while our studies help clarify the role of chirality on phase selection in complexes of charged polypeptides, other polyelectrolyte complex systems also form both solid and fluid phases. We suggest that the causes of solid phase formation in polyelectrolyte complexes are to be found in short-range forces, which may be influenced by tacticity, hydration packing and other factors, acting in concert with longer range electrostatic forces.

The patterning and assembly techniques developed in this work for synthetic polymers are now being extended to a variety of other projects: i.) controlling the orientation of ionic domains in cation conducting block copolymer electrolytes (i.e., use of poly(styrene-*block*-tert-butyl acrylate), where the tert-butyl protective group is cleaved to make acrylic acid moieties after assembling the block copolymer), ii.) comparing the anionic conductivity of PSbP2VNMP⁺ of different morphologies (i.e., parallel lamellae versus perpendicular lamellae versus in-plane cylinders versus perpendicular cylinders) and iii.) bridging the ionic domains in PSbP2VNMP⁺ perpendicular lamellae directly between two gold electrodes using a graphoepitaxy process (i.e., straight-line lamellae that yields a tortuous pathway of one). We anticipate that these approaches will improve ion conductivity in polymer electrolytes for energy conversion and storage devices and water treatment and be useful as an analytical platform for fundamental studies aimed at connecting how polymer electrolyte architecture influences ion transport in such materials.

On the modeling front, we are actively pursuing detailed studies of defect formation and elimination in directed assembly, as well as sophisticated treatments of solvent and electrostatic

interactions in order to arrive at a complete description of the non-equilibrium processes that arise in solvent-assisted charge-driven polymer complexation.

Publications Over Past Year (2014-2015)

1. Freeman, G.S., Lequieu, J.P., Hinckley, D.M., Whitmer, J.K. and de Pablo, J.J. (2014) DNA Shape Dominates Sequence Affinity in Nucleosome Formation. *Physical Review Letters*, **113**, 168101.
2. Jung, I. H.; Lo, W.-Y.; Jang, J.; Chen, W.; Zhao, D.; Landry, E. S.; Lu, L.; Talapin, D. V.; Yu L. "Synthesis and Search for Design Principles of New Electron Accepting Polymers for All-Polymer Solar Cells", *Chem. Mater.* 2014, 26, 3450–3459.
3. Li, W., Nealey, P.F., de Pablo, J.J. and Mueller, M. (2014) Defect Removal in the Course of Directed Self-Assembly is Facilitated in the Vicinity of the Order-Disorder Transition. *Physical Review Letters*, **113**.
4. Whitmer, J.K., Chiu, C.-c., Joshi, A.A. and de Pablo, J.J. (2014) Basis Function Sampling: A New Paradigm for Material Property Computation. *Physical Review Letters*, **113**, 168301.
5. Onses, M.S., Ramirez-Hernandez, A., Hur, S.-M., Sutanto, E., Williamson, L., Alleyne, A.G., Nealey, P.F., de Pablo, J.J. and Rogers, J.A. (2014) Block Copolymer Assembly on Nanoscale Patterns of Polymer Brushes Formed by Electrohydrodynamic Jet Printing. *Acs Nano*, **8**, 6606-6613.
6. Priftis, D., Xia, X., Margossian, K.O., Perry, S.L., Leon, L., Qin, J., de Pablo, J.J. and Tirrell, M. (2014) Ternary, Tunable Polyelectrolyte Complex Fluids Driven by Complex Coacervation. *Macromolecules*, **47**, 3076-3085.
7. Qin, J., Priftis, D., Farina, R., Perry, S.L., Leon, L., Whitmer, J., Hoffmann, K., Tirrell, M. and de Pablo, J.J. (2014) Interfacial Tension of Polyelectrolyte Complex Coacervate Phases. *Acs Macro Letters*, **3**, 565-568.
8. Ramirez-Hernandez, A., Suh, H.S., Nealey, P.F. and de Pablo, J.J. (2014) Control of Directed Self-Assembly in Block Polymers by Polymeric Topcoats. *Macromolecules*, **47**, 3520-3527.
9. Hur, S.-M., Khaira, G.S., Ramírez-Hernández, A., Müller, M., Nealey, P.F. and de Pablo, J.J. (2015) Solvent-assisted directed self-assembly of block copolymer films *ACS Macro Letters*, **4**, 11-15.
10. D. Priftis , X. Xia, K. O. Margossian, S. L. Perry, L. Leon, J. Qin, J. J. de Pablo and M. Tirrell, Ternary, Tunable Polyelectrolyte Complex Fluids Driven by Complex Coacervation, *Macromolecules*, **47**, 3076–3085 (2014).
11. Perry, Sarah L.; Li, Yue; Priftis, Dimitrios; et al. The Effect of Salt on the Complex Coacervation of Vinyl Polyelectrolytes, *Polymers*, **6**, 1756-1772 (2014).

12. Perry, Sarah L.; Li, Yue; Priftis, Dimitrios; et al. *Polymers* **2014**, *6*(6), 1756-1772; doi:[10.3390/polym6061756](https://doi.org/10.3390/polym6061756) -
13. S. L. Perry, L. Leon, K. Q. Hoffmann, M. J. Kade, D. Priftis, K. A. Black, D. Wong, R. A. Klein, C. F. Pierce III, K. O. Margossian, J. K. Whitmer, J. Qin, J. J. de Pablo, M. Tirrell, Chirality-selected phase behavior in ionic polypeptide complexes, *Nature Comm*, **6**, 6052 | DOI: 10.1038/ncomms7052 (2015).
14. Yang, Y.; Chen, W.; Dou, L.; Chang, W.-H.; Duan, H.-S.; Bob, B.; Li, G.; Yang, Y. “Molecular Compatibility Enabling High-Performance Multiple Donor Bulk Heterojunction Solar Cells”, Nat. Photon. Advance Online Publication (AOP) on Feb 9, 2015.
15. Lu, L.; Xu, T.; Chen, W.; Landry, E. S.; Yu, Y. “Ternary Blend Polymer Solar Cells with Power Conversion Efficiency of 8.22%”, Nat. Photon. 2014, *8*, 716-722.
16. Shao, M.; Keum, J.; Chen, J. H.; He, Y. J.; Chen, W.; Browning, J. F.; Jakowski, J.; Sumpter, B. G.; Ivanov, I. N.; Ma, Y. Z.; Rouleau, C. M.; Smith, S. C.; Geohagan, D. B.; Hong, K. L.; Xiao, K. “The isotopic effects of deuteration on optoelectronic properties of conducting polymers”, Nat. Commun. 2014, *5*, 4180.
17. Gao, J.; Chen, W.; Dou, L.; Chen, C.-C.; Chang, W.-H.; Liu, Y.; Li, G.; Yang, Y. “Elucidating Double Aggregation Mechanisms in the Morphology Optimization of Diketopyrrolopyrrole-Based Narrow Bandgap Polymer Solar Cells”. *Adv. Mater.* 2014, *26*, 3142–3147.
18. Gao, J.; Dou, L.; Chen, W.; Chen, C.-C.; Guo, X.; You, J.; Bob, B.; Chang, W.-H.; Strzalka, J.; Wang, C.; Li, G.; Yang, Y. “Improving Structural Order for a High-Performance Diketopyrrolopyrrole-Based Polymer Solar Cell with a Thick Active Layer”. *Adv. Energy Mater.* 2014, *4*, 1300739.
19. Wen, J.; Miller, D. J.; Zaluzec, N. J. Chen, W.; Darling, S. B.; Xu, T.; He, F.; Yu L. “Direct Visualization of Hierarchical Nanomorphologies in Polymer-Fullerene Bulk Heterojunction Solar Cells Using Chromatic Aberration-Corrected Transmission Electron Microscopy”, *Microscopy and Microanalysis* 2014, *20*, 1507-1513.

Self-healing and Self-regulating Bio-inspired Materials

Seb Doniach, Sarah Heilshorn, Nick Melosh, Andy Spakowitz

SLAC National Accelerator Laboratory and Stanford University

Program Scope

The focus of this multi-disciplinary research program is to characterize and exploit the tailored molecular interactions inherent in biological systems. Such understanding will enable engineering of responsive, biomimetic materials that exhibit self-healing and self-regulating transformations. These materials will lead to fundamentally new designs in biomimetic organic/inorganic devices for energy storage, catalysis, solar cells, and fuel cells. The team integrates a wide range of experimental and theoretical approaches to assemble, characterize, and model dynamic assembly. Our recent collaborative effort has focused on experimental and theoretical insights into the fundamentals of biomimetic self-assembly in two and three dimensions, including the development of an Artificial Clathrin Mimetic system that exhibits many of the properties and behaviors of natural clathrin. Furthermore, we are investigating the effects of local topological transformations on the structure and dynamics of supercoiled DNA in order to develop a DNA-based system with novel nanoscale behavior that can assemble responsive materials. Our team is developing novel synthesis and characterization strategies to enable the creation and analysis of our biomimetic materials, including the development of advanced x-ray characterization techniques for atomic scale resolution of biomimetic materials with local order but disorder at large length scales.

Recent Progress

Clathrin templates to direct nanoparticle clustering and bimetallic composites. We previously reported the functionalization of self-assembled clathrin protein cages to enable synthesis of nanoparticles from a range of inorganic materials. Recently, we investigated the ability of this engineered biomolecular complex to act as a tunable nanoreactor for the formation of different arrangements of gold nanoparticles in 3D. We found that self-assembled clathrin cages functionalized with engineered bi-functional peptides induced formation of gold nanoparticles to generate solutions of either dispersed or clustered gold nanoparticles on demand. The 3D arrangement of nanoparticles is dependent on the concentration of the engineered peptide, which fulfills multiple roles in the synthesis process including stabilization of the nanoparticle surface and localization of the nanoparticles within the self-assembled clathrin cage. We proposed and experimentally verified a mechanism that allows us to predict the peptide concentration at which the nanoreactor behavior switches, **Fig. 1**. This work provides insight into peptide-based

surfactants and the potential for incorporating them into strategies for tuning biological templating processes in mild solution conditions to generate complex structures.

A biomimetic system for 2-dimensional assembly of multi-functional subunits. Our FWP has built a platform system that can leverage the insights learned from the clathrin system, but with more control over geometry and more amenable to fabrication of larger yields. In particular, we have created “Artificial Clathrin Mimetics” (ACMs) out of thin metal structures with several of the characteristics of clathrin (3-armed legs, localized binding sites, propensity to attach to 2D interfaces) in order to reproduce the dynamic assembly and sampling behavior of native clathrin. By selective functionalization of the ACM faces, we can order them onto fluid 2D air-water interfaces and manipulate their self-assembly structurally and chemically. These particles have been fabricated as micron-sized structural analogues of clathrin, with their self-assembling behavior visualized by optical microscopy at liquid-air interfaces. This general class of behaviors could recreate one of the most advanced and dynamic processes in biology, and would open up an entirely new, micron scale sampling and assembly method.

Theoretical modeling of clathrin structure and responsive transformations. Theoretical efforts in the project have developed a predictive theoretical model for the structure and dynamics of clathrin to establish responsive nanoscale assemblies. Our modeling of clathrin structural transformations led to new insight into the pivotal role of topological transformations within protein networks in dictating large-scale structural transitions. Our recent work in modeling the bud formation in clathrin was featured on the cover the *Soft Matter* in January 2015. The clathrin subunit is modeled as a three-legged pinwheel with elastic deformation modes and inter-subunit binding interactions, **Fig. 2**. The pinwheels are constrained to lie on the surface of an elastic sheet that opposes bending deformation and is subjected to tension. Through Monte Carlo simulations, we predicted the equilibrium phase behavior of clathrin lattices at various levels of tension, predicting the conditions where the lattice exhibits solid and fluid phases. These results provided an approach for collective changes in assembly behavior from subtle environmental cues. We then addressed the impact of local nanoscale indentations in modulating the local phase behavior of the clathrin lattices. Our work provides a basis for utilizing local deformations in triggering 3-dimensional vesicle budding from reorganization of 2-dimensional clathrin lattices.

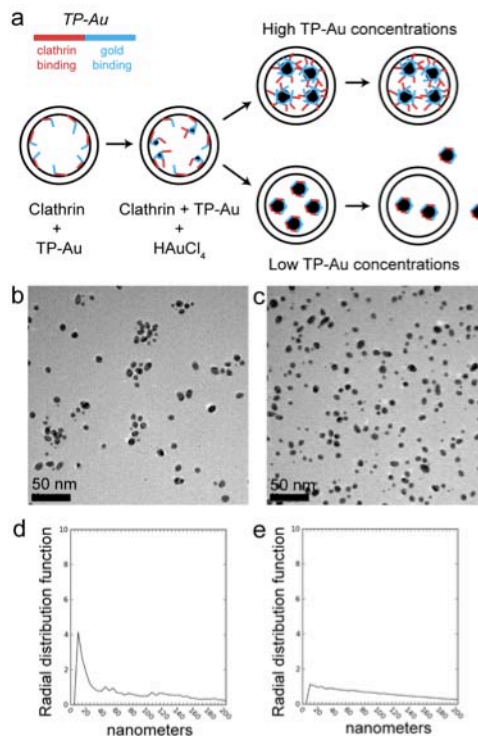


Figure 1. a) Schematic of potential particle growth mechanism in the case of high TP-Au peptide concentration (top) or low peptide concentration (bottom). (b, c) TEM micrographs of gold nanoparticle synthesis reactions containing clathrin cages and 67.6 mM (b) or 33.8 mM (c) TP-Au peptide. (d, e) Radial distribution function analysis of TEM data, indicating the degree of clustering present in panels (b) and (c), respectively.

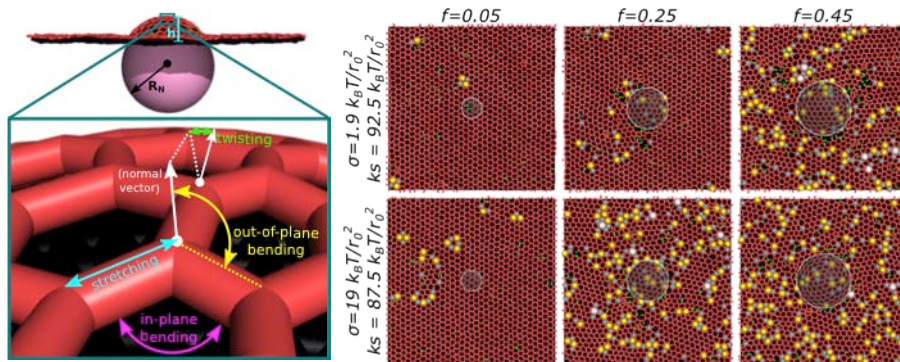


Figure 2. Left, our model of clathrin on a fluctuating membrane that subjected to a nanoscale indentation. Right, Monte Carlo simulations reveal a physical mechanism where local curvature induces a phase transition to a fluid phase, resulting in a responsive lattice that is able to form local 3D budding indentations on the membrane.

Ongoing work involves direct comparison of the theoretical predictions with experimental measurements. To complement our work on clathrin, we are currently developing a DNA-based system that utilizes local topological changes to trigger structural transformations. This system will be used to create novel structures at the nanoscale, and incorporating such structures into 2D membranes and 3D gels will result in materials that exhibit large-scale structural changes in response to local dynamic transformations. Double-stranded DNA behavior is strongly influenced by two topological contributions: twist-induced supercoiling and knotting. We have developed a new approach to modeling proteins and nucleic acids that permits us to predict behavior over a range of length and time scales that were previously inaccessible. Furthermore, our new model permits the efficient evaluation of topological quantities associated with supercoiling and knotting. Our theoretical model shows good agreement with the measured structure of supercoiled DNA from dynamic light scattering, and we are currently preparing a manuscript that elucidates the progression of structural transformations in supercoiled DNA.

A breakthrough in X-ray science: Correlated X-ray Scattering of nano and soft materials.

Tools to study disordered systems with local structural order, such as proteins in solution, remain limited. Such understanding is essential for determining molecular structure of biopolymer materials that are locally ordered but disordered at large length scales. Use of Correlated X-ray Scattering (CXS) to study molecular structure was proposed theoretically by Kam in 1977.¹ The advent of improved X-ray sources and detectors since that time has led to the experimental feasibility of this structural technique. Correlated X-ray scattering (CXS) has recently attracted new interest as a way to leverage next-generation light sources to study such disordered matter. The CXS experiment measures angular correlations of the intensity caused by the scattering of X-rays from an ensemble of identical, internally structured particles with disordered orientation and position. The Doniach lab has recently achieved a breakthrough in X-ray science by demonstrating for the first time the feasibility of CXS to obtain structural information at atomic resolution for disordered systems of ordered objects, **Fig. 3**. In our publication, we report on experimental work in which CXS signals were obtained for an ensemble of 20 nm silver nanoparticles in three dimensions. We averaged over 15,496 snapshot X-ray images obtained by exposing a series of samples of silver nanoparticles in solution to a micro-focused synchrotron radiation beam. Of order 10^9 particles were exposed to the X-ray beam in each shot. Angular correlations were measured at wide angles corresponding to atomic resolution and were shown to

match theoretical predictions. Recent data acquisition has been obtained on a series of DNA samples with varying topological properties. Data analysis and interpretation is currently underway and will be directly compared with the theoretical models described above.

Future Plans

One of the most exciting goals for the next year is fully recreating the ‘sampling’ of extracellular contents that clathrin normally performs in the cell. This would create truly advanced biomimetic behavior that could eventually be leveraged for continuous fluidic monitoring, non-destructive single-cell sampling, and self-healing structures. By changing the shape and functionalization of the ACM particles, we aim to mechanically control the underlying lipid support in a similar way to clathrin. We also aim to use the surface properties of these particles to localize secondary, non-membrane-interacting structures to the membrane-assembling particles. These secondary self-assembled structures would allow us to add additional functionality to the clathrin mimicking particles, and recreate interesting biophysical functionality. Theoretically, we will establish a predictive model for a biomimetic clathrin system that spontaneously assembles at an interface. Our efforts in modeling correlated X-ray scattering (CXS) will be used to determine dynamic DNA structural properties ranging from 1 to 100 nanometers. Models are currently being compared with experimental data sets obtained at the free-electron laser at SACLA (Japan). These efforts will be used as a structural characterization of supercoiled DNA, which will aid in the development of DNA-based, responsive materials that utilize local topological changes to elicit large-scale structural changes. We plan to study the effects of topoisomerases on the conformations of DNA plasmids using CXS. This will provide a direct measure of the degree of supercoiling of the DNA as a function of the degree of winding of the DNA by various topoisomerase enzymes. We have performed simulations of the CXS expected from DNA and expect to use these as a template for analysis of experimental data acquired in the coming 1-2 years. These data will inform our design of a DNA-based material composed of interconnected rings of DNA. Introducing local topological changes of the DNA supercoiling will result in large-scale changes in material shape and rheological properties.

References 1. Z. Kam. *Macromolecules*, 1977, 10(5): 927-934.

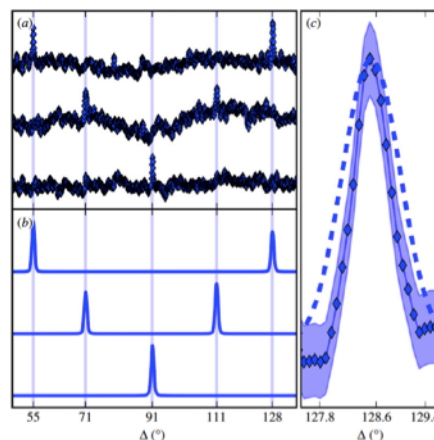


Figure 3. (a) From top to bottom, measured correlation functions $D(q_{111}, q_{200}, D)$, $D(q_{111}, q_{111}, D)$ and $D(q_{200}, q_{200}, D)$ from 20 nm silver NPs. The angular range is truncated to highlight the correlation peaks. Regions not shown contain similar artifacts, with nothing greater in magnitude than the CXS peaks. (b) Corresponding simulations of the correlations plotted in (a). Vertical lines mark analytical predictions. (c) Simulation (dashed line) and measurement (diamond marker) of a correlation peak width. Peak width scales inversely with particle size, hence we expect the measured CXS resulted from particles larger than 20 nm. Shading represents 95% confidence intervals.

Publications

Peer-Reviewed Journal Articles - Fully Supported by this FWP

1. J.J. VanDersarl, S. Mehraeen, A.P. Schoen, S.C. Heilshorn, A.J. Spakowitz, N.A. Melosh. "Rheology and simulation of 2-dimensional clathrin protein network assembly." *Soft Matter*, 2014, 10(33): 6219-6227.
2. N. Cordella, T.J. Lampo, S. Mehraeen, A.J. Spakowitz. "Membrane fluctuations destabilize clathrin protein lattice order." *Biophysical Journal*, 2014, 106(7): 1476-1488.
3. K.N.L. Huggins, A.P. Schoen, M.A. Arunagirinathan, S.C. Heilshorn. "Multi-site functionalization of protein scaffolds for bimetallic nanoparticle templating." *Advanced Functional Materials*, 2014, 24(48): 7737-7744.
4. N. Cordella, T. Lampo, N. Melosh, A.J. Spakowitz. "Membrane indentation triggers clathrin lattice reorganization and fluidization." *Soft Matter*, 2015, 11(3): 439-448.
5. A.P. Schoen, K.N.L. Huggins, S.C. Heilshorn. "Engineered clathrin nanoreactors provide tunable control over gold nanoparticle synthesis and clustering." *Journal of Materials Chemistry B*, 2013, 1:6662-6669.
6. A.P. Schoen, N. Cordella, S. Mehraeen, M.A. Arunagirinathan, A.J. Spakowitz, S.C. Heilshorn. "Dynamic remodeling of disordered protein aggregates is an alternative pathway to achieve robust self-assembly of nanostructures." *Soft Matter*, 2013, 9(38): 9137-9145.

Peer-Reviewed Journal Articles - Partial FWP Support

7. S.A. Mollinger, B.A. Krajina, R. Noriega, A. Salleo, A.J. Spakowitz. "Percolation, tie-molecules, and the microstructural determinants of charge transport in semicrystalline conjugated polymers." *Macro Letters*, 2015, 4:708-712.
8. D. Mendez, T.J. Lane, J. Sung, J. Sellberg, C. Levard, H. Watkins, A.E. Cohen, M. Soltis, S. Sutton, J. Spudich, V. Pande, D. Ratner, S. Doniach. "Observation of correlated X-ray scattering at atomic resolution." *Philosophical Transactions of the Royal Society B*, 2014, 369(1647):20130315.
9. S.H. Hong, E. Toro, K.I. Mortensen, M.A. Díaz de la Rosa, S. Doniach, L. Shapiro, A.J. Spakowitz, H.H. McAdams. "Caulobacter chromosome in vivo configuration matches model predictions for a supercoiled polymer in a cell-like confinement." *Proceedings of the National Academy of Sciences USA*, 2013, 110(5):1674-1679.

Bioinspired Materials

PIs: Surya Mallapragada, Mufit Akinc, David Vaknin, Marit Nilsen-Hamilton, Alex Travesset, Wenjie Wang, Ruslan Prozorov and Tanya Prozorov, Ames Laboratory; Dennis Bazylinski, Univ. Nevada Las Vegas

Mailing Address: Division of Materials Sci. and Eng., Ames Laboratory, Ames, IA 50011

Email: suryakm@iastate.edu

Program Scope: Nature is replete with hierarchically assembled hybrid materials where their multi-scale structures confer unique properties and functions. This FWP uses organic and biological templates as seen in nature to control the growth of inorganic/metallic phases to form hierarchically self-assembled functional nanocomposite materials for energy relevant systems. The interdisciplinary FWP team has successfully demonstrated the value of an integrated experimental approach guided by computational work for room-temperature synthesis of a variety of bioinspired nanostructures materials *in vitro*, including hydroxyapatite, zirconia and complex magnetic nanocrystals, mimicking natural systems such as bone and magnetotactic bacteria to recreate such structures *in vitro*, both in bulk and at the surface. Solid-state NMR, advanced X-ray and neutron scattering methods, and *in situ* fluid cell transmission electron microscopy (TEM), have been coupled with molecular biology techniques to elucidate the hierarchical assembly in these nanocomposites and understand the role of biomolecules in facilitating mineralization. Experimental techniques were complemented by the development of advanced high performance computational methods to model the dynamics and thermodynamics of the self-assembly processes at the nanoscale and to guide the experimental efforts. Future work in this FWP will move “beyond” nature and use bioinspired approaches and biological templates to synthesize systems not found in living organisms. Taking advantage of our ability to manipulate nanoscale particles into self-assembled architectures with spatial control over multiple length scales, we are now at the point where we can target function using bioinspired approaches. We now plan to create “use-inspired” functional tailored metamaterials to illustrate targeting function and, to directly address DOE’s Grand Challenge #3, which is to orchestrate atomic and electronic constituents to control material properties.

Recent Progress: Research in this FWP has focused on the development of hierarchically self-assembling block copolymer templates coupled with biological molecules to form nanocrystals and self-assembling nanocomposites. This approach has been demonstrated successfully for the synthesis and assembly of nanocrystals of different inorganic phases such as magnetite and zirconia, using natural systems such as bone and magnetotactic bacteria as inspiration to recreate structures and nanocomposites found in nature. We have also investigated the role of biomolecules such as the protein Mms6 that facilitate the mineralization process. We have used these bioinspired approaches to create mesoporous zirconia with large surface areas and enhanced thermal stability under mild conditions in aqueous solutions. Building on our successes, we have expanded our efforts to include the synthesis of complex magnetic nanoparticles not found in nature in living organisms, such as gadolinium-doped magnetite, and have focused on moving from bulk synthesis to synthesis on patterned surfaces, allowing for control over formation and placement of nanocrystals on a surface. The use of complementary DNA strands to link proteins to polymers confers reversibility, to allow dynamic processes, and is being guided by our own computational studies of programmed DNA-mediated self-assembly. Our simulations have also focused on templated self-assembly in the presence of nanoparticles to guide experiments. The key results are summarized below.

Templated nanocrystal synthesis and assembly: A family of tri- and pentablock copolymers that self-assemble at different length scales to form nanoscale micelles and macroscale gels/solids was synthesized and used as templates for mineralization in conjunction with biomolecules. We published the first report of mesoporous zirconia synthesized in completely aqueous media with biomolecules conjugated to these polymer templates. Cationic pentablock copolymers designed and synthesized in our FWP were found to replace cationic proteins and serve as effective templating agents. Mesoporous zirconia synthesized with these copolymer templates showed the highest surface area and improved thermal stability up to 900°C, which is crucial for applications such as in solid oxide fuel cells. This shows that an understanding of the role of the mineralization proteins can enable the design of effective robust synthetic analogues of the mineralization biomolecules. Using these self-assembling polymers and a similar bioinspired room-temperature approach, we have created nanostructured magnetic materials *in vitro* using the mineralization protein, Mms6. The protein, found in the magnetotactic bacteria, promotes shape-specific magnetite nanocrystal growth. Using this protein, we have synthesized and characterized magnetic properties of magnetite nanocrystals similar to those found in nature, but also and Gd-doped materials at mild room-temperature conditions, not occurring naturally in living organisms. We were able to influence the magnetosome magnetite biomineralization in bacteria to produce Mn-doped magnetosome magnetite nanocrystals with novel magnetic properties.

Our results suggest that Mms6 undergoes a slow structural change as it organizes iron and that catalysis is part of the Mms6 mechanism for assembling magnetite nanocrystals, as it exhibits ferric reductase activity in aerobic aqueous solution. Besides Mms6, we are investigating other mineralization proteins, found in strains of magnetotactic bacteria that produce magnetic nanocrystals with various morphologies, such as bullet-shaped nanocrystals etc.

Methods development and characterization: We have developed new solid-state NMR, *in situ* TEM and scattering methods to characterize the bioinspired products, as well as to probe the mechanisms of self-assembly and mineralization. We have systematically established solid-state NMR as a tool for characterizing these hierarchically assembled nanocomposites. We have also collaborated with the *Emerging Atomic and Magnetic Structures* FWP (Early Career Project) to use *in situ* fluid cell scanning TEM methods to directly visualize the biomimetic iron oxide nucleation mediated by Mms6. We have developed surface sensitive synchrotron X-ray reflectivity (XR), fluorescence near total reflection (XFNTR), and grazing incidence X-ray diffraction (GIXD) techniques to determine the accumulation of ferric iron Fe (III) or ferrous iron Fe (II) at templates formed by the protein Mms6. Small-angle (X-ray and neutron) scattering studies, carried out at DOE national research

facilities (Advanced Photon Source and High Flux Isotope Reactor), provided 3D colloidal structural information for Mms6 in the bulk at a length scale over 1-100 nm. The micellar characteristics of Mms6 as an amphiphilic macromolecule was verified in the SAXS experiments as it exhibited a core-shell structure. The iron

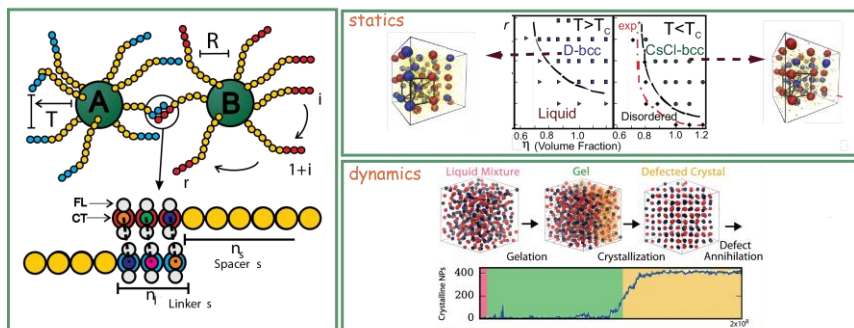


Fig. 1:(Left) Coarse-grained model for DNA programmed self-assembly. (Left Top) Phase diagram for $T > T_m$ and $T < T_m$ as a function of r number of grafted ssDNA strands and volume fraction (Left Bottom) Number of solid particles as a function of time

ions in the bulk induced protein organization, forming a precursor for magnetite formation. We have identified the high affinity iron binding site on Mms6 from alanine scanning experiments.

Computational studies of phase behavior and self-assembly: The experimental studies are being complemented with predictive theoretical studies that involve coarse-grained molecular dynamics simulations of block copolymer assembly and templating, and programmed DNA self-assembly of inorganic nanoparticles. This work will also help guide the future directions of the project involving DNA templates and self-assembling biomolecular templates. We have already demonstrated ways to synthesize nanostructured inorganic materials and control their placement in an organic matrix through self-assembly in the bulk, and on surfaces. Immobilizing and patterning the Mms6 on hydrophobic surfaces (such as octadecanethiol (ODT) monolayers on gold) using reversible or irreversible linkages, provides an opportunity to create localized assemblies of magnetic nanocrystals on patterned surfaces. Computational studies are guiding experimental design. We have provided a theoretical understanding for the complementary DNA-based experiments, predicting a new class of materials in which nanoparticles are linked by hybridized grafted single-stranded DNA (ssDNA) attached to hydrophobic blocks. The computational work also has focused on developing methods to simulate the self-assembly of nanocomponents into mesoscale structures. To date, work has been focused on two complementary methods, Self-Assembly Simulations (SAS) and Free Energy Calculations (FEC). SAS consists of an initial random configuration that evolves in molecular dynamics using the HOOMD-blue (Highly Optimized Object-oriented Many-particle Dynamics) code, pioneered by our FWP and used widely by many BES funded efforts and others. These methods provide a rigorous description of the dynamics and characterization of the equilibrium phase free of bias. FEC provides the free energy of the system for a given crystal structure. These methods have been applied with great success to various systems as described here.

Free energy methods have used our recently developed HOODLT, (software that enables the calculation of all thermodynamical parameters within Dynamical Lattice Theory (DLT) developed by our FWP). A comparison between the excess free energies of an inverse $p = 6$ potential calculated within DLT and using the Einstein crystal integration (ECTI) shows that the error is less than 0.2% for bcc and even less for fcc. The quadratic approximation obtained from HOODLT can be scripted to run in HOOMD. The phase diagram of a binary system of NPs with different diameters has been characterized for a system of soft particles interacting with a given potential. The relevance of the work is that it enables us to go beyond hard-sphere systems, whose well known phase diagrams do not successfully describe experimental results. The coarse-grained system models NPs as rigid bodies and ssDNA with beads and springs, with additional interactions for complementary ssDNA strands. Not only are the simulations in complete agreement with existing experimental data, (red dashed lines in **Fig. 1**) and additional studies on the dynamics from other groups, but also they contain new predictions on both dynamics and equilibrium with dynamics characterized by four stages: Liquid Mixture \rightarrow Gel \rightarrow Defected Crystal \rightarrow Equilibrium. The gel stage, which plays a crucial role in the dynamics, is absent if DNA is described implicitly (as done in most previous models). Below the DNA melting transition, MD converges to equilibrium only over a narrow temperature range, related to the cooperativity in the hybridization process. This limitation in the range of temperatures where equilibration occurs is also observed in experiments, enhancing the model reliability. Subsequent work has focused on the self-assembly of nanocubes. The phases for standard hybridization are in complete agreement with experiment. The computational demands for the calculations are significant, and made possible by the use of

graphics processing units (GPUs). Our FWP pioneered the use of GPUs in MD simulations and developed the first MD code that runs entirely on GPUs, HOOMD (now HOOMD-blue). The software is freely available under an open source license from Ames Laboratory with over three thousand users. Scripts of all our simulations are available to the broad community.

Future Plans: The ability to synthesize and self-assemble a variety of uniform nanostructures under ambient synthesis conditions in the bulk and on surfaces through the use of biomimetic approaches involving self-assembling polymers and biomolecules, opens up new possibilities for extending these approaches to the synthesis of functional metamaterials. Metamaterials are tailored man-made assemblies composed of sub-wavelength metallic building blocks that are densely packed into an effective material. We propose to develop bioinspired bottom-up synthesis approaches where biological macromolecules serve as templates for metallization to create nanoscale structures and to provide options for higher-level 2D and 3D mesoscale organization and alignment. These approaches can potentially overcome the challenges involved in creating functional metamaterials. Long a unique strength of Ames Laboratory, metamaterials provide an ideal example of synergistic use-inspired focus and targeting of function for the multi-scale bioinspired synthesis approaches that are a focus of this FWP. The complex architectures required for functional metamaterials are at the length scales ideally suited to bioinspired approaches, and are difficult to achieve using conventional top-down methods. We now have sufficient insight into the self-assembly for controlled fabrication of complex hierarchical structures by mimicking nature's self- and directed-assembly by using DNA and polymer templates for metallization.

Publications (which acknowledge DOE support; from 2013 to 2015)

1. H. Zhang, X. Liu, S. Feng, W. Wang, K. Schmidt-Rohr, M. Nilsen-Hamilton, D. Vaknin, and S.K. Mallapragada, "Morphological Transformations in the Magnetite Biomineralizing Protein Mms6 in Iron Solutions: A Small-Angle X-ray Scattering Study", *Langmuir*, **31**, 2818-2825 (2015).
2. A. Travesset, "Binary Nanoparticle Superlattices of Soft-Particle Systems", *PNAS* (in press).
3. C. Valverde-Tercedor, M. Montalban-Lopez, T. Perez-Gonzalez, M.S. Sanchez-Quesada, T. Prozorov, E. Pineda-Molina, M.A. Fernandez-Vivas, A.B. Rodriguez-Navarro, D. Trubitsyn, D.A. Bazylinski, and C. Jimenez-Lopez, "Size Control of *In Vitro* Synthesized Magnetite Crystals by the MamC Protein of Magnetococcus Marinus Strain MC-1, *Appl. Microbiol. Biotechnol.*, **99**, 5109-5121 (2015).
4. S. Kashyap, T. Woehl, X.P. Liu, S.K. Mallapragada, and T. Prozorov, "Protein-Mediated Nucleation of Nanoparticles *In situ*", *ACS Nano*, **8**, 9097-9106 (2014).
5. T. Prozorov, T. Perez-Gonzalez, C. Valverde-Tercedor, C. Jimenez-Lopez, A. Yebra, A. Kornig, D. Faivre, S.K. Mallapragada, P.A. Howse, D. Bazylinski, and R. Prozorov, , "Manganese Incorporation into Magnetosome Magnetite: Magnetic Signature of Doping", *Eur. J. Minerol.*, **26**, 457-471 (2014).
6. V. Malik, J. Goodwill, S.K. Mallapragada, T. Prozorov, and R. Prozorov, "Comparative Study of Magnetic Properties of Nanoparticles by High Frequency Heat Dissipation and Conventional Magnetometry", *IEEE Magn. Lett.* **5**, 4000104 (2014).
7. C. Knorowski and A. Travesset, "Self-Assembly and Crystallization of Hairy (f-Star) and DNA-Grafted Nanocubes," *JACS*, **136**, 653-659 (2014).
8. Q. Ge, X.P. Liu, G. Parada, S.K. Mallapragada, and M. Akinc, "Synthesis of Mesoporous Zirconia Templated by Block Copolymer- Lysozyme Conjugate in Aqueous Media", *Sci. Adv. Mater.*, **6**, 2106-49 (2014).

9. V. Morillo, F. Abreu, A. C. Araujo, L. G. P. de Almeida, A. Enrich-Prast, M. Farina, A. T. R. de Vasconcelos, D. A. Bazylinski, and U. Lins, "Isolation, Cultivation and Genomic Analysis of Magnetosome Biomineralization Genes of a New Genus of South-Seeking Magnetotactic Cocci within the Alphaproteobacteria," *Front. Microbiol.*, **5**, 72 (2014).
10. C. Valverde-Tercedor, F. Abadia-Molina, M. Martinez-Bueno, E. Pineda-Molina, L. Chen, Z. Oestreicher, B. H. Lower, S. K. Lower, D. A. Bazylinski, and C. Jimenez-Lopez, "Subcellular Localization of the Magnetosome Protein Mamc in the Marine Magnetotactic Bacterium *Magnetococcus Marinus* Strain Mc-1 Using Immunoelectron Microscopy," *Arch. Microbiol.*, **196**, 481-488 (2014).
11. S. S. Rathnayake, M. Mirheydari, A. Schulte, J. E. Gillahan, T. Gentit, A. N. Phillips, R. K. Okonkwo, K. N. J. Burger, E. K. Mann, D. Vaknin, W. Bu, D. M. Agra-Kooijman, and E. E. Kooijman, "Insertion of Apolp-Iii into a Lipid Monolayer Is More Favorable for Saturated, More Ordered, Acyl-Chains," *Biochim. Et Biophys. Acta-Biomembr.*, **1838**, 482-492 (2014).
12. W. Bu, D. Kim, and D. Vaknin, "Density Profiles of Liquid/Vapor Interfaces Away from Their Critical Points," *J. Phys. Chem. C*, **118**, 12405-12409 (2014). 10.1021/jp504374z
13. W. J. Wang, I. Kuzmenko, and D. Vaknin, "Iron near Absorption Edge X-ray Spectroscopy at Aqueous-Membrane Interfaces," *Phys. Chem. Chem. Phys.*, **16**, 13517-13522 (2014).
14. A. Travasset, "Phase Diagram of Power law and Lennard-Jones systems: Crystal Phases", *J. Chem. Phys.* **141**, 164501 (2014).
15. W. R. Lindemann, W. Wang, F. Fungura, J. Shinar, R. Shinar, and D. Vaknin, "The Effect of Cesium Carbonate on 1-(3-methoxycarbonyl)propyl-phenyl[6,6]C₆₁", *Appl. Phys. Lett.* **105**, 191605/1-5 (2014).
16. S. R. Feng, L. J. Wang, P. Palo, X. P. Liu, S. K. Mallapragada, and M. Nilsen-Hamilton, "Integrated Self-Assembly of the Mms6 Magnetosome Protein to Form an Iron-Responsive Structure," *Int. J. Mol. Sci.*, **14**, 14594-14606 (2013). 10.3390/ijms140714594
17. R. B. Frankel, Pósfai, M., C.T. Lefèvre, D. Trubitsyn, D.A. Bazylinski, and R.B. Frankel. "Phylogenetic significance of composition and crystal morphology of magnetosome minerals", *Front. Microbiol.* **4**, 344 (2013).
18. X. P. Liu, Q. W. Ge, A. Rawal, G. Parada, K. Schmidt-Rohr, M. Akinc, and S. K. Mallapragada, "Templated and Bioinspired Aqueous Phase Synthesis and Characterization of Mesoporous Zirconia," *Sci. Adv. Mater.*, **5**, 354-365 (2013).

Directed Organization of Functional Materials at Inorganic-Macromolecular Interfaces

PI: Aleksandr Noy¹; Co-Is: Jim De Yoreo², Tony Van Buuren¹ and Chun-Long Chen²

Mailing address: ¹Physical & Life Sciences Directorate, Lawrence Livermore National Laboratory, Livermore, CA; ²Physical Sciences Division, Pacific Northwest National Laboratory, Richland, WA.

E-mail: noy1@llnl.gov

Program Scope

The purpose of this project is to develop a quantitative physical picture of macromolecular organization and its relationship to function, and to use macromolecular organization to derive new functionality. To date, we have approached this problem from several different yet converging directions. In the first, we used hierarchical assembly of phospholipids and membrane proteins on 1D silicon nanowire templates to create versatile interfaces between biological objects and electronic circuits. In the second, we created artificial membrane nanopores using carbon nanotube scaffolds, assembling them into 2D biological membrane environments, and studying transport characteristics of these assemblies. In the third, we created 3D artificial light harvesting complexes in which MS2 viral capsids functionalized on their exterior surfaces with DNA linkers and modified to include light adsorbing centers. These structures were assembled with nm-scale control over separation distance from Au nanoparticles using DNA origami tiles to achieve plasmonic enhancement of fluorescence. All of these tasks were supported by fundamental studies of the mechanisms and controls on macromolecular assembly in 1D (collagen), 2D (S-layer protein) and 3D (virus capsid) systems. Taking lessons from those studies and using the natural biological structures as an inspiration, we are now transitioning to all-synthetic macromolecular systems. Membranes formed from biomimetic sequence-defined polymers—peptoids—either serve as scaffolds for assembly of carbon nanotube pores, or directly self-assemble into porous networks in which the pores size and chemistry is controlled by the peptoid sequence. Several complementary characterization efforts cut across these tasks: atomic-scale characterization using small-angle x-ray scattering (SAXS) x-ray diffraction (XRD), x-ray imaging (STXM), and high-speed AFM imaging.

Recent Progress

Templated assembly creates biologically driven and regulated bioelectronic devices. We used templated assembly of lipids and biological pores on silicon nanowire templates to create bioelectronic transistors that incorporate biological functionality into an electronic circuit. (Fig. 1a). In this cycle we have investigated devices that use photoactivated proton pump bacteriorhodopsin (Fig. 1a) to regulate the device current output. We observed a pronounced response upon illumination in the green spectral region (Fig. 1b) as the protein pumps protons into the confined space under the lipid bilayer. To explain the device behavior we have built a kinetic model that connected

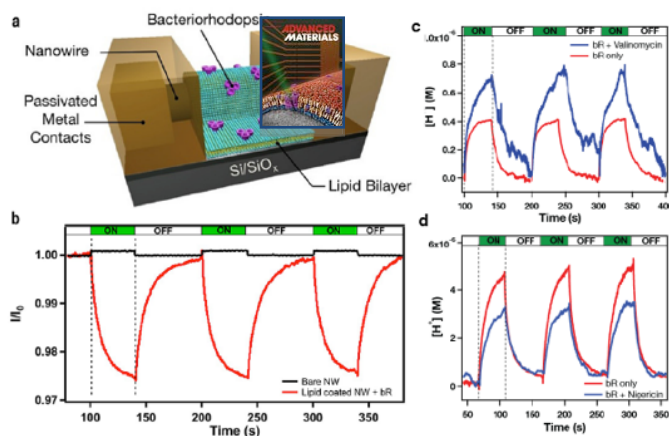


Fig. 1. Biologically-regulated 1D bilayer devices. (a) A SiNW transistor incorporating photoactivated bacteriorhodopsin (bR) protein pumps. (b). Normalized device current recorded under 3 cycles illumination for the uncoated SiNW device (black trace) and the device containing bR (red trace). (c,d) Proton concentration in vicinity of the nanowire during 3 consecutive illumination cycles for bR devices incorporating ionophores (c) valinomycin, and (d) nigericin. **Adv. Mater.** (2015) **Front Cover**

proton concentration rise and fall kinetics with the physical dimensions of the device and proton permeability characteristics of the lipid bilayer. We also implemented another layer of complexity in this system by employing biological modifiers of proton and ion permeability of the lipid layer to change the device response. Specifically, two ionophores, valinomycin and nigericin, up-regulate and down-regulate the device output (Fig. 1c,d). Remarkably, an analytical model based on the proton-ion equilibrium across the membrane reproduced the changes in the device response based on the published ion permeabilities of the lipid bilayers in presence and absence of ionophores. Thus, templated assembly can build bioelectronic structures with complex biologically regulated functionality and analytically tractable performance.

The performance of 1D bilayer devices could be critically impacted by spatial variations in the bilayer structure. We have used a combination of in-situ SAXS and STXM to determine atomic level structural ordering in these systems. The data show that Si NWs are coated with a single bilayer structure with thicker, multilayered structures formed only in the nodes between touching Si NWs (which are typically absent in the device geometry). STXM provided the capability to resolve angular dependence in specific bonds within the lipids that compose these thin structures. The data show that the C=C bond has a more upright than prostrate orientation with respect to the Si surface, which is consistent with prior MD simulations and NMR/infrared spectroscopy studies, and that any tilt away from the surface normal is predominantly in a direction perpendicular to the long axis of the NW. Neither the C=O, nor C-C bonds of the DOPC lipids exhibit comparable angular dependence.

Carbon nanotube porins create a versatile biomimetic nanopores with exceptional transport properties.

To address the need for more robust and tunable membrane transport systems, we have created a new type of artificial nanopore—*carbon nanotube porin* (CNTP). This structure is based on a short segment of carbon nanotube wrapped with lipid molecules, which allow CNTPs to self-insert into the lipid membrane (Fig. 2a,b), the behavior that we verified using cryogenic electron microscopy (Fig. 2b) and single pore transport measurements (Fig 2c, d, e). Narrow and hydrophobic inner pores of carbon nanotubes share several key structural characteristics with biological channels, the mechanism of the water and proton transport through carbon nanotubes has a distinct similarity to those pores, and indeed CNTPs reproduce the biological channel’s ability to transport protons, water, ions, and macromolecules such as DNA. We have also observed stochastic gating behavior, which we attributed to an ionic liquid-vapor transition that is unique to narrow hydrophobic nanopores. The structure of the CNT-lipid complexes is critical to the identification of the mechanisms of CNT insertion into lipid vesicles to form the CNT-porins. Several morphology models exist where CNTs can be encapsulated within cylindrical micelles, or covered with either hemispherical micelles, or randomly adsorbed molecules. We have used in situ SAXS to study CNTs-lipid complexes and found the structure to be consistent with a single layer of DOPC on the surface of CNTs. Overall, CNTPs give our team a versatile experimental platform that

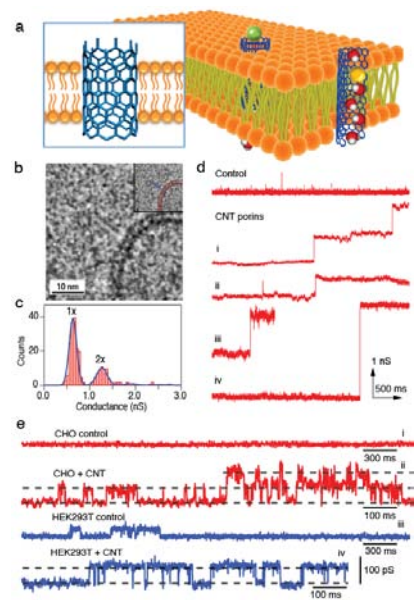


Fig. 2. Carbon Nanotube Porins. **a.** Structure of a CNT porin. **b.** Cryogenic TEM image of a carbon nanotube porin in a lipid membrane. **c.** Histogram of ionic conductance of individual CNT porins in 1M KCl solution. **d.** Conductance traces showing spontaneous incorporation of CNT porins into a lipid membrane from solution. Each conductance jump of ca. 0.62 nS corresponds to an individual porin incorporation. **e.** Conductance traces showing CNT porin incorporation into membranes of two live cell lines. **Nature** (2014).

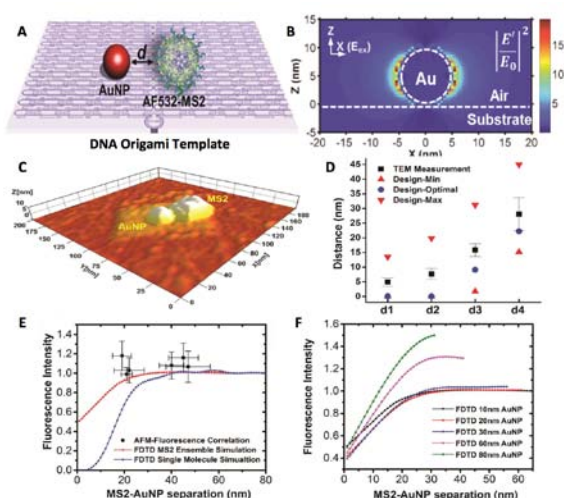


Fig. 3. (A) DNA origami templates organize fluorophore-labeled capsids and AuNPs (B) Numerical simulation of E-fields. (C) AFM image of capsid and AuNP on DOT. (D) Comparison of design points to actual AuNP-capsid separation. (E) Measured intensity vs. prediction for ensemble of dyes on capsid (red) and single dye molecule (blue). (F) Predictions for other NP diameters showing optimization at larger size.

To assemble peptoids into hexagonal pore networks, similar to many natural protein membranes, we designed a series of 3-fold peptoids, such as Pep-1 and Pep-2, in which hubs with different lengths were introduced to tune pore size (Fig. 5a). These hubs were designed to be self-complementary through inter-peptoid hydrogen bonds and hydrophobic interactions. The formation of such intra-peptoid interactions is expected to drive the formation of honeycomb-like networks through homodimerization between peptoids (Fig. 5a). When the amine-containing Pep-1 was exposed to basic conditions, vesicles with ~ 500 nm diameters were formed. In contrast, Pep-2 assembled into ~ 4 μm vesicles at neutral pH, because each hub contains three $-\text{COOH}$ groups and three $-\text{NH}_2$ groups, it is known that $-\text{COOH}$ and $-\text{NH}_2$ groups form charge-assisted hydrogen bonds. Structure of the peptoid assemblies/ vesicle has been determined by XRD. When Pep-2 vesicles were deposited on freshly-cleaved mica surface, the introduction of peptoid-mica interactions drove formation of 2D macromolecular scaffolds with uniform pore sizes of ~ 12 nm. This size is close to that expected for a perfect hexagonal network generated from ~ 5.0 nm hubs of Pep-2. Because the pore size of 2D macromolecular scaffolds is determined by the size of the 3-fold building block, we are currently tuning the length of peptoid hubs to target pores sizes ranging from 0.5 nm to 2.0 nm, and investigating the assembly mechanisms.

Future plans

Going forward, our overarching objective is to integrate the transport studies

should be flexible enough to adapt to a variety of transport measurements, and is capable of integration into a variety of membranes.

Using virus scaffolds and DNA templates to build plasmonic devices. We used DNA origami tiles (DOTs) to organize MS2 virus capsids and Au nanoparticles (NPs) and create hierarchical plasmonic nanostructures presenting a fluorophore ensemble to a plasmonic antenna (Fig. 3). The capsid served as a programmable scaffold providing molecular level control over the fluorophore distribution, while the DNA template controlled the distance between the capsid and the AuNP that served as a plasmonic antenna. By combining finite-difference time-domain numerical simulations with AFM and correlated scanning confocal fluorescence microscopy, we showed that this design kept the majority of fluorophores out of the quenching zone, leading to increased fluorescence. These bio-inspired plasmonic structures provide a flexible design for manipulating photonic excitation and photoemission.

Building peptoid-based 2D macromolecular scaffolds and molecule-selective pore networks.

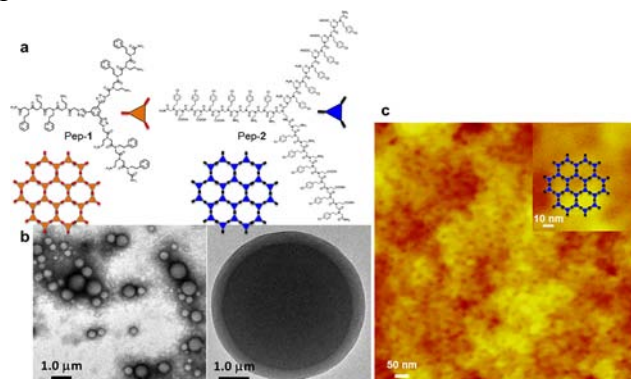


Fig. 4. Self-assembly of 3-fold amphiphilic peptoids into porous vesicles and 2D macromolecular scaffolds. a. Structures of two 3-fold peptoid sequences (Pep-1 and Pep-2) and their honeycomb-like packing to form pore networks. **b.** Vesicles assembled from Pep-1 and Pep-2 in solution. **c.** Pep-2 vesicles transformed into porous 2D macromolecular scaffolds on inorganic surface.

and the investigation of macromolecular assembly through the creation of completely artificial macromolecular matrices and functional units, with a focus on membranes for molecular separation and transport. Our next efforts are going to leverage the results that we have achieved in three areas: (1) controlling transport through molecular pores in 1D lipid bilayer bioelectronic devices, (2) investigating the controls that protein-solvent-surface interactions and conformational dynamics exert over organization of macromolecules at inorganic surfaces, and (3) synthesizing self-assembling 2D materials and pore networks from biomimetic sequence-defined polymers. Thus our approach continues to integrate synthesis of novel biomimetic materials and structures with the most advanced in situ characterization capabilities and theory-driven simulations of structure and assembly. This approach will lead to a predictive understanding of: (1) the link between sequence and organization of 2D biomimetic matrices, (2) the controls on assembly and ordering, and (3) transport through nanoscale pores. Together, these advances will build a foundation for design of functional materials based on an understanding of the link between sequence, assembly, and function, and lead to a new generation of biomimetic membrane materials in which the pore size and chemical selectivity can be tuned for applications in a wide range of energy systems.

Publications

- C. M. Ajo-Franklin, A. Noy *Crossing Over: Nanostructures that Move Electrons and Ions Across Cellular Membranes* **Adv. Mater.**, DOI: 10.1002/adma.201500344 (2015).
- P.J.M. Smeets, K-R. Cho, R.G.E. Kempen, N.A.J.M. Sommerdijk and J.J. De Yoreo, *Calcium carbonate nucleation driven by ion binding in a biomimetic matrix revealed by in situ electron microscopy*, **Nature Mater.** *14*, 394-399 (2015).
- J. R. I. Lee, M. Bagge-Hansen, R. Tunuguntla, K. Kim, M. Bangar, T. M. Willey, I.C. Tran, D. Kilcoyne, A. Noy, T. van Buuren, *Ordering in Bio-inorganic Hybrid Nanomaterials Probed by In Situ Scanning Transmission X-ray Microscopy* **Nanoscale, Advance Article**, DOI: 10.1039/C5NR00622H (2015).
- R. Tunuguntla, M. Bangar, K. Kim, P. Stroeve, C. P. Grigoropoulos, C.M. Ajo-Franklin, A. Noy *Light-powered bioelectronic devices with biologically-tunable performance*, **Adv. Mater.**, *27*, 831-836 (2015). **Front Cover**.
- K. Kim, J. Geng, R. Tunuguntla, C. P. Grigoropoulos, C. M. Ajo-Franklin, A. Noy *Osmotically-Driven Transport In Carbon Nanotube Porins*, **Nano Lett.**, *14*, 7051–7056 (2014).
- J. Geng, K. Kim, J. Zhang, R. Tunuguntla, L. R. Comolli, F. I. Allen, K. R. Cho, D. Munoz, Y. M. Wang, C. P. Grigoropoulos, C. M. Ajo-Franklin, A. Noy *Stochastic Transport and Gating in Carbon Nanotube Porins in Lipid Membranes*, **Nature**, *514*, 612-615 (2014).
- D. Wang, S.L. Capehart, S. Pal, M. Liu, L. Zhang, P.J. Schuck, Y. Liu, Y. Hao, M.B. Francis, J.J. De Yoreo, *Hierarchical Assembly of Plasmonic Nanostructures using Virus Capsid Scaffolds and DNA Origami Tiles*, **ACS Nano**, *8*, 7896 (2014).
- B. Narayanan, G. Gilmer, J. Tao, J.J. De Yoreo and C. Ciobanu, *Self-assembly of collagen on surfaces: the interplay of collagen-collagen and collagen-substrate interactions* **Langmuir** *30*, 1343–1350 (2014).
- J.J. De Yoreo, “Mimicking Biomineral Systems: What have we achieved and where do we go from here?” In M. Knecht and T. Walsh, Eds. Bio-inspired Nanotechnology-From Surface Analysis to Applications, pp. 290-314 (Springer, NY, 2014).
- R. Tunuguntla, M. Bangar, K. Kim, P. Stroeve, C.M. Ajo-Franklin, A. Noy, *Lipid Bilayer Composition can Influence the Orientation of Proteorhodopsin in Artificial Membranes*, **Biophys. J.**, *105*, 1388 (2013).
- J. R. I. Lee, T. Han, T. Willey, M. Nielsen, L. Klivansky, Y. Liu, S.W. Chung, L. Terminello, T. van Buuren, J. De Yoreo, *Cooperative Reorganization of Mineral and Template during Directed Nucleation of Calcium Carbonate*, **J. Phys. Chem. C**, *117* (21), 11076–11085 (2013).
- S-W. Chung, J.J. De Yoreo, “In situ Atomic Force Microscopy as a tool for investigating assembly of protein matrices”, In: Biomineralization Sourcebook: Characterization of Biominerals and Biomimetic Materials, (Eds.: Dimasi, E. and Gower, L. (Taylor & Francis Group, 2013).
- K-R. Cho and J.J. De Yoreo, “Probing protein assembly, biomineralization, and biomolecular interactions by atomic force microscopy”, In: NanoCellBiology: Multimodal Imaging in Biology & Medicine, Eds: Jena, B.P. and Taatjes, D.J., (Pan Stanford Publishing, Singapore, 2013).
- J.J. De Yoreo, S. Chung, and R.W. Friddle, *In situ AFM as a tool for investigating interactions and assembly dynamics in biomolecular and biomineral systems* (Invited Review) **Adv. Func. Mat.**, *23*, 2525-2538, (2013) **Inside Cover Article**.
- L.R. Comolli, C.E. Siegerist, S-H. Shin, C.R. Bertozzi, W. Regan, A. Zettl and J.J. De Yoreo, *Conformational transitions at an S-layer growing boundary resolved by cryo-TEM* **Agew. Chem. Int. Ed.**, *52*, 4829-4832, **Inside Cover Article** (2013).
- Bagge-Hansen, M.; Wichmann, A.; Wittstock, A.; Lee, J. R. I.; Ye, J. C.; Willey, T. M.; Kuntz,

- J. D.; van Buuren, T.; Biener, J.; Baumer, M.; Biener, M. M. *Quantitative Phase Composition of TiO₂-Coated Nanoporous Au Monoliths by X-ray Absorption Spectroscopy and Correlations to Catalytic Behavior*. **J. Phys. Chem. C.**, 118, 4078-4084 (2014).
- Bagge-Hansen, M.; Wood, B. C.; Ogitsu, T.; Willey, T. M.; Tran, I. C.; Wittstock, A.; Biener, M. M.; Merrill, M. D.; Worsley, M. A.; Otani, M.; Chuang, C. H.; Prendergast, D.; Guo, J. H.; Baumann, T. F.; van Buuren, T.; Biener, J.; Lee, J. R. I. *Potential-Induced Electronic Structure Changes in Supercapacitor Electrodes Observed by In Operando Soft X-Ray Spectroscopy*. **Adv. Mater.** 27, 1512. (2015) (**Cover Article**)
- Wright, J. T.; Su, D.; van Buuren, T.; Meulenberg, R. W. *Electronic structure of cobalt doped CdSe quantum dots using soft X-ray spectroscopy*. **J. Mater. Chem. C.** 2, 8313-8321 (2014)

Early Career: Real-Time Studies of Nucleation, Growth and Development of Ferromagnetism in Individual Protein-Templated Magnetic Nanocrystals

PI: Tanya Prozorov, Ames Laboratory

Mailing Address: Division of Materials Sci. and Eng., Ames Laboratory, Ames, IA 50011

Email: tprozoro@ameslab.gov

Project Scope

In biological systems, nucleation and crystallization of biogenic inorganic materials is controlled by diverse biomineralization proteins. Using the recombinant iron-binding protein, Mms6, and corresponding peptides, well-formed nanocrystals of magnetite and cobalt ferrite can be grown in polymeric matrices in a process mimicking the growth of magnetite in live magnetotactic bacteria. However, neither the structure of Mms6, nor the detailed process of protein-assisted nanoparticle nucleation and growth are established. The major issue is that common characterization techniques only work with large, macroscopic assemblies of nanoparticles, so that interactions and collective effects mask the behavior of individual nanoparticles.

The research in my *Emergent Magnetic and Atomic Structures* Group is aimed at investigating the nucleation, growth, the emergence of crystal structure and development of ferromagnetism in the *individual* bio-templated magnetic nanocrystal by utilizing advanced and novel electron microscopy techniques. Uniform magnetic nanoparticles with large magnetic moment and controlled magnetic anisotropy have important technological applications from data storage, to catalysis and drug delivery. Biomimetic synthetic routes offer room-temperature pathways to placement control, formation, and assembly of a variety of magnetic nanostructures with unique shapes and sizes. We work on gaining a better understanding on how the assembly of biomacromolecules dictates nanoparticle formation and functional properties. Magnetite biomineralization by magnetotactic bacteria is used as model system with the individual microorganisms monitored throughout the various steps of the biomineralization process, from the incipient nuclei to the fully developed crystalline and magnetic structures.

Recent Progress

My group worked on a direct visualization of nucleation of iron oxide nanoparticles mediated by an acidic bacterial recombinant protein, Mms6. Using *in situ* fluid cell transmission electron microscopy (TEM) holder customized for the project by Hummingbird Scientific, we utilized the *in situ* STEM analysis to follow the reaction induced and controlled by the slow addition of NaOH at a fixed rate and imaged the particle formation process at nanometer resolution as it occurred in solution. We observed preferential formation of the amorphous liquid precursor phase and incipient nuclei on the surface of protein micelles, pointing to the importance of presence of extended protein surface in the process. Formation of the amorphous

precursor phase leads to depletion of the micelle-bound iron and diminishes nucleation in the surrounding bulk solution, as shown in **Figure 1**. Our results represent a significant step forward in understanding the role of the biomineralization protein in the highly-dynamic biomimetic *nucleation processes* and will aid in optimizing the biomimetic synthesis of magnetic nanoparticles [9].

Using the liquid cell STEM holder, we have visualized viable cells of *Magnetospirillum magneticum* strain AMB-1 *in situ*. To access viability of the bacterial culture after the STEM characterization *in-situ*, we developed and implement a correlative microscopy approach involving exposure of the imaged cells to the fluorescent dyes and imaging them with the fluorescent microscope to verify their cell wall

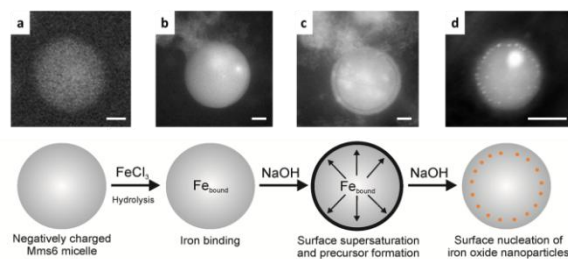


Figure 1. Protein-mediated formation of iron oxide nanoparticles *in situ*: (a) protein micelles bind ferric iron and become visible (b); surface-bound iron reacts with NaOH, leading to formation of liquid-like precursor formation (c); upon further addition of NaOH, amorphous iron oxide nanoparticles form on the micellar surface (d). Scale bar: 50 nm.

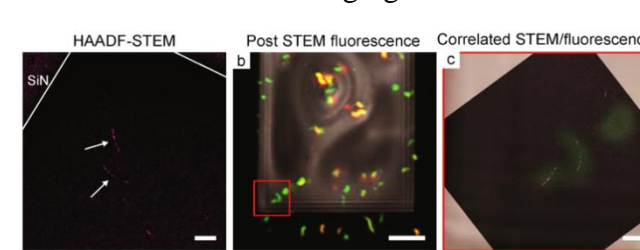


Figure 2. False-colored HAADF STEM image of AMB-1 bacteria (a) is overlaid with fluorescence image of the ROI (b) to produce a composite correlated FM-STEM image (c). Scale bar: 1 μ m.

membrane integrity. Based on the post-STEM fluorescence imaging, the bacterial cell wall *membrane does not sustain damage during STEM analysis at low electron dose conditions*, as shown in **Figure 2**. Correlative STEM and fluorescence imaging of magnetotactic bacteria is a first step in directly observing biomineralization of magnetite nanocrystals, currently monitored *ex situ* [8]. We investigated the early stages of magnetosome formation in this work and correlated the size and emergent crystallinity of formed magnetosomes with the changes in chemical environment of iron and oxygen by utilizing advanced analytical electron microscopy techniques. Magnetosomes in the early stages of biomineralization with the sizes of 5-10 nm were disordered ferric hydroxide, while the fully matured magnetosomes were indexed to magnetite. The magnetosomes with the sizes 10-13 nm showed partially crystalline structure with a majority of iron present as Fe^{3+} and trace amounts of Fe^{2+} . Our approach provided spatially resolved structural and chemical information of individual magnetosomes with different particle sizes, attributed to particles at different stages of biomineralization, as illustrated in **Figure 3**.

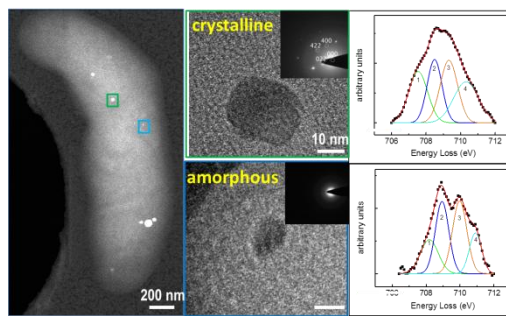
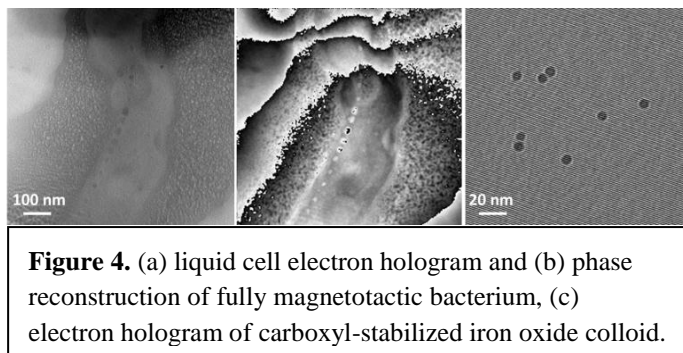


Figure 3. Magnetosome nanoparticles exhibit different sizes, crystalline structure and chemical environment of iron.

Off-axis electron holography has been widely used to enable phase imaging of electrostatic and magnetic fields with nanoscale resolution, however it is restricted to dry specimens due to the high vacuum requirements, thus posing limitations to the analysis of soft matter. To obtain a realistic picture of interparticle interactions and their role in response of the entire ensemble of particles, it is necessary to study these systems in liquid state. The *in situ* liquid cell TEM characterization is crucial for direct visualization of such interparticle interactions.

In collaboration with Rafal E. Dunin-Borkowski of the Ernst Ruska-Centre for Microscopy, Peter Grünberg Institute, Forschungszentrum Jülich, Germany, we pioneered electron holographic imaging of magnetic nanoparticles suspension in liquid, using studied magnetotactic bacteria as a model system. Notably, these experiments are currently deemed impossible. We have applied off-axis electron holography, in combination with the use of an *in situ* fluid cell, to characterize the local magnetic properties of aqueous colloid containing 15 nm carboxyl-stabilized iron oxide nanoparticles, as shown in **Figure 4**.



Future Plans

Extending the electron holography to liquid environments opens *a new era in materials characterization*, as this is the only technique permitting visualization of the variation of electrostatic potential across the liquid specimen. The novel science enabled by this approach will produce a new body of knowledge in many fundamental areas of research, from dynamics of interacting nano- and meso- scale objects in liquids, to nucleation and crystallization events and mean inner potentials of solvents and biological molecules, to visualization of interactions between the individual magnetic nanoparticles and understanding of how this influences the properties of nanoparticle assembly. We will monitor the evolution of the magnetic response of the protein-templated nanocrystal *in situ* at different stages of its growth by combining the dynamic electron diffraction with the electron holography data.

Publications

1. Woehl, T. J., Prozorov, T. “*Future prospects in liquid cell EM of biomaterials*” in: Liquid Cell Electron Microscopy. Editors: Ross, F., de Jonge, N. **2016**, Cambridge University Press, invited book chapter, *Revised chapter submitted*.
2. Prozorov, T. “*TEM and associated techniques (Liquid Cell, Holography)*” in: Iron Oxides. From Nature to Applications. Editor: Faivre, D. **2016**, Wiley-VCH, invited book chapter, *Submitted*.

3. Prozorov, T. “*Magnetic microbes: bacterial magnetite biomineralization*”, Special issue on Biomineralization, Seminars in Cell and Developmental Biology, **2015**, invited review, *Submitted*.
4. Woehl, T. J., Prozorov, T. “The Mechanism for Nanoparticle Chain Self-Assembly Determined from Real-Time Nanoscale Kinetics in Liquid”, *Nano Lett.*, **2015**, *Submitted*.
5. Firlar, E., Çınar, S., Kashyap, S., Akinc, M., Prozorov, T. “Direct Visualization of the Hydration Layer on Alumina Nanoparticles with the Fluid Cell STEM *in situ*”, **2015**, *Scientific Reports*, *5*, 9830. DOI:10.1038/srep09830.
6. Valverde-Tercedor, C.; Montalbán-López, M.; Trubitsyn, D.; Pineda-Molina, E.; Perez-Gonzalez, T.; Prozorov, T.; Bazylinski, D. A.; Jimenez-Lopez, C. “Size Control of *in vitro* Synthesized Magnetite Crystals by MamC from *Magnetococcus marinus* MC-1”, *Appl. Microbiol. Biotechnol.*, **2015**, *99*, 5109. DOI 10.1007/s00253-014-6326-y.
7. Malik, V.; Goodwill, J.; Mallapragada, S. K.; Prozorov, T.; Prozorov, R. “Comparative Study of Magnetic Properties of Nanoparticles by High Frequency Heat Dissipation and Conventional Magnetometry”, **2014**, *IEEE Magnet. Lett.*, *5*, 4000104. DOI: 10.1109/LMAG.2014.2368517.
8. Woehl, T. J.; Kashyap, S.; Perez-Gonzalez, T.; Faivre, D.; Trubitsyn, D.; Bazylinski, D. A.; Prozorov, T., “Correlative Electron and Fluorescence Microscopy of Magnetotactic Bacteria in Liquid: Toward *In Vivo* Imaging”, **2014**, *Sci. Rep.*, *4*, 6854. DOI:10.1038/srep06854.
9. Kashyap, S., Woehl, T. J., Liu, X., Mallapragada, S. K., Prozorov, T., “Protein-Mediated Nucleation of Nanoparticles *In-Situ*”, **2014**, *ACS Nano*, *8*, 9097. <http://dx.doi.org/10.1021/nn502551y>.
10. Prozorov, T., Perez-Gonzalez, T.; Valverde-Tercedor, C., Jimenez-Lopez, C., Yebra, A., Mallapragada, S. K., Howse, P., Bazylinski, D. A., Prozorov, R., “Iron *et al.*: Magnetic Signature of Magnetosome Magnetite Doping”, **2014**, *Europ. J. Mineral.* *26*, 457. DOI: 10.1127/0935-1221/2014/0026-2388.
11. Prozorov, T., Bazylinski, D. A.; Prozorov, R.; Mallapragada, S. K., “Novel Magnetic Nanomaterials Inspired by the Magnetotactic Bacteria: Topical Review”, *Materials Sciences and Engineering R: Reports*, **2013**, *Invited Topical Review*, *173*, 133-172.
12. Sizova, M.V., Muller, P., Panikov, N., Mandalakis, M., Hohmann, T., Hazen, A., Fowle, W., Prozorov, T., Bazylinski, D.A., Epstein, S.S. “Stomatobaculum longum gen. nov., sp nov., an obligately anaerobic bacterium from the human oral cavity,” **2013**, *Int. J. System. Evol. Microbiol.*, *63*, 1450.
13. Perez-Gonzalez, T., Valverde-Tercedor, C., Yebra-Rodriguez, A., Prozorov, T., Gonzalez-Munoz, M.T., Arias-Penalver, J.M., Jimenez-Lopez, C. “Chemical Purity of *Shewanella oneidensis*-Induced Magnetites,” **2013**, *Geomicrobiol. J.* *30*,731.

Active Assembly of Dynamic and Adaptable Materials: Artificial Microtubules

Task Lead: Erik D. Spoerke

Principal Investigator: George D. Bachand

Co-Investigators: Erik D. Spoerke, Mark Stevens, and Darryl Sasaki

Mailing Address: Electronic, Optical, and Nano Materials, Sandia National Laboratories,
PO Box 5800, MS 1411, Albuquerque, NM 87185

Email: edspoer@sandia.gov

Program Scope

The *Active Assembly of Dynamic and Adaptable Materials* program explores materials science questions arising from the integration of biology, nanomaterials, chemistry, and hybrid material interfaces. As an overarching objective, this program seeks to understand Nature's strategies for non-equilibrium assembly and manipulation of materials, and to translate the principles behind these processes in biohybrid or bio-inspired synthetic systems. In particular, we investigate molecular and biomolecular systems which utilize energy consumption to enable dynamic and adaptive materials behaviors that exceed limitations imposed by diffusion and chemical equilibria. Current research tasks are focused on (1) the active assembly of hybrid nanomaterials employing motor protein-driven nanomaterial transport and dynamic polymerization of cytoskeletal filaments (microtubules), and (2) the exploration of "artificial microtubule" supramolecular chemistries which incorporate/mimic key attributes and dynamic, non-equilibrium behaviors of natural MT filaments in synthetic systems.

Many of the unique behaviors found in living systems (e.g., self-replication, adaptivity) are commonly associated with dynamic self-assembly and energy dissipation.¹ Our program focuses on one of Nature's active, adaptive transport systems, specifically microtubules (MTs) and their associated motor proteins (Fig. 1). MTs are hollow filaments composed of $\alpha\beta$ tubulin dimers whose energy-dissipative assembly is used to push, pull, or rearrange the cell's cytoskeleton. These filaments also serve as "train tracks" for the coordinated bidirectional transport of macromolecules and organelles by the motor proteins kinesin and dynein through the conversion of chemical energy into mechanical work. Living organisms use the concerted and dynamic interactions between kinesin and MT to control physiological processes ranging from chromosome segregation at the cellular level to macroscopic color changing behaviors at the organismal level.² Learning to exploit, mimic, and/or translate the role of active proteins in emergent biological behaviors will create invaluable opportunities to dramatically advance nanoscale and biomolecular materials assembly.

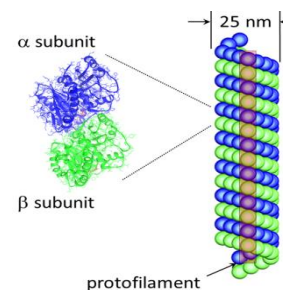


Fig. 1. Crystal structure of tubulin and model of an assembled MT.

Recent Progress

Recent activities in the *Artificial Microtubules* subtask have utilized a combination of theory and experiment to explore synthetic molecular systems that mimic elements of natural

MT form and function. In particular, we have emphasized the study of novel peptide-based systems with structures and self-assembly behaviors inspired by the unique and remarkable molecular chemistry of MTs.

The $\alpha\beta$ tubulin dimer (Fig. 1) not only assembles to define the tubular structure of MTs, but also introduces the chemical functionality that governs the dynamic assembly and disassembly of the MTs and regulates interactions of the MTs with other biomolecules. For example, the binding and hydrolysis of guanosine triphosphate (GTP) to tubulin dimers critically regulates the MT assembly and disassembly, and the association of microtubule associated proteins (MAPs) with MTs critical impacts the stabilization of MTs undergoing dynamic instability. Our recent focus has emphasized the study of reversibly self-assembling synthetic peptides that incorporate chemical and structural elements designed to mimic selective aspects of tubulin form or function.

Diphenylalanine-Based Peptides

Inspired by the $\alpha\beta$ tubulin dimer motif, we are exploring chemical modifications to the simplified peptide dimer, diphenylalanine, known to assemble with crystalline order into tubules.³ By introducing functional changes that affect the molecular conformation or chemical interactions of this self-assembling dipeptide, we aim to manipulate the dynamic self-assembly of the peptide and control its interactions with secondary biomolecules. For example, we have attached boronic acid (BA) onto the FF peptide and studied the self-assembly behavior this molecule (BFF). BAs are mild Lewis acids, that undergo reversible complexation with select diols and polyols, such as catechol and sugars, to form cyclic boronate esters.⁴ Our studies show that BA functionalization greatly enhances peptide solubility in physiological media and consequently enables the reversible self-assembly into nanoribbon hydrogels. Moreover, we observed that the reversible binding of polyols to BFF can be used as a new route to modulate the peptide between its assembled and disassembled states (Fig. 2).

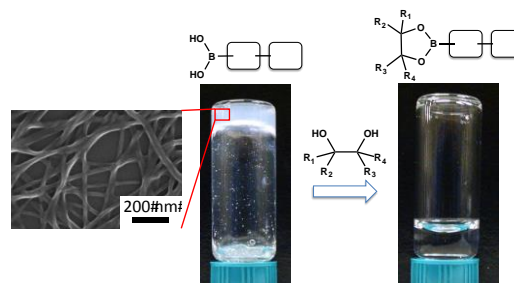


Fig. 2. SEM image (left) and optical images of a self-assembled BFF nanoribbon hydrogel and polyol-mediated disassembly. (FF represented by red blocks.) (Jones, et al., *Chem Comm.*, 2015.)

Multifunctional Block Peptides

In parallel efforts, we continue to study multifunctional peptides comprising “blocks” designed to introduce specific structural or functional properties that influence self-assembly. Selective engineering of these blocks can play critical roles in determining molecular shape, peptide/solvent interactions, electrostatics, and the balance of molecular interactions laterally (e.g., around a tube) or vertically (e.g., along a tube) that collectively direct self assembly in both natural MT and bioinspired systems.⁵⁻⁷

Expanding on these concepts, we have studied a series of MT-inspired peptides, such as the “bola” peptide shown in Fig. 3. This peptide comprises two similar amphiphilic peptide units

(α and β), joined by an enzymatically-cleavable phenylalanine linker. We have shown that self-assembly of this $\alpha\beta$ dimer in water is triggered by its cooperative interactions with a charged surfactant, sodium dodecyl sulfate (SDS). Electrostatic binding of the dodecyl sulfate (DS) to the peptide introduces critical solvation-based driving forces needed to induce assembly into a self-supporting hydrogel composed of one-dimensional, β -sheet rich nanostructures (Fig. 3). By moderating pH, the DS binding and resulting hydrogel formation can be reversed. Interestingly, the introduction of the SDS to the system also imparts unique function to the gel, making it resistant to enzymatic cleavage of the central phenylalanine linker. Not only does this MT-inspired peptide system offer parallels to the dimerized structure of the tubulin building blocks, but the collaborative influences from secondary molecules on both molecular assembly and stability represent additional functional analogues to the natural system.

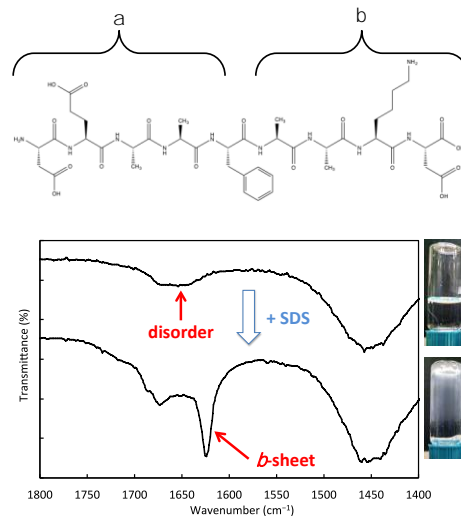


Fig. 3. Scheme of $\alpha\beta$ bola peptide and fourier transform infrared spectra showing β -sheet formation in hydrogels collaboratively assembled by the peptide and SDS. (Jones, et al, *Soft Matter*, 2015).

We have also utilized computation and theory to guide the design of new multicomponent peptides. We have previously employed molecular dynamics (MD) and self-consistent field theory (SCFT) to inform both molecular design and interpretation of self assembly behavior of amphiphilic wedge peptides.⁵⁻⁷ We have recently expanded this approach, utilizing SCFT to predict the self-assembly of unique triblock amphiphiles and guide the experimental synthesis of peptide-based molecules inspired by these predictions. These ABC

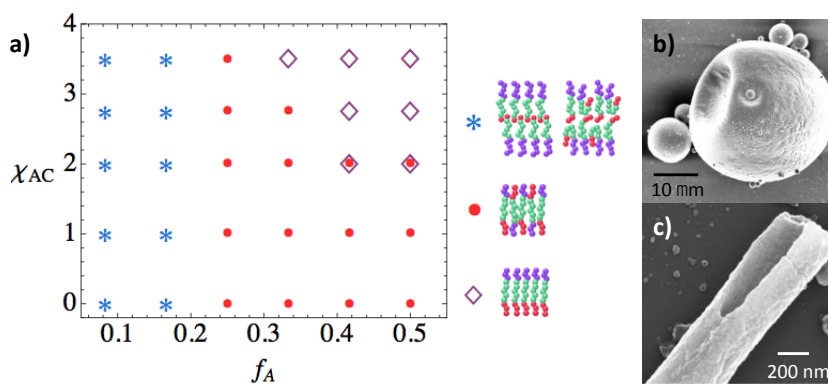


Fig. 4. a) Phase diagram as a function of interaction asymmetry χ_{AC} and molecular asymmetry f_A . Schematic legend shows symmetric bilayers (stars), symmetric monolayer (circles), and asymmetric monolayer (diamonds) (Ting, et al, *Soft Matter*, 2015). b) Scanning electron micrograph (SEM) of vesicle formed from ABC triblock Gln₆-Phe₇-PEG₈. c) SEM of tubule formed from modified ABC triblock with increased Gln block size.

triblock systems comprise two dissimilar hydrophilic blocks (A and C) linked by a hydrophobic core block (B). SCFT simulations predict that variations in block size and the relative interaction strengths of the blocks will affect molecular assembly into varied bilayers and monolayers. (Fig. 4a). These varied layered structures are expected to correlate with assembled morphologies ranging from planar sheets to

spherical vesicle and tubes (Fig. 4a). Of particular interest here are asymmetric monolayers, expected to form vesicles and tubules. Target ABC peptides (e.g., Gln₆-Phe₇-PEG₈) predicted to form these asymmetric monolayers were synthesized to test these SCFT predictions. As seen in Fig. 4b, initial results indicate that these simulation-inspired peptides do self-assemble into spherical vesicles. Moreover, we have observed that selective variations in the ABC peptide composition can influence the formation of either spherical vesicles or tubules (Fig 4c). Continued work on this emerging system will inform a more comprehensive understanding of the critical elements ultimately governing MT-inspired self-assembling materials.

Future Plans

We intend to follow parallel paths forward that will allow us to expand our understanding of the principles behind bio-inspired molecular assembly while beginning to realize the potential functional value of these dynamic and adaptable chemistries as tools for the secondary manipulation of nanomaterials. We will continue to employ complementary theory and experiment to identify and understand new chemical systems capable of responsive and adaptive self assembly into a variety of controllable architectures (tubes, vesicles, sheet, fibers, etc.). As these bio-inspired systems continue to develop, however, we intend to interface them with secondary biomolecular and nanomaterial elements to explore new opportunities for advanced, bio-inspired materials manipulation and organization (e.g., 3D architectures, environmentally responsive materials, alternative motility). The true value of the dynamic and adaptive character of MTs lies in their ability to facilitate complex, dynamic processes and organize other functional materials within a cell. Analogously, we intend to explore how the bio-inspired synthetic systems studied in this program can enable alternative strategies to manipulate the transport, organization, and non-equilibrium function of biomolecular and synthetic nano materials.

References

1. Fialkowski, M., et al. *J. Phys. Chem. B* **2006**, 110, (6), 2482-2496.
2. Goldstein, L. S. B.; Yang, Z. H. *Annu. Rev. Neurosci.* **2000**, 23, 39-71.
3. Reches, M.; Gazit, E. *Science* **2003**, 300, (5619), 625-627.
4. Hall, D. G., *Boronic Acids: Preparation and Applications in Organic Synthesis and Medicine*. Wiley-VCH: Weinheim, Germany, 2005.
5. Cheng, S. F.; Aggarwal, A.; Stevens, M. J. *Soft Matter* **2012**, 8, (20), 5666-5678.
6. Gough, D., et al. *Langmuir* **2014**, 30, 9201-9209.
7. Ting, C., et al. *J. Phys. Chem. B* **2014**, 118, (29), 8624-8630.

Acknowledgement

This research was supported by the U.S. Department of Energy, Office of Basic Energy Sciences, Division of Materials Sciences and Engineering, Project KC0203010. Sandia National Laboratories is a multi-program laboratory managed and operated by Sandia Corporation, a wholly owned subsidiary of Lockheed Martin Corporation, for the U.S. Department of Energy's National Nuclear Security Administration under contract DE-AC04-94AL85000.

Publications

1. Rao, V, Navath, S, Kottur, M, McElhanon, JR, and McGrath, DV (2013) An efficient reverse Diels–Alder approach for the synthesis of N-alkyl bismaleimides. *Tetrahedron Letters* **54**, 5011-5013.
2. Stevens, MJ (2014) How shape affects microtubule and nanoparticle assembly. *Science* **343**, 981-982.
3. Spoerke, ED, Connor, BA, Gough, DV, McKenzie, BB, and Bachand, GD (2014) Microtubule-templated cadmium sulfide nanotube assemblies. *Particle & Particle Systems Characterization* **31**(8), 863-870 (*cover*).
4. Cheng, S, Stevens, MJ (2014) Self-assembly of chiral tubules. *Soft Matter* **10**, 510-518.
5. Ting, CL, Frischknecht, AL, Stevens, MJ, and Spoerke, ED (2014) Electrostatically tuned self-assembly of branched amphiphilic peptides. *Journal of Physical Chemistry B* **118**(29), 8624-8630.
6. Vandelinder, V, Bachand, GD (2014) Photodamage and the importance of photoprotection in biomolecular-powered device applications. *Analytical Chemistry* **86**(1), 721-728.
7. Bachand, GD, Bouxsein, NF, VanDelinder, V, Bachand, M (2014) Biomolecular motors in nanoscale materials, devices, and systems. *Wiley Interdisciplinary Reviews: Nanomedicine and Nanobiotechnology* **6**, 163-177 (*invited review*).
8. Gough, DV, Wheeler, JS, and Spoerke, ED (2014) Supramolecular assembly of asymmetric self-neutralizing amphiphilic peptide wedges. *Langmuir* **30**(30), 9201–9209.
9. Bouxsein, NF and Bachand, GD (2014) Divalent counter-ion regulation of microtubule stability, flexibility and motility. *Biomacromolecules* **15**(10), 3696-705
10. Bachand, M, Bouxsein, NF, Cheng, S., von Hoyningen-Huene, S, Stevens, MJ, and Bachand, GD (2014) Directed self-assembly of 1D microtubule nano-arrays. *RSC Advances*, **4**, 51641-54649.
11. Momin, N, Lee, S, Gadok, AK, Busch, DJ, Bachand, GD, Hayden, CC, Stachowiak, JC, and Sasaki, DY (2015). Designing lipids for selective partitioning into liquid ordered membrane domains. *Soft Matter* **11**, 3241-3250.
12. Bachand, GD, Spoerke, ED, and Stevens, MJ (2015) Microtubule-based Nanomaterials: Borrowing from Nature’s dynamic biopolymers. *Biotechnology and Bioengineering* **112**(6), 1065-1073 (*invited review*).
13. Jones, BH, Martinez, AM, Wheeler, JS, and Spoerke, ED (2015) Surfactant-induced assembly of enzymatically-stable peptide hydrogels” *Soft Matter* **11**(18), 3572-3580 (selected for “2015 Soft Matter Hot Papers”).
14. Paxton, WF, Bouxsein, NF, Henderson, I, and Bachand GD (2015) Dynamic assembly of polymer nanotube networks via kinesin powered microtubule filaments. *Nanoscale* **7**, 10998-11004.
15. Ting, CL, Jones, BH, Frischknecht, AL, Spoerke, ED, and Stevens, MJ. (2015_ Amphiphilic Triblocks to control assembly of mixed or segregated bilayers and monolayers. *Soft Matter*, (In Press.)
16. Jones, BH, Martinez, AM, Wheeler, JS, McKenzie, BB, Miller, LL, Wheeler, DR, and Spoerke, ED (2015) A Multi-Stimuli Responsive Self-Assembling Boronic Acid Dipeptide. *Chem. Comm.* (In revision)
17. Jones, BH, Wheeler, DR, Wheeler, JS, Miller, LL, Alam, TM, and Spoerke, ED (2015) Anomalous isomer-sensitive deboronation in reductive aminations of aryl boronic acids. *Tetrahedron Letters* (In review).

18. Greene, AC, Henderson, IM, Gomez, A, Paxton, WF, VanDelinder, V, and Bachand, GD (2015) "Leviathan" polymersomes formed via simple gel-assisted rehydration. *Angewandte Chemie* (In review).

***UNIVERSITY GRANT
PROJECTS***

Bioinspired Hierarchical Design of Chiral Mesoscale Liquid Crystalline Assemblies

Nicholas L. Abbott, University of Wisconsin-Madison (Principal Investigator) and Juan J. de Pablo, University of Chicago (Co-Investigator)

Program Scope

Biology uses elastic stresses, defects, chirality and hierarchical design strategies to create a range of functional materials. This hierarchical organization serves as an amplifier that allows highly localized, molecular events to propagate into the mesoscale, resulting in dynamic functional properties of biological systems that have not yet been fully realized in synthetic material designs. We are pursuing a program of research in which we seek to recreate such principles using synthetic liquid crystals (LC) as a versatile platform. We are elucidating new hierarchical design strategies that heavily leverage chirality and topological defects to realize equilibrium and non-equilibrium, dynamic mesoscale phenomena in the context of nano- and micrometer-sized LC droplets containing nanoparticles. Specifically, we are unmasking how equilibrium and dynamical phenomena emerge from hierarchical organizations in responsive, chiral liquid crystalline assemblies. Overall, this research will advance new hierarchical designs of meso-scale materials in which biomimetic principles, including the propagation of events or information over multiple temporal and spatial scales, are enacted in a facile manner.

Recent Progress

The simplest chiral nematic phase is the cholesteric LC in which the director exhibits a twist along an axis that is orthogonal to the director. We have investigated the structure of cholesteric LC droplets with the goal of using their internal structure to guide the positioning of colloids. Our recent experimental observations of LC-in-water emulsion microdroplets have revealed that the confined cholesteric LCs exhibit three dominant configurations, namely a Radial Spherical Structure (RSS), a Diametrical Spherical Structure (DSS), and a Bipolar Structure (BS). These structures differ from each other by the symmetry and morphology of topological defects. An example of one of the structures that we have observed, the RSS, is shown in Figure 1. Inspection of Figure 1 reveals a double twisted disclination that runs from the center to the surface of the droplet (arrows in Figure 1). In

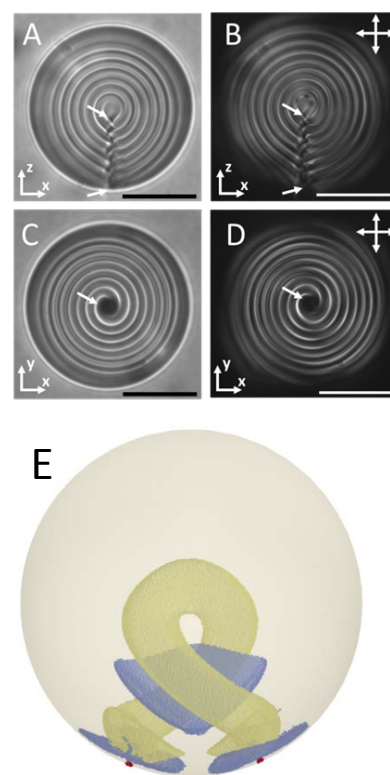


Figure 1. Representative (A and C) bright field and (B and D) polarized light micrographs of a chiral LC droplet with a radial spherical structure (RSS) taken along (A and B) y-axis or (C and D) z-axis. Scale bars: 20 μm . (E) Schematic representation of the RSS structure predicted from our simulations.

contrast, for the DSS, the defect lines span the diameter of each droplet and for the BS configuration the defects were singular and localized at two poles of the droplets. Comparisons of our experimental observations of RSS structures to numerical simulations (Fig 1E) reveal excellent agreement.

We have also quantified experimentally the influence of the size of cholesteric LC droplets on their internal configurations using the parameter N , where N is the number of π -turns along a distance corresponding to the diameter of a droplet. Size-dependent stabilization of the various configurations of the cholesteric droplet was observed, with good correspondence between experiment and simulation (Fig. 2).

In many experimental situations, however, the anchoring of the LC is not expected to be strong.

To explore the consequences of “weak planar anchoring”, we performed a series of numerical simulations in this limit. We used the splay-bend order parameter (S_{SB}), defined as a second derivative of the order tensor with respect to orientation to quantify the extent of splay and bend

deformations in the various droplet configurations. Inspection of Fig. 3 reveals that a weak planar anchoring energy allows droplets to adopt a perpendicular orientation at the surface, leading to a range of new LC droplet morphologies that have not previously been reported. Our results reveal that the magnitude of the anchoring energy of the cholesteric LC plays a central role in dictating the internal configurations of cholesteric droplets, and that changes in the

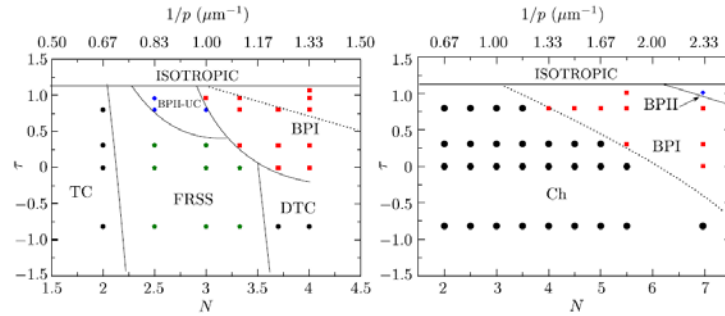


Figure 2 - (Left) Simulated phase diagram of chiral droplets with weak planar degenerate anchoring. The morphologies found in the diagram include the twist cylinder (TC) (see Fig.3a), the frustrated radial spherical structure (FRSS) (see Fig.3b), the deformed twist cylinder (DTC) (see Fig.3c), blue phase I (BPI) (see Fig.3e) and blue phase II (BPILUC) (see Fig.3d). The dashed line corresponds to the division between the cholesteric and BPI regions in the bulk for a chiral system. (Right) Phase diagram in the bulk.

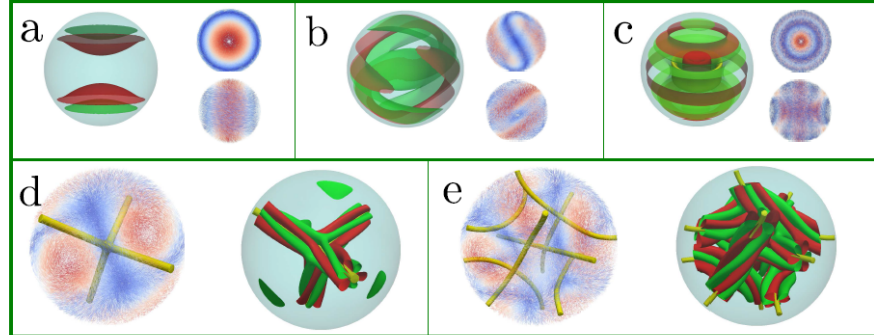


Figure 3 - Representative morphology of chiral LC droplets. For a, b and c, the splay-bend iso-surfaces for $S_{SB} = -0.0001$ and $S_{SB} = 0.0001$ are shown in red and green, respectively. We show the z-view (top) and lateral view (bottom) of the director field for a TC (a), FRSS (b) and DTC (c). The DTC configuration exhibits a defect region represented by the iso-surface with $S = 0.57$. For BPII (d) and BPI (e), the splay-bend iso-surfaces correspond to $S_{SB} = -0.001$ in red and $S_{SB} = 0.001$ in green, respectively, and rotate along the defect ($S = 0.35$).

anchoring energy provide a powerful approach for accessing a rich range of potential chiral templates for directing the self-assembly of nanoparticles. In addition, numerical simulations performed over the past year clearly establish that the experiments that we have performed to date correspond to the limit of strong anchoring.

Building from the results above, we have investigated how the morphologies of the chiral LC droplets impact localization of nanoparticles at their interfaces. Inspection of Figure 4 shows how the interactions of colloids with the disclinations of RSS droplets lead to their precise positioning (Figure 4). Surprisingly, we have observed that colloids can also be targeted to the center of cholesteric LC droplets (Fig. 4c). Ongoing investigations seek to understand the mechanism by which this occurs.

At high loadings of chiral dopant in a nematic LC, so-called blue phases (BP) form. These phases comprise well-defined three dimensional networks of double twisted cylinders. Between the double twisted cylinders, period arrays of defects appear (Fig. 5a and b). These periodic arrays of defects underlie many of the properties of BPs, including their optical appearance due to Bragg diffraction of visible wavelengths of light. Over the past year, we have conducted a synergistic experimental and computational study of BP confined to spherical droplets. As hypothesized in our original proposal to DOE, our results indicate that, in addition to the so-called BP I and II, several new morphologies arise under confinement. Our results also suggest

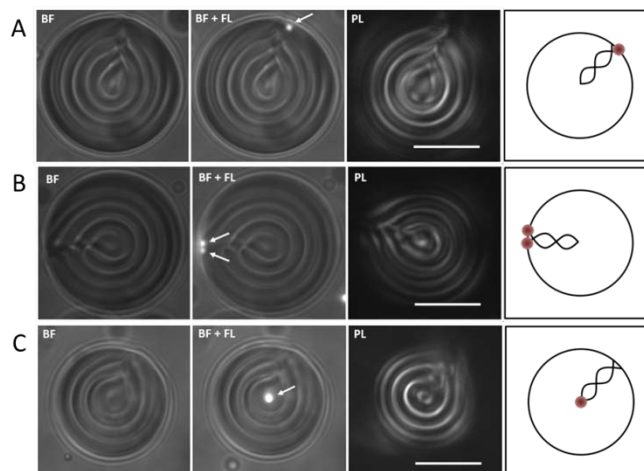


Figure 4. Bright field, fluorescence and cross-polarized light images of RSS droplets with (A) single-colloid and (B) two colloids localized on surface defects, and (C) single-colloid engulfed within the droplet. Scale bars: 10 μm .

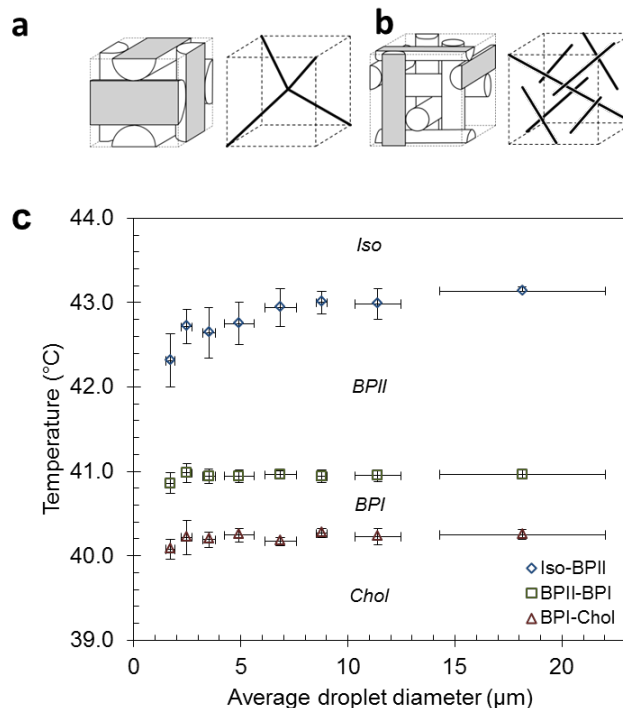


Figure 5. Organization of double-twist cylinders and defect lines in (a) BPI and (b) BPII. Phase transition temperatures of 37.5 wt% S-811 doped MLC 2142 confined within droplets of differing size.

that confinement increases the range of stability of BP, thereby providing intriguing prospects for applications.

As shown in Fig. 6, we have made the first observations of BP monodomains formed in aqueous dispersions of LC droplets. Quantitative analysis of the wavelength and intensity of the light diffracted from the BP droplets shown in Fig. 6a-c revealed a strained BP lattice (Fig 6d-f), which has also been confirmed using simulations (Fig. 6g). Interestingly, we have made the additional observation that the coassembly of biological lipids with BP droplets can change the internal morphologies of the BP droplets, which is evident in the Bragg diffraction of light from the droplets (Fig. 7).

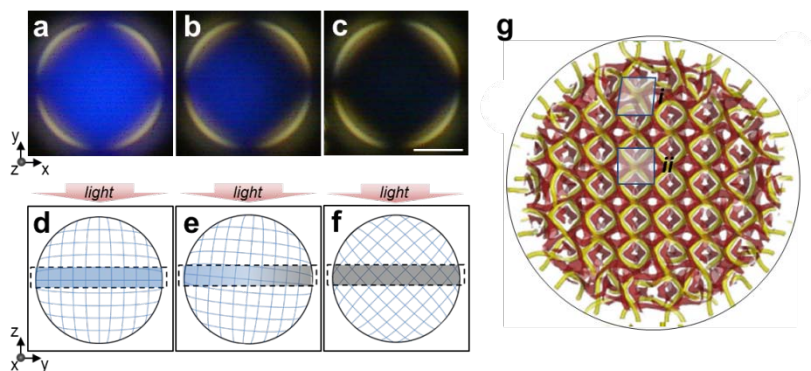


Figure 6. (a-c) Optical appearance of a rotating BPII droplet at 41.0 °C. Scale bar: 10 μm . (d-f) 2D sketches of the internal organization (orientation of unit cells) of BPII droplets with respect to the incident light. (g) A snapshot of a BPII droplet from computer simulations. Yellow lines indicate the defect lines of BP, and red regions are splay-bend isosurfaces corresponding to $S_{\text{SB}} = -0.001$.

Overall, these results reveal that chiral LC droplets are remarkably rich in terms of the range of morphologies and defects that can form within the LC droplets. Such findings are particularly promising in the context of the broader goals of our DOE project, as defects play a central role in mediating the interactions of LCs and nanoparticles. Thus our results to date support the key concept that chiral LC droplets represent a promising class of templates for directing the organization of nanoparticles.

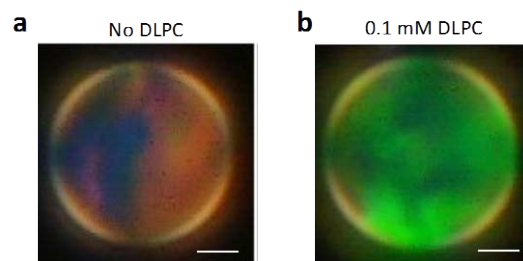


Figure 7. Optical appearance of droplets of BP at a temperature corresponding to BPI (40.0 °C). Droplets were incubated in (a) water, and (b) 0.1 mM DLPC. Scale bars: 5 μm .

Future Plans

Future plans will include experiments and complementary simulations to explore the influence of molecular adsorbates on the structure of BP droplets to understand how adsorbates stabilize the orientation/periodicity of defect lattice. We will also investigate the effects of ions on the structure of cholesteric droplets as an experimental approach to realizing weak anchoring energies, and compare observations to simulations shown in Fig 3 of this extended abstract. We also plan to continue our studies of the studies of the “positioning” of achiral nanoparticles with cholesteric and BP droplets via both simulation and experiment.

Publications

Rahimi, M.; Roberts, T. F.; Armas-Pérez, J. C.; Wang, X.; Bukusoglu, E.; Abbott, N. L.; de Pablo, J. J., Nanoparticle Self-assembly at the Interface of Liquid Crystal Droplets. Proceedings of the National Academy of **Sciences** **2015**, 112, 5297-5302

“Homeotropic Nano-Particle Assembly on Degenerate Planar Nematic Interfaces: Films and Droplets”, Londono-Hurtado, A; Armas-Perez, JC; Hernandez-Ortiz, JP; de Pablo, JJ, *Soft Matter*, 11(25), 5067-5076, 2015.

“Nematic-Field-Driven Positioning of Particles in Liquid Crystal Droplets”, Whitmer, JK; Wang, XG; Mondiot, F; Miller, DS; Abbott, NL; de Pablo, JJ, *Physical Review Letters*, 111 (22), 2013.

“Blue Phases of Chiral Liquid Crystals under Spherical Confinement,” Jose Adrian Hernandez, Ye Zhou, Mohammed Rahimi, Nicholas Abbott, Juan de Pablo, submitted for publication, 2015.

“Nanoparticle Localization in Chiral Liquid Crystal Droplets,” Ye Zhou, Jose Adrian Ramirez, Julio Armas, Nicholas Abbott and Juan de Pablo, submitted for publication, 2015.

“Effects of Confinement on the Structure of Blue Phases”, Emre Bukusoglu, Xiaoguang Wang, Juan de Pablo and Nicholas L. Abbott, submitted for publication, 2015.

“Modeling the Polydomain-Monodomain Transition of Liquid Crystal Elastomers”, Whitmer, JK; Roberts, TF; Shekhar, R; Abbott, NL; de Pablo, JJ, *Physical Review E*, 87(2), 2013.

“Dynamics of the Chemo-Optical Response of Supported Films of Nematic Liquid Crystals”, Hunter, JT; Abbott, NL, *Sensors and Actuators B - Chemical*, 183, 71-80, 2013.

“Liquid-Crystal Mediated Nanoparticle Interactions and Gel Formation”, Whitmer, JK; Joshi, AA; Roberts, TF; de Pablo, JJ, *Journal of Chemical Physics*, 139(19), 2013.

Program Title: Harnessing Chemo-mechanical Energy Transduction to Create Systems that Selectively Catch and Release Biomolecules

Principle Investigator: Prof. Joanna Aizenberg¹ (jaiz@seas.harvard.edu); Co-PI: Prof. Anna Balazs² (balazs@pitt.edu); Subcontractor: Dr. Ximin He³ (Ximin.He@asu.edu)

Mailing Address: ¹John A. Paulson School of Engineering and Applied Sciences, Harvard University, Cambridge, MA 02138; ²Department of Chemical and Petroleum Engineering, University of Pittsburgh, Pittsburgh, PA 15261; ³Materials Science and Engineering, Arizona State University

Program Scope

We are pursuing the design and creation of biomimetic and bioinspired integrated systems, in which man-made materials utilize biomimetic coupling of chemical and mechanical energy provided by a responsive gel, with the feedback to the embedded microstructures being a centerpiece of the energy conversion. We are also looking broadly at engineering modularity and tunability into the individual components of these integrated systems, namely gels and microstructure arrays. The critical issue in designing new materials, that are both functional and borrow concepts from biology, is establishing design rules for making the materials adaptive; that is, we must determine how to engineer responsiveness to environmental changes and the ability to perform important functions into the framework of the material. In our studies, the components are integrated to enable adaptive functionality and encompass feedback. Notably, biological systems use feedback as a crucial component to provide efficient performance. Yet, the use of feedback has not been exploited to a sufficient extent in the design of new materials systems and it remains a highly desirable target¹.

The specific goal of this project is to create dynamically reconfigurable surfaces that interconvert chemical and mechanical energy and thereby exhibit unprecedented adaptive and self-regulating behavior. We aim to utilize a variety of environmental cues as stimuli, including temperature, pH, humidity, light, biomolecules, salt, magnetic and electric fields, redox state, etc. The inspiration for these studies comes from the stunning sensitivity and efficiency of such biological structures as the cilia on single cells, the pedicellaria and spines on the skin of echinoderms and sensors on the legs of spiders. These hair-like structures act as mechanochemical receptors that can extract meaningful information from a noisy environment, and allow the organisms to respond, adapt and move essentially instantaneously. It is this exceptional performance in biological mechanochemical systems that inspire our efforts to engineer the next-generation of adaptive, self-regulating materials and devices with energy transduction at their core.² The far-reaching goal is to harness the chemo-mechanical energy transduction to develop materials capable of structural reconfiguration that triggers responsive changes in chemistry, wetting behavior, affinity for biological molecules, optical or thermal properties among others.^{3,4} We have recently developed self-regulated mechanochemical adaptively reconfigurable tunable systems (SMARTS),⁵ which created built-in chemo-mechano-chemical ($C \rightleftharpoons M$) feedback loop and demonstrated autonomous, self-sustained regulation of local condition such as temperature. By further expanding on this platform and beyond, we have recently explored several different modes of chemo-mechanical modulation for a variety of purposes, including: chemo-mechanically regulated oscillation of an enzymatic reaction; catching and releasing target proteins for energy-efficient separation; self-regulation of material surface property and material healing. Many of the aspects and features of this platform have been recently summarized in a detailed account.⁶

The program capitalizes significantly on synergy and cross-pollination between the broad expertise of Aizenberg group in material chemistry and mechanics, polymer

synthesis, biochemistry, fabrication of micro/nanomaterial systems, characterization techniques, and extensive expertise of Balazs group in theoretical modeling and computational simulation.

Recent Progress

1) Chemomechanically Regulated Oscillation of Biomolecular Reaction.⁷ We have utilized the robustness of the chemo-mechanical transductions in the system to efficiently sort and transport biomolecules from a solution mixture (e.g. $C1 \rightarrow M \rightarrow C2$ where $C2$ is a biochemical or binding process), with inspiration drawn from vesicle-carrying kinesins and dyneins that shuttle different biomolecules along the microtubule network. High-aspect-ratio epoxy microfins decorated with an enzyme and partially embedded in a hydrogel reversibly actuate as the gel swells/contracts in response to a chemical stimulus ($C1$) (Fig.1). When tuning the pH of the lower fluid, this actuation (M) moves the enzyme on the microfin tips into and out of a top “nutrient” layer of reactants, such that the reaction ($C2$) of the enzyme and reagent luciferase is turned on and off, realizing a synchronized bioluminescence oscillation via the cascade of chemo-mechanical energy inter-conversions ($C1 \rightarrow M \rightarrow C2$).^{6, 8-10} The potential variety of switchable biochemical reactions can be tailored to a wide range of stimuli, representing an important step toward biomimetic, responsive materials and paving the way for more applications in minituarized energy-efficient biomimetic sensors with novel readouts.

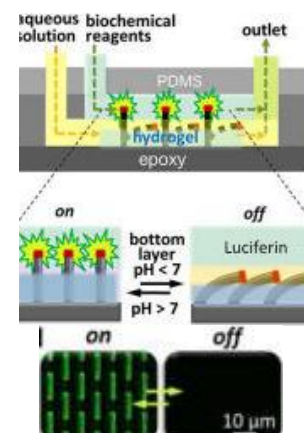


Fig.1 Schematic and dynamic light emission of a mechanically controlled bioluminescence reaction.

2) Protein Catch and Release by Aptamer-functionalized Adaptively Reconfigurable Systems¹¹ A major goal is to further expand the capabilities of the reconfigurable SMARTS for biomolecular material

applications, while concurrently developing the computational methods to describe enhancements made to the system. The efficient extraction of (bio)molecules from fluid mixtures is vital for a variety of applications, including energy-efficient means of removing waste from the environment as well as capturing valuable minerals or other resources from fluid mixtures. Inspired by biological processes that seamlessly synchronize the capture, transport and release of biomolecules, we designed a robust chemomechanical sorting system capable of the concerted catch and release of target biomolecules from a solution mixture. (Fig. 2) We functionalized the SMARTS with

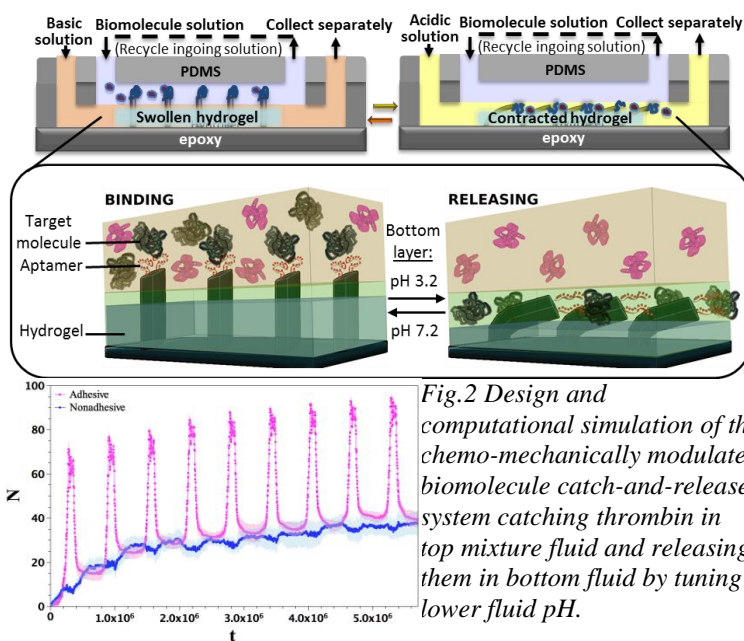


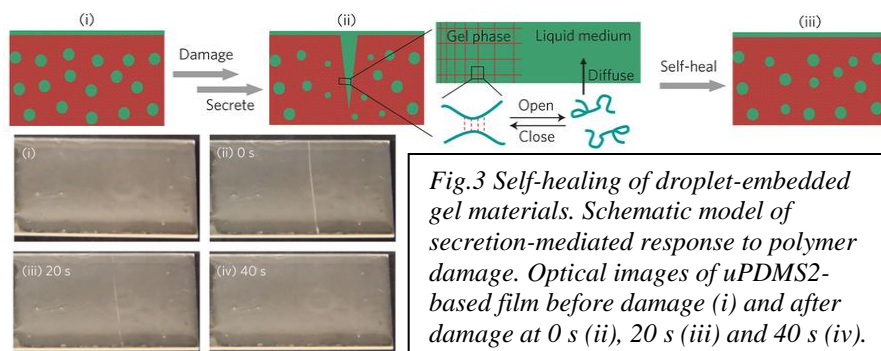
Fig.2 Design and computational simulation of the chemo-mechanically modulated biomolecule catch-and-release system catching thrombin in top mixture fluid and releasing them in bottom fluid by tuning lower fluid pH.

specific protein-binding DNA aptamer on the microfin tips. The designed system demonstrated effective separation of thrombin by synchronizing the pH-dependent binding strength of a thrombin-specific aptamer with volume changes of the pH-responsive hydrogel in a biphasic microfluidic regime, and showed a non-destructive separation that has a quantitative sorting efficiency, as well as the system’s stability and amenability to multiple solution recycling. It achieved almost quantitative recovery of thrombin in an eight-pass recycle, and a very high specificity for thrombin collection over other proteins, as well as in the real complex biofluid,

human serum. The variability and tunability of the hydrogel, aptamer-binding strength, geometry and material of the microstructure, and flow characteristics make this system a broad-based, customizable platform for multiple applications. Computational simulation results captured the key features of the process and allowed us to assess the contributions of different variables. The process could ultimately be tailored to allow for purification or desalination of water to the desired purity.

3) Autonomous Self-regulation of Material Surface Property and Material Healing¹² Approaches for regulated fluid secretion, which typically rely on fluid encapsulation and release from a shelled compartment, do not usually allow a fine continuous modulation of secretion, and can be difficult to adapt for monitoring or function-integration purposes.

They also often require energy input for pumping or otherwise transporting the fluid to desired locations. We have designed self-regulated, self-reporting systems that consist of liquid-storage compartments in a



supramolecular polymer-gel matrix with a thin liquid layer on top, and demonstrated that dynamic liquid exchange between the compartments, matrix and surface layer allows repeated, responsive self-lubrication of the surface and cooperative healing of the matrix (Fig. 3). Depletion of the surface liquid or local material damage induces secretion of the stored liquid via a dynamic feedback between polymer crosslinking, droplet shrinkage and liquid transport that can be read out through changes in the system's optical transparency. We foresee diverse applications in on-demand fluid delivery, wetting, lubricity and adhesion control, and material self-repair.

Future Plans

(1) Cell Capture and Release with Aptamer-functionalized SMARTS We will further explore the mammalian cells separation by SMARTS. We plan to use leukemia T-lymphoblast cells to prove the versatility of our system. We will carry out experiments to characterize the capacity of the microdevice to capture the cells with optimized flow rate, as well its selectivity for the CCL-119 cells over other cell types. We will measure the capture/release capacity, sorting efficiency through repeated actuation cycles, and selectivity of cell-sorting. Detailed computer simulation work analyzing a parameter space determining performance of such systems is in progress.

(2) Light-responsive Hydrogel for Local Actuation of a Hydrogel-embedded Microstructure Array

Aiming to broaden the capabilities of our hydrogel-actuated integrated responsive system, we are working to expand the different types of responses the system can be sensitive to from pH, temperature, humidity, to light. With the ability to actuate by light, we aim to introduce resolved, local actuation defined by the light beam width on the sample. In order to achieve this, we will add a light-responsive moiety, a benzospiropyran, and graft the molecule onto the backbone of the pH responsive hydrogel (e.g., by free radical polymerization). We aim to achieve the light-induced actuation by a laser source, which irradiates in the visible range.

(3) Electric Stimuli-responsive Hydrogel-Actuated Integrated Responsive Systems (HAIRS).

To add another new functionality to our systems, we plan to develop HAIRS that are responsive to electric stimuli. For example, crosslinking a polyacrylic acid hydrogel upon complexation of the carboxylic

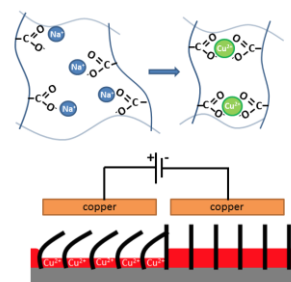


Fig.4 Schematic of copper-mediated electric stimuli-responsive HAIRS

acid groups with Cu^{2+} -ions that are introduced via a positively charged copper-electrode will allow us to actuate the microstructures locally, independent of pH- or temperature and such that the system “memorizes” the stimulus. The reverse action (swelling) should be possible to obtain upon removal of the Cu^{2+} -ions with either a negative copper-electrode or upon extraction of Cu^{2+} with a ligand (Fig. 4).

4) Guiding the Out-of-equilibrium Assembly of Elongated Bilayer Assemblies via Microstructures. We aim to assemble simple surfactant molecules into lipid bilayers that form long, cylindrical vesicles and eventually highly complex myelin structures. To control and direct the growth of these elongated assemblies, their formation will be confined by applying micro-sized channels, i.e. microplates positioned on a substrate such that 1D channels are formed. Our elongated assemblies are envisioned to resemble a number of naturally occurring high-aspect ratio objects. Whereas in nature the growth of these structures is generally facilitated by the energy-dissipating phenomena like the cytoskeleton build-up, here the out-of-equilibrium assembly is driven by an osmotic pressure gradient of lipid bilayer swelling. We foresee that the out-of-equilibrium growth of these structures will provide new strategies in microfluidics, drug-delivery and energy technologies by facilitating transport phenomena beyond Brownian motion.

References

1. Stuart, M. A. C.; Huck, W. T. S.; Genzer, J et al. “Emerging applications of stimuli-responsive polymer materials.” *Nature Materials* 9, 101-113, 2010.
2. Sidorenko, A.; Krupenkin, T.; Taylor, A.; Fratzl, P.; Aizenberg, J. “Reversible Switching of Hydrogel-Actuated Nanostructures into Complex Micropatterns.” *Science* 315, 487-490, 2007.
3. Kim, P.; Zarzar, L. D.; Zhao, X.; Sidorenko, A.; Aizenberg, J. “Microbristle in gels: Toward all-polymer reconfigurable hybrid surfaces.” *Soft Matter* 6, 750-755, 2010.
4. Zarzar, L. D.; Liu, Q.; He, X.; Hu, Y.; Suo, Z.; Aizenberg, J. “Multifunctional actuation systems responding to chemical gradients” *Soft Matter* 8, 8289-8293, 2012.
5. He, X., Aizenberg, M., Kuksenok, O., Zarzar, L. D., Shastri, A., Balazs, A. C., Aizenberg, J. “Synthetic homeostatic materials with chemo-mechano-chemical self-regulation” *Nature* 487, 214-218, 2012
6. Zarzar, L. D.; Aizenberg, J.. “Stimuli-Responsive Chemomechanical Actuation: A Hybrid Materials Approach” *Acc. Chem. Res.* 47, 530-539, 2014.
7. He, X.; Friedlander, R. S.; Zarzar, L. D.; Aizenberg, J. “Chemo-Mechanically Regulated Oscillation of an Enzymatic Reaction” *Chem. Mater.* 25, 521-523., 2013.
8. Grinthal, A. Kang, S. H.; Epstein, A. K.; Aizenberg, M., Khan, M., Aizenberg, J. “Steering nanofibers: An integrative approach to bio-inspired fiber fabrication and assembly” *Nano Today* 7, 35-52, 2012.
9. Grinthal, A., Aizenberg, J. “Adaptive all the way down: Building responsive materials from hierarchies of chemomechanical feedback” *Chem. Soc. Rev.* 42, 7072-7085, 2013.
10. Grinthal, A., Aizenberg, J. "Hydrogel-Actuated Integrated Responsive Systems (HAIRS): Creating Cilia-like "Hairy" Surfaces" *Artificial Cilia* (ed.: J. den Toonder, P. Onck) RSC, Cambridge, U.K., 162-185 (2013).
11. Shastri, A., McGregor, L. M., Liu, Y., Harris, V., Nan, H., Mujica, M., Vasquez, Y., Bhattacharya, A., Ma, Y., Aizenberg, M., Kuksenok, O., Balazs, A. C.; Aizenberg, J., He, X. “An aptamer-functionalized chemomechanically modulated biomolecule catch-and-release system” *Nature Chem.* 7, 447-454, 2015.
12. Cui, J., Daniel, D., Grinthal, A., Lin, K., Aizenberg, J. "Dynamic polymer systems with self-regulated secretion for the control of surface properties and material healing" *Nature Mater.* 2015, doi:10.1038/nmat4325

Publications (2-year list, supported by DoE BES)

1. Shastri, A., McGregor, L. M., Liu, Y., Harris, V., Nan, H., Mujica, M., Vasquez, Y., Bhattacharya, A., Ma, Y., Aizenberg, M., Kuksenok, O., Balazs, A. C.; Aizenberg, J., He, X. "An aptamer-functionalized chemomechanically modulated biomolecule catch-and-release system" *Nature Chem.* 7, 447-454, 2015.
2. Cui, J., Daniel, D., Grinthal, A., Lin, K., Aizenberg, J. "Dynamic polymer systems with self-regulated secretion for the control of surface properties and material healing" *Nature Mater.* 2015, doi:10.1038/nmat4325
3. Hashmi, B., Zarzar, L. D., Mammoto, T., Mammoto, A., Jiang, A., Aizenberg, J., Ingber, D. E. "Developmentally-Inspired Shrink-Wrap Polymers for Mechanical Induction of Tissue Differentiation" *Adv. Mater.* 26, 3253-3257, 2014.
4. Zarzar, L. D.; Aizenberg, J. "Stimuli-Responsive Chemomechanical Actuation: A Hybrid Materials Approach" *Acc. Chem. Res.* 47, 530-539, 2014.
5. He, X.; Friedlander, R. S.; Zarzar, L. D.; Aizenberg, J. "Chemo-Mechanically Regulated Oscillation of an Enzymatic Reaction" *Chem. Mater.* 25, 521-523., 2013.
6. Grinthal, A., Aizenberg, J. "Adaptive all the way down: Building responsive materials from hierarchies of chemomechanical feedback" *Chem. Soc. Rev.* 42, 7072-7085, 2013.
7. Grinthal, A., Aizenberg, J. "Hydrogel-Actuated Integrated Responsive Systems (HAIRS): Creating Cilia-like "Hairy" Surfaces" *Artificial Cilia* (ed.: J. den Toonder, P. Onck) RSC, Cambridge, U.K., 162-185 (2013).
8. Liu, Y., Bhattacharya, A., Kuksenok, O., He, X., Aizenberg, M., Aizenberg, J., Balazs, A. C. "Utilizing Oscillating Fins to "Catch and Release" Targeted Nanoparticles in Bilayer Flows", *ACS Nano*, *submitted*.
9. Liu, Y., Yong, X., McFarlin, G. IV, Kuksenok, O., Aizenberg, J., Balazs, A. C. "Designing a Gel-Fiber Composite to Extract Nanoparticles from Solution" *Soft Matter*, *submitted*.

Biomimetic Templated Self-Assembly of Light Harvesting Nanostructures

Alfredo Alexander-Katz, Department of Materials Science and Engineering, MIT.

Program Scope

In this project we are interested in studying computationally the self-assembly of antenna-like structures with very specific features using block copolymers as templates. This system mimics naturally-occurring ultra-efficient light harvesting antennas found in Green Sulfur Bacteria, so-called Chlorosomes. The complex organization of these antennas, which are composed of small organic chromophores (BacterioChlorophyll C in this case) is dictated by the shape of the mesostructure as well as the internal interactions between the chromophores themselves and the polymer-chromophore interactions. With this in mind, the overall aim of this project is to find which are the design rules for creating tailored antenna-like assemblies. Such design rules will be important not only for forming light harvesting antennas, but to understand self-assembly of different nano objects under confinement in general.

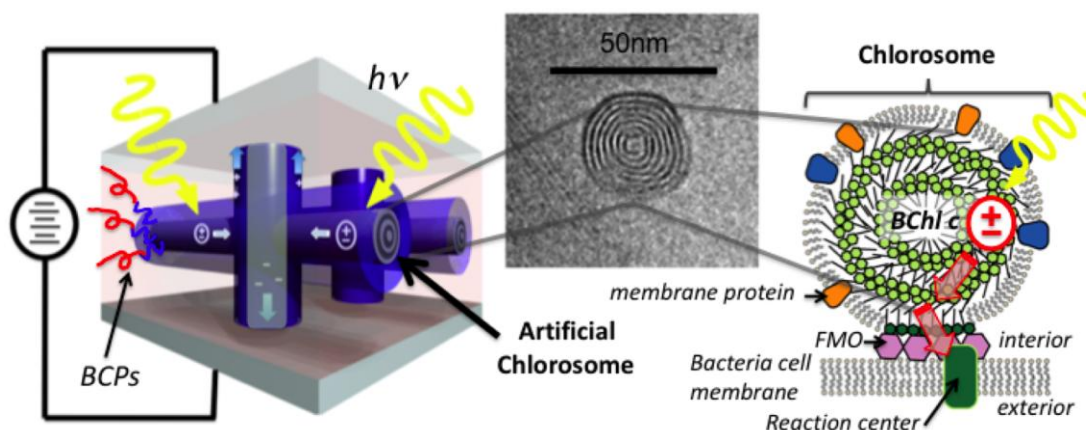


Figure 1. **Conceptual illustration of Biomimetic Self-Assembled Light Harvesting Nanostructures.** Block copolymers will template the self-assembly of a supramolecular dye aggregates (concentric cylinders within the blue phase in the sketch at the left). Notice that this approach is equivalent to that utilized by nature to assemble the chlorosome where a single lipid layer templates the assembly of hundreds of thousands of Chlorophyll molecules (right). A cryo-TEM image is provided in the center panel. In the future, we can construct biomimetic devices that could convert light into electricity (left sketch).

In particular, the specific objectives of this program are to i) understand block copolymer templated supramolecular assembly, ii) control the spatial location and morphology of the supramolecular structures based on the template, and iii) understand under what conditions such assemblies can occur based on the physical properties of the dyes and the polymers.

Recent Progress

Our program has recently focused on parts i and ii. We have found that defects in the block copolymer (BCP) templates can serve as attractors for nano objects inside such BCP microphases. This provides a route to localize such nanomaterials (e.g. chromophores) in very particular locations. Such BCP defects can be induced by a template in the so-called top-down approach. Furthermore, the shape of the nano object is quite important and allows one to not only localize it, but have a preferential orientation. In this respect, we have found what are the preferred orientations for different chromophore structures such as rods (short stiff highly conjugated organic molecules) or disks (planar conjugated organic molecules, as porphyrin or nanographene). Such molecules also have preferred orientations confined in the cylindrical phase of BCPs, yet the confinement is quite soft and such objects are able to fluctuate. Our first studies in this area where performed using a self-consistent formalism (known as SCFT) for the polymers, while the nano objects where placed as boundary conditions. This is a mean-field approach and allows us to find the free energies of the system, yet it does not include fluctuation effects. To find how the system evolves one needs to compute a large number of nano object orientations and positions and interpolate the solutions. Furthermore, it is necessary to perform a true multiscale simulation because the boundaries between the object and the BCPs need to be resolved for numerical accuracy. We have used a hybrid Lattice Boltzmann approach, originally developed in our group, to achieve such resolutions. An example of what is possible is shown in Fig. 2.

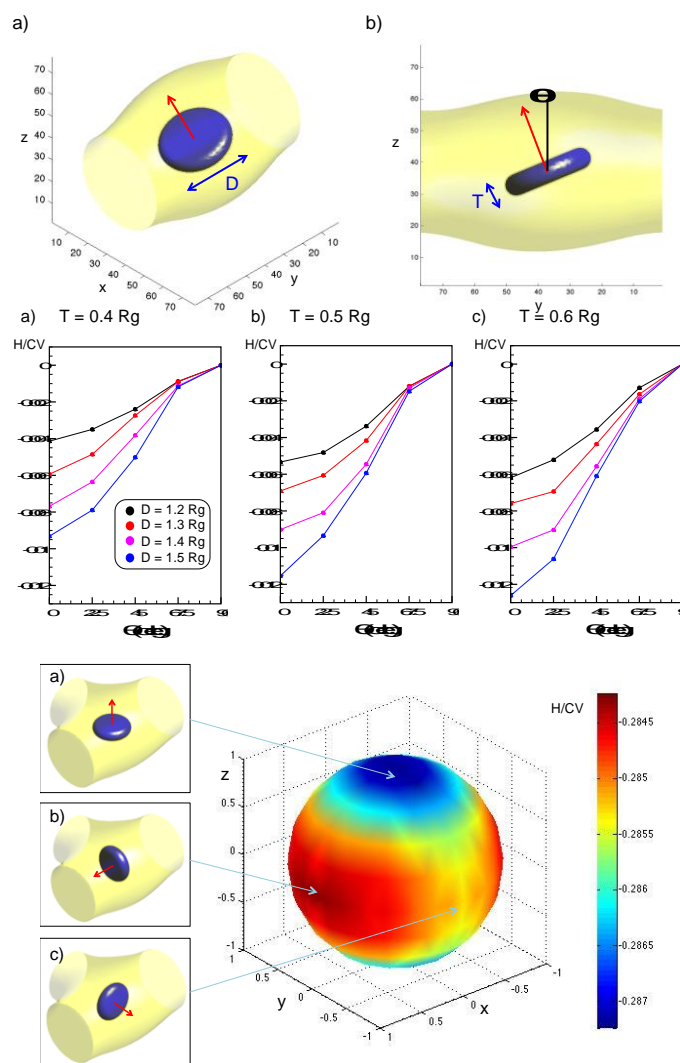


Figure 2. (Upper row) Schematic of a disk in a cylindrical phase of a block copolymer. (Middle row) The preferred orientation of a single disk confined within a cylindrical morphology is always perpendicular to the axis of the cylinder. (Lower row) 3D angular free energy landscape of a disk in a model T junction point. Notice that the position and the orientation of the disk is constrained at the core of the defect.

While such a description of the system is useful, it has many problems when a many body assembly is to be studied due to intrinsic long relaxation times for the density and chemical fields as one changes the configuration of the system. To overcome this we have implemented a biased Monte Carlo method where we can study from single chromophores to highly dense systems. The single molecule results utilizing this method are in excellent agreement with the

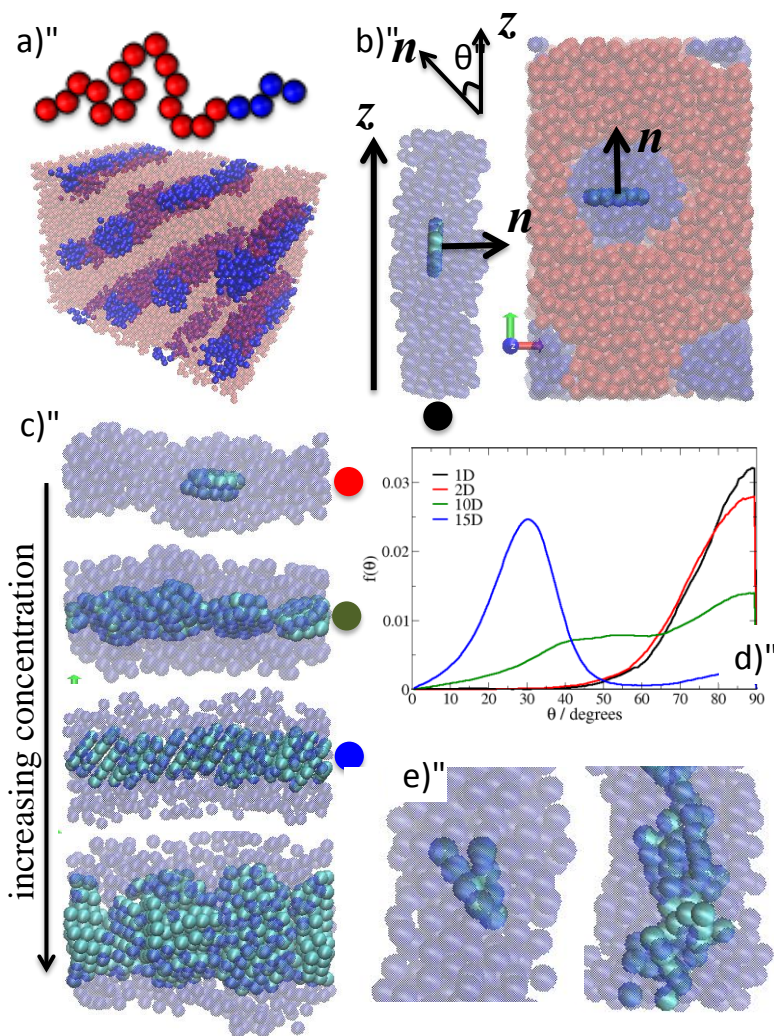


Figure 2. Biased Monte Carlo results on supramolecular self-assembly. a) Schematic of the block copolymer chain used in the simulations, and snapshot of the self-organization of the system. b) Single disk in cylinder. The different vectors correspond to the normal to the disk \mathbf{n} , and the axis of the cylinder \mathbf{z} . The angle between both of these vectors is denoted by θ . c) Snapshots of different concentrations of disks within one cylinder. The colored dots are for reference to part d). Notice the stacking and change in orientation of the disks. d) The probability distribution of the angle θ for different concentrations of disks. e) Preliminary results on the interactions and ordering of rod like chromophores. Notice that compared to disks, rods are not ordered.

SCFT results, and show interesting many body physics for the dense systems. In particular we found a strong depletion attraction for disk-like molecules mediated by the BCP chains that leads to stacks oriented perpendicular to the axis of the confining soft channel, which in this case is a cylinder corresponding to the minority phase of the BCP. As the density is increased we have observed a transition into a tilted phase and a reentrant transition into a dense array of stacks. Some of these results can be found in Figure 3.

Besides this, we have also established the tolerance limits of top-down approaches for BCP self assembly, and have developed extremely fast LB codes that have been used for BCP calculations and fluid dynamics calculations as well.

Future Plans

In the next year we will continue to study the self-assembly of disks and rods in BCP matrices. However, we will include specific interactions from molecular models. In particular we will focus more and more in porphyrins, and the interactions arising in this class of molecules. Competition between polymer-induced and specific chemical interactions in such molecules promise to yield a complex and rich self-assembly landscape.

Publications

- 1.- **Artificial tribotactic microscopic walkers: walking based on friction gradients**, J. Steimel, J. L. Aragoes and A. Alexander-Katz, *Phys. Rev. Lett.* **113**, 178101 (2014).
(Highlighted in Physics from the American Physical Society)
- 2.- **Anisotropic nanoparticle distribution in block copolymer model defects**, YJ. Kim and A. Alexander-Katz, (2015) in revision.
- 3.- **Limits on Template Tolerance in Directed Self Assembly of Block Copolymers**, Y. Ding, R. Pablo-Pedro, K. R. Gadelrab, H. Chen, K. Gotrick, D. Tempel, V. Vitelli, C. Ross, and A. Alexander-Katz, (2015) to be submitted.

Design and Synthesis of Structurally Tailored and Engineered Macromolecular (STEM) Gels

PI: Anna C. Balazs, University of Pittsburgh; Co-PI: Krzysztof Matyjaszewski, Carnegie Mellon University

Program Scope.

Our goal is to take full advantage of controlled/living polymerization techniques to develop a new platform of “living” hierarchical polymeric materials with broadly tunable chemical composition, structure and function based on chemical modification of precursor molecular frameworks comprised of swollen polymer gels. The framework backbone of these gels contains initiation sites for further grafting (polymerization) of an extremely broad range of modifying components, and thus, serves as a “stem” for functional branching (see **Fig. 1**). This, in turn, facilitates further diversification of the precursor material’s structure and function. Given our aim to create *structurally tailored and engineered macromolecular* gels, we refer to these materials as “stem” gels. The name also reflects the “stem-branch” architecture, which ultimately enables the material to exhibit a remarkably diverse range of functionalities.

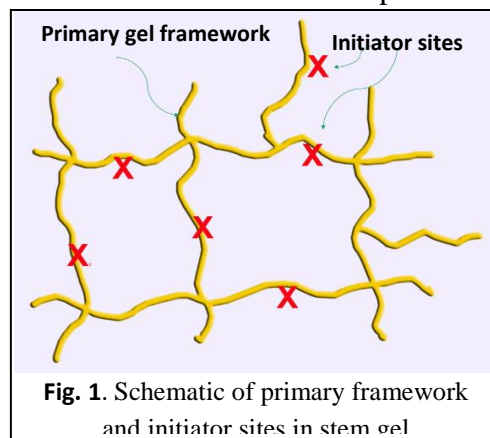


Fig. 1. Schematic of primary framework and initiator sites in stem gel

The studies are *inspired by the structural hierarchy found in biological materials* that involves the seamless integration of multiple components into one construct, which enables the system to perform remarkably complex and adaptive behavior. Motivated by this principle, we aim to design and synthesize a single material that encompasses an analogous and useful level of interlocking hierarchical structures. In the proposed stem gels, the primary structural elements (the frameworks) are covalently linked to the secondary structural elements (e.g., dangling chains). Importantly, both of these elements can be readily tailored to achieve the desired properties or global behavior. In this respect, the stem gels provide a remarkable level of adaptability. Moreover, each element can be stimuli-responsive, and hence, the stem gel can exhibit collective behavior that might not be achieved without the interlocking of the constituent parts. Finally, the stem gel is a “living” material, which can be dynamically modified, and thus, tailored “on demand” to meet new needs for new applications.

From the chemist’s perspective, the decision about material composition is typically taken as a first step, dictating the choice of ingredients and reactions used to achieve the final goal. Further tuning of materials’ composition is then usually achieved through physical means (e.g. by forming polymer blends, composites, etc.). Modification of the material’s composition *after* it has achieved its final physical form is usually greatly limited by its ability to accommodate additional ingredients. The departure point for the proposed study is the realization that this limitation is not present in swollen polymer networks, where the polymer “matrix” may comprise as little as 1% (by volume) of the material. We propose to undertake concerted synthetic, characterization and modeling studies aimed at extending the stem approach to a broad range of compositions, molecular architectures and length scales, and to explore some of its most promising applications.

Recent Progress

We recently combined modeling and experiments¹ to create multilayered gels where each layer is “stacked” on top of the other and covalently interconnected to form mechanically robust materials, which could integrate the properties of the individual layers (see **Fig. 2**). In this process, a solution of new initiator, monomer, and cross-linkers is introduced on top of the first gel and these new components then undergo living copolymerization to form the subsequent layer. We simulated this process using dissipative particle dynamics (DPD) to isolate factors that affect the formation and binding of chemically identical gel, as well as incompatible layers. We first investigated the polymerization kinetics and gelation processes of two-layer hydrophilic-hydrophilic gels. We

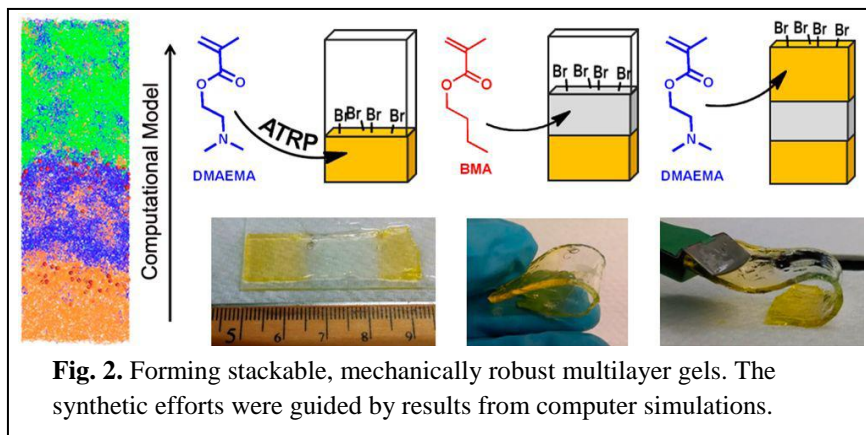


Fig. 2. Forming stackable, mechanically robust multilayer gels. The synthetic efforts were guided by results from computer simulations.

We characterized the interfacial strength between the layers by calculating the number of inter-gel cross-links. The findings indicated that the contribution of the active chain ends to the binding of the two layers at high conversion is dominant, as compared to that of residual cross-links with dangling vinyl groups. Hence, the analysis indicated that the covalent bond formation between the different layers is primarily due to reactive chain-ends, rather than residual cross-linkers.

Following the prediction from the computational modeling, we experimentally realized the two-layer gel system by the multi-step polymerization. Mechanical evaluation of the materials showed that both multi-layered gels prepared either by ATRP or FRP preserved their integrity. Their mechanical properties were slightly reduced in comparison with single layered gels. Experiments suggest that interpenetration between chemically identical layers created a sufficiently strong interface even in the gels with only residual vinyl bonds contributing to the inter-gel cross-links (FRP). Simulations suggest that gels with chemically incompatible layers prepared by ATRP in the same solvent should have a strong interface between the layers. This behavior is attributed to the formation of inter-gel cross-links between the first and second layer due to the preserved active chain ends from the first layer. Results of experimental studies support this mechanism. Namely, the three-layer composite gels prepared by ATRP preserved their connectivity upon bending, while the samples prepared by FRP broke. Thus, multi-layered gels prepared by ATRP are characterized by a stronger interface between layers than gels prepared by FRP.

Overall, our approach provides a robust route for designing multi-layered, “stackable” gels, where each subsequent layer is effectively “stacked” on top of the previous layer. With each gel layer being covalently bound to the neighboring layers, the system displays considerable mechanical integrity. Such robust “stackable” gels introduce two particularly advantageous features. First, we can formulate completely new materials where each layer encompasses a distinct property and thus, the composite material can exhibit a range of novel behavior. In other words, we can compartmentalize different functionalities into the different layers and incorporate a new functionality by simply adding a new layer. Second, the approach allows us to repair the

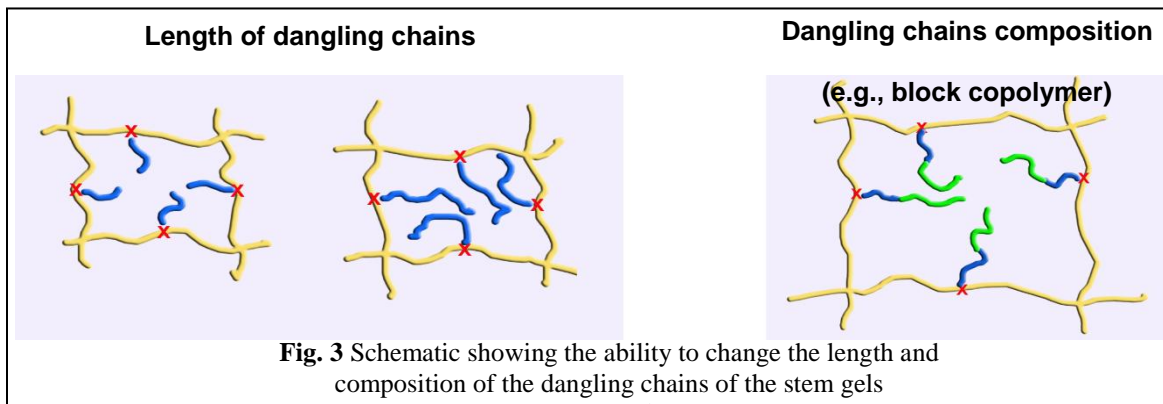
gel if layers are severed. Notably, the new layer can be grown from the living chain ends in the existing underlying layer. This process ensures the formation of covalent bonds between the different layers, and thus, the creation of strong interfaces between the different layers.

Future Plans

We will extend the approach described above to bind alternating multi-layer stacks of hydrophilic and hydrophobic gels. The challenge in developing these versatile systems is creating strong interfaces between the chemically different layers. We will investigate the use of miktoarm stars as a “glue” to bind two separate incompatible gels, and thereby, establish a powerful means of combining the distinct layers. We will also establish routes for introducing nanoparticles into specific layers. Hence, the system could encompass alternating layers of particle-filled and non-filled gels. Moreover, the different layers can contain different particles. Depending on the thickness of the layers, the system could display remarkable optical properties, and thus, be used for novel photonic applications. On the mesoscopic scale, the alternating layers of filled and unfilled gels could exhibit novel mechanical behavior. To the best of our knowledge, such stackable composite gels have not been fabricated and thus, we have a unique opportunity to uncover as yet unexplored behavior.

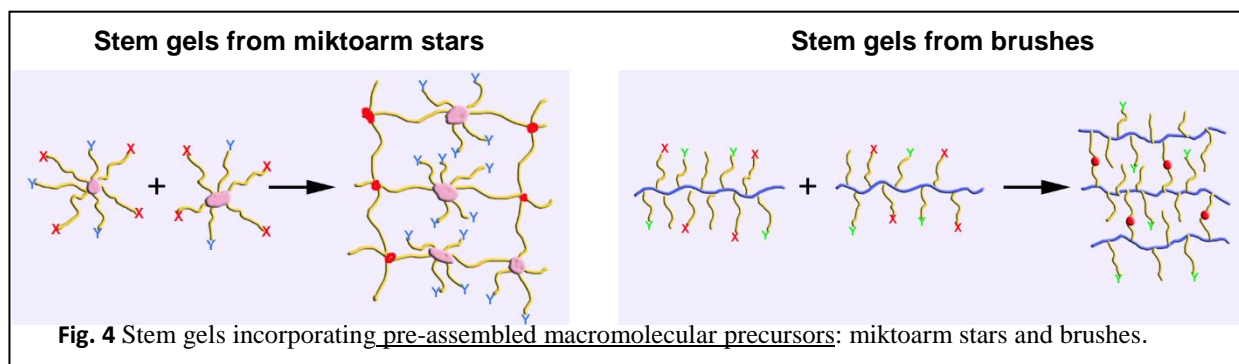
Moving forward, we will consider the following systems:

1. Stem gels comprised of cross-linked linear polymers Precise control of the characteristics of these gels will be made possible through the use of controlled radical polymerizations (CRPs) such as atom transfer radical polymerization (ATRP). Use of CRPs will also facilitate control over the composition of the secondary elements of the stem gels, i.e., the dangling chains that emanate from the framework. In particular, with respect to the dangling chains, we will establish approaches for controlling the following features (see **Fig. 3**): chemical structure (hard, soft, crystallizable, hydrophilic, hydrophobic, or thermo-responsive behavior), length, shape (linear or branched) and composition (block, statistical, periodic, and gradient structures).

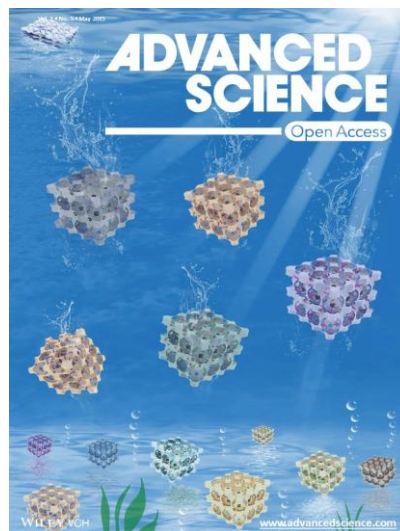


With respect to the bulk composition of the material, we will create systems with either uniform or non-uniform composition. Notably, non-uniform and asymmetric compositions can be of particular interest in applications such as mechanotransduction and separations. One potentially straightforward way of achieving asymmetric concentrations of the dangling chains will be based on the control of the diffusive monomer feed into the pre-formed stem gel matrix. More complex spatial control and 3-D patterning will be achieved by light-activated initiator sites.

2. Control of stem gel architecture and nanostructure through the use of pre-assembled macromolecular precursors In addition to the structures indicated above, we will attempt to create stem gels with more complex architectures and hierarchical nanostructures, and thereby, introduce greater functionality into these systems. One means of accomplishing this goal is through the addition of pre-assembled precursors to the framework structure. Here, we will focus on two major types of such precursors: stars and polymer brushes (see **Fig. 4**), both of which can be readily prepared using CRPs. We will also study systems where the miktoarm stars form the fundamental units in the system; namely, they are cross-linked to form the stem gel. Of particular interest are the systems where a nanoparticle forms the core of the star, and hence, the system forms the polymer-grafted nanoparticle (PGN) networks. The synthesis of these PGN networks will allow us to test our theoretical predictions from the last funding period on the self-healing behavior of such composite materials.



3. Multifunctional hydrogels with reversible 3D ordered macroporous structures Hydrogels were prepared by colloidal crystals templating with unique three-dimensionally ordered macroporous (3DOM) structures.² (The work was featured on the cover of the issue—see image on the right.) The highly reversible macroporous structures and intrinsic shape memory properties of 3DOM hydrogels were demonstrated for the first time. Two approaches were utilized for the characterizations of 3DOM structures: one procedure was electron microscopy imaging of their inverse replicas, and the other was non-invasive and non-destructive nano-scale resolution X-ray microscopy imaging of the hydrated hydrogels. The 3DOM hydrogels are promising as robust platforms for constructing novel functional materials with preselected properties targeting a wide range of applications, including thermoresponsive systems, fluorescent, magnetic, electrically conductive, catalytic and biorelated materials



Publications supported by this grant (which started Jan. 2015)

1. Yong, X., Simakova, A., Averick, S., Gutierrez, J., Kuksenok, O., Balazs, A.C., and Matyjaszewski, K., “Stackable, Covalently-Fused Gels: Repair and Composite Formation”, *Macromolecules*, **48** (2015) 1169-1178.
2. He, H.; Averick, S.; Mandal, P.; Ding, H.; Li, S.; Gelb, J.; Kotwal, N.; Merkle, A.; Litster, S.; Matyjaszewski, K., Multifunctional Hydrogels with Reversible 3D Ordered Macroporous Structures, *Advanced Science* **2** (2015) 1500061-1500066.

Designing Dual-functionalized Gels that Move, Morph and Self-organize in Light

PI: Anna C. Balazs, University of Pittsburgh, Pittsburgh, PA 15261

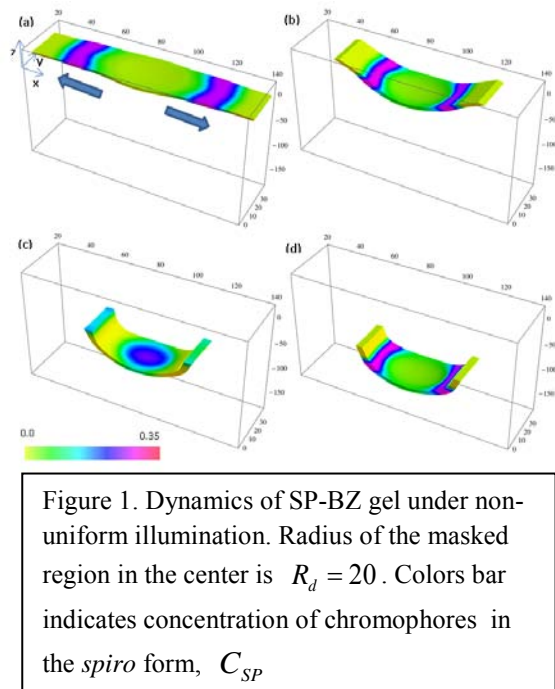
Program Scope

Our goal is to design synthetic gels that exhibit unprecedented biomimetic behavior, which can be regulated by external stimuli. The ideal materials for achieving these aims are “SP-BZ” gels¹ that contain both spirobenzopyran (SP) chromophores and the ruthenium catalysts that drive the oscillating Belousov-Zhabotinsky (BZ) reaction. The BZ reaction occurring within these gels enables the polymer networks to oscillate autonomously,² and thereby, produce mechanical work. In the presence of light, the SP groups provide a means of dynamically reconfiguring the shape of the gels. Furthermore, the BZ reaction is light-sensitive and samples can undergo spontaneous, directed movement under non-uniform illumination.³ Therefore, by integrating the SP and BZ functionality into one “dual-functionalized” system, we can design gels where structural reconfiguration and directed motion become interlinked, and thus, lead to new modes of dynamic behavior. We have developed the first model for gels that combines both these SP and BZ functionalities¹ and our current studies reveal exemplar systems that exhibit dramatic shape changes as the gels undergo self-propelled motion in the presence of light (see Fig. 1).

Notably, polymer chains that contain both the SP and BZ functionalities have just recently been synthesized.⁴ In the latter experiments, the SP and BZ functionalities are anchored to a poly(*N*-isopropylacrylamide) backbone; these poly(*N*IPAAm-co-Ru(*bpy*)₃-co-Sp) chains are referred to as “PNRS”.⁴ The SP-BZ gels are formed by cross-linking these PNRS chains.⁴ To the best of our knowledge, there have been no systematic studies of the SP-BZ gels. Thus, our studies¹ were the first to reveal the properties of this novel class of active, self-oscillating materials, and provide guidelines for controlling the synergy between the structural reconfiguration and motion. Hence, our findings lay the groundwork for exploiting the capabilities of these unique gels.

Recent Progress

In order to capture the behavior of these novel materials, we extended our gel lattice spring model (gLSM)³ to include both the SP and BZ functionality.¹ The effect of light in our SP-BZ gels is introduced through the reaction rate constant $k_L(I(\mathbf{r}))$, which describes light-induced ring closure of the SP, and the coefficient $\Phi(I(\mathbf{r}))$, which accounts for the additional



production of bromide ions in the presence of light.⁵ Both values are assumed to be proportional to the light intensity at a given point, $I(\mathbf{r})$; the temperature of the SP-functionalized gels remains constant when it is illuminated with blue light.⁶ In the studies described below, we investigated the dynamic behavior of the dual-functionalized samples in non-uniform light. We also determined the effect of varying the total concentration of the spirobenzopyran chromophores, C_{SP}^t , on the motion of these systems.

Figure 1 illustrates the dynamic behavior in these SP-BZ gels. Here, an initially flat sample roughly $6.5\text{mm} \times 1.7\text{mm} \times 0.2\text{mm}$ in size is illuminated at both edges, leaving a central non-illuminated region of radius $R_d=20$ units (approximately 0.8mm). The sample morphs into a bent structure that promotes its self-sustained downward motion. Importantly, neither the SP nor the BZ gel alone would yield such net translational motion.¹

In Figure 1, the intensity of the light illuminating the ends is higher than the critical intensity needed to suppress the oscillations in a uniformly illuminated sample of the BZ gel. Hence, the chemical waves originate only in the dark, central region and then propagate to the illuminated ends. Due to the spirobenzopyran chromophores, the illuminated ends of the gel shrink. Compared to these collapsed ends, the central region is relatively swollen. This uneven distribution of solvent within the gel causes the central region to bulge out of the plane (in the *negative* z -direction for the case in Fig. 1). With the bending of the gel, the traveling chemical waves move not only in the lateral direction (the x -direction), but also upward from the depressed center to the ends of the sample (along the *positive* z -direction). Due to the inter-diffusion of the polymer and solvent, the movement of the chemical wave in the positive z -direction causes the gel to move in the opposite direction;³ i.e., the *negative* z -direction, and hence, migrate to the bottom of the simulation box for the example in Figure 1.

To characterize the observed motion, we plotted the temporal evolution of the z -coordinate of the central node on the bottom face of the gel, z_c , for different values of C_{SP}^t (Fig. 2). During the first stage of the motion, the sample remains flat and localized in one plane (as indicated by the flat portion of the curve). During the second stage, the sample moves downward (along the negative z -direction) with approximately constant velocity; however, this seemingly monotonic movement of the sample involves small-scale oscillatory motion, as can be seen from the enlargement of a portion of the curve (Fig. 2a). Figure 2b reveals that the velocity of the downward motion is fastest for the lowest C_{SP}^t and decreases with an increase in C_{SP}^t .¹ Hence, our findings provide design rules for controlling the rate of the autonomous motion.

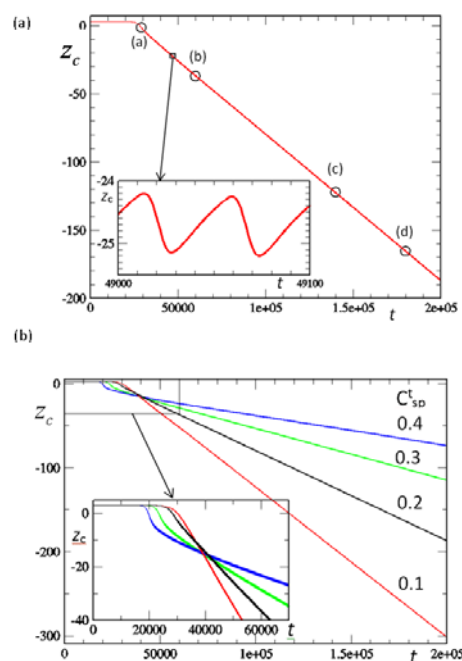
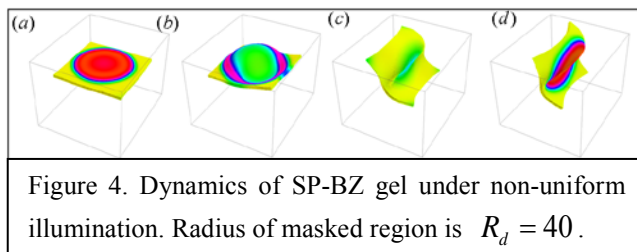
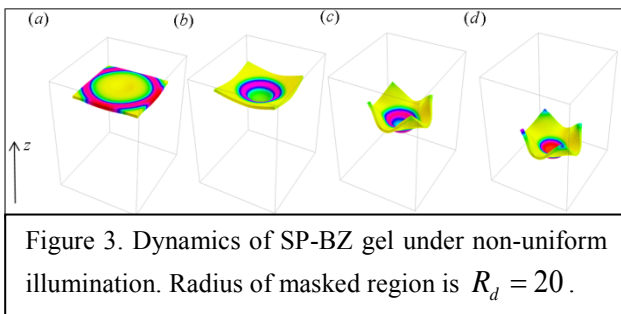


Figure 2. Time evolution of the z -coordinate of the bottom face of the center of the gel, z_c , for the simulation in Figure 1. Points marked (a)-(d) correspond to the respective images in Fig. 1a-d. (b) Time evolution of z_c for gels at four different values of C_{SP}^t .

To demonstrate the generality of the behavior seen in Figure 1, we considered a relatively large, square sample that is $90 \times 90 \times 5$ nodes in size and is illuminated along all four edges, so that only the central region of radius $R_d = 20$ is in the dark (Fig. 3). Again, the out-of-plane bulging of the swollen center is accompanied by the bending of the collapsed edges, resulting in the directed motion of the gel. This behavior is robust for a range of R_d values. If, however, we increase R_d beyond some critical size (thereby significantly decreasing the size of the ends that undergo light-induced shrinking),¹ we find that the dynamic behavior of the gel is similar to that of a pure BZ gel. Namely, with $R_d = 40$, the sample exhibits negative phototaxis; it reorients to fit within the relatively wide dark, central region, and thereby, avoid the light (see Fig. 4).



In the above examples, we focused on chemically uniform samples placed in non-uniform illumination. Patterned SP-BZ gels can exhibit remarkable dynamics even under uniform illumination. In the example shown in Figure 5 only the central area encompasses dual SP-BZ functionalization while the outer regions of the samples include only functionalization with the Ru catalyst. Here, the overall shape of the sample is dictated by the concentration of the chromophores and can be controlled by the light intensity. As discussed below, we will exploit different patterns of light to control the shapes and folding of the patterned gels, as well as the translational motion of the sample.

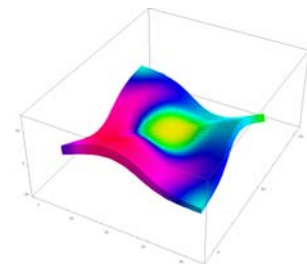


Figure 5. Patterned gel under *uniform* light. The radius of the SP-BZ area in the center is $R_d = 20$.

Future Plans

1. Model Patterned Gels

(a) *Localize the Ru catalyst within distinct domains.* In the previous studies, we used non-uniform illumination to break the symmetry in the system. We will now break the symmetry by localizing the Ru catalyst into specific patches within the gel. This mode of patterning will allow us to harness uniform illumination to tailor the shape of the sample, and thus, the motion of the gel.

(b) *Confine the SP functionalization to specific regions* With the SP moieties localized in specific regions, we can confine the light-induced shrinking of the gel to particular areas. Our aim is to develop fundamental relationships that correlate the structure of the patterned material to its response to uniform illumination, as well as variations in light. In particular, we will pinpoint the factors that control the novel form of photo-chemo-mechanical energy transduction in these systems.

2. Translate the Light Source Over the Sample We previously showed ⁷ that by swiping a light source over the length of a SP-functionalized gel, the sample could undergo directed motion. We anticipate that by rastering the light over the SP-BZ system, we can controllably direct the movement of self-oscillating gels of various sizes and shapes. Notably, the SP-functionalized domains become hydrophobic under light. Hence, by swiping the light along the length of the SP-BZ gels, we can controllably transport hydrophobic particles or droplets along the pulsating “conveyor belt”. In the absence of light, the gel is hydrophilic. Hence, SP-BZ gels can be switched from a hydrophilic to a hydrophobic conveyor simply by the application of light. This attribute can greatly extend the functionality and utility of microfluidic devices.

3. Examine Multiple, Interacting Gel Pieces In our prior studies,³ we showed that BZ gels can undergo auto-chemotaxis, where each individual piece emits a chemical signal that drives the autonomous motion and self-organization of multiple units. We anticipate that multiple pieces of the SP-BZ gels will exhibit rich dynamic behavior, where the localized shrinking of the illuminated SP-BZ samples will modulate the “communication” between the samples, and hence, affect the spontaneous self-organization. We will determine how to drive the self-organization of these SP-BZ pieces into small-scale machines, such as gear-like objects, which can operate in an autonomous manner. Moreover, we will determine how to control this autonomous motion through light. These self-organized gears will be coupled through photo-chemical interactions, and can be utilized to perform mechanical work that is modulated by light.

References

1. O. Kuksenok, A. C. Balazs, Designing dual-functionalized gels for self-reconfiguration and autonomous motion. *Scientific Reports* **5**, 9569 (2015).
2. R. Yoshida, T. Takahashi, T. Yamaguchi, H. Ichijo, Self-oscillating gel. *J Am Chem Soc* **118**, 5134 (1996).
3. (a) P. Dayal, O. Kuksenok, A. C. Balazs, Directing the behavior of active, self-oscillating gels with light. *Macromolecules* **47**, 3231 (2014). (b) Dayal, P., Kuksenok, O., and Balazs, A.C., “Reconfigurable assemblies of active, auto-chemotactic gels”, *PNAS* **110**, 431 (2013).
4. T. Yamamoto, R. Yoshida, Self-oscillation of polymer and photo-regulation by introducing photochromic site to induce LCST changes. *React Funct Polym* **73**, 945 (2013).
5. H. J. Krug, L. Pohlmann, L. Kuhnert, Analysis of the modified complete Oregonator accounting for oxygen sensitivity and photosensitivity of Belousov-Zhabotinsky systems. *J Phys Chem-US* **94**, 4862 (1990).
6. A. Szilagyi *et al.*, Rewritable microrelief formation on photoresponsive hydrogel layers. *Chem Mater* **19**, 2730 (2007).
7. O. Kuksenok, A. C. Balazs, Modeling the photoinduced reconfiguration and directed motion of polymer gels. *Adv Funct Mater* **23**, 4601 (2013).

Publications from this BES grant (which started in Jan. 2015)

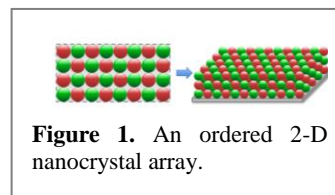
1. O. Kuksenok, A. C. Balazs, Designing dual-functionalized gels for self-reconfiguration and autonomous motion. *Scientific Reports* **5**, 9569 (2015).

Program Title: Rigid Biopolymer Nanocrystal Systems for Controlling Multicomponent Nanoparticle Assembly and Orientation in Thin Film Solar Cells

Principle Investigator: Jennifer N. Cha

Program Scope

The focus of the proposed research is to **direct the assembly of single or binary nanoparticles into well-ordered meso- or macroscale assemblies without using prohibitively expensive lithographic processes.** The ability to control nanoparticle organization in both 2- and 3D can revolutionize technologies for energy to generate new types of energy harvesting and conversion materials that show optimal efficiencies. For example, it has been proposed that having a nanostructured solid-state bulk hetero-interface will enable efficient charge-carrier separations, similar to organic based heterojunction cells but with potential improvements, including thermal and long-term stability, tunability of energy levels, large adsorption coefficients and carrier multiplication. *Furthermore, controlling the orientation of different photoactive nanostructures can have significant value toward engineering new catalysts for fuel generation from water and solar energy. However, engineering such devices requires nanoscale control and ordering in both 2- and 3-dimensions which is often difficult to achieve.*



In Nature, bulk organic and inorganic materials are arranged into precise and ordered programmed assemblies through the sequestration of raw materials into confined spaces and association through highly specific non-covalent interactions between biomolecules. Using similar strategies, a portion of the proposed research will focus on confining metal and semiconductor nanocrystals to pre-determined surface patterns and controlling their arrangement through tunable, orthogonal biomolecular binding (Fig. 1). The proposed research utilizes the ability of biomolecules to bind specific targets in a tunable, orthogonal, multivalent, and reversible manner. When conjugated to nanoparticles, these biomolecules can control particle arrangements on chemically defined surfaces. Through careful balance of the attractive and repulsive forces between the particles, the array, and the outside surface, it is envisioned that single or binary nanoparticles can be packed to adopt highly ordered, well-defined assemblies in two and three dimensions from simple mixing and annealing of biomolecule-nanoparticle systems with biomolecule-stamped surfaces. To control the crystallographic alignment of each particle with its neighbors, the nanoparticles will be assembled using a mixture of DNA interactions.

Over the last few years, we have demonstrated that using such tunable biomolecular interactions can lead to creating thin film quantum dot (QD) assemblies with control over film thickness, particle organization and surface roughness. In this work, we also demonstrated the potential of utilizing DNA interactions to control the interparticle distances between neighboring semiconductor nanocrystals. Furthermore, through charge conduction studies, we show that DNA does not necessarily impede electron or hole mobility from one QD to the next to yield photocurrent activity that depends to a large extent on the relative band edge energy levels of the different semiconductors with respect to the measured HOMO LUMO levels of the DNA sequences. We do however also demonstrate that in order to improve device performances, future work at controlling the various interfaces and the amount of DNA loading per QD will need to be optimized as well as future single QD-DNA constructs. More recently, we have focused our studies at using DNA to control the assembly of different photocatalytic nanocrystals to cause a significant gain in hydrogen production from TiO_2 and CdS. Finally, as a

means to increase the variety of materials that can be used for water splitting, we have developed methods to synthesize well-defined nanostructures of BiVO_4 which has in recent report shown promise for water oxidation

Recent Progress

Scalable Assembly of 3D Quantum Dot Assemblies by using DNA Interactions

To translate the use of DNA to mediate particle packing and orientation in 3-D thin films directly from a substrate, we recently showed that highly ordered hexagonally close packed nanocrystal superlattices could be obtained on geometrically and chemically confined DNA patterns on a substrate by using DNA sequences that mediate interparticle hybridization as well as thermal annealing. This work underscored the proven ability of biomolecules, particularly DNA, to bind specific targets in a tunable, orthogonal, multivalent, and reversible manner. In order to extend these discoveries toward assembling quantum dots (QDs), we first developed methods to conjugate DNA directly to semiconductor nanocrystals to produce QDs with uniform coatings of DNA. These DNA-conjugated QDs were found to be stable to oxidation and remain suspended in high ionic strength environments. Furthermore, we show that these DNA-conjugated nanocrystals can be used to produce QD thin films with control over thickness and roughness. The films were formed in only a few steps with minimal material waste and use of benign solvents, as opposed to

processes such as spin coating or dip-coating which also require multiple layer-by-layer deposition steps. Furthermore, because the method only requires adsorption of a single solution followed by drying and thermal annealing, it was very simple to produce films of variable thicknesses by tuning the initial DNA-CdTe concentrations (Figure 2). Cross-sectional SEM

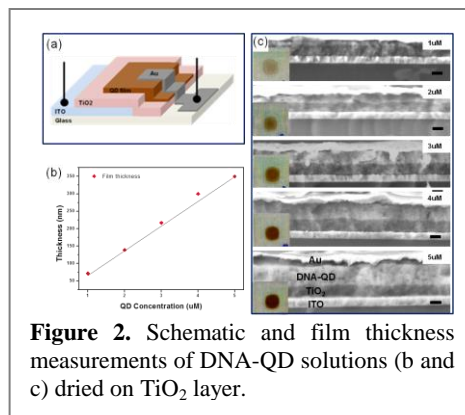


Figure 2. Schematic and film thickness measurements of DNA-QD solutions (b and c) dried on TiO_2 layer.

images of the DNA-CdTe films on TiO_2 showed not only a clear correlation between film thickness and QD concentration but that the films remained relatively smooth and that the QD-DNA layers were intact throughout the film (Figure 2). For these studies, the DNA-conjugated CdTe nanocrystals

were assembled onto TiO_2 films to fabricate ITO/ TiO_2 /DNA-CdTe/Au thin film test devices. Based on the relative energy levels of the assembled ITO/ TiO_2 /DNA-CdTe/Au devices, the DNA-CdTe and TiO_2 would act as a hole and electron transport layer respectively (Figure 3a). To test this, DNA-CdTe QD films composed of different sized nanocrystals were prepared and devices were tested as a function of linker DNA, QD size and film thickness. First as a measure of comparison, films made with no linker DNA showed absolutely little to no consistency in current-voltage characteristics as a function of QD size (Figure 3b). It is hypothesized that the random formation of QD organization within the no DNA linker films could only result in irreproducible and overall poor device performance. In direct contrast, devices with linker DNA showed consistent current-voltage characteristics where in all of the three sets of devices with different QD sizes, the V_{oc} values were set around 400mV and the short circuit current (J_{sc})

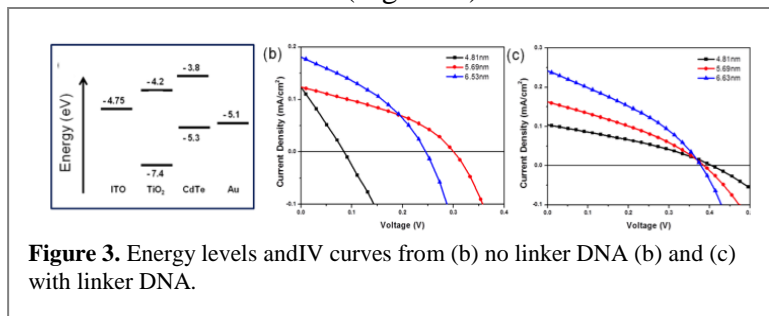


Figure 3. Energy levels and IV curves from (b) no linker DNA (b) and (c) with linker DNA.

were assembled onto TiO_2 films to fabricate ITO/ TiO_2 /DNA-CdTe/Au thin film test devices. Based on the relative energy levels of the assembled ITO/ TiO_2 /DNA-CdTe/Au devices, the DNA-CdTe and TiO_2 would act as a hole and electron transport layer respectively (Figure 3a). To test this, DNA-CdTe QD films composed of different sized nanocrystals were prepared and devices were tested as a function of linker DNA, QD size and film thickness. First as a measure of comparison, films made with no linker DNA showed absolutely little to no consistency in current-voltage characteristics as a function of QD size (Figure 3b). It is hypothesized that the random formation of QD organization within the no DNA linker films could only result in irreproducible and overall poor device performance. In direct contrast, devices with linker DNA showed consistent current-voltage characteristics where in all of the three sets of devices with different QD sizes, the V_{oc} values were set around 400mV and the short circuit current (J_{sc})

showed an increase as a function of a size of the CdTe QDs (Figure 3c). Overall, the J_{sc} values measured from the films with linker DNA were comparable to a previously reported use of pyridine coated CdTe/CdSe nanocrystals where ligand exchange was run but the nanocrystals were not sintered.

Effective separation of electron-hole pairs is critical to achieve a photovoltaic effect. In the case of nanocrystals, the electronic coupling between particles decreases exponentially as a function of interparticle distance. For example, when the ligands on the QDs are the hydrocarbons used for their synthesis, the coupling energy diminishes an order of magnitude every $\sim 2\text{\AA}$ increase in interparticle distance. In previous work with small area (3-5 micron) DNA-gold nanoparticle superlattices, we determined that the interparticle distance is primarily driven by the lengths of the dsDNA used. If this is roughly maintained with these large area (over $3 \times 3\text{mm}^2$) DNA-QD films, the spacing (surface to surface distance) between the CdTe nanocrystals is theoretically calculated to be $\sim 3\text{nm}$. Should this be the case, the distance between neighboring CdTe QDs is potentially too long to assume easy carrier hopping from one particle to the next which lends to the possibility that the DNA itself plays a role in enabling carrier migration. Because electron mobility through double stranded DNA has been demonstrated, it is not implausible that an electron generated in a QD could move through the surrounding DNA to the next QD. To study this in more detail, charge transport measurements were run in collaboration with Prof. Prashant Nagpal's group which showed that the energy levels of the QDs and the DNA strands need to be considered for effective charge mobility from one QD to the next.

Enhanced Hydrogen Production from DNA Assembled Z-scheme TiO_2 -CdS Photocatalyst Systems

With increasing demands for alternative sources of fuel, extensive research has focused on discovering methods to generate renewable energy from earth abundant resources. In recent years, a wide range of inorganic nanostructures with high surface areas and tunable band gaps have been synthesized and used as photocatalysts for splitting water into hydrogen and oxygen. To increase their activity, "Z-scheme" photocatalytic systems have been implemented in which multiple types of photoactive materials simultaneously oxidize water and reduce molecules upon photoillumination. In some cases, redox molecules or electron mediators have also been used to aid in electron shuttling between the different catalysts, facilitate charge separation, and inhibit recombination events. Recently, solid-state Z-scheme systems have also been synthesized in which control over the interface between the different materials was found to be critical for higher fuel production.

In almost all of these cases, optimal catalysis is typically obtained by interfacing different materials through aggregation (e.g. electrostatic interactions) or epitaxial nucleation of one material on top of another. These methods, however, tend to decrease the overall accessible catalytic surface area because of the limited control over spatial organization of the separate components. In addition, the scope of different materials that can be produced by direct chemical synthesis is limited.

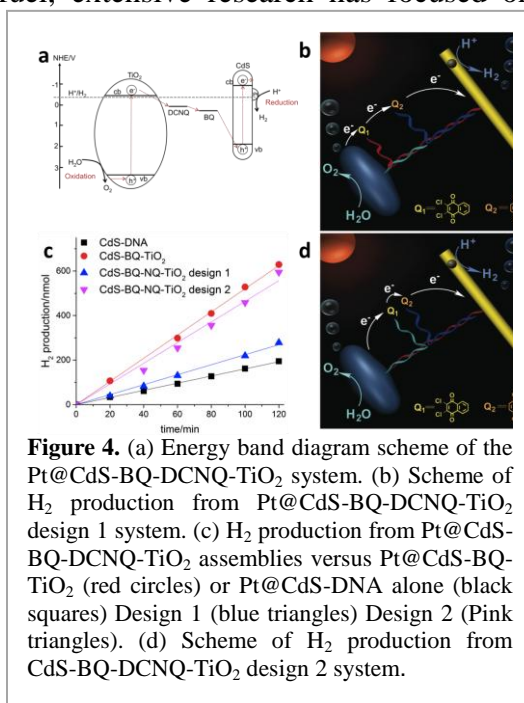


Figure 4. (a) Energy band diagram scheme of the Pt@CdS-BQ-DCNQ-TiO₂ system. (b) Scheme of H₂ production from Pt@CdS-BQ-DCNQ-TiO₂ design 1 system. (c) H₂ production from Pt@CdS-BQ-DCNQ-TiO₂ assemblies versus Pt@CdS-BQ-TiO₂ (red circles) or Pt@CdS-DNA alone (black squares) Design 1 (blue triangles) Design 2 (Pink triangles). (d) Scheme of H₂ production from CdS-BQ-DCNQ-TiO₂ design 2 system.

Finally, since electron transfer largely depends on diffusion, simply mixing electron mediators with different catalysts in solution requires a high concentration of redox molecules to avoid rate limitations but which can lead to undesired side oxidation/reduction reactions. To address these challenges, we recently utilized DNA as a structure-directing agent to spatially organize well-defined TiO_2 and Pt decorated CdS (Pt@CdS) nanocrystals. By using DNA as an assembler a significant increase in H_2 production was observed upon photoillumination as compared to Pt@CdS or TiO_2 alone directly in solution. Potential limitations in H_2 production caused by negatively charged DNA on the Pt@CdS nanoparticles was simply fixed by controlling the amount of DNA per CdS nanorod. DNA also allowed positioning of a single or series of electron mediators site-specifically in between the two catalysts. The inclusion of benzoquinone (BQ) equidistant between the TiO_2 and CdS through DNA assembly further increased H_2 production (Figure 4). While the use of a second quinone in conjunction with BQ showed no more improvement, its location within the Z-scheme was found to strongly influence catalysis.

New Materials for Water Oxidation

While wide-band gap semiconductors like TiO_2 and WO_3 have been studied as photocatalysts for water-splitting, more recent efforts have turned to BiVO_4 due to its bandgap of 2.4eV and ability to absorb in the visible. In the presence of electron scavengers such as AgNO_3 or NaIO_3 , BiVO_4 has also shown a strong ability to oxidize water and generate oxygen. Despite these successes in producing photoactive BiVO_4 however, the synthesis of well-defined nanostructures of BiVO_4 with control over both size and shape has remained challenging. Because of this, we have recently developed methods to obtain monodisperse and well-defined BiVO_4 nanoparticles (NPs) and nanorods (NRs) (Figure 5). Next ligand exchange techniques that removed the large hydrocarbons from the particle surfaces and enabled their effective transfer to aqueous solutions were developed. Despite their blue shift in absorbance with respect to bulk, when testing the photocatalytic performance of the BiVO_4 NPs and NRs, a significant improvement in water oxidation as compared to micron-sized BiVO_4 in the presence of sodium persulfate as an electron acceptor was observed.

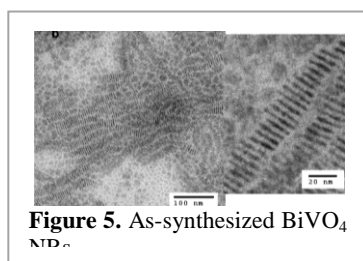


Figure 5. As-synthesized BiVO_4 NPs.

Future Studies

In future studies, we propose to continue to explore the production of energetic fuels from water and CO_2 . For this, we will either apply similar approaches to what was used for the H_2 studies and utilize linear DNA oligonucleotides or we will employ self-assembled 2D DNA templates as templating agents. All of the different DNA conjugated photocatalysts (e.g. BiVO_4 , modified CdS) will be assembled by DNA hybridization in the absence or presence of a series of different electron mediators site specifically placed in between the different nanoparticles.. After DNA conjugation and characterization, the ability of the semiconductor QDs to controllably reduce and oxidize cofactors such as benzoquinones upon photoillumination will also be examined. Finally, in order to more qualitatively measure the redox activities of the photocatalysts with the electron mediators, the oxidation/reduction states of the different meditatots will be monitored through UV-Vis measurements. For the CO_2 reduction itself, a series of pyridine like molecules and derivatives will be studies. We hypothesize that using organic catalysts that can both associate with CO_2 as well as assist in hydride transfer will cause improvements in CO_2 reduction. The use of enzymes for CO_2 reduction will also be studied.

List of publications (with DOE support: Financial support from July 2013-June 2015)

1. K. Ma, O. Yehezkeli, D.W. Domaille, H.H. Funke, **J.N. Cha***, “Enhanced Hydrogen Production from DNA Assembled Z-scheme TiO₂-CdS Photocatalyst Systems” *Angew. Chem. Int. Ed. In press* (2015) DOI: 10.1002/anie.201504155
2. O. Yehezkeli, A. Harguindey, D.W. Domaille, L. He, **J.N. Cha***, “Synthesis and Phase Transfer of Well-Defined BiVO₄ Nanocrystals for Photocatalytic Water Splitting” *RSC Advanced, in press* (2015)
3. O. Yehezkeli, D. R.D. Barcellos, **J.N. Cha***, “Electrostatically Assembled CdS-Co₃O₄ Nanostructures for Photo-assisted Water Oxidation and Photocatalytic Reduction of Dye Molecules”, *Small*, **11**, 668-674 (2015)
4. G. Hafenstine, D.W. Domaille, **J.N. Cha***, A.P. Goodwin*, “Self-assembly and reassembly of fiber-forming dipeptides for pH-triggered DNA delivery” *J. Polym. Sci. part A*, **53**, 183-187 (2015)
5. S.M. Goodman, H. Noh, V. Singh, **J.N. Cha**, P. Nagpal*, “Charge transport through exciton shelves in cadmium chalcogenide quantum dot-DNA nano-bioelectronic thin films”, *Appl. Phys. Lett.*, **106**, 083109 (2015)
6. J.H. Lee, D.W. Domaille, H. Noh, T. Oh, C. Choi, S. Jin, **J.N. Cha***, “High-Yielding and Photolabile Approaches for Covalent Attachment of Biomolecules to Surfaces via Hydrazone Chemistry”, *Langmuir*, **30**, 8452-8460 (2014)
7. D.D. McKinnon, D.W. Domaille, **J.N. Cha***, K.S. Anseth* “Bis-Aliphatic Hydrazone-Linked Hydrogels Form Most Rapidly at Physiological pH: Identifying the Origin of Hydrogel Properties with Small Molecule Kinetic Studies”, *Chemistry of Materials*, **26**, 2382-2387 (2014)
8. D.W. Domaille, **J.N. Cha***, “DNA-Templated Organocatalytic Hydrazone Formation with Aniline-Terminated DNA”, *Chem. Comm.*, **50**, 3831--3833 (2014)
9. J.H. Lee, P.F. Xu, D.W. Domaille, C. Choi, S. Jin, **J.N. Cha***, "Quantitative Surface Enhanced Raman Scattering Based Protein Detection and Identification via DNA-Conjugated M13 Bacteriophage and SERS active DNA core shell nanoparticles", *Advanced Functional Materials*, **24**, 2079-2084 (2014)
10. H. Noh, S.M. Goodman, P. Mohan, A.P. Goodwin, P. Nagpal, **J.N. Cha***, “Scalable Assembly of 3D Excitonic Nanocrystal Assemblies by using DNA Interactions and DNA Mediated Charge Transport”, *RSC Advances*, **4**, 8064-8071 (2014)
11. D.D. McKinnon, D.W. Domaille, **J. N. Cha**, K.S. Anseth, “Covalently adaptable networks as biophysical-ECM mimics for cell culture”, *Advanced Materials*, **26**, 865-872(2014)

12. L.M. Forbes, S. Sattayasamitsathit, P.F. Xu, A. O'Mahony, I.A. Samek, K. Kaufmann, J. Wang, **J.N. Cha***, Improved Oxygen Reduction Reaction Activities with Amino Acid R Group Functionalized PEG at Platinum Surfaces, *J. Mater. Chem.* **1**, 10267 – 10273 (2013)
- 13 P.F. Xu, H. Noh, J.H. Lee, D.W. Domaille, M. Nakatsuka, A.P. Goodwin*, **J.N. Cha***, “The Role and Potential of DNA for Next-Generation Materials”, *Materials Today*, **16**, 290-296 (2013)
14. D.W. Domaille, J.H. Lee, **J.N. Cha***, “Conformationally Independent, Reversible DNA Conjugation to M13 Bacteriophage For Colorimetric and Fluorescence-Based Protein Biosensors”, *Chemical Communications*, **49**, 1759 - 1761 (2013)
15. P.F. Xu, A.M. Hung H. Noh, **J.N. Cha*** “Switchable Nanodumbbell Probes for Analyte Detection”, *Small* **9**, 228–232 (2013)

Self-Assembly and Self-Replication of Novel Materials from Particles with Specific Recognition

Principle Investigator: P. Chaikin*, Co-PIs: N. Seeman†, M. Weck†, D. Pine*

*Dept. of Physics, †Dept. of Chemistry, New York University, New York, NY 10003

Program Scope

The goals of our program are to understand, discover, design and control the basic interactions between nanoscopic and microscopic units so that complex self-assembly processes and architectures are enabled. We are particularly interested in specific interactions between particles which potentially allow the design of functional structures involving many different components precisely arranged. To this end we have been using DNA with its specific hybridization only between complementary sequences to make both reversible and irreversible bonds. We have also used depletion interactions and shown that such complementary colloidal assembly techniques is more complex, interesting and useful than previously believed. Depletion was taken as temperature independent, but temperature dependent solvent quality leads to weak absorption, melting and then bridging of colloidal crystals/clusters. We have extended our work on colloids to include emulsion droplets with the advantage that the DNA linker strands are mobile on the surfaces. This permits the formation of droplets with controlled valency, one, two.. bonds between complementary droplets as well as the use protected DNA strands for programmed sequential self-assembly. Most of our effort has been spent on developing systems that can self-replicate and eventually evolve. These systems are based on DNA origamis and we have demonstrated self-replication and exponential growth over 24 cycles with more than 7 million amplification of the introduced seeds.

Recent Progress

DNA Functionalized Emulsions In collaboration with the group of Jasna Brujic at NYU, we have functionalized silicon oil emulsions with DNA and demonstrated not only that they specifically bind but that the effective valency of the droplets is controllable. When droplets come together the mobile DNA on their surface migrates to an adhesion patch whose size and DNA content depend on the surface tension of the droplets, the binding of DNA and excluded volume effects. The adhesion patch contains a certain maximum number of DNA strands. If we coat the droplets with that amount or less we have one patch – valency one. If we have enough for two patches – valency two, etc.

Sequential assembly Fig. 1. The fact that we can functionalize emulsion droplets enables a number of scenarios where mobile DNA links on the surface are important. We can protect one DNA strand by hybridization to another. A deprotector strand can displace the protector freeing the protected strand which can migrate on the surface and bind to another droplet. If the freed strand is a deprotector for the next particle the sequence can

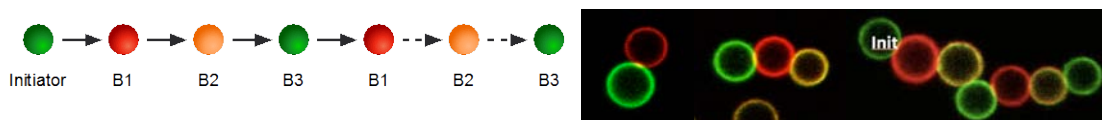


Fig.1 Above is designed sequence and left is assembled emulsions. Far right are green initiator assembling one and then two droplets.

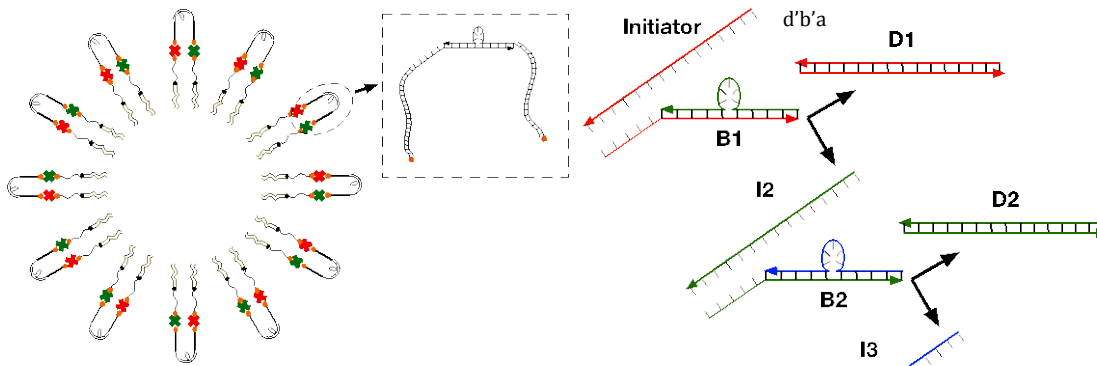


Fig. 2 The scheme used for sequential assembly – emulsion droplets are coated with partially hybridized DNA strands whose active regions are protected. An initiator deprotects the active region which can move on the droplet as I2 then join to another droplet and act as an initiator for its protected strands.

proceed in an order prescribed by the strands Fig. 2. Forced sequential assembly is a new design paradigm for self assembly.

DNA Origami Directed Assembly. We are trying to use DNA origami to organize colloidal particles. We will replace conventional 'hairy particles' with 'belted particles.'

A belted particle, wherein the belt consists of a DNA origami construct, is illustrated in Figure 3. Each point on the belt is, in principle, an addressable 2D patch that can contain several parallel DNA helices, each of which can have site-specific staple strands long enough to address the outside environment with a unique sequence, thereby specifying the orientation of the particle with which it interacts. These can include not merely the cardinal points (*e.g.*, 100, 110, 111, etc.), but any others that are useful for construction. We will make a micron-scale Zometool™-like construct that can interact with other species directly. The approach is not limited to orthogonal belts. other arrangements (*e.g.*, hexagonal belts) can be produced, as well as belts of higher connectivity (a variety of latitude lines and longitude lines). Arbitrary-length origami scaffolds have recently

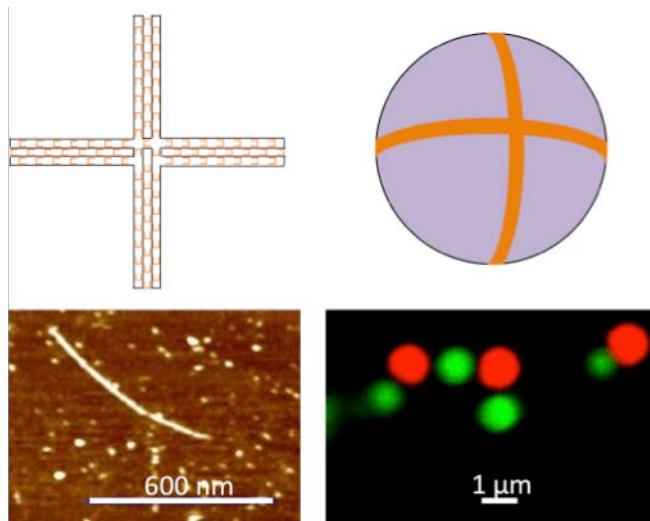


Fig 3. (top left) A “plus” shaped four-helix arm origami made from 52K base S3113 viral DNA of linear dimension 2π microns attached on a one micron colloidal particle allows for positioning of ligands, motors, reactants, or nanoparticles with 6 nm accuracy on the colloid. (top right) schematic of a four-helix arm on a colloidal particle surface. (bottom left) AFM image of a straight four-helix arm 7249 base M13 virus origami 600nm long with sticky ends complementary to red and green colloids at each end. (bottom right) Confocal image of 1-micron particles tethered by origami.

become available from genomic DNA molecules, not just those derived from specific viral constructs. All of the simple known packings should be available from such belted particles. For example, a set of 24 spheres could be used to form a huge-cavity version of Zeolite A, by making a truncated octahedron whose exterior is readily deprotected by Yurke isothermal strand displacement. In addition to other particles, origami belts allow precise positioning of other specific DNA strands, aptamers, chemical modifications, antibodies and other proteins and a variety of nanoparticles with respect to each other. The simple principles of viral construction owing to Fuller (adopted by Casper and Klug) could also be employed using belts that enable icosahedral arrangements. Stronger materials could be made by specific connections of deltahedral arrangements of contacts, for example a tetrahedron and an octahedron in face-sharing mode would yield a face-centered cubic packing. It is unclear whether algorithmic assemblies will have higher fidelity on this scale, but they can be explored so that this question can be answered.

Self-replication, exponential growth

One of the primary goals of our proposed research was to develop a process for self-replication of microscopic objects. This would add the most fundamental aspect of living systems to materials science. A major accomplishment of our research during the previous grant period was to develop such a system using DNA origami. The system doubles its progeny every cycle exhibiting exponential growth. A schematic of the system is shown in Fig. 4. The system consists of two types of tiles, DNA origamis made from a backbone of M13 bacteriophage single stranded DNA (7249 bases) and ~ 200

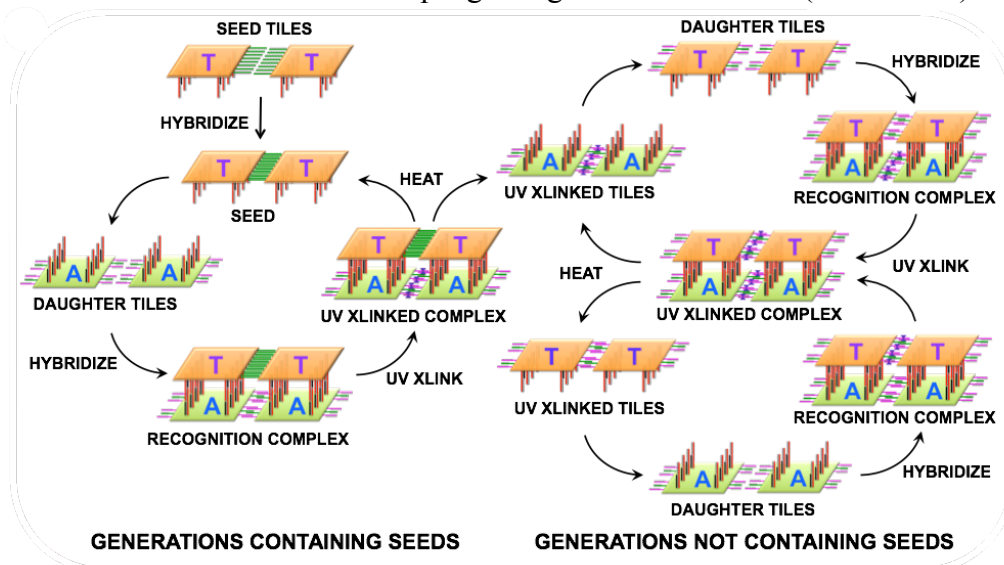


Fig.4 Self-replication cycles. A dimer ‘TT’ seed is constructed from two T-tiles using sticky-end cohesion and blunt exterior edges. The seed is introduced into a bath of A and T tiles. On lowering the temperature to 4C the vertical sticky ends from the TT seed faces attract and bind two A tiles. At this stage if the system is heated the A’s separate from each other and from the seed. If UV is applied while the system is cold the edge sticky ends on the A’s permanently binds them in an AA dimer. After UV exposure, heating to 40C results in the separation of the original TT dimer seed and a daughter AA dimer. On repeated cycling the TT seeds keep on producing AA dimers. The AA dimer cycles to produce TT progeny and both types of dimers then proliferate to make TT and AA offspring doubling the number of dimers each cycle.

“staple strands” of DNA complementary to regions of the backbone forming a

rectangular structure $\sim 100\text{nm} \times 80\text{nm} \times 2\text{nm}$. The “T” tiles are complementary to the “A” tiles. We have demonstrated exponential growth over 24 cycles for a seed amplification of greater than 7 million. We have also demonstrated that with TT seeds there are only TT and AA offspring while with TA seeds offspring are only AT and TA.

Future Plans

Functionalize colloids with DNA origami belts to allow patchy particles with complete control of positions and angles including dihedral. Spontaneous mutation and controlled mutation, selection, competition and evolution of self-replicating DNA origami molecules.

Publications (Supported by this DOE grant over past two years)

1. Lang Feng, Remi Dreyfus, Ruojie Sha, Nadrian C. Seeman, Paul M. Chaikin, “DNA Patchy Particles”, *Advanced Materials* **25**, 2779-2783 (2013)
2. Kun-Ta Wu, Lang Feng, Ruojie Sha, Remi Dreyfus, Alexander Y. Grosberg, Nadrian C. Seeman, and Paul M. Chaikin, “Kinetics of DNA-coated sticky particles”, *PHYSICAL REVIEW E* **88**, 022304-8 (2013)
3. D.A. Rusling, A.R. Chandrasekaran, Y. Ohayon, T. Brown, K.R. Fox, R. Sha, C. Mao & N.C. Seeman, Functionalizing Designer DNA Crystals with a Triple-Helical Veneer, *Angew. Chemie Int. Ed.* **53**, 4060-4063 (2014).
4. N.C. Seeman, Art as a Stimulus for DNA Nanotechnology, *Leonardo* **47** (2), 143-149 (2014).
5. R. Sha, J.J. Birktoft, N. Nguyen, A.R. Chandrasekaran, J. Zheng, X. Zhao, C. Mao, N.C. Seeman, Self-Assembled DNA Crystals: The Impact on Resolution of 5'-Phosphates and the DNA Source, *NanoLett.* **13**, 793-797 (2013).
6. N.C. Seeman, Another Important 60th Anniversary, *Advances in Polymer Science* **261**, *Hierarchical Polymer Structures: 60 Years after the Staudinger Nobel Prize*, V. Percec ed., Springer, 217-228 (2013).
7. M. Ye, J. Guillaume, Y. Liu, R. Sha, R. Wang, N.C. Seeman & J.W. Canary, Site-Specific Inter-Strand Cross-Links of DNA Duplexes, *Chem. Sci.* **4**, 1319-1329 (2013).
8. L. Feng, J. Romulus, M. Li, R. Sha, J. Royer, K.-T. Wu, Q. Xu., N.C. Seeman, M. Weck, P.M. Chaikin, Cinnamate-Based DNA Photolithography, *Nature Materials* **12**, 747-753 (2013).
9. L. Feng, L.L. Pontani, R. Dreyfus, P. Chaikin, J. Brujic, “Specificity, flexibility and valence of DNA bonds guide emulsion architecture”, *Soft Matter*, **9**, 9816-9823 (2013)
10. Feng, Lang, Laderman, Bezia, Sacanna, Stefano, and Chaikin, Paul, "Re-entrant solidification in polymer–colloid mixtures as a consequence of competing entropic and enthalpic attractions", *Nature Materials* **14**, 61-65 (2015)

Hierarchical active matter: from extensile bundles to flowing gels, streaming liquid crystals and motile emulsions

Principle Investigator: Zvonimir Dogic, Department of Physics, Brandeis University, Waltham, MA 02474.

Program Scope:

The laws of equilibrium statistical mechanics impose severe constraints on the properties of conventional materials assembled from inanimate building blocks. Consequently, such materials cannot exhibit spontaneous motion or perform macroscopic work. Inspired by diverse biological phenomena ranging from ciliary beating and cellular motility to *Drosophila* cytoplasmic streaming our goal is to develop a new category of materials assembled from animate, energy-consuming building blocks. Released from the constraints of equilibrium, such active materials acquire fundamentally new functionalities that have so far been mainly restricted to living organisms. For example, in contrast to well-studied conventional polymer gels, which remain quiescent unless driven by external forces, active gels can spontaneously flow through channels and openings or even push on the boundaries of a rheometer to generate a macroscopic force. Such force-producing self-pumping active fluids are just one example of desirable biomimetic functionalities that become possible once the materials are released from the constraints of equilibrium. Our long-term goal is to imbue traditional soft materials with the remarkable functionalities of living organisms, including their ability to regenerate and self-heal, flow through constrictions, crawl on surfaces and swim through suspensions.

To accomplish our goals we assemble soft materials from filamentous microtubules (MTs) and energy consuming molecular motors and characterizes their emergent hierarchical dynamics. At the most basic level we quantify the microscopic dynamics of an elemental structural motif comprised from an extensile microtubule bundle and driven by energy consuming molecular motors. Subsequently we incorporate this force-generating structural element into diverse soft matter systems, including cross-linked isotropic gels, streaming nematic liquid crystals, emulsion droplets and deformable lipid vesicles. Our goal is not to reverse-engineer any specific biological process, but rather by starting from the bottom up, to systematically explore a nearly limitless space of functionalities that arise once soft materials are released from the tight constraints imposed by the laws of equilibrium statistical mechanics. For example, by incorporating molecular motors into microtubule-based liquid crystals we have assembled active nematics and quantified their structure and streaming dynamics that exhibits continuous self-fracturing and healing as well as unbinding and annihilation of highly motile topological defects. By connecting the behaviour of active systems across all length scales and levels of complexity we will elucidate design principles required for the engineering of the next generation soft non-equilibrium materials with biomimetic functionalities.

Recent Progress:

Mechanics of passive and active microtubule bundles: We have developed a single-molecule experimental technique that allows us to assemble a MT bundle of predefined structure, polarity as well as the number of filaments. Simultaneously using optical tweezers we have interrogated the mechanical properties of such composite filamentous materials. Using this newly developed

technique we have first measured the depletion-induced interactions between a pair of MT filaments (**Fig. 1**). Our results demonstrate that the extensively studied Asakura-Oosawa model of the depletion interaction fails to quantitatively describe the interaction between a pair of MTs. Tentatively we have ascribed this discrepancy to the presence of a disordered amino-acid sequence that coats the MTs surface and acts as a repulsive polyelectrolyte brush. Subsequently, by introducing clusters of molecular motor kinesin, which simultaneously bind to and move along neighboring filaments, we have rendered filamentous bundles active. Using our experimental setup we have measured the interfilament sliding velocity and how it depends on the relevant molecular parameters such as concentration of kinesin clusters and their translocation velocity. We have also quantified the extensile force created by sliding filaments and have thus measured the force-velocity relationship of multi-motor clusters. When clamped at both of their ends, internally generated extensile force induces spontaneous bundle buckling (**Fig. 2**). This phenomenon is an active analog of the well-known Euler buckling which is usually induced by applying an external force on a passive material. Once the curvature reaches a critical value the cohesive forces can no longer sustain uniform structure and the composite bundle frays into individual MTs. Buckling and self-fracture of extensile bundles is the essential microscopic structural motif that drives macroscopic dynamics of diverse non-equilibrium materials. Thus our quantitative characterization of active extensile bundles will provide important design principles that will guide development of entirely new categories of active matter.

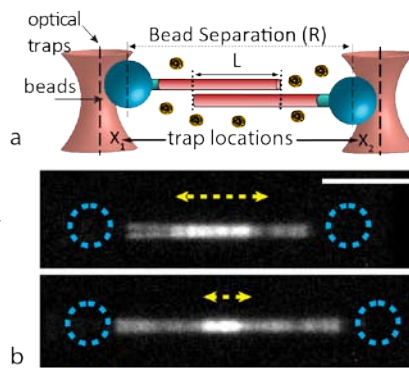


Fig. 1. a) Schematic of a MT configuration used to measure depletion cohesion force. **b)** Experimental setup allows for control of MT overlap length. Scale bar 5 μm .

Self-pumping isotropic active gels: Increasing concentration of extensile bundles leads to the formation of a percolating isotropic network that continuously rearranges on microscopic scale and exhibits emergent properties such as spontaneous chaotic mixing flows. We have discovered a method that transforms the chaotic dynamics of bulk isotropic gels into coherent flows that can be used to transport materials on macroscopic scales and thus harvest energy. Preliminary data suggest that confinement within an annulus induces the formation of autonomous directional circular flows that persist over the entire sample lifetime (up to 24 hours) (**Fig. 3**). This striking phenomenon illustrates the essential difference between active soft matter and its more conventional equilibrium analogues. The later materials only flow in response to applied external pressure while our results indicate that this is not the case for the former systems, as predicted by theoretical models. The self-organized directional flows can serve as a valuable model system that exhibits transition between two inherently non-equilibrium steady states. Using tunable active gels we are systematically characterize the properties of such a non-equilibrium transition. In particular we are varying microscopic parameters such as ATP and MT concentration, confinement geometry and topology to determine how they influence the development of self-organized currents.

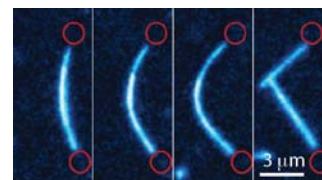


Fig. 2. Motor driven extensile bundles clamped at their end with optical traps buckle and upon reaching a critical curvature fracture.

Orientational Order of Motile Defects in Active Nematics:

The study of conventional equilibrium liquid crystals has led to fundamental insights into the nature of ordered materials, as well as to practical applications such as display technologies. Active nematics are a fundamentally different class of liquid crystals, driven away from equilibrium by the autonomous motion of their constituent rod-like particles. Currently very little is known about the dynamics and structure of these intriguing materials. Increasing the concentration of MTs confined on a 2D oil-water interface leads to assembly of highly ordered nematic domains and robust formation of active liquid crystals. The internally generated activity by molecular motors powers the continuous creation and annihilation of topological defects, which leads to complex streaming flows whose chaotic dynamics appear to destroy any long-range order. We have studied defect dynamics in MT based realization of active nematics. By tracking thousands of defects over centimeter-scale, we have identified a novel non-equilibrium phase characterized by system-spanning orientational order of defects. This emergent order persists over hours despite defect lifetimes of only seconds. Similar dynamical structures are observed in coarse-grained simulations, suggesting that defect-ordered phases are a generic feature of active nematics.

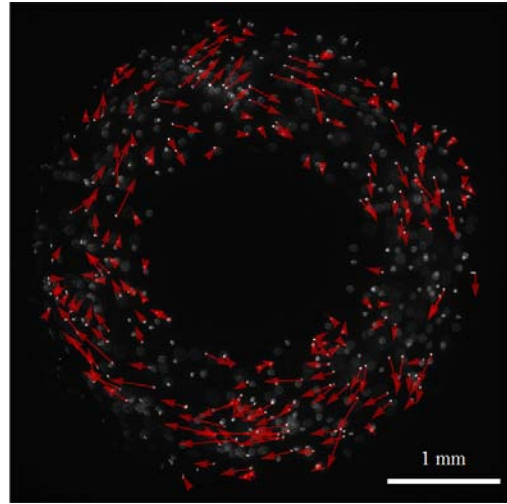


Fig. 3. Fluorescence image demonstrates that circular flows spontaneously emerge when active gel is confined within a torus. The magnitude and direction of red arrows indicates the velocity of tracer beads as they are being advected by the autonomous flow generated by the active gel.

Similar dynamical structures are observed in coarse-grained simulations, suggesting that defect-ordered phases are a generic feature of active nematics.

Oscillatory dynamics of confined active nematics: In order to simplify the complex dynamics of bulk 2D active nematics and thus facilitate comparison to theoretical models we have investigated the behaviour of active nematics confined on surfaces of varying topology and geometry. These explorations demonstrated that confined active nematics exhibit intriguing and highly robust spatiotemporal patterns that have not been predicted by theoretical models. For example, active nematics covering a 2D circular liquid interface organize into a self-spinning vortex-like state that is interrupted by periodic invagination patterns of remarkable regularity (**Fig. 5**). The net circular motion activity induced effective “centrifugal force” that drives outward flux of MT filaments and their accumulation at the edge of the confining geometry. Upon reaching a critical density the extensile edge-bound MTs becomes unstable and buckle, forming a $+1/2$ defect that invaginates the mostly empty interior. This initiates another cycle of outward net MT migration and another subsequent instability that is reminiscent of a

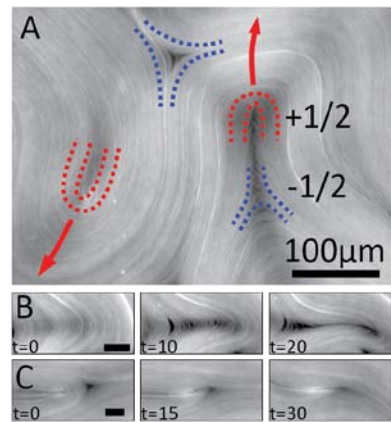


Fig. 4. a) 2D active nematic exhibits motile defects. **b)** Time sequence of images showing how bend instability gives rise to a pair of disclination. **c)** Annihilation of a pair of oppositely charged defects.

gastrulation processes occurring in the development of biological organisms. Each occurrence of instability can switch the handedness of the autonomous circular flows. The dynamics of circular active nematics is an intriguing intermediate case between highly complex unconfined 2D active nematics and much simpler 3D spherical nematics, since it allows for both spatial and temporal control of defect generation.

Future Plans: An important future goal will be to quantitatively characterize how geometrical confinement induces transition of chaotic flows of bulk isotropic gels into a different dynamical state characterized by steady-

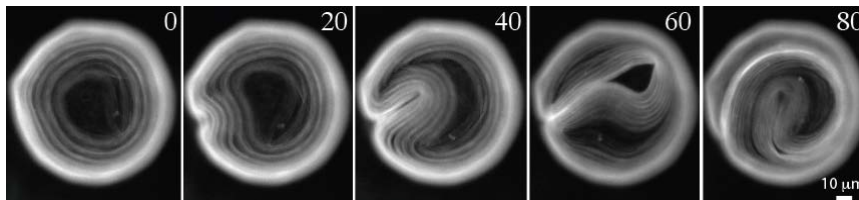


Fig. 5. Dynamics of circularly confined active nematics. Oil is below the image plane while water is above. The plastic sheet covers the interface except for a circular opening which is covered by active nematics. MTs lie parallel to the sample edges. Sample exhibits a periodic gastrulation-like instability of remarkable regularity. Images are 20 sec apart.

state currents capable of material transport. We will also characterize the flow of 2D active nematics and initiate work to develop analogous 3D materials. In particular we will quantify how flows in active nematics are coupled to the dynamics of nematic field, which will be measured separately. We have demonstrated that confined active nematics behave as tunable oscillators. Finally, we will develop quantitative models of confined and will explore the possible hydrodynamic coupling between such oscillators

Publications which acknowledge full or partial DOE support:

1. DeCamp SJ, Redner GS, Baskaran A, Hagan MF, Dogic Z. Orientational Order of Motile Defects in Active Nematics. *Nature Materials*, accepted for publication **2015**.
2. Hilitski F, Ward AR, Cajamarca L, Hagan MF, Grason GM, Dogic Z. Measuring Cohesion between Macromolecular Filaments One Pair at a Time: Depletion-Induced Microtubule Bundling. *Physical Review Letters* **2015**, 114 (13).
3. Henkin G, DeCamp SJ, Chen DTN, Sanchez T, Dogic Z. Tunable dynamics of microtubule-based active isotropic gels. *Philosophical Transactions of the Royal Society a-Mathematical Physical and Engineering Sciences* **2014**, 372 (2029).
4. Keber FC, Loiseau E, Sanchez T, DeCamp SJ, Giomi L, Bowick MJ, et al. Topology and dynamics of active nematic vesicles. *Science* **2014**, 345 (6201): 1135-1139.
5. Ward A, Hilitski F, Schwenger W, Welch D, Lau AWC, Vitelli V, et al. Solid friction between soft filaments. *Nature Materials* **2015**, 14(6): 583-588.

Virus-enabled Biomaterials: Linking Biological Unit, Topology and Thermodynamics in Virus-like Particles

Bogdan Dragnea, Chemistry Department, Indiana University, Bloomington, IN 47405

Program Scope

The overall goal of the program is to establish design principles by which self-assembled subunits organized by biomolecular interactions could lead to formation of three-dimensional coupled networks exhibiting collective responses to light, magnetic fields, etc. While a multitude of other strategies are intensely being pursued, ours is based on encapsulating nanoparticles and other macromolecular cargoes inside symmetric virus shells by self-assembly and relying on innate or engineered biomolecular interactions to further organize these abiotic nanomaterials into a desired network. The plans for program execution can be separated in two parts: a) studies of the building block, i.e. of the virus or virus-like particle, and b) of means to lattice formation under internal and external driving forces.

The virus-enabled approach has some unique advantages and potential side benefits:

- 1) Stoichiometric control of the building block. In many cases of interest, virus self-assembly is a process leading to the spontaneous organization of macromolecules in **finite-size mesoscopic systems** that are **structurally and functionally identical** down to molecular scale.
- 2) Potential for emergent complexity from simple anisotropic building blocks (1). Interactions between proteins and nucleic acid molecules that make a virus are anisotropic. This anisotropy translates to higher scales.
- 3) Versatility via established biomolecular engineering approaches including genetic and chemical modification methods.
- 4) Bioinspiration: viruses have evolved under stringent constraints of scale and chemical environment. Fundamental understanding of their physical and chemical properties provides inspiration. For instance, to maintain the advantages brought by icosahedral symmetry, large viruses will use scaffold proteins to guide assembly. We have used nanoparticles and even other viruses to same effect.
- 5) Viruses are gene carriers. A native virus particle will not have much more room to carry extra genes than its own. Engineered capsids, however, can afford larger cargo volumes. Thus, there is potential for indirect impact on energy technologies such as biofuels via improved gene delivery approaches.

The building block for biomaterials under study is a virus-like particle (VLP), a biotic/abiotic hybrid composed of a symmetric virus coat protein cage assembled from a magic number of proteins, which form an optimal number of contacts.

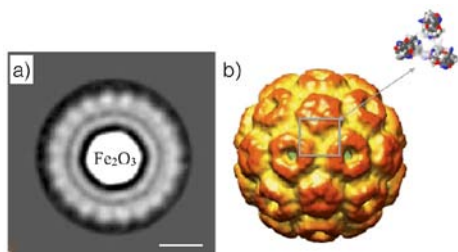


Figure 1. a) Highest-reported resolution cryo-em micrograph of a VLP (maghemite core) and 3D reconstruction of the protein shell structure. The inset shows a map of hydrophobic and cationic patches on the shell surface (2). We have discovered that mechanical properties are echoing such chemical anisotropy. Scale bar: 10 nm.

In certain conditions, the protein cage will efficiently and spontaneously grow around a variety of cargoes from free proteins in solution, if they possess the appropriate chemical functionality promoting self-assembly, Fig. 1. An important feature is that the magic number of proteins forming the cage can be controlled (3). However, until recently, it was not known how thermodynamic stability varies as a function of the cage size.

Recent Progress

Topology and thermodynamics. Control of the magic number of proteins in the regular shell opens the way, in principle, to heterostructures in which functionally

and structurally different building blocks can be combined. Interesting, new properties such as optical magnetism without magnetic materials (4) and optical surface tension are expected. These will make the medium-term objectives of our studies.

In recent past, we have focused on the relationship between biological subunit, topology of assembly. More precisely, we have established thermodynamic analysis protocols to determine how the free energy of a cage formed from brome mosaic virus (BMV) coat proteins depends on the number of protein subunits. Studies include the experimental measurement of equilibrium concentrations of VLPs with a gold nanoparticle core and of free capsid proteins. From the equilibrium free protein concentration and initial conditions, a Gibbs free energy was extracted for a limited number of nanoparticle diameters. The data set is currently incomplete this being work in progress, but from the partial data we have gathered so far, it looks like the Gibbs free energy of the native virus structure is an absolute free energy minimum, much deeper than the theoretical expectations based on isotropic subunit packing. To gain an understanding on the role of each of the factors potentially involved, we have teamed up for modeling work with the theory groups of Roya Zandi at UC Riverside and Paul van der Schoot at T.U. Eindhoven (5). Moreover, our studies of the interaction between the native RNA cargo and the coat protein (6,7) taught us important lessons that could be followed to extend the range of cage sizes from 18 nm diameter (60 proteins) to 60 nm diameter (720 proteins), Fig. 2.

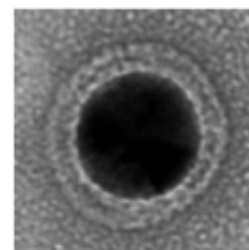


Figure 2. Largest stable BMV VLP to date. It contains ~ 720 proteins wrapped around a 50 nm Au particle. Its structure is not yet known, but AFM indicated local hexagonal symmetry.

Non-icosahedral shells. Being able to explore cages that form away from prescribed magic numbers brings in focus the question of defects, which must appear in order to accommodate the topological constraint imposed by the scaffold. A hexameric sheet of proteins requires defects in order to gain curvature. As the VLP radius increases, so does bending strain which tends to accumulate mainly at pentameric sites in the case of regular, icosahedral capsids. At a certain subunit size to radius of curvature ratio, the isolated pentamers characteristic of icosahedral symmetry become unstable. Bending of the close-packed protein sheet is acquired by introducing other types of crystallographic defects. This is a poorly understood phenomenon due to lack of structural methods of study. To acquire enough spatial resolution, established ultrastructural methods such as X-ray diffraction or cryo-em with single particle reconstruction rely on averaging. States of low symmetry and low abundance are not normally accessible by these methods. Yet, the template assembly method we have developed can stabilize such states. However, spherical assembly templates formed of metal nanoparticles have drawbacks for cryo-em due to strong scattering and electron absorption in gold with respect to the comparatively weak signal from the protein shell. To alleviate this challenge and avoid averaging among dissimilar particles, we have developed a novel method by which the recombinant procapsids of another virus, a bacteriophage, were functionalized with nucleic acid, enabling them to act as templates around which the structural protein of another virus (HIV-1) assembled into isometric virus-like particles, Fig. 3.

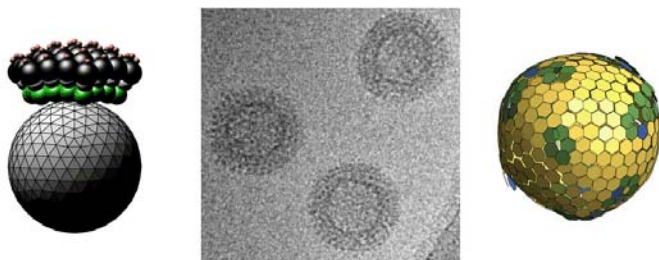


Figure 3. A phage (P22) encased in a HIV virus cage: schematic, cryo-em image, cryo tomographic reconstruction of the HIV Gag protein colored according topology.

The ability to provide Gaussian curvature, electron beam transparency, and reduced size polydispersity enabled the analysis, at a single-particle scale, of the assembly subunit coordination network (topology), and extract morphological features which afforded new insights into the assembled-state subunit interactions.

Future Plans

From recent studies it became clear that encapsulated cargo by virus-like particles can play a central role to the thermodynamic stability of the particle. The focus will be on thermodynamics and dynamics of protein subunits organizing on the surface of a spherical template and we will continue to pay close attention to the link between topology and thermodynamics. We have started experiments that aim at generating a free energy landscape of the virus-like particle assembly process. The results will be compared with those obtained from molecular dynamics simulations of isotropic and anisotropic subunits packed on the surface of a sphere. The outcome will be a quantitative picture of the weight of biological adaptation vs. the classical geometrical optimization principles set forward fifty years ago by Caspar and Klug. Other experiments will concern formation and crystallization of nonicosahedral VLPs, e.g. using

short silver nanorod templates, Fig. 4, which we expect will also be characterized by shell closeness and protein magic numbers albeit in a different series than the quasi-equivalent. Low-symmetry subunits such as nano rods hold technological promise for magneto-optical materials, but are challenging to produce in reproducible fashion. We hypothesize that stability associated with a closed shell of proteins can provide a means towards narrowing nanorod VLP distribution.

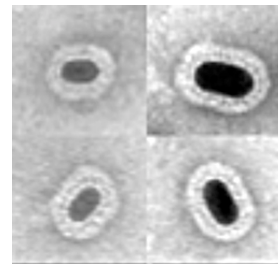


Figure 4. Non-icosahedral closed cages formed by template-assembly on short Au rods 10 nm diameter. The protein shell structure is unknown.

We have also started experiments of co-crystallization of Ag-VLPs and Au-VLPs. The goal is to construct a phase diagram and hopefully discover phase space parameters that lead to co-crystallization.

References

- (1) Fejer, S. N.; Chakrabarti, D.; Wales, D. J. Emergent Complexity from Simple Anisotropic Building Blocks: Shells, Tubes, and Spirals. *ACS Nano* **2010**, *4*, 219–228.
- (2) Malyutin, A. G.; Easterday, R.; Lozovyy, Y.; Spilotros, A.; Cheng, H.; Sanchez-Felix, O. R.; Stein, B. D.; Morgan, D. G.; Svergun, D. I.; Dragnea, B.; *et al.* Virus-like Nanoparticles with Maghemite Cores Allow for Enhanced MRI Contrast Agents. *Chem. Mater.* **2015**, *27*, 327–335.
- (3) Sun, J.; DuFort, C.; Daniel, M.-C.; Murali, A.; Chen, C.; Gopinath, K.; Stein, B.; De, M.; Rotello, V. M.; Holzenburg, A.; *et al.* Core-Controlled Polymorphism in Virus-like Particles. *Proc. Natl. Acad. Sci. U. S. A.* **2007**, *104*, 1354–1359.
- (4) Monticone, F.; Alù, A. The Quest for Optical Magnetism: From Split-Ring Resonators to Plasmonic Nanoparticles and Nanoclusters. *J. Mater. Chem. C* **2014**, *2*, 9059–9072.
- (5) Kusters, R.; Lin, H.-K.; Zandi, R.; Tsvetkova, I.; Dragnea, B.; van der Schoot, P. Role of Charge Regulation and Size Polydispersity in Nanoparticle Encapsulation by Viral Coat Proteins. *J. Phys. Chem. B* **2015**, *119*, 1869–1880.
- (6) Vaughan, R.; Tragesser, B.; Ni, P.; Ma, X.; Dragnea, B.; Kao, C. C. The Tripartite Virions of the Brome Mosaic Virus Have Distinct Physical Properties That Affect the Timing of the Infection Process. *J. Virol.* **2014**, *88*, 6483–6491.
- (7) Smith, V. M.; Dragnea, B. In Singulo Probing of Viral RNA Dynamics by Multichromophore Fluorescence Dequenching. *J. Phys. Chem. B* **2014**.

Publications

- (1) Tsvetkova, I. B.; Dragnea, B. Encapsulation of Nanoparticles in Virus Protein Shells. In *Methods in molecular biology (Clifton, N.J.)*; **2014**.

- (2) Smith, V. M.; Dragnea, B. In Singulo Probing of Viral RNA Dynamics by Multichromophore Fluorescence Dequenching. *J. Phys. Chem. B* **2014**, 18, 14345-52.
- (3) Vaughan, R.; Tragesser, B.; Ni, P.; Ma, X.; Dragnea, B.; Kao, C. C. The Tripartite Virions of the Brome Mosaic Virus Have Distinct Physical Properties That Affect the Timing of the Infection Process. *J. Virol.* **2014**, 88, 6483–6491.
- (4) Malyutin, A. G.; Easterday, R.; Lozovyy, Y.; Spilotros, A.; Cheng, H.; Sanchez-Felix, O. R.; Stein, B. D.; Morgan, D. G.; Svergun, D. I.; Dragnea, B.; *et al.* Virus-like Nanoparticles with Maghemite Cores Allow for Enhanced MRI Contrast Agents. *Chem. Mater.* **2015**, 27, 327–335.

Semiconductor Nanocrystals as Light Harvesters for Biomimetic Solar Fuel Generation

PI: Gordana Dukovic, Department of Chemistry and Biochemistry, University of Colorado Boulder

Program Scope

The goal of this project is to understand how the remarkable light-harvesting properties of semiconductor nanocrystals could be synergistically combined with the outstanding efficiencies of enzymes that catalyze fuel-forming reactions to enable efficient fuel production under solar irradiation. This approach is inspired by photosynthesis, where light absorption is coupled to catalysis via electron transfer steps. We aim to provide design principles for synthetically tailoring the optimal light absorbers and integrating them with enzymatic catalysts in a way that minimizes energy-wasting processes. This is critical because the rates of light absorption, electron and hole transfer, and redox reactions must be balanced and matched with the solar flux in order for solar energy to be efficiently transferred into new chemical bonds and prevent light-induced damage.

Recent Progress

In order to examine how semiconductor nanocrystals and redox enzymes can be coupled to photochemically produce fuels, we have focused on our prototypical system: CdS nanorods (NRs) coupled with [FeFe]-hydrogenase from *Clostridium acetobutylicum* (CaI). In collaboration with King and co-workers, we have demonstrated that complexes of CdS NRs and CaI generate H₂ under illumination, with quantum yields (QY(H₂)) of up to 20%.¹ The CdS-CaI complexes form via a biomimetic interaction in which CdS NRs, capped with negatively-charged surface ligands, bind to CaI as analogs of the electron-donating protein ferredoxin.¹ We proposed a model for photochemical H₂ generation that involves light absorption by CdS NRs and injection of photoexcited electrons (i.e., electron transfer, ET) into CaI, which can then utilize two electrons to reduce two protons and generate one H₂ molecule.¹ Photoexcited holes are scavenged by ascorbate in solution.

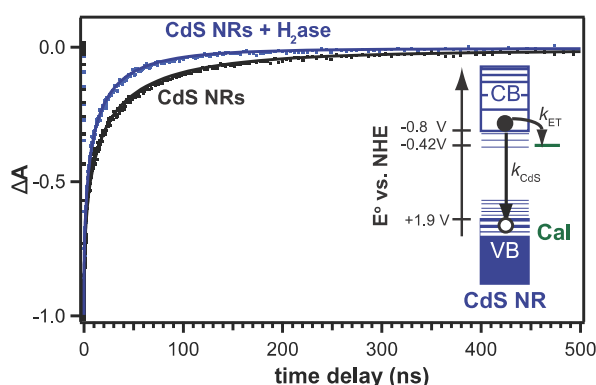


Figure 1. TA kinetics of the band gap feature for CdS NRs (black) and CdS-CaI complexes (molar ratio 1:1, blue). Inset: Energy level diagram depicting the competition between ET and electron-hole recombination.

Critical to our understanding of photochemical H₂ generation in CdS-CaI complexes is the fact that electron relaxation pathways in nanocrystals, such as trapping and recombination, are in kinetic competition with ET to CaI. The quantum efficiency of ET to CaI (QE_{ET}), defined as (electrons transferred)/(photons absorbed), depends on the ratio of the ET rate constant (k_{ET}) and the rate constant of the internal electron decay processes (k_{CdS}). The value of QE_{ET} defines the upper limit on the value of QY(H₂) because only electrons delivered to CaI can be incorporated into H₂ molecules. Semiconductor nanocrystals are highly

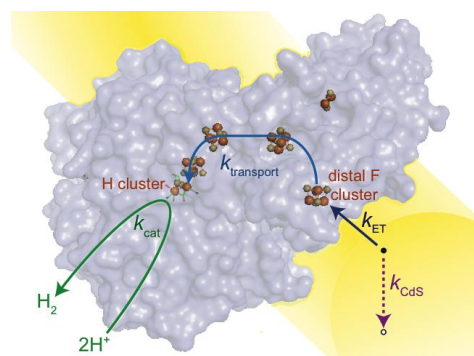


Figure 2. Schematic of the electron pathway resulting in H_2 generation by photoexcited CdS-CaI complexes.

Measurement of ET kinetics using transient absorption (TA) spectroscopy. In order to examine how nanocrystal structure controls ET to CaI, we first measured the rates and efficiencies of ET in our prototypical system, CdS NRs capped with 3-mercaptopropionic acid (3-MPA) and coupled to CaI.^{2,3} To accomplish this, we employed transient absorption (TA) spectroscopy.³ Upon excitation, TA spectra of CdS NRs exhibit a transient bleach feature that directly reports on electron relaxation kinetics (Figure 1). In the presence of the enzyme, in a 1:1 ratio, electron decay in CdS NRs is approximately a factor of two faster, indicating that ET and electron relaxation in CdS are in direct competition and occur with similar probabilities. Similar ET kinetics were observed when the enzyme active site was inactivated. This observation is consistent with the biomimetic model for H_2 generation, in which electron injection occurs at the distal iron sulfur cluster near the ferredoxin binding pocket, and is followed by electron transport to the active site, located 2.9 nm away (Figure 2). Average ET rate increases linearly with the number of enzymes adsorbed. However, binding more enzymes on each NR does not aid H_2 production because of the competition for the second electron among multiple enzymes on each NR.

It is challenging to develop a quantitative understanding the kinetics of nanocrystal-enzyme ET because the excited states of nanocrystals decay nonexponentially over many decades in time, which results from structural heterogeneities present in an ensemble sample. Additionally, the number of enzymes adsorbed varies in the ensemble sample. To understand how specific electron decay processes in CdS NRs compete with ET to CaI, it is necessary to use

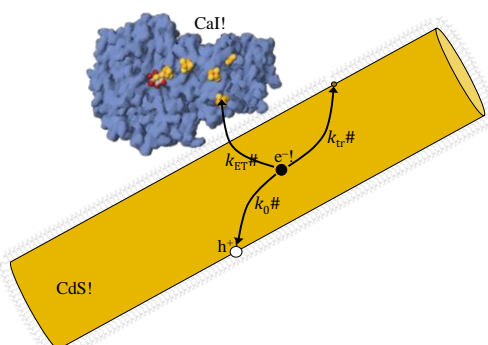


Figure 3. Schematic depiction of a CdS-CaI complex and the photoexcited electron decay pathways, including electron-hole recombination (k_0), electron trapping (k_{tr}), and electron transfer (k_{ET}).

synthetically tunable, with procedures available for the control of particle size, shape, composition, and surface chemistry. Thus, their electronic structure, including absorption spectra and driving forces for photochemical redox reactions, can be designed and optimized for specific applications. In principle, the rate constants for processes involved in photochemical H_2 generation, k_{ET} and k_{CdS} , can be controlled through synthetic modifications of CdS NRs. Here, we examine how aspects of nanocrystal structure can be used to control ET kinetics and, ultimately, H_2 generation.

a kinetic model that accounts for CdS NR heterogeneity as well as the number distribution of bound CaI moieties per NR.

We developed and employed such a kinetic model to analyze the decay of the electron population observed in the TA signal of CdS NRs and CdS-CaI complexes.² We determined the intrinsic rate constants for three electron decay processes: electron-hole recombination in CdS NRs (k_0), electron trapping (k_{tr}), and ET to CaI (k_{ET}) (Figure 3). We found k_0 to be $1.5 \times 10^7 \text{ s}^{-1}$, and k_{tr} to be 7-fold larger ($1.1 \times 10^8 \text{ s}^{-1}$), with the average electron trap density ($\langle N_{tr} \rangle$) of 0.6 per NR. k_{ET} ($2.4 \times 10^7 \text{ s}^{-1}$) is within a factor of two of k_0 . This

value of k_{ET} is lower than those usually observed for molecules and metal particles adsorbed on the nanocrystal surfaces. It is, however, consistent with an ET process that depends on electron tunneling to the injection site (distal cluster), as is common in biological systems. We found a quantitative agreement between QE_{ET} and the quantum yield of H_2 generation using CdS-CaI complexes.¹ This similarity suggests that CaI converts electrons from photoexcited CdS NRs into H_2 with close to 100% efficiency, illustrating the remarkable electrocatalytic properties of this enzyme. This result supports the idea that the key to improving H_2 production lies in increasing QE_{ET} .

Modeling the excited state relaxation of CdS-CaI complexes in this way provides insights into the factors that play a critical role in photochemical H_2 generation. QE_{ET} in the ensemble sample is a function of both the ratios of the intrinsic rate constants and of the average numbers of traps and enzymes. While it depends strongly on the ratio k_{ET}/k_0 , the dependence on k_{tr}/k_0 is weak because $\langle N_{tr} \rangle$ is small. Thus the key to more efficient photochemical H_2 generation lies in improving the efficiency of ET from CdS NRs to CaI by manipulating the individual contributions of k_{ET} and k_0 . Our current work in manipulating the surface and electronic structure of semiconductor nanocrystals to control the value of k_{ET}/k_0 is summarized next.

Impact of surface-capping ligands on ET kinetics. In our prototypical CdS NR-CaI system, the nanocrystal surfaces are capped with 3-MPA.^{1,3} By tuning the ligand length, we can examine the role of the surface-capping ligands in ET and H_2 production. We have varied the length of the ligand from 3 to 11 carbons in the aliphatic chain, while maintaining the same functional groups

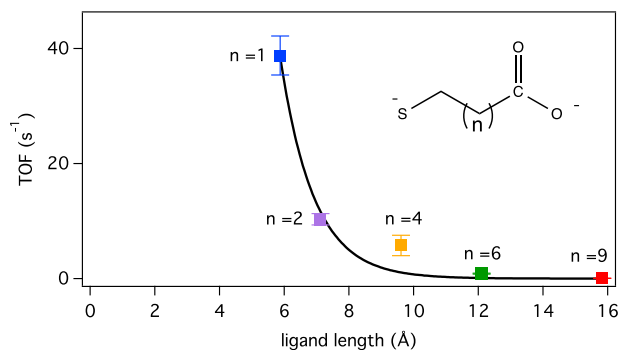


Figure 4. Light-driven hydrogen production as a function of ligand length. The solid line is an exponential decay according to Eq 4.1 where $\beta=0.96 \text{ \AA}^{-1}$.

that interact with the nanocrystal surface and the enzyme. The photochemical H_2 production decreased exponentially as a function of ligand length, as shown in Figure 4. This data is suggestive of electron tunneling through the surface-capping ligand layer to the injection site in CaI. Light-driven H_2 production is not a direct measure of ET, but is rather a result of the competition between ET and the photophysical decay processes in the nanocrystal, represented by QE_{ET} . A change in surface-capping ligand can impact multiple competing pathways for

the electron. We are currently carrying out TA measurements and kinetic modeling to determine how the ET rates and efficiencies in CdS-CaI complexes depend on the surface-capping ligands.

Impact of nanocrystal electronic structure on ET kinetics. In addition to examining the role of surface-capping ligands in determining QE_{ET} primarily by controlling k_{ET} , we are also examining how charge-separating nanocrystal heterostructures, which are expected to have smaller values of k_0 than CdS NRs^{4,5} can enhance the competitiveness of ET with recombination processes in the nanocrystal. Two heterostructures are currently under investigation: CdSe/CdS dot-in-rods (DIRs) and ZnSe/CdS DIRs. These materials have considerably more complicated photophysics than CdS NRs. We are currently developing kinetic models that will enable us to

quantitatively analyze the already acquired TA data on these structures in the presence of CaI and provide the level of detail that we have achieved with CdS NRs.

Future Plans

In addition to completing the work on currently in progress, as described above, there are two main directions for the near future. The first direction relates to the role of surface-capping ligands in determining the rate of ET between a nanocrystal and an enzyme. The information we have to date points to the ligand serving as a tunneling barrier. For this reason, we will explore alternative ligand designs that could enhance ET and H₂ generation by manipulating this tunneling barrier.

The second major direction will involve extending the strategy of using nanocrystals to mimic the interactions between redox enzymes and their biological redox-transfer partners to photochemical CO₂ reduction. In contrast to most artificial, inorganic CO₂ reduction catalysts, enzymes catalyze the reaction selectively, without a significant amount of H₂ generation from protons. They also operate at a low overpotential. CO₂ reduction is a more kinetically complicated reaction than H₂ generation, and understanding how enzymes catalyze it selectively can inform future artificial catalyst designs. We will focus on how nanocrystal structural parameters can be tuned to control the rates and efficiencies of photochemical CO₂ reduction.

References

- (1) Brown, K. A.; Wilker, M. B.; Boehm, M.; Dukovic, G.; King, P. W. *J. Am. Chem. Soc.* **2012**, *134*, 5627.
- (2) Utterback, J. K.; Wilker, M. B.; Brown, K. A.; King, P. W.; Eaves, J. D.; Dukovic, G. *Phys. Chem. Chem. Phys.* **2015**, *17*, 5538.
- (3) Wilker, M. B.; Shinopoulos, K. E.; Brown, K. A.; Mulder, D. W.; King, P. W.; Dukovic, G. *J. Am. Chem. Soc.* **2014**, *136*, 4316.
- (4) Kim, S.; Fisher, B.; Eisler, H. J.; Bawendi, M. *J. Am. Chem. Soc.* **2003**, *125*, 11466.
- (5) Eshet, H.; Grunwald, M.; Rabani, E. *Nano Lett.* **2013**, *13*, 5880.

Publications (supported by this award):

M. B. Wilker, K. E. Shinopoulos, K. A. Brown, D. W. Mulder, P. W. King, G. Dukovic. "Electron transfer kinetics in CdS nanorod-[FeFe] hydrogenase complexes and implications for photochemical H₂ generation." *Journal of the American Chemical Society*, **2014**, *136*, 4316-4364. **Featured in JACS Spotlights.**

J. K. Utterback, M. B. Wilker, K. A. Brown, P. W. King, J. D. Eaves, G. Dukovic. "Competition between electron transfer, trapping, and recombination in CdS nanorod-hydrogenase complexes." *Physical Chemistry Chemical Physics*, **2015**, *17*, 5538-5542.

K. A. Brown, N. Khadka, M. B. Wilker, S. Keable, G. Dukovic, J. W. Peters, L. C. Seefeldt, P. W. King. “Light-Driven Catalysis by Nitrogenase MoFe Protein-Nanorod Complexes.” *Submitted.*

Experimental Realization of ‘Repair-and-Go’ Using Microencapsulation of Nanomaterials

Principle Investigator: Todd Emrick

Affiliation: Polymer Science and Engineering Department

University of Massachusetts Amherst, MA 01003

E-mail: tsemrick@mail.pse.umass.edu

Program scope. This project develops new materials and methods for microencapsulation and advanced concepts in materials repair that exploit lessons from biology, specifically processes associated with wound healing and delivery/repair. Our experimental work benefits from theoretical findings of Balazs,^[1] who simulates delivery of encapsulated particulates to damaged regions (cracks) of substrates. We find that such specified delivery is possible using polymer-stabilized oil-in-water emulsion droplets on substrates having differentiated wetting properties between the pristine surface and the damaged regions. We have realized this so-called ‘repair-and-go’ concept through deposition of CdSe quantum dots into the cracks of damaged substrates,^[2] and more recently by deposition of SiO₂ nanoparticles that afford measurable materials repair of the substrates. In conjunction with ‘repair-and-go’, we are engaged in complementary efforts to develop functional droplets that locate and pickup nanoparticles from substrates in a process related conceptually to the *in vivo* action of osteoclasts that function to balance bone density. The theoretical basis for this work, again inspired by Balazs,^[3] utilized synthetic vesicles to probe substrates and capture Janus-type NPs with distinct hydrophobic and hydrophilic hemispheres. We have generalized the concept to employ functional droplets and nanoparticles, including hydroxyapatite (HA) NPs that mimic the chemical makeup of human bone.

Recent Progress. Our experimental approach to ‘repair-and-go’, illustrated in **Figure 1A**, utilizes microcapsule carriers of nanoparticles that deposit the particles into the damaged regions of cracked polymer films. Key to the success of these experiments is the robust nature of the polymer surfactant that stabilizes the droplets. Phosphorylcholine (PC) functionality in the polymer prevents irreversible droplet adsorption (or surface fouling) onto the pristine surface. In ‘repair-and-go’, PC-polyolefins stabilize the emulsion droplets and encapsulate nanoparticles (*i.e.*, CdSe quantum dots or fluorescent SiO₂ nanoparticles) in an oil phase, while the droplets are dispersed in a continuous aqueous phase. The droplets are introduced to a fluidic system and enter a flow cell containing the cracked substrate, and are circulated with a peristaltic pump that produces laminar flow (flow rate 0.5 mL/sec, Reynolds number ~300). A typical “repair-and-go” experiment involves 100-200

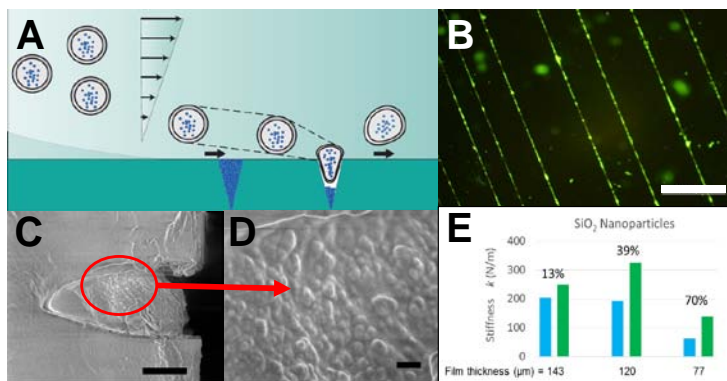


Figure 1. (A) ‘Repair-and-go’ illustration, from White and coworkers,^[4] highlighting the theoretical work of Balazs; (B) fluorescence micrograph of a substrate after ‘repair-and-go’, with the green fluorescent lines reflecting nanoparticle deposition into the cracks (scale bar = 500 nm); (C, D) SEM image of the cross-section of a filled crack after ‘repair-and-go’, with visualization of the 50 nm (on average) diameter SiO₂ nanoparticles. Scale bars: 1 micron in (C) and 200 nm in (D); (E) Stiffness of PDMS films before and after “repair-and-go”. Blue column: damaged polymer film; green column: after “repair-and-go”. The percentage shown above each column is the corresponding healing efficiency.

pulsed intervals, each interval consisting of flow and rest periods of 5-30 seconds duration. The fluorescence of the deposited nanoparticles allows their identification by electron microscopy in the damaged regions (**Figure 1B**) and confirms a relative absence of nanoparticles on the pristine surface. Samples for SEM characterization were prepared by freeze-fracturing the substrate in liquid nitrogen to expose a cross-sectional view, imaged on a 90° sample mount at 1 kV. **Figures 1C and D** show the SiO₂ NPs (~50 nm diameter) embedded in the cracks. This nanoparticle deposition afforded considerable recovery of properties, as judged by the stiffness of the material after ‘repair-and-go’ relative to the initially damaged material. This is shown in **Figure 1E**, using data derived from dynamic mechanical analysis (DMA), and work is progressing towards optimizing repair as a manuscript draft is prepared for submission.^[5]

Developing polymer-stabilized droplets that perform nanoparticle deposition, nanoparticle pickup, or both (*i.e.*, pickup and drop off) under fluid flow represents a significant advance in surfactant/materials science owing to biological inspiration. To this end, we are studying transport systems for nanoparticles, using polymer-stabilized droplets, in

which functional groups on the polymer interact with the nanoparticles of interest. As depicted in **Figure 2**, the droplets

traverse a surface to locate, pick up, and carry away the nanoparticles (the droplets are termed ‘*ostedroplets*’ for their conceptual relationship to the action of osteoclasts *in vivo*). The fundamental characteristics observed in nanoparticle pickup include: 1) PC-polyolefin stabilized ‘smart droplets’ that promote nanoparticle insertion *onto the fluid-fluid interface*; and 2) PC-polyolefin stabilized droplets that *engulf NPs into the interior oil phase*.

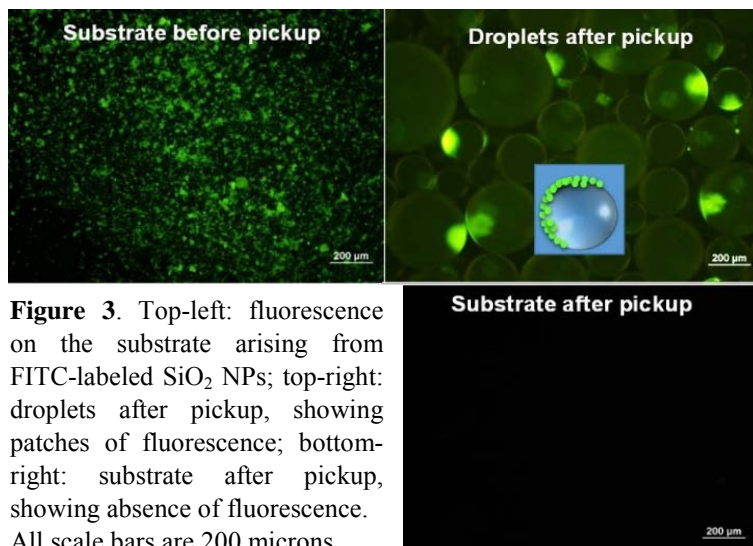


Figure 3. Top-left: fluorescence on the substrate arising from FITC-labeled SiO₂ NPs; top-right: droplets after pickup, showing patches of fluorescence; bottom-right: substrate after pickup, showing absence of fluorescence. All scale bars are 200 microns.

These “Janus droplets” reflect the formation of a cross-linked polymer/nanoparticle network at the fluid-fluid interface, rationalized by reaction of the multifunctional nanoparticles with the multifunctional polyolefin. **Figure 3** (bottom-right) shows the efficiency of the technique - nanoparticles are removed entirely from the substrate with no trace of residual fluorescence. Control experiments showed that nanoparticles were retained on the substrate when subjected only to flowing pure water,^[6] or when

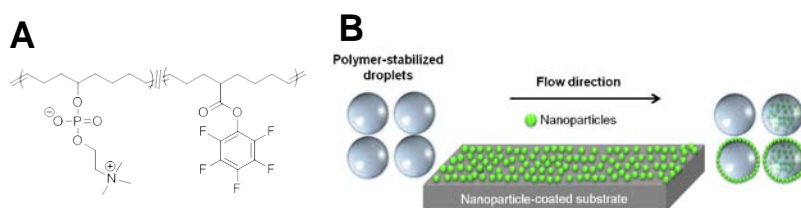


Figure 2. (A) Smart droplets from PFPE-functionalized polymer surfactants; (B) possible pickup scenarios using functional droplets and nanoparticle-contaminated surfaces.

subjected to flow with non-functional droplets (no PFPE groups). This ‘osteodroplet’ technique simultaneously cleans and collects/encapsulates debris from substrates, avoiding uncontrolled dispersal into the fluid phase.

Moving close to biological mimicry, we are developing droplets that pickup nanoparticle with compositions more typical of bone, including hydroxyapatite (HA) NPs having the chemical structure $\text{Ca}_5(\text{OH})(\text{PO}_4)_3$. Commercial HA NPs are polydisperse, with TEM analysis showing 30-300 nm diameter structures. Embedding catechols (1,2-dihydroxybenzene) into PC-polyolefins affords new functional surfactants that both stabilize droplets and provide functionality for recognition and pickup of HA NPs. Catechol interacts with calcium ions of HA (i.e., non-nanoparticulate structures), known from the bone imaging reports of Moriguchi;^[7] in our work catechols prove well-suited for integration into these nanoparticle-transporting droplets. Catechol groups were integrated smoothly into PC-poly(cyclooctene) by copolymerization and nucleophilic substitution onto the PFPE-substituted intermediates. Fortunately, PC-catechol copolymers effectively stabilize oil-in-water droplets, with pendant drop tensiometry giving interfacial tension values of 9-11 mN/m at the TCB/water interface, confirming a strong surfactant character (similar to that of PC-polyolefin homopolymer) and suitability for evaluation in HA NP pickup experiments.

Pickup experiments on HA nanoparticles were performed using a pump-driven flow system to pass droplets over 2 x 1 cm Si wafers coated with HA nanoparticles. Oil-in-water droplets stabilized with PC-catechol polyolefins were formed by agitation of a 2 mg/mL aqueous polymer solution in TCB, then introduced to the substrate at a flow rate of 0.5 mL/sec. **Figure 4** shows the HA nanoparticles by optical microscopy as black spots (aggregates) on the substrate, and by SEM (insets). We found that HA nanoparticle ‘debris’ was cleaned from the substrate using PC-catechol droplets containing 28 mole percent catechol. Image J[®] analysis revealed that nearly all of the HA nanoparticle coverage was removed by the droplets. Notably, the droplets remained intact following the experiment, and were imaged by TEM to confirm that the HA NPs originally on the silicon wafer became associated with the droplets. Control experiments were crucial for confirming the role of the catechol-functionalized droplets in HA NP pickup. In the absence of the droplets, but under otherwise identical aqueous flow conditions, no significant reduction in HA nanoparticle content was seen. Moreover, attempted HA NP experiments using droplets stabilized with PC-polyolefins (i.e., without catechol functionality) similarly failed to clean the substrate of HA NPs.

Figure 4 shows the HA nanoparticles by optical microscopy as black spots (aggregates) on the substrate, and by SEM (insets). We found that HA nanoparticle ‘debris’ was cleaned from the substrate using PC-catechol droplets containing 28 mole percent catechol. Image J[®] analysis revealed that nearly all of the HA nanoparticle coverage was removed by the droplets. Notably, the droplets remained intact following the experiment, and were imaged by TEM to confirm that the HA NPs originally on the silicon wafer became associated with the droplets. Control experiments were crucial for confirming the role of the catechol-functionalized droplets in HA NP pickup. In the absence of the droplets, but under otherwise identical aqueous flow conditions, no significant reduction in HA nanoparticle content was seen. Moreover, attempted HA NP experiments using droplets stabilized with PC-polyolefins (i.e., without catechol functionality) similarly failed to clean the substrate of HA NPs.



Figure 4. Optical microscopy images (scale bar: 500 μm) of Si substrates before (left) and after (right) HA pickup (SEM image insets are of the same substrates, scale bar: 500 nm).

Future Plans. Highly sensitive assessment of HA nanoparticle pickup would benefit absorption or fluorescence measurements that are precluded by the lack of such properties in the native HA nanoparticles. Chelating dyes such as alizarin red will be used to functionalize HA nanoparticles to provide spectroscopic handles^[7] for fluorescence imaging before and after attempted pickup. The effect of substrate composition will be investigated systematically, by varying the charge of the substrate through selection of different substrates (polymeric, inorganic, metallic) and by surface modification of substrates that produce self-assembled monolayers of well-defined charge. Presently, we know that HA nanoparticles are picked up successfully from silicon, mica, and

UV/Ozone-treated PDMS, but not from plastic films such as poly(ethylene terephthalate) (PET), the later possibly affected by the hydrophobic character of this aromatic polyester (water contact angle = 72°) that minimizes droplet wetting of the substrate and resultant droplet-to-substrate contact time. The results described above using PC-catechol polyolefins will allow examination of a breadth of nanoparticles compositions, especially metal oxides, in NP pickup. Titania, iron oxide, and numerous other nanoparticles will be tested as the platform of pickup capabilities expands during the course of the project. Furthermore, experiments are underway in which droplets stabilized with PC-catechol copolymers pick up HA nanoparticles, transport them along the substrate, then drop them off at defined locations on the substrate. This controlled nanoparticle relocalization (*pickup and drop off*) would represent an advance over our accomplished work to-date, and more closely mimic Nature's elegant and cooperative action of osteoclasts/osteoblasts. Demonstrating such capabilities would open new possibilities for controlling the placement of NPs with properties relevant to catalysis, magnetic materials, and other applications.

References.

1. Kolmakov, G. V.; Revanur, R.; Tangirala, R.; Emrick, T.; Russell, T. P.; Crosby, A. J.; Balazs, A. C., Using nanoparticle-filled microcapsules for site-specific healing of damaged substrates: creating a 'repair-and-go' system. *ACS Nano* **2010**, 4, 1115-1123. DOI: 10.1021/nn901296y.
2. Kratz, K.; Narasimhan, A.; Tangirala, R.; Moon, S.; Revanur, R.; Kundu, S.; Kim, H.S.; Crosby, A.J.; Russell, T.P.; Emrick, T.; Kolmakov, G.; Balazs, A. C., Probing and repairing damaged surfaces with nanoparticle-containing microcapsules. *Nature Nanotechnology* **2012**, 7(2), 87-90. DOI: 10.1038/nnano.2011.235.
3. Salib, I.; Yong, X.; Crabb, E. J.; Moellers, N. M.; McFarlin IV, G. T.; Kuksenok, O.; Balazs, A. C., Harnessing fluid-driven vesicles to pick up and drop off Janus particles. *ACS Nano* **2013**, 7(2), 1224-1238. DOI: 10.1021/nn304622f.
4. White, S. R.; Geubelle, P. H., Self-healing materials: Get ready for repair-and-go. *Nature Nanotechnology* **2010**, 5(4), 247-248. DOI: 10.1038/nnano.2010.66.
5. Bai, Y.; Chang, C. C.; Zhao, X.; Ribbe, A.; Kosif, I.; Szyndler, M.; Crosby, A.; Emrick, T., Mechanical restoration of damaged polymer films by "repair-and-go". Manuscript in preparation.
6. Kosif, I.; Chang, C. C.; Bai, Y.; Ribbe, A. E.; Balazs, A. C.; Emrick, T., Picking up nanoparticles with functional droplets. *Advanced Materials Interfaces* **2014**, 1(5), 1400121. DOI: 10.1002/admi.201400121.
7. Moriguchi, T.; Yano, K.; Nakagawa, S.; Kaji, F., Elucidation of adsorption mechanism of bone-staining agent alizarin red S on hydroxyapatite by FT-IR microspectroscopy. *Journal of Colloid and Interface Science* **2003**, 260(1), 19-25. DOI: 10.1016/S0021-9797(02)00157-1.

Publications.

1. Kosif, I.; Chang, C. C.; Bai, Y.; Ribbe, A. E.; Balazs, A. C.; Emrick, T., Picking up nanoparticles with functional droplets. *Advanced Materials Interfaces* **2014**, 1(5), 1400121. DOI: 10.1002/admi.201400121.
2. Bai, Y.; Chang, C. C.; Zhao, X.; Ribbe, A.; Kosif, I.; Szyndler, M.; Balazs, A.C.; Crosby, A.; Emrick, T., Mechanical restoration of damaged polymer films by “repair-and-go”. In preparation.
3. Bai, Y.; Chang, C. C.; Kosif, I.; Emrick, T., Polymer Osteodroplets for Picking up Hydroxyapatite Particles. In preparation.

Controlling Structure Formation Pathways in Functional Bio-Hybrid Nanomaterials

PI: Lara A. Estroff; Co-PI: Ulrich Wiesner

Department of Materials Science and Engineering, Cornell University, Ithaca, NY 14853

Program Scope

This project aims to understand the structure formation pathways in organic-inorganic hybrid materials in which information transfer from the organic into the inorganic phase is critical to directing the assembly of the composites. Self-assembly of silica nanomaterials directed by small molar mass surfactants is the simplest system of study, both in terms of the organic, as well as the amorphous, inorganic phase. The second system uses synthetic block copolymers to direct the assembly of amorphous calcium phosphate hybrids. The structural complexity of the organic structure-directing agents, as well as the inorganic phase is enhanced over the first system, resulting in an increase in the complexity of the expected chemical pathways. Finally, we are using synthetic/peptide block copolymers to direct the formation of crystalline calcium phosphate bio-hybrids. In this system, we are looking at the effect of peptide sequence, i.e. a significantly increased information transfer from the organic phase, on the crystallization of the calcium phosphate phase. In all three cases, controlling interactions at the interfaces of organic and inorganic materials and elucidating assembly pathways is a central focus. Efforts include synthesis of all organic/inorganic precursors and their composites, as well as in-depth characterization of local, global, and where possible interface structure, of assembly intermediates and final products to elucidate governing principles for structure/shape control in the materials synthesis. When successful, results will provide general guidelines and methodologies for the controlled synthesis of hybrid nanomaterials with increasing complexity offering enormous scientific and technological promise, in areas ranging from energy conversion and storage to drug delivery and bone repair.

Recent Progress

Formation pathways to mesoporous silica nanoparticles with dodecagonal tiling

Quasicrystals exhibit highly ordered local structure but lack long range translational periodicity, and permit symmetry operations that are forbidden in classical crystallography, e.g. five-, eight-, ten- and twelve-fold rotations (1). Since 1984, quasicrystalline order has been observed

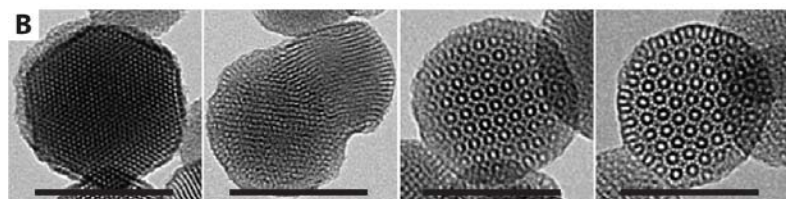


Fig. 1. TEM images of MSNs prepared from EtOH/TEOS, surfactant, and, from left to right, increasing concentrations of a pore expander.

experimentally in a large variety of materials, including metal alloys (1, 3), thin films (4), liquid crystals (5), polymers (6), colloids (7) and mesoporous networks (8), and therefore is now considered a universal form

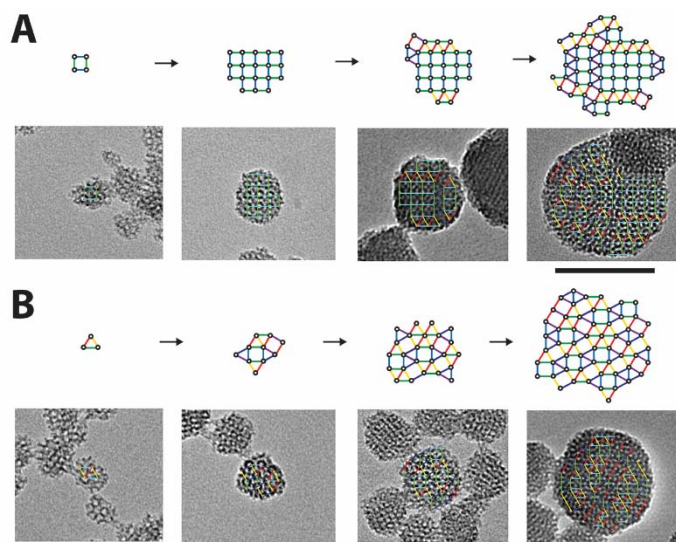


Fig. 1. Proposed quasicrystal particle growth pathways from simulations and corresponding TEMs from experiment. (A) When the first particle is a square, growth of a cubic core occurs. (B) When the first particle is a triangle, a quasicrystal is more likely to form.

of ordering (9). Despite increasing attention to identifying various quasicrystalline materials, little is known experimentally about early pathways to their formation. Although multiple formation mechanisms have been proposed via simulations (10-12), direct experimental observation of early formation stages and processes still remains a challenge. Here, we show that, by taking advantage of highly tunable silica sol-gel chemistry, the early formation steps of random tiling quasicrystals (14) with dodecagonal quasiperiodic tiling (DQT) can be experimentally preserved as mesoporous silica nanoparticles (MSNs). Through varying reaction conditions, the size of

MSNs with DQT can be tuned from >100 nm, for which the DQT is well developed, down to <30 nm where particles consist of only a single elementary DQT unit, e.g. a triangle or a square. Simultaneously, the quasicrystallinity can be controlled, via a single experimental parameter, from cubic crystalline to quasicrystalline (Fig. 1, *in prep.*). Based on these observations, a library of MSNs with varying size and quasicrystallinity is synthesized and their structures are compared to simulations (Fig. 2, *in prep.*). Results elucidate not only early formation pathways to random tiling quasicrystals, but also the structural transition from DQT to crystalline ordering, thereby providing detailed insights into early quasicrystal formation mechanisms.

Pathway Complexity in the Formation of Periodically-Ordered Calcium Phosphate Nanostructures by Block Copolymer-Directed Self-Assembly

The mechanical properties of biomineralized tissues are directly related to their nano-, meso-, and macroscale structures (15). In this work, we use block copolymers (BCPs) to direct the self-assembly of organosilicate-modified amorphous calcium phosphate nanoparticles (osm-ACP NPs) to obtain nanocomposites with continuous inorganic phases and tailored mechanical properties. We studied the solution behavior of an amphiphilic BCP as a function of solvent composition, and developed a synthetic strategy in which osm-ACP NPs swell the hydrophilic domains of the BCP, resulting in composites with well-defined periodic BCP lattices with lamellar, hexagonal, and cubic symmetries (Fig. 3, *in preparation*). Accessing this structure control required an understanding of three key “bifurcations” in the assembly pathway: 1) As was already known from previous studies involving BCPs and NPs, the size of the NPs needed to be smaller than the radius of gyration of the solvating, hydrophilic block (16). To obtain such

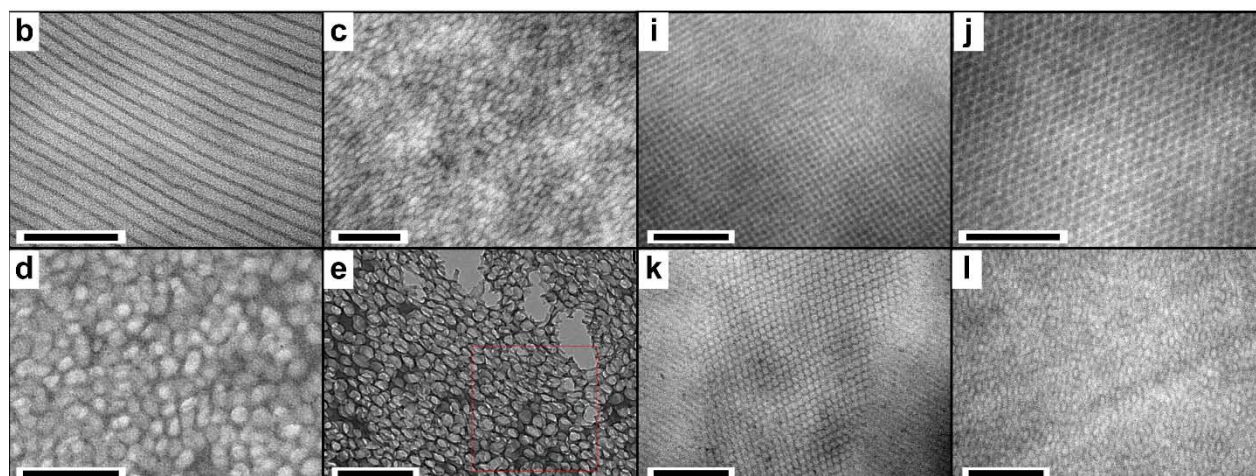


Figure 3. (b-e) TEM images of BCP1 and varying concentrations of osm-ACP NPs (b) lamellar (c, d) disordered micellar network, and (e) plasma-etched sample of (d). (i-l) TEM images of BCP2 and varying concentrations of osm-ACP NPs (i,j), cubic bicontinuous phase (k) hexagonal, (l) disordered network. All scale bars are 200 nm. For (i) and (j), sample slices were stained with osmium tetroxide, in all others contrast comes from the osm-ACP NPs.

small particles, we developed a sol-gel based synthesis of ultra-small (< 3 nm) osm-ACP NPs. 2) The second “decision point” in the assembly pathway is the choice of solvent and understanding of the solution behavior of the amphiphilic BCPs. With an increasing amount of water/ethanol, the polymer solution behavior changed from unimers to micellar aggregates, which in turn switched the solvent evaporation induced self-assembly pathway: At low sol content, unimer based self-assembly occurred (Fig. 3b, i, j, k) while at higher sol content, micelle-based self-assembly lead to nanocomposites with cellular/micellar morphologies independent of composition (Fig. 3c-d, l). 3) The third key experimental variable, as in other BCP/NP systems (17, 18), is the BCP composition and sol NP/copolymer composition. By tuning this variable, we obtained nanocomposites with a series of morphologies expected from increased swelling of only one block of the BCP.

Our ability to tune the composite composition and structure led to a substantial variation in mechanical properties of the resulting composites. To this end, we demonstrated that as a result of continuous NP network formation, nanostructured composites with inorganic NP loading as low as ~ 10 vol% had an order of magnitude higher indentation modulus as compared to a disordered composite with the same loading. Insights provided by this study may enable access to a broad range of well-controlled osm-ACP nanostructures with potential applications in areas including dental repair and hard tissue engineering.

Future Plans

We are currently applying what we have learned about pathway complexity in the BCP + osm-ACP NP systems to tri-block terpolymers (TTPs). We anticipate that by understanding the solvent-dependent structure of TTPs, coupled with control over composition, we will obtain access to new bicontinuous composite structures with tailored mechanical properties. In

addition, we are working to replace the organosilane modifier in the ACP NP synthesis with silicon-free molecules that still are able to control size of the particles. By removing silicon from the system, we aim to obtain hierarchically-structured, crystalline calcium phosphates, after processing and heating the composite films. We are also developing polymer-peptide hybrids that will allow nanostructure control of the assembly process by the BCP, while the peptide sequence will be varied to promote the low-T formation of crystalline HA and control crystallographic orientation with respect to the assembly, something unattainable with previous techniques. Thus, we are implementing a strategy utilizing thiol-ene “click” chemistry, by which a thiol-terminated peptide can be attached to a pendant alkene on polymer backbone, in one block of the BCP, with near 100% efficiency. In particular, we are now exploring the self-assembly of these new polymer architectures both in the absence of inorganic additives, as well as with ACP nanoparticles.

References

1) Shechtman, D., Blech, I., Gratias, D. & Cahn, J. *Phys. Rev. Lett.* **53**, 1951 (1984). 2) Levine, D., Steinhardt, P. *Phys. Rev. Lett.* **53**, 2477 (1984). 3) Bindi, L., Steinhardt, P., Yao, N., Lu, P. *Science* **324**, 1306 (2009). 4) Förster, S., Meinel, K., Hammer, R., Trautmann, M., Widdra, W. *Nature* **502**, 215 (2013). 5) Zeng, X. et al. *Nature* **428**, 157 (2004). 6) Hayashida, K., Dotera, T., Takano, A., Matsushita, Y. *Phys. Rev. Lett.* **98**, (2007). 7) Talapin, D. et al. *Nature* **461**, 964 (2009). 8) Xiao, C., Fujita, N., Miyasaka, K., Sakamoto, Y., Terasaki, O. *Nature* **487**, 349 (2012). 9) Tolbert, S. *Nature Mater* **11**, 749 (2012). 10) Joseph, D., Elser V. *Phys. Rev. Lett.* **79**, 1066 (1997). 11) Achim, C., Schmiedeberg, M., Löwen, H. *Phys. Rev. Lett.* **112**, (2014). 12) Engel, M., Damasceno, P., Phillips, C., Glotzer, S. *Nature Mater* **14**, 109 (2014). 13) Levine, D., Steinhardt, P. *Phys. Rev. B* **34**, 596 (1986). 14) Oxborrow, M., Henley, C. *Phys. Rev. B* **48**, 6966 (1993). 15) Wegst, U. G. K.; Bai, H.; Saiz, E.; Tomsia, A. P.; Ritchie, R. O., *Nature Mater* **14**, 23 (2015). 16) Warren, S. C., Disalvo, F. J., Wiesner, U. *Nature Mater.* **6**, 156 (2007). 17) Warren, S. C. et al. *Science* **320**, 1748 (2008). 18) Zhao, Y. et al. *Nature Mater.* **8**, 979 (2009).

Publications Supported by BES 2013-2015

1) Moore, D.T.; Tan, K.W.; Sai, H.; Barteau, K.P.; Wiesner, U.; Estroff, L.A. “Direct crystallization route to methylammonium lead iodide perovskite from an ionic liquid.” *Chem. Mater.*, **2015**, 27, 3197. 2) Moore, D.T.; Sai, H.; Tan, K.W.; Smilgies, D.M.; Zhang, W.; Snaith, H.J.; Wiesner, U.; Estroff, L.A. “Crystallization kinetics of organic-inorganic trihalide perovskites and the role of the lead anion in crystal growth.” *J. Am. Chem. Soc.*, **2015**, 137, 2350. 3) Zhang, W.; Saliba, M.; Moore, D. T.; Pathak, S.; Horantner, M.; Stergiopoulos, T.; Stranks, S. D.; Eperon, G. E.; Alexander-Webber, J. A.; Abate, A.; Sadhanala, A.; Yao, S.; Chen, Y.; Friend, R. H.; Estroff, L. A.; Wiesner, U.; Snaith, H. J. “Ultra-smooth organic-inorganic perovskite thin-film formation and crystallization for efficient planar heterojunction solar cells.” *Nat. Commun.* **2015**, 6, 6142.

Material Lessons from Biology: Nano-to-Mesoscale Organization of Biominerals by Mollusk Shell Proteins.

John Spencer Evans, Center for Skeletal Sciences, New York University, 345 E. 24th Street, NY, NY 10010.

Program Scope

Biological organisms offer many potential models where multiple material properties and construction phenomena intertwine at the mesoscale. A case in point is biomineralization, a process by which organisms employ very unique and important assembly mechanisms to create inorganic skeletal elements over different length scales (nano to macro). In some biomineralizing systems, such as the invertebrate mollusk, the biomineralized skeletal elements (i.e., the shell) possess some very energy-relevant material properties. For example, in mollusk shell nacre (inner layer, **Fig 1A**) the properties of fracture-toughness and resistant to crack propagation co-exist, which provide the mollusk with a protective armor that resists pressures (and predators) at underwater depths under high salinity conditions.¹⁻⁶ Once the shell has formed the mollusk retains the ability to repair and regenerate portions of the shell that do experience fracture.⁴

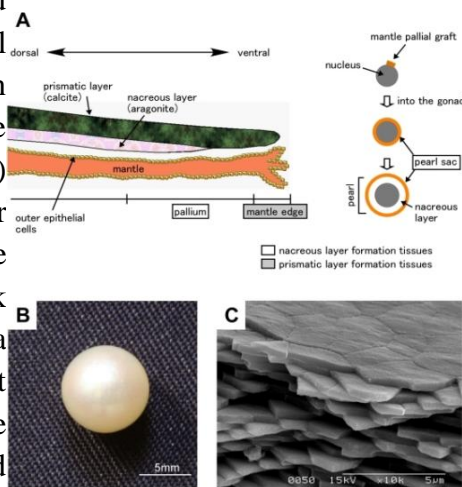


Fig 1. A) Diagram of mollusk shell and pathway to pearl formation; B) A nacre pearl; C) SEM image of fractured nacre layer illustrating the “brick and mortar” layered mineral structure. Taken from Ref 6.

These materials properties arise from mesoscale aragonite single crystals which are organized into a “brick and mortar” arrangement (**Fig 1C**). What is even more interesting is that the mesoscale materials properties arise from nanoscale features, such as nano-asperities (mineral surface roughening); mineral bridges which physically link each tablet to its neighbor; the presence of elastomeric intercrystalline organic hydrogel layers; physical interlocking of tablets; and the presence of nanoscale intracrystalline organic voids, which enables interception of force-generated cracks within each tablet.^{1-3,5} Thus, the nacre layer is a complex material that combines many important material attributes into one “package”.

The most likely agents which introduce these meso- and nanoscale properties to nacre tablets are protein families or proteomes.⁶⁻⁹ Genomic and proteomic sequencing have now revealed several mineral-specific shell proteomes, such as the intracrystalline, framework, silk, and pearl/repairative families. But do any of these proteomes control mineral nanoparticle formation and subsequent assembly?

Recent Progress

Using recombinant or chemically synthesized forms of five representative aragonite-associated proteins (AP7, AP24, PFMG1, n16.3, Pif97) we found that these proteins were aggregation-prone, forming disordered protein phases or hydrogels that contained organized mineral nanoparticles within the protein phase (**Fig 2, LEFT**).⁷⁻¹² Subsequently, STEM flow-cell studies with one of these proteins, AP7, demonstrated that the protein phases assemble mineral nanoparticles over time to form larger protein-mineral assemblies that approach the mesoscale (**Fig 2, RIGHT**).⁹ These seminal studies directly implicate intracrystalline, framework, and pearl-

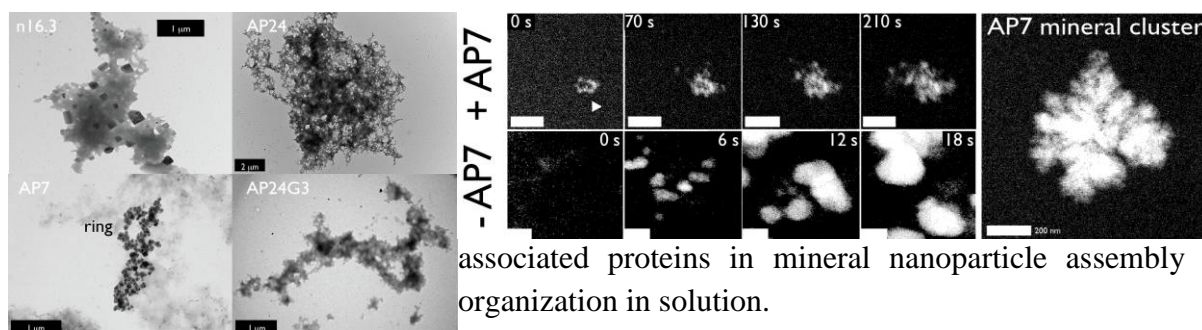


Fig 2. (LEFT) Representative TEM images of nacre protein phases or hydrogels containing calcium carbonate mineral nanoparticles. (RIGHT) STEM flow-cell video stills of mineral nanodeposits forming in the presence and absence of AP7.

This assembly phenomena was not the only functional feature identified for these representative nacre proteins. In the presence of nucleating calcite crystals, nacre protein phases were found to: a) create organized nanoparticle surface coatings; b) create new crystal growth directions and nanotexturing; and c) become occluded within the calcite crystals, thereby creating randomly distributed nanoporosities and nanochambers that possess heterogeneous dimensions (i.e., micro, meso, and macro).^{8,10,11} The nature of the surface and subsurface

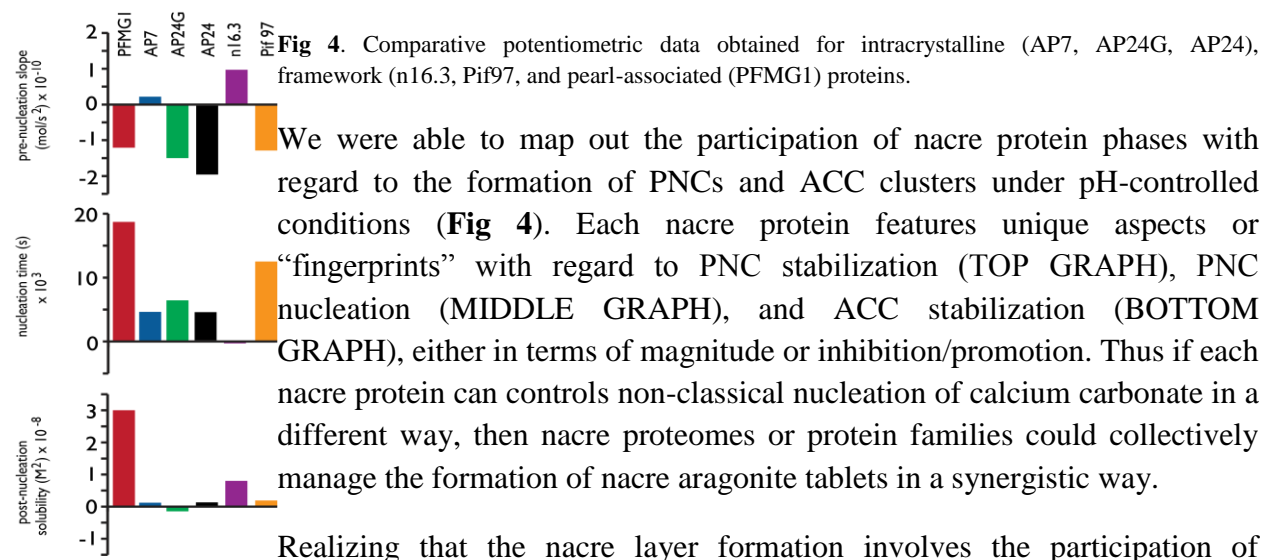


modifications were found to be unique for each protein, suggesting that protein sequence plays a role in the protein
Fig 3. (LEFT) Calcite crystal modified by AP7 protein phases (note organized nanodeposits on surfaces; (MIDDLE) 3-D tomographic reconstruction of AP7-modified calcite crystal surface (green) and subsurface (blue) regions; (RIGHT) Intracrystalline calcite nanoporosities generated by AP7 protein phases

phase composition and its ability to direct nucleation events once in contact with a growing crystal. Thus, in addition to organizing nanoparticles in solution, these same protein phases modify growing crystals and become occluded within them, creating random nanoporosities that mimic that found *in situ* within nacre tablets.

But what about the participation of nacre proteins during early events in nucleation? The non-classical nucleation scheme for calcium carbonates *in vitro* posits that disordered ionic clusters (1-3 nm), termed pre-nucleation clusters (PNCs), form initially in supersaturated

solutions. These PNCs then co-assemble to form stable amorphous calcium carbonate (ACC) clusters (100-300 nm diameter).^{9,12} Ultimately, the ACC clusters can either undergo Ostwald ripening and form crystalline solids or, can persist in the amorphous state if stabilization agents are present. What is attractive about the non-classical scheme is that it accounts for the presence of amorphous phases in biological systems, and, offers several stages of mineral growth, and thus, several opportunities for biomineralization proteins to control transitional steps, such as PNC formation, PNC to ACC aggregation, and so on.^{9,12}



Realizing that the nacre layer formation involves the participation of numerous proteins over time, we have migrated our research towards studying *in vitro* mineralization in the simultaneous presence of several nacre proteins. Our first test case was the combination of the intracrystalline protein, AP7, with the pearl reparative protein, PFMG1. Although these proteins originate from different mollusks and would not be present together under normal conditions, they do have individual *in vitro* functions that are very distinctive and thus relatively easy to trace within a two-component system (**Fig 4**). Thus, this “artificial” pairing of two different nacre proteins provides a foundation to develop approaches that can successfully monitor natural protein pairs, such as the intracrystalline AP7 – AP24 and framework n16.3 – Pif97 pairs.

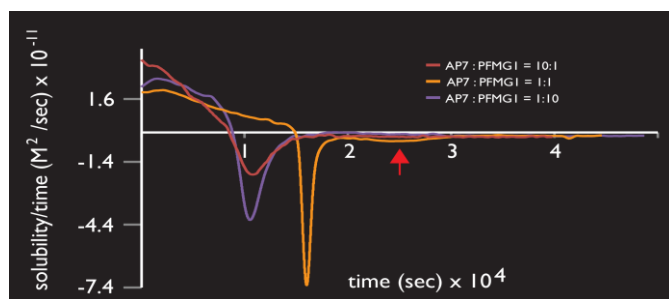


Fig 5. First derivative potentiometric plot of time-dependent ACC stability in the presence of AP7 and PFMG1. Second nucleation event noted by red arrow.

Using potentiometric titrations, we find that AP7 and PFMG1 in a 1:1 mole ratio jointly create 2 separate ACC nucleation events which exhibit different timescales (**Fig 5**). Typically, this type of result has been witnessed in single component polyelectrolyte systems but to date never observed for individual nacre proteins (**Fig 4**). Further, using STEM flow cell imaging and parallel mineral assay conditions, we were able to visualize both proteins creating a protein phase which dramatically slows down ACC nucleation. In other words, instead of interfering with each other, both proteins cooperatively do their job and produce a novel result. This result opens up a new avenue for exploiting combinatorial organic modifiers to augment and direct inorganic solid formation at the nano- and mesoscales.

Future Plans

We will be characterizing the nacre protein hydrogels in more detail to determine chemical and physical features that enable protein-specific modification of crystal growth and organization of mineral nanoparticles. We intend to investigate multiple nacre protein systems in calcite- and aragonite-based to determine if the same or different synergistic mineralization phenomena occur in known framework (n16.3 – Pif97) and intracrystalline (AP7 - AP24) protein pairs. With external collaborators we are also performing data mining of Pacific gastropod and mollusk genomes to identify potential protein candidates that may also organize nanoparticles and introduce intracrystalline nanoporosities. Finally, going farther afield from calcium carbonates, we are currently testing the ability of nacre proteins to organize other forming inorganic nanoparticles, such as magnetite, within *in vitro* settings.

References

- [1] Zhang, G., Li, X. (2012) *Cryst. Growth Design* 12, 4306-4310.
- [2] Li, X., Chang, W.C., Chao, Y.J., Wang, R., Chang, M. (2004) *NanoLetters* 4, 613-617.
- [3] Sun, J., Bhushan, B. (2012) *RSC Adv.* 2, 7617-7632.
- [4] Su, X.W., Zhang, D.M., Heuer, A.H. (2004) *Chem. Mat.* 16, 581-593.
- [5] Li, X., Huang, Z. (2009) *Phys. Rev. Lett.* 102, 075502-075506.
- [6] PLOS One
- [7] Perovic, I., Mandal, T., and Evans, J.S. (2013) *Biochemistry* 52, 5696-5703.
- [8] Chang, E.P., Williamson G., Evans, J.S. (2015) *Crystal Growth and Design* 15, 1577-1582.
- [9] Perovic, I., Chang, E.P., Verch, A., Rao, A., Cölfen, H., Kroeger, R., Evans, J.S. (2014) *Biochemistry* 53, 7259-7268.

[10] Chang, E.P., Russ, J.A., Verch, A., Kroeger, R., Estroff, L.A., Evans, J.S. (2014) *Biochemistry* 53, 4317-4319.

[11] Chang, E.P., Russ, J.A., Verch, A., Kroeger, R., Estroff, L.A., Evans, J.S. (2014) *Cryst. Eng. Commun.* 16, 7406-7409.

[12] Perovic, I., Chang, E.P., Lui, M., Rao, A., Cölfen, H., Evans, J.S. (2014) *Biochemistry* 53, 2739-2748.

Publications

Chang, E.P., Williamson G., Evans, J.S. (2015) Focused ion beam tomography reveals the presence of micro-, meso-, and macroporous intracrystalline regions introduced into calcite crystals by the gastropod nacre protein AP7. *Crystal Growth and Design* 15, 1577-1582.

Perovic, I., Chang, E.P., Verch, A., Rao, A., Cölfen, H., Kroeger, R., Evans, J.S. (2014) An oligomeric C-RING nacre protein influences pre-nucleation events and organizes mineral nanoparticles. *Biochemistry* 53, 7259-7268.

Chang, E.P., Russ, J.A., Verch, A., Kroeger, R., Estroff, L.A., Evans, J.S. (2014) Engineering of crystal surfaces and subsurfaces by an intracrystalline biomineralization protein. *Biochemistry* 53, 4317-4319.

Chang, E.P., Russ, J.A., Verch, A., Kroeger, R., Estroff, L.A., Evans, J.S. (2014) Engineering of crystal surfaces and subsurfaces by framework biomineralization protein phases. *Cryst.Eng. Commun.* 16, 7406-7409.

Brown, A.H., Rodger, P.M., Evans, J.S., Walsh, T.R. (2014) Equilibrium conformational ensemble of the intrinsically-disordered peptide n16N: Linking sub-domain structures and function in nacre. *Biomacromolecules* 15, 4467-4479.

Perovic, I., Chang, E.P., Lui, M., Rao, A., Cölfen, H., Evans, J.S. (2014) A framework nacre protein, n16.3, self-assembles to form protein oligomers that participate in the post-nucleation spatial organization of mineral deposits. *Biochemistry* 53, 2739-2748.

Seto, J., Picker, A., Evans, J.S., Cölfen, H. (2014) A nacre protein sequence organizes the mineralization space for polymorph formation. *Crystal Growth and Design* 14, 1501-1505.

Evans, J.S. (2014) The Realities of Disordered or Unfolded Proteins: Relevance to Biomineralization. In *Biomineralization Sourcebook: Characterization of Biominerals and Biomimetic Materials*. Eds E. DiMasi, L.B. Gower. CRC Press, NY, NY USA.

Evans, J.S. (2013) “Liquid-like” biomineralization protein assemblies: A key to the regulation of non-classical nucleation. *Crystal Engineering Communications* 15, 8388 - 8394.

Perovic, I., Mandal, T., and Evans, J.S. (2013) A pseudo EF-hand pearl protein self-assembles to form protein complexes that amplify mineralization. *Biochemistry* 52, 5696-5703.

Dynamic self-assembly of DNA nanotubes

Elisa Franco, Department of Mechanical Engineering University of California at Riverside

Program Scope

Many biological materials result from the spontaneous self-assembly of monomeric elements. The cytoskeleton, for instance, is a complex, active network of filaments that assemble from individual actin monomers (Fig. 1). The main advantage of this type of architecture is that large, scalable structures can be built with relatively simple components and few interaction rules. This scalable growth mechanism usually goes hand in hand with ease of reconfiguration; the cytoskeleton is again a great example, because its tubular structures can disassemble as fast as they assemble in response to stimuli, resulting in the striking capacity of biological cells for growth, shape adaptation and self-repair. Our project aims at building monomer-based artificial biomolecular materials where assembly and disassembly can be triggered by chemical or physical stimuli. We pursue this goal using nucleic acids as a self assembling material, due to the programmability of their Watson-Crick interactions, their inexpensive synthesis, and the variety of existing, well characterized nucleic acid circuits [1,2,3] and nanostructures [4,5,6,7] that can be modularly combined. We focus on DNA nanotubes [4], which assemble from tile monomers via sticky end interactions and can grow up to microns in length. We direct dynamic growth and decay of DNA nanotubes with DNA and RNA molecules that interact with the tile sticky ends, promoting assembly or disassembly. These nucleic acid control signals can be released in solution in response to environmental signals via nucleic acid aptamers [8] and circuits. Thus the material response can be programmed modularly by choosing nucleic acid sensors and signal processing elements. This project is developed in collaboration with the Schulman lab at Johns Hopkins University.



Figure 1: Dynamic self assembly of microtubules (Garland Science)

Recent Progress

1. DNA nanotube control of assembly and disassembly.

Growth and decay in materials such as cytoskeletal filaments occurs dynamically and reversibly, and is driven by the concentration of chemical signals that favor monomer binding or unbinding. We achieved dynamic and reversible assembly of DNA

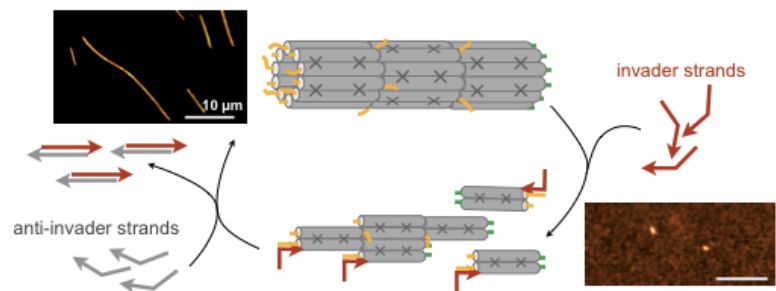


Figure 2: Our nanotube dynamic assembly pathway

nanotubes [4] by designing tile monomers whose binding domains are sensitive to the concentration of specific DNA inputs (Fig. 2). In particular, DNA molecules we named

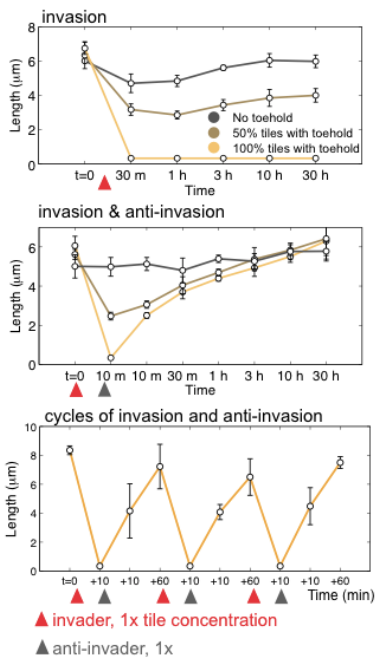


Figure 3: Reversible control of assembly and disassembly (unpublished data)

“invaders” are designed to target the intra-tile bonds via exposed domains, or toeholds, and weaken these bonds. We modulated the abundance, length, and location of the toeholds, achieving control over the disassembly mechanism. The toehold abundance and length control disassembly speed and mean length of the nanotubes (Fig. 3). The toehold location, which can be internal or external to the nanotube surface, controls the breakage mechanism spatially: an external toehold results in uniform breakage, while an internal toehold results in breakage localized at the nanotube extremities. If the invader strand is sequestered by a complementary “anti-invader” strand, nanotubes spontaneously regrow within one to two hours to a mean length comparable to the pre-breakage length. The breakage-regrowth process can be repeated isothermally in several subsequent cycles. Our monomer-based architecture for dynamic control of assembly allows us to control temporal and spatial parameters of growth and decay of the material in a scalable and programmable manner.

2. Directing DNA nanotube assembly with

transcriptional networks. Cell division is a periodic event where the cytoskeletal scaffold reorganizes and distributes dynamically all cellular components. To reproduce a similarly sophisticated behavior in an artificial material, a timer circuit is required to direct temporally and spatially the material itself [3]. We thus aim at identifying design principles and methods that enable us to grow our nanotubes with an autonomous oscillator. Because currently available in vitro oscillators rely on transcription, and thus a biocompatible environment, we developed strategies to control assembly using transcriptional systems. First, we identified design parameters (tile binding strength in particular) to guarantee that nanotubes are stable in biocompatible conditions, which substantially differ from typical conditions at which DNA nanostructures are produced. We discovered that bacteriophage enzymes favor disassembly of nanotubes with weak inter-tile bonds; a model elucidating this phenomenon is under development. The growth of biocompatible nanotubes can be successfully directed using RNA outputs of synthetic genes; this shows that nucleic acid systems have remarkable programmability and can be redesigned to operate at a variety of environmental conditions. A molecular oscillator, built with two synthetic genes, is currently being tested as a signal source to direct nanotubes assembly and disassembly. Oscillator and nanotubes are coupled via a “buffer” circuit that transmits the oscillatory signal to the nanotubes, without altering the oscillations. Preliminary data indicate that the circuit successfully breaks and promotes regrowth of the nanotubes with at least one oscillation cycle. Current work focuses on

improving growth rates by employing nucleation seeds developed by the Schulman lab (co-PI on this project).

3. Mathematical modeling of nanotube growth. Classical protein or DNA tiling polymerization models capture the binding dynamics of individual monomers to the growing structure. Our AFM data show that sticky end strand invasion causes nanotubes to break in chunks of variable size, rather than monomers, where each chunk is composed by a variable number of assembled tiles. Thus, we built a macroscopic model to capture average parameters of breakage, monomer binding, and tube joining events. The model is a set of ordinary differential equations (built from equivalent chemical reactions) that capture joining and breakage of nanotubes in a range of lengths. We fitted the model to the measured length distributions, obtaining average breakage and assembly rates. This model will be further fitted to nanotubes growing in different conditions, to gain quantitative insight on the influence of various parameters such as temperature, ionic concentration, length and sequence content of tile sticky end and toehold domains.

4. Reversible nucleic acid sensors.

This project aims at using various physical and chemical signals to direct nanotube assembly. Aptamers [8] will be employed as sensors, which will transduce and transmit these signals to nucleic acid circuits. Dynamic external signals will require sensors capable of reversible dynamics. We explored this concept by designing strand displacement reactions for reversible binding and unbinding of aptamers to their target. As model targets, we considered light-up aptamers (Fig. 4) and RNA polymerases and we have shown that strand displacement works well to reverse aptamer-target binding.

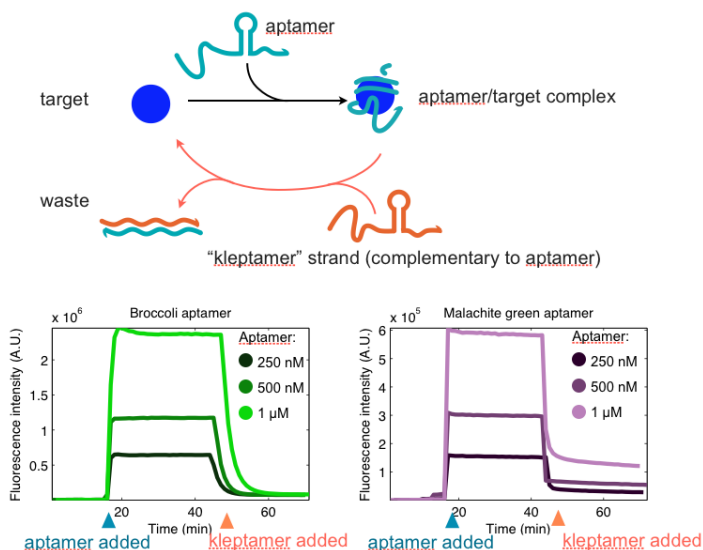


Figure 4: Reversible sensing via RNA aptamers. We can reverse aptamer/target binding via strand displacement (unpublished data)

Future Plans

The achievement of isothermal, reversible control of assembly and disassembly in our DNA nanotubes is a stepping stone toward the development of a variety of active behaviors in synthetic biomaterials. Future work will focus on combining temporal control of assembly with spatial control at different scales. The local organizations of individual nanotubes could be controlled by enabling assembly of a specific tile type as a function of time, achieving for instance tubes with a striped color pattern or diverse functional domains for decoration with

other ligands. These patterns could be driven by sensed environmental signals via nucleic acid aptamers. Finally, we aim at expanding the types of structures for which we can achieve dynamic control of assembly. A disadvantage of monomer-based assembling materials like DNA nanotubes is the complexity of achievable structures is limited by the properties of individual components and interaction rules. This limitation can be addressed by using different monomer types and designing hierarchical assembly of relatively simple structures into more complex supra-structures. For instance, tubular and flat structures in the cytoskeleton interact to form complex scaffolds; similarly, tiles with different geometric properties could yield different shape primitives (e.g. tubes and ribbons), and the assembly of these primitives could be triggered by external signals resulting in a composite material. Monomers with externally controllable binding strength could again be directed to disassemble or reassemble, yielding responsive, active materials. Components such as seeds, nunchucks, and organizing structures (currently developed by the Schulman lab) will be essential to direct higher-level assemblies.

References

- [1] G. Seelig, D. Soloveichik, D.Y. Zhang, E. Winfree, *Science* 314(5805), 1585 (2006)
- [2] D.Y. Zhang, G. Seelig, *Nature Chemistry* 3(2), 103 (2011)
- [3] E. Franco, E. Friedrichs, J. Kim, et al., *Proceedings of the National Academy of Sciences* 108(40), E784 (2011)
- [4] P.W.K. Rothmund, A. Ekani-Nkodo, N. Papadakis, et al., *Journal of the American Chemical Society* 126(50), 16344 (2004)
- [5] P.W.K. Rothmund, *Nature* 440, 297 (2006)
- [6] R.D. Barish, R. Schulman, P.W.K. Rothmund, E. Winfree, *Proceedings of the National Academy of Sciences USA* 106(15), 6054 (2009)
- [7] P. Yin, H.M.T. Choi, C.R. Calvert, N.A. Pierce, *Nature* 451, 318 (2008)
- [8] R. Stoltenburg, C. Reinemann, B. Strehlitz, *Biomolecular Engineering* 24(4), 381 (2007)

Publications

1. Deepak Agrawal, Elisa Franco and Rebecca Schulman. A Self-Regulating Biomolecular Comparator for Processing Oscillatory Signals. *Proceedings of American Control Conference*, 2015. Journal article submitted.
2. Dynamic self-assembly of DNA nanotubes. LN Green, HKK Subramanian, V Mardanlou, J Kim, RF Hariadi, E Franco. In preparation.
3. Reversing aptamer-target binding via strand displacement. C. Tran, J. Lloyd, H. K. Subramanian and E. Franco. In preparation.
4. Stability of self-assembled nanostructures in transcriptional environment. L.N. Green, H. K. Subramanian and E. Franco. In preparation.

Long Range van der Waals-London Dispersion Interactions for Biomolecular and Inorganic Nanoscale Assembly: Duplex to Quadruplex DNA

Principal Investigators: R. H. French*, N. F. Steinmetz[†],

In collaboration with V. A. Parsegian[‡] and W. Y. Ching[§]

Sen. Res. Assoc.: Rudolf Podgornik[‡], Grad. Students: Yingfang Ma*, Selcuk Yasar[‡], Puja Adhikari[§], Undergrad. Students: Taylor Nguyen*, Jacob Schimelman[†], Katherine Kraweic[†], Diana Acosta*

Mailing Address: *Materials Science and Engineering, [†]Biomedical Engineering, Case Western Reserve Univ., Cleveland, Ohio, 44106; [‡]Physics Dept., Univ. of Mass.-Amherst, Amherst, MA, 01003; [§]Dept. of Physics and Astronomy, Univ. of Missouri-Kansas City, Kansas City, MO, 64110

Email: rxfl31@case.edu, nfs11@case.edu, parsegian@physics.umass.edu, Chingw@umkc.edu

Program Scope

In the first three years of the DOE-funded proposal “Long Range van der Waals-London Dispersion Interactions for Biomolecular and Inorganic Nanoscale Assembly,” we directed our activities into several research areas that we believe are relevant for the implementation of our immediate goals: to provide a long-overdue practical access to the rigorous modern theory of van der Waals dispersion, polar and electrostatic long-range interactions (Fig. 1.) and to use the modern theory of these organizing long-range interactions in the assembly of organic/inorganic materials, such as filamentous molecules of the double stranded (duplex) DNA type, globular molecules of the BSA protein type as well as their more complex analogues such as the planar macromolecules of the inorganic berlinite aluminum phosphate type. This is the starting point to investigate also inorganic and metallic materials and nanoparticles that are parts of organic-inorganic material composites.

We have continued to develop expertise in LRI and vdW to identify and characterize optical properties and electronic structures of various DNA morphologies which prove useful for applications in biology-inspired materials, bioelectronics and mesoscale self-assembly. Optical spectra and properties were determined using VUV and UV/vis spectroscopy techniques, and these spectra and properties are compared to those calculated using *ab initio* methods (UMKC). Stacking sequence and base composition have been interchanged to investigate the general electronic properties of DNA variants. From initial calculations, we predict that optical spectra and consequently the vdW interactions of (thin) duplex DNA and (thicker) quadruplex DNA are fundamentally different with the latter being larger. Static light scattering (SLS) was used to measure the second virial coefficient, quantifying the net interaction strength between biomolecules. X-ray diffraction methods were used to deduce interactions in condensed arrays of duplex DNA vs. quadruplex DNA, and estimate the role LRIs play at their condensation transitions. The electronic structure of quadruplex was determined using *ab initio* calculations.

Recent Progress

Topic 1: Oligonucleotide Sequence Effects in DNA

Composition and Stacking sequence effects in DNA¹ (UMass, CWRU, UMKC): The electronic transitions and optical properties of three DNA oligonucleotide sequences ((AT)₁₀, (AT)₅(GC)₅, (AT-GC)₅) were studied as a function of composition and stacking sequence. Full UV absorbance spectra were obtained for the three DNA oligonucleotide sequences (Figure 1). A strong dependence in position and intensity of UV absorbance features with correlation to the corresponding oligonucleotide composition and stacking sequence was found. This dependence elucidates the benefits of full spectral analysis of DNA as opposed to reductive methods that consider solely 260 nm absorbance (A₂₆₀) or purity ratios such as A₂₆₀/A₂₈₀ or A₂₆₀/A₂₃₀. These insights are useful for biology-inspired materials, and mesoscale self-assembly.

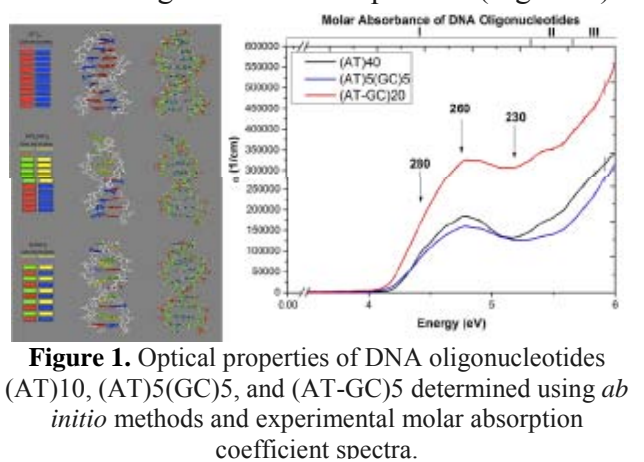


Figure 1. Optical properties of DNA oligonucleotides (AT)₁₀, (AT)₅(GC)₅, and (AT-GC)₅ determined using *ab initio* methods and experimental molar absorption coefficient spectra.

Topic 2: DNA solvation and solute binding

DNA/Doxorubicin Solvation and Binding² (UMass, CWRU, UMKC): The electronic structure and partial charge of doxorubicin (DOX) in three different molecular environments - isolated, solvated, and intercalated in a DNA complex—are studied by first-principles density functional methods. It is shown that the addition of solvating water molecules to DOX, together with the proximity to and interaction with DNA, has a significant impact on the electronic structure as well as on the partial charge distribution. Significant improvement in estimating the DOX–DNA interaction energy is achieved. The results are elucidated by resolving the total density of states and surface charge density into different functional groups. It is concluded that the presence of the solvent and the details of the interaction geometry matter greatly in determining the stability of DOX complexation. *Ab initio* calculations on realistic models are an important step toward an accurate description of the interactions in biomolecular systems.

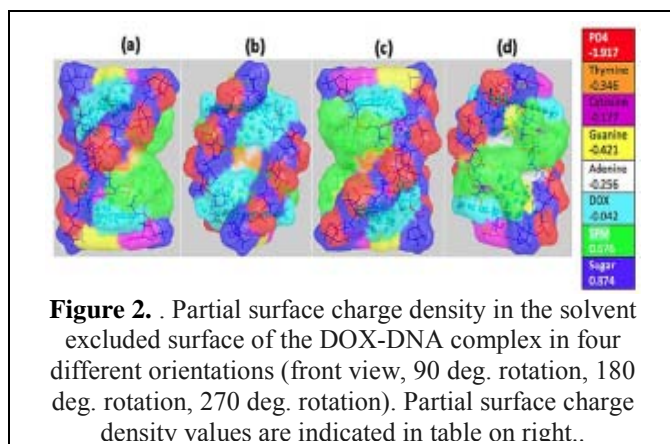


Figure 2. Partial surface charge density in the solvent excluded surface of the DOX-DNA complex in four different orientations (front view, 90 deg. rotation, 180 deg. rotation, 270 deg. rotation). Partial surface charge density values are indicated in table on right.

Topic 3: Tetraplex & Quadruplex DNA analogues

Preparation of Quadruplex Analogues (CWRU): Quadruplex DNA has been prepared using the following protocol: oligonucleotides of the sequence d[AG₃(T₂AG₃)₃] (d=4-12), obtained from IDT (Integrated DNA Technologies), will be dissolved and stored in (100 μM) sodium or potassium phosphate buffers at pH 6.5-7.0 with or without 0.1-0.5 mM EDTA. Oligonucleotides will be denatured at 95 °C for 5 min, and then annealed by cooling to room temperature. Samples were analyzed using circular dichroism (CD) spectroscopy to ensure proper crystal structure formation.

Electronic Structure of G-Quadruplex DNA analogue³

(UMKC): Density functional theory study on the electronic structure, charge distribution and bonding of G-quadruplex (G4) DNA for parallel and anti-parallel configurations with presence of water and alkali counterions. Water molecules, K⁺ and Na⁺ ions are present in parallel G4 but only Na⁺ ions are present in the anti-parallel G4. The structure orientation of G4, together with the proximity and interaction with water molecules and K⁺ counterions has a significant impact on the electronic structure, the partial charge distribution and bonding on G4-DNA. The calculated HOMO- LUMO gaps of parallel and anti-parallel G4 are 1.99 eV and 2.67eV respectively. The HOMO and LUMO state of two G4 models are located in different functional groups. Sugar and counterions are positively charged and all of the nucleobases, PO₄ units and water molecules are negatively charged. The Hoogsteen hydrogen bonds of O-H are stronger than N-H in tetrad of guanine in both G4 models and their strength increases with presence of water and K⁺ ions in the channel of guanine bases. This indicates that K⁺ ions at the center of tetrad of guanine and explicit presence of water molecules play a pivotal role for structure and stability of G4-DNA.

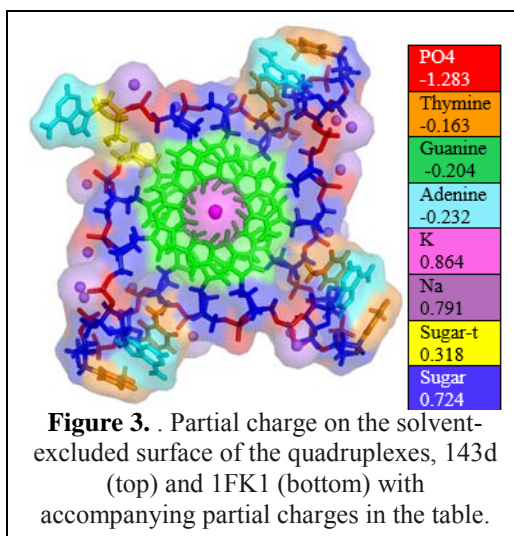


Figure 3. . Partial charge on the solvent-excluded surface of the quadruplexes, 143d (top) and 1FK1 (bottom) with accompanying partial charges in the table.

Molecular interactions in condensed phases of DNA analogues (UMass): We measured the cholesteric-to-hexatic transition of duplex DNA as well as the condensation transitions (having nature and features similar to the cholesteric-to-hexatic transition) of higher-order DNA structure, tetraplex DNA (or GMP-tetraplex). Tetraplex DNA is similar to human telomeric quadruplex DNA, a stack of tetramericly-arranged guanine nucleotides (i.e., G4), not attached by the sugar-phosphate backbone. We explored the sensitivity of the transitions and condensation (including the DNA density change at the transition) to thermodynamic variables such as osmotic pressure, ionic strength, and temperature. DNA analogues revealed relations between the interaction potentials which govern high-density DNA packing and the helical and elastic characteristics of the DNA structures, relevant for the high-density DNA packing and stabilization of chromatin telomeres. The nature of the condensation transition is the same for both duplex and tetraplex DNA, but the free energy and entropy changes differ. Therefore: (i) in the less-ordered phase the repulsion due to chain fluctuations is much larger for tetraplexes than for duplexes; (ii) the lowering of free energy induced by azimuthal orientation of the chains (due to helical interactions) at the transition is larger for tetraplexes than for duplexes. Changes in positional order and azimuthal order in DNA phases occur concurrently. To account for an abrupt change in the electrostatic part of the free energy at the transition, we must also

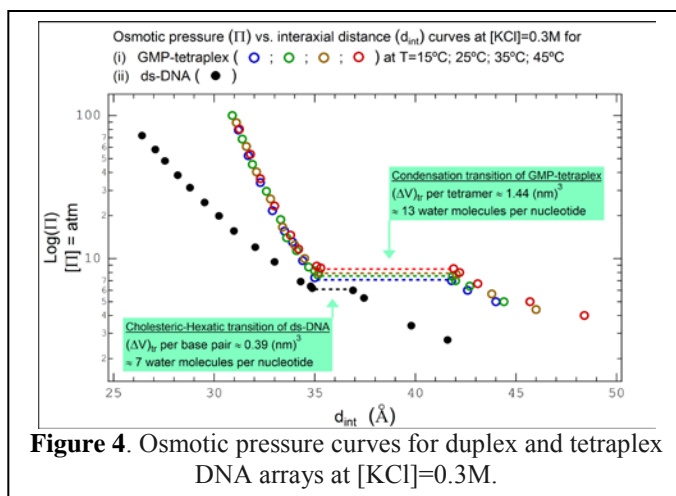


Figure 4. Osmotic pressure curves for duplex and tetraplex DNA arrays at $[KCl]=0.3M$.

consider (iii) counterion localization and charge neutralization.

Future Plans

Topic 1: Oligonucleotide Sequence Effects in DNA

CG vs GC base ordering in DNA^d (UMKC, CWRU): Ab initio and UV-vis measurements were used to characterize short DNA oligonucleotides. The difference in pure purine-base strand and pyrimidine-base strand ((AT)₅(GC)₅ and (AT-GC)₅) versus the oligonucleotides comprised of alternating purine-pyrimidine-bases strands ((AT)₅(CG)₅ and (AT-CG)₅) was studied. Initial measurements indicate a presence of a sharp peak found for the alternating duplex sequences compared to the homogenous strands that leak a peak.

Topic 3: Tetraplex & Quadruplex DNA analogues

Molecular interactions in dilute phases and virial coefficients of DNA analogues (CWRU): 22 based duplex DNA samples have been acquired from IDT with base sequence of AG₃(T₂AG₃)₃. This duplex sequence will be compared to the quadruplex DNA samples that have been successfully made. Static light scattering measurements will be done on both duplex and quadruplex under comparable salt conditions to investigate the potential of quadruplex existing in monovalent (physiological) salt conditions versus polyvalent salt conditions that duplex DNA requires.

Molecular interactions in condensed phases of DNA analogues (UMass): Building on the previous study of tetraplex and duplex DNA molecules, the next step in this study is to compare the interactions between DNA tetraplexes (which lack a sugar-phosphate backbone) to triplexes and quadruplexes (where the bases do have backbone linkages). The goal is to infer the stabilizing contributions of the backbone. We have been using the sequence the sequence d[AG₃(T₂AG₃)₃] (with d=4) and the protocol to prepare not in air.

References

1. J. B. Schimelman, D. M. Dryden, L. Poudel, K. E. Krawiec, Y. Ma, R. Podgornik, V. A. Parsegian, L. K. Denoyer, W.-Y. Ching, R. H. French, N. F. Steinmetz: Optical Properties and Electronic Transitions of DNA Oligonucleotides as a Function of Composition and Stacking Sequence, **Phys. Chem. Chem. Phys.** 17 4589-99 (2015).
2. L. Poudel, A. M. Wen, R. H. French, V. A. Parsegian, R. Podgornik, N. F. Steinmetz, W.-Y. Ching: Electronic structure and partial charge distribution of doxorubicin under different molecular environments, **Chem. Phys. Chem.** (2015) DOI: 10.1002/cphc.201402893.
3. L. Poudel, W.-Y. Ching, Exploring the electronic structure, charge distribution and bonding on human telomeric G-quadruplex DNA, In preparation.
4. J. B. Schimelman, Y. Ma, R. H. French, Optical Properties and Electronic Structure of Duplex AT-GC vs. AT-CG DNA, In preparation.

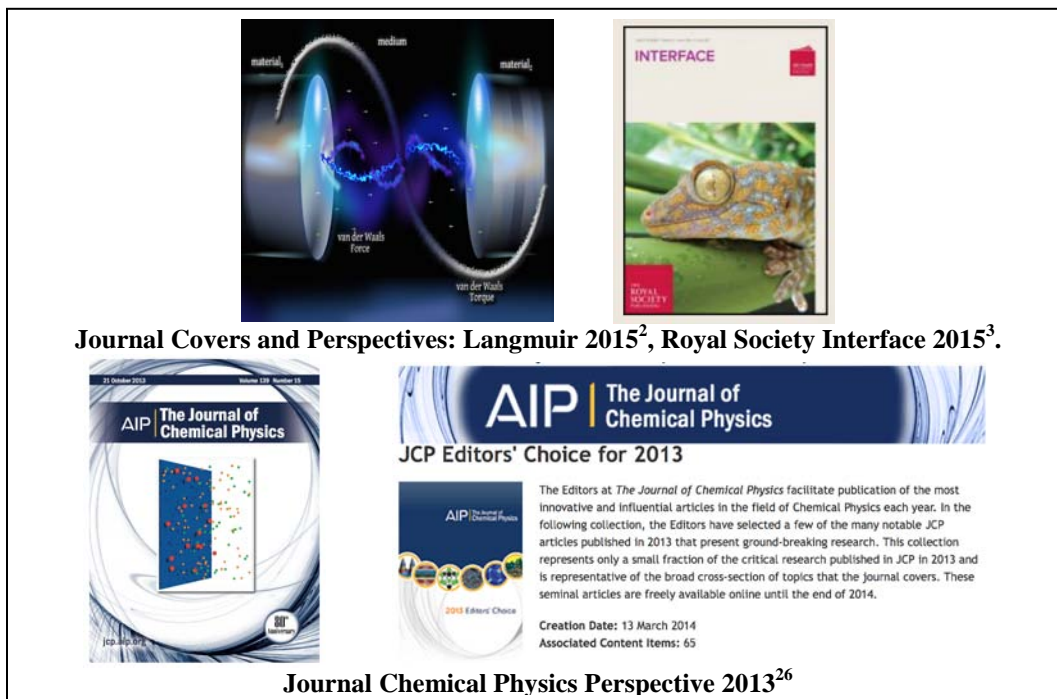
Publications

1. J. C. Hopkins, R. Podgornik, W.-Y. Ching, R. H. French, and V. A. Parsegian: Disentangling the Effects of Shape and Dielectric Response in Van Der Waals Interactions Between Anisotropic Bodies, **J. Colloid and Interface Sci.**, submitted.
2. A. Y. Stark, D. M. Dryden, J. Olderman, K. A. Peterson, P. H. Niewiarowski, R. H. French, and A. Dhinojwala: Adhesive Interactions of Geckos with Wet and Dry Fluoropolymer Substrates,” **J. The Royal Society Interface** 12, 108, 20150464 (2015).
3. D. M. Dryden, J. C. Hopkins, L. K. Denoyer, L. Poudel, N. F. Steinmetz, W.-Y. Ching, R. Podgornik, V. A. Parsegian, and R. H. French: Van Der Waals Interactions on the Mesoscale: Open-Science Implementation, Anisotropy, Retardation, and Solvent Effects, **Langmuir** (2015). doi:10.1021/acs.langmuir.5b00106.
4. J. B. Schimelman, D. M. Dryden, L. Poudel, K. E. Krawiec, Y. Ma, R. Podgornik, V. A. Parsegian, L. K. Denoyer, W.-Y. Ching, N. F. Steinmetz, and R. H. French: Optical properties and electronic transitions of DNA oligonucleotides as a function of composition and stacking sequence, **Phys. Chem. Chem. Phys.** 17, 6, 4589-4599, (2015). Doi: 10.1039/C4CP03395G
5. A. M. Wen, R. Podgornik, G. Strangi, and N. F. Steinmetz: Photonics and Plasmonics Go Viral: Self-Assembly of Hierarchical Metamaterials, **Rendiconti Lincei**, 1-13, March 5th 2015. doi:10.1007/s12210-015-0396-3.
6. L. Poudel, A. M. Wen, R. H. French, V. A. Parsegian, R. Podgornik, N. F. Steinmetz, and W.-Y. Ching: Electronic Structure and Partial Charge Distribution of Doxorubicin in Different Molecular Environments, **Chem. Phys. Chem.**, 16, 7, 1451-60, (2015). doi: 10.1002/cphc.201402893.
7. D. Dean, R. Podgornik, V. A. Parsegian: Fluctuation mediated interactions due to rigidity mismatch and their effect on miscibility of lipid mixtures in multicomponent membranes, **J. Phys.: Condens. Matter** 27, 21, 214004 (2015). Doi: 10.1088/0953-8984/27/21/214004
8. D. M. Dryden, G. L. Tan, and R. H. French: Optical Properties and van der Waals–London Dispersion Interactions in Berlinite Aluminum Phosphate from Vacuum Ultraviolet Spectroscopy, **J. Am. Ceram. Soc.** 97, 4, 1143-50, (2014). Doi: 10.1111/jace.12757
9. S. Yasar, R. Podgornik, and V. A. Parsegian: Continuity of States in Cholesteric - Line Hexatic Transition in Univalent and Polyvalent Salt DNA Solutions, **MRS Proceedings** 1619 (2014). doi:10.1557/opl.2014.358.
10. Y. Ma, D. M. Acosta, J. R. Whitney, R. Podgornik, N. F. Steinmetz, R. H. French, and V. A. Parsegian: Determination of the second virial coefficient of bovine serum albumin under varying pH and ionic strength by composition-gradient multi-angle static light scattering, **J Biol Phys**, 1-13, Jan. 2015. Doi: 10.1007/s10867-014-9367-7

11. L. Poudel, P. Rulis, L. Liang, and W. Y. Ching: Electronic structure, stacking energy, partial charge, and hydrogen bonding in four periodic B-DNA models, **Phys. Rev. E**, 90, 2, 022705 (2014). Doi: 10.1103/PhysRevE.90.022705
12. R. J. Nap, A. L. Božič, I. Szleifer, and R. Podgornik: The Role of Solution Conditions in the Bacteriophage PP7 Capsid Charge Regulation, **Biophysical Journal**, 107,8, 1970-79 (2014). Doi: 10.1016/j.bpj.2014.08.032
13. M. D. Glidden, J. F. Edelbrock, A. M. Wen, S. Shukla, Y. Ma, R. H. French, J. K. Pokorski, and N. F. Steinmetz: Application of engineered viral nanoparticles in materials and medicine, in **Chemoselective and Bioorthogonal Ligation Reactions: Concepts and Applications**, Wiley-VCH, 2014.
14. N. Li and W.-Y. Ching: Structural, electronic and optical properties of a large random network model of amorphous SiO₂ glass, **J. Non-Crystalline Solids** 383. 28-32, (2014). Doi: 10.1016/j.jnoncrysol.2013.04.049
15. S. Yasar, R. Podgornik, J. Valle-Orero, M. R. Johnson, and V. A. Parsegian: Continuity of states between the cholesteric → line hexatic transition and the condensation transition in DNA solutions, **Scientific Reports** 4, 6877 (2014). Doi: 10.1038/srep06877
16. D. S. Dean and R. Podgornik: Relaxation of the thermal Casimir force between net neutral plates containing Brownian charges, **Phys. Rev. E** 89, 3, 032117, (2014). Doi: 10.1103/PhysRevE.89.032117
17. J. C. Hopkins, D. M. Dryden, W.-Y. Ching, R. H. French, V. A. Parsegian and R. Podgornik: Dependence of the Strength of van Der Waals Interactions on the Details of the Dielectric Response Variation, In **MRS Proceedings** 1648 (2014). doi:10.1557/opl.2014.426.
18. D. M. Dryden, Y. Ma, J. Schimelman, D. Acosta, L. Liu, O. Akkus, M. Younesi: Optical Properties and van Der Waals-London Dispersion Interactions in Inorganic and Biomolecular Assemblies, **MRS Proceedings** 1619 (2014). doi:10.1557/opl.2014.301.
19. J. Eifler, P. Rulis, R. Tai, and W.-Y. Ching: Computational Study of a Heterostructural Model of Type I Collagen and Implementation of an Amino Acid Potential Method Applicable to Large Proteins, **Polymers**, 6, 2, 491-514, (2014). Doi: 10.3390/polym6020491
20. P. Adhikari, A. M. Wen, V. A. Parsegian, N. Steinmetz, R. Podgornik, W.-Y. Ching: Electronic Structure, Dielectric Response, and Surface Charge Distribution of RGD (1FUV) Peptide, **Scientific Reports** 4, 5605 (2014). Doi: 10.1038/srep05605
21. J. C. Hopkins, D. M. Dryden, W.-Y. Ching, R. H. French, V. A. Parsegian, and R. Podgornik: Dielectric response variation and the strength of van der Waals interactions, **J. of Colloid and Interface Sci.** 417, 278-84 (2014). Doi: 10.1016/j.jcis.2013.10.040
22. A. M. Wen, P. H. Rambhia, R. H. French, and N. F. Steinmetz: Design rules for nanomedical engineering: from physical virology to the applications of virus-based materials in medicine, **J. Biol. Phys.**, 39, 1-25, (2013). Doi: 10.1007/s10867-013-9314-z

23. A. Naji, M. Kanduč, J. Forsman, and R. Podgornik: Perspective: Coulomb fluids—Weak coupling, strong coupling, in between and beyond, **J. Chem. Phys.**, 139, 15, 150901, (2013). Doi: 10.1063/1.4824681
24. N. Li, R. Sakidja, S. Aryal, and W.-Y. Ching: Densification of a continuous random network model of amorphous SiO₂ glass, **Phys. Chem. Chem. Phys.**, 16, 4, 1500-14, (2013). Doi: 10.1039/C3CP53192A

Other References:



Program Title: A Hybrid Biological/Organic Photochemical Half-Cell for Generating H₂

Principal Investigator: John H. Golbeck; Co-PI: Donald A. Bryant

Mailing Address: Department of Biochemistry and Molecular Biology, The Pennsylvania State University, University Park, PA 16802, E-mail: jhg5@psu.edu, dab14@psu.edu

Program Scope

The goal of the current program is to develop a hybrid biological/organic photo-electrochemical half-cell that couples Photosystem I (PSI), an enzyme that captures and stores energy derived from sunlight, with hydrogenase (H₂ase), an enzyme that catalyzes H₂ evolution with an input of two electrons and two protons. In past grant periods, we assembled the half-cell by directly connecting the surface-located F_B [4Fe-4S] cluster in PSI with the surface-located distal [4Fe-4S] cluster in H₂ase via a molecular wire. The wire serves to tether the two proteins so that an electron can quantum mechanically tunnel between with the FeS clusters of the two enzymes (**Figure 1**) at a rate faster than the competing charge recombination between P₇₀₀⁺ and F_B⁻. We reported that the PSI-wire-[FeFe]H₂ase nanoconstruct evolves H₂ at a rate of 2850 μmoles mg Chl⁻¹ h⁻¹, which is equivalent to an electron transfer throughput of 142 e⁻ PSI⁻¹ s⁻¹. This electron throughput is 2.5 to 3-times than the rate of oxygenic photosynthesis, thereby validating the concept of tethering proteins to overcome diffusion-based rate limitations on electron transfer¹. In the current grant period, we focused on enhancing the performance of our biohybrid nanoconstruct.

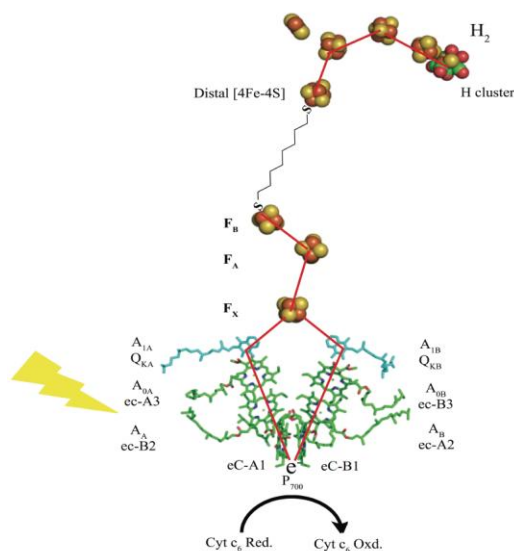


Figure 1. Depiction of the electron transfer pathway in the PSI-wire-FeFe]-H₂ase nanoconstruct.

Recent Progress

The quantum yield of H₂ production in the PSI-wire-FeFe]-H₂ase nanoconstruct.

We measured the quantum yield for light-induced H₂ generation in our optimized bio-hybrid cytochrome c₆ (Cyt c₆) cross-linked PSI_{C13G}-1,8-octanedithiol-[FeFe]H₂ase_{C97G} nanoconstruct. Illumination of the nanoconstruct with visible light between 400 nm and 700 nm resulted in the production of 0.10 to 0.20 molecules of H₂ per photon absorbed (**Figure 2**), which equates to the requirement of 6 to 16 photons of light per H₂ molecule generated. The theoretical quantum yield for the light induced H₂ production for the optimized nanoconstruct should be 0.50 molecules of H₂ produced per photon absorbed, or two photons of light per H₂ molecule generated. These results indicate that the Cyt c₆ cross-linked PSI_{C13G}-1,8-octanedithiol-[FeFe]H₂ase_{C97G} nanoconstruct may not assemble in the predicted 1:1:1 molar ratio, thereby limiting the quantum yield of H₂ production. The reason for the difference between theoretical and experimental yields includes the presence of free PSI_{C13G} and [FeFe]H₂ase_{C97G} proteins from unproductive coupling

reactions, and the occurrence of non-productive, cross-linked [FeFe]H₂ase_{C97G}-1,8-octanedithiol-[FeFe]H₂ase_{C97G} and PSI_{C13G}-1,8-octanedithiol-PSI_{C13G} complexes. Because the masses of the unproductive complexes are different from the productive PSI_{C13G}-1,8-octanedithiol-[FeFe]H₂ase_{C97G} nanoconstruct, it may be possible to remove them by ultrafiltration or chromatography.

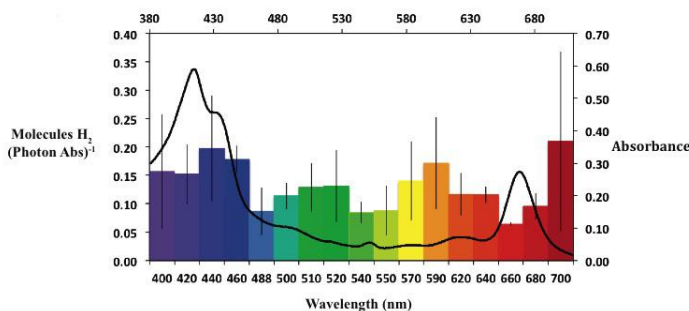


Figure 2. Quantum yield of H₂ production as a function of wavelength of incident radiation.

Increasing the optical cross-section of PSI for greater electron throughput.

When cyanobacteria are grown under iron-limiting conditions, they express IsiA, a peripheral chlorophyll *a* antenna protein, and IsiB, a flavodoxin that substitutes for ferredoxin. The IsiA protein forms single rings around trimeric PSI, presumably to increase the optical cross-section. In 2011², we reported that that at even lower Fe concentrations, the PSI trimer is encircled by two complete IsiA rings. Nevertheless, in spite of the many studies have been carried out to show that IsiA serves as an efficient light-harvesting structure, none have been carried out that show the increased optical cross-section actually leads to an enhanced rate of electron transfer through PSI. Our studies with iron-stressed *Synechococcus* sp. PCC 7002 showed a more rapid transient accumulation of the A₁⁻ phyllosemiquinone anion radical by EPR spectroscopy in iron-depleted cells than in iron-replete cells after a block of white light (**Figure 3**). A derivative-shaped optical signal around 500 nm in the light-minus-dark difference spectrum from an electrochromic bandshift of a carotenoid located near the A₁ phylloquinones is enhanced in iron-depleted wild-type cells and in an iron-depleted *isiB* deletion strain, which lacks flavodoxin, but it is greatly diminished in an iron-depleted *isiA* deletion strain, which lacks IsiA and flavodoxin. These findings confirm that the transient accumulation of electrons on A₁ occurs more rapidly in the IsiA/PSI supercomplex than in the PSI complex alone. Thus, the increased absorption cross-section from the IsiA proteins does translate to an enhanced rate of electron transfer through PSI. We would therefore expect that electron throughput and H₂ generation could be enhanced by a factor greater than two in the case of one ring of IsiA and by a factor between three and four in the case of two rings of IsiA were the PSI-wire-[FeFe]H₂ase nanoconstruct to be assembled with IsiA-containing PSI complexes.

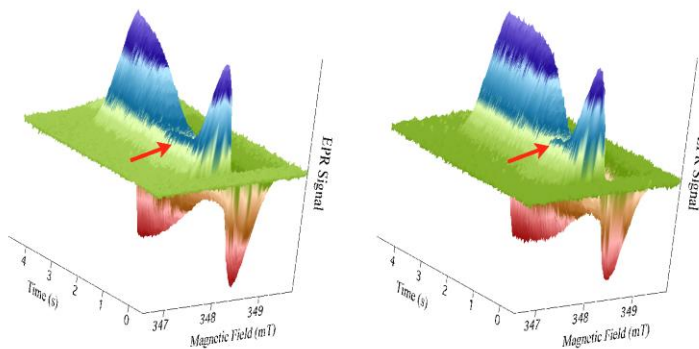


Figure 3. Field-modulated EPR studies of Fe-replete and Fe-depleted WT cultures. The intensity of the EPR signals are plotted against magnetic field and time as a three-dimensional plot for Fe-replete (left) and Fe-depleted (right) WT cells.

Extracting the electron from the lower-potential A_{1A} and A_{1B} phylloquinone-containing sites

We found that a molecular wire consisting of 1-[15-(3-methyl-1,4-naphthoquinone-2-yl)]pentadecyl thiol [(NQ(CH₂)₁₅SH)] can be incorporated into the A_{1A} and A_{1B} sites of PSI (see **Figure 1**) in the *menB* variant of *Synechocystis sp.* PCC 6803. When a Pt nanoparticle is attached to the other end of the molecular wire, the PSI-NQ(CH₂)₁₅S-Pt nanoconstruct evolves H₂ at a rate of 67.3 μmol of H₂ mg of Chl⁻¹ h⁻¹, which is equivalent to 3.4 e⁻ PSI⁻¹ s⁻¹. We proposed that although the rate of electron transfer from A_{1A}/A_{1B} to the tethered Pt nanoparticle is kinetically unfavorable relative to the rate of forward electron transfer to the FeS clusters, the FeS clusters are nevertheless involved in stabilizing the electron. The ~50 ms residence time of the electron on F_A or F_B provides sufficient time for Cyt c_6 to reduce P_{700}^+ , thereby eliminating the recombination channel. We tested this model by sequentially removing the FeS clusters, F_B , F_A , and F_X from PSI, and determining the concentration of Cyt c_6 at which the backreaction was outcompeted and H₂ production was observed. We confirmed that the concentration of Cyt c_6 needed to produce H₂ was comparable to that needed to suppress the backreaction. The FeS clusters therefore serve to ‘park’ the electron and thereby extend the duration of the charge-separated state; however, in doing so, the redox advantage of removing the electron at A_{1A}/A_{1B} is lost. Thus, either a more rapid means of extracting the electron from the A_{1A}/A_{1B} sites or a more rapid means of reducing P_{700}^+ to eliminate the recombination channel will be needed if the low redox potential of the A_{1A}/A_{1B} sites is to be exploited. Nevertheless, because the NQ(CH₂)₁₅SH molecular wire contains two different prosthetic groups, unproductive PSI-PSI complexes that were generated when the 1,8-octanedithiol wire was attached to the F_B cluster can be avoided.

Anchoring PSI onto an electrically conducting solid support containing oligoelectrolytes

In this work, we explored methods to anchor PSI onto an electrically conducting solid support to realize the ultimate goal of this project, the construction of a hybrid biological/organic photoelectrochemical half-cell that can function as a working photocathode. The problem is that the long distance between the electrode surface and P_{700} leads to slow electron transfer rates. We utilized oriented 2-dimensional (2D) PSI crystals on a conductive polymer support and measured photocurrents comparable with thick film (~1.5 μm) devices. Self-assembly was induced through dialysis to produce 2D PSI lipid crystals, providing an environment that mimics the native membrane. 2D crystals are traditionally used for structure determination of membrane proteins by electron microscopy and their application to photovoltaics has not been previously considered. In the 2D crystal form, PSI is stabilized at a very high concentration (weight lipid-to-

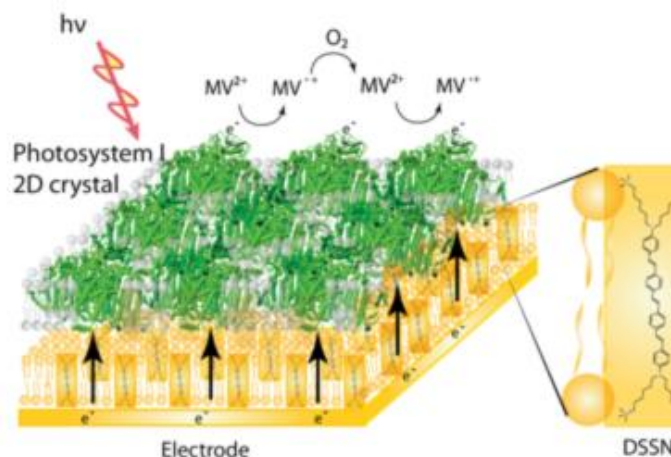


Figure 4. Architecture of assembled biomimetic device. This artificial design aligns PSI proteins in a packed two-dimensional array within a lipid membrane. A conductive oligoelectrolyte-containing bilayer stabilizes the crystals and provides a molecular wire to the crystals.

protein ratio of 0.4-1.0 w/w) and aligned in an orientation that allows for electron transfer between artificial electron acceptor/donors. We prepared 2D PSI crystals on gold electrodes using a stabilizing conductive bilayer (**Figure 4**). The conductive bilayer support was assembled using conductive oligoelectrolyte polymers inserted into a tethered bilayer lipid membrane on gold electrodes. Incorporation of conductive oligoelectrolytes into lipid bilayers was found to be necessary to provide electron transfer across the bilayers. The vertical architecture of the electrode, conductive bilayer, and 2D crystal mimics the native electron transfer pathway that occurs across the thylakoid membrane.

Future Plans

In the next grant period, we plan to (1) develop methods to chromatographically isolate productive PSI_{C13G}-1,8-octanedithiol-FeFe]-H₂ase_{C97G} nanoconstructs from non-productive complexes, (2) incorporate a larger antenna of IsiA proteins in the PSI_{C13G}-1,8-octanedithiol-FeFe]-H₂ase_{C97G} nanoconstruct to increase the optical cross section, (3) generate a PSI-NQ(CH₂)₁₅S-[FeFe]H₂ase nanoconstruct to pass electrons from the A_{1A} and A_{1B} sites to a H₂ase enzyme, and (4) assemble a PSI_{C13G}-1,8-octanedithiol-FeFe]-H₂ase_{C97G} or a PSI-NQ(CH₂)₁₅S-[FeFe]H₂ase nanoconstruct on a solid support containing conductive oligoelectrolytes.

References (Supported by BES Contract Number DE-FG02-05ER46222)

- (1) Lubner, C. E., Applegate, A. M., Knörzer, P., Ganago, A., Bryant, D. A., Happe, T., and Golbeck, J. H. (2011) Solar hydrogen-producing bionanodevice outperforms natural photosynthesis, *Proc Natl Acad Sci U S A*, 108, 20988-91.
- (2) Chauhan, D., Folea, I. M., Jolley, C. C., Kouril, R., Lubner, C. E., Lin, S., Kolber, D., Wolfe-Simon, F., Golbeck, J. H., Boekema, E. J., and Fromme, P. (2011) A photosynthetic strategy for adaptation to low-iron aquatic environments, *Biochemistry*, 50, 686-92.

Publications (Supported by BES Contract Number DE-FG02-05ER46222)

- Saboe, P. O., Lubner, C.E., McCool, N.S., Vargas-Barbosa, N.M., Yan, H., Chan, S, Ferlez, B., Bazan, G.C., Golbeck, J.H., and Kumar, M. (2014) Two-dimensional protein crystals for solar energy conversion, *Advanced Materials* 26, 264-269.
- Gorka, M., Schartner, J., van der Est, A., Rögner, M., and Golbeck, J.H. (2014) Light-mediated hydrogen generation in Photosystem I: attachment of a naphthoquinone-molecular wire-Pt nanoparticle to the A_{1A} and A_{1B} sites, *Biochemistry* 53, 2295-306.
- Lubner, C, Applegate, A., and Golbeck, J.H. (2014) Rerouting redox chains for directed photocatalysis, in *Biohydrogen* (M. Rögner, ed), de Gruyter, Berlin, pp. 239-264.
- Applegate, A. M., C. E. Lubner, P. Knörzer, T. Happe, and Golbeck, J.H. (2015) Quantum yield measurements of light-induced H₂ generation in a photosystem I-[FeFe]-H₂ase nanoconstruct, *Photosynth Res* (in press: DOI 10.1007/s11120-014-0064-y).
- Sun, J. and Golbeck, J.H. (2015) The presence of the IsiA-PSI supercomplex leads to enhanced Photosystem I electron throughput in iron-starved cells of *Synechococcus sp.* PCC 7002, *J. Phys. Chem. B*. (in press: DOI 10.1021/acs.jpcc.5b02176).
- Gorka, M., Perez, A., Baker, C.S., Ferlez, B, van der Est, A., Bryant, D. and Golbeck, J.H. (2015) Electron transfer from A_{1A} and A_{1B} to a tethered Pt nanoparticle requires the FeS clusters for suppression of the recombination channel, *Photochem. Photobiol. B*. (in review).

Project Title: Optical and electro-optic modulation of biomimetically-functionalized nanocarbon materials

PI's and Affiliations: Padma Gopalan (Materials Science and Engineering and The Department of Chemistry, University of Wisconsin-Madison), David McGee, (Department of Physics, College of New Jersey) (Collaborators: Francois Leonard (Sandia National Lab), Bryan Wong (UC Riverside), Franz Himpsel (Department of Physics, University of Wisconsin-Madison)

Program Scope

Light-driven molecular transformations have been long explored for various applications from photorefractives, electro-optics, and energy storage to photodetectors. Natural photo-transduction processes such as vision rely on the *cis* to *trans* isomerization of a small molecule “retinal”, which induces conformational changes in the surrounding protein and triggers a cascade of biochemical events culminating in transmission of an electrical impulse through the optic nerve to the brain¹. Many of these light absorbing molecules found in natural systems are not stable outside their biological environment as they photo-bleach quite easily. However, there are a number of synthetic analogues that can potentially mimic the natural photoconduction process. The fascination with the class of synthetic photochromic or photo-switchable molecules is due to accessibility to a wide range of properties, stability to multiple cycles and fast response. Among many classes of light switchable molecules, azobenzene molecule, which can reversibly isomerize between *trans* and *cis* form by illumination with UV light (*trans* to *cis*) and visible light (*cis* to *trans*), has been of great interests as the dipole moment can be tuned with chemistry, and are remarkably photochemically stable. In the synthetic world coupling these molecules to known semiconductors can result in an ultrasmall light-driven switching device in solid state which mimics natural phototransduction processes. Our research led to the very first demonstration of an optically active nanotube hybrid material by noncovalent functionalization of SWNT field-effect transistors with an azo-based chromophore. The functionalized transistors showed repeatable switching for many cycles, and the low ($100 \mu\text{W}/\text{cm}^2$) intensities necessary to optically modulate the transistor are in stark contrast to measurements of intrinsic nanotube photoconductivity, which typically require $1 \text{ kW}/\text{cm}^2$ intensity². Subsequently, this approach was extended to demonstrate photodetection with tunability over the visible range by changing the chromophore structure³. Our research is focused on understanding the chromophore/ nanotube interactions and gaining mechanistic insight into the effect photo-switching in the molecule on the nanocarbon electronic properties.

Recent Progress: We have made significant progress towards the goals articulated in the proposal. Specifically 1) We have studied the nature of interaction of the chromophore with graphene using Raman Spectroscopy⁴, 2) synthesized a range of dipolar chromophores, 3) quantified the orientation of these molecules on nanotubes by NEXAFS⁵, 4) Studied the effect of reversal of internal dipole of the molecule on the electronic properties⁶, 5) integrated theoretical effort to understand the observed experimental results by collaborating with Bryan Wong (who is now at UC Irvine and formerly at Sandia National Lab), 6) Discovered the formation of phase and surface relief gratings in these functionalized nanocarbon solids. Below is a summary of our main findings in topics related to 1-6.

1) Orientation of a Monolayer of Dipolar Molecules on Graphene from X-ray Absorption Spectroscopy:

Previously, we reported the effect of tethering an azobenzene chromophore (pyrene tethered Disperse Red 1, DR1P) to the surface of SWNTs. The orientation and the photoisomerization kinetics of the chromophores were investigated in nanotube networks using optical second harmonic generation (SHG). While SHG can give the macroscopic polarization of the molecules on the substrate, XAS can provide complementary information by directly probing the orientation of specific molecular orbitals. The element- and bond-specific nature of X-ray absorption spectroscopy (XAS) allows us to look specifically at the most relevant part of the chromophores for determining their orientation. Here we use XAS to gain complementary information on the orientation of chromophores with different terminal groups which are non-covalently latched to graphene

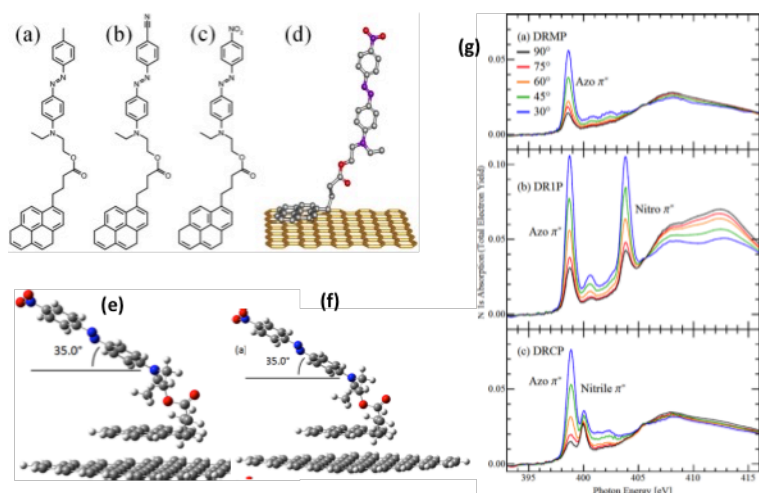


Figure 1: Structure of (a) DRMP, (b) DRCP, and (c) DR1P. Each chromophore is identical except for the terminal group (methyl for DRMP, nitrile for DRCP, and nitro for DR1P). (d) Diagram showing the anchoring of DR1P to graphene via a pyrene tether (in the trans conformation). Two stable configurations of DR1P on graphene, optimized by density functional theory. Configuration (e) is slightly more stable than configuration (f). The tilt angles from DFT calculations for each configuration are indicated. (g) Polarization-dependent N 1s absorption spectra for sub-monolayers of (a) DRMP, (b) DR1P, and (c) DRCP, taken with p-polarized light at various incidence angles. (90° is normal incidence).

instead of SWNTs. Of particular interest is the question of how the transition from a contoured to a planar substrate affects the molecular orientation.

A large polarization dependence is found for three terminal groups, both polar and non-polar. All three chromophores are oriented with the azobenzene moiety tilted by an angle of $\leq 34^\circ$ from the surface. Density functional calculations for one of the three are in good agreement with experimental results and give two similar, stable configurations (Figure 1). The terminal groups thus have only a minor effect on the orientation of the chromophores. In this case the two other factors that could affect the tilt angle are fairly constant, namely surface coverage and the length of the tethers to the surface. Hence, the dipole moment of these molecules can be changed by varying the end group functionalities to probe purely the effect of the dipole on the charge transfer to graphene and hence any possible Raman enhancement effect. More importantly, this brings in a new set of tools to probe molecular orientation at these unconventional interfaces.

2) Mechanistic Insight into Raman Enhancement of Dipolar Molecules on Graphene:

Upon noncovalently latching a dipolar chromophore, namely a pyrene tethered Disperse Red 1 (DR1P), to graphene which effectively p-doped graphene with a hole concentration of $\sim 5 \times 10^{12} \text{ cm}^{-2}$, we detected intense Raman modes from the molecule even with sub-monolayer coverage implying that the interaction of DR1P with graphene potentially led to enhanced Raman signal.

Based on our understanding of the electronic properties of the DR1P/graphene hybrid, we examined this effect through systematic studies of Raman scattering from the graphene/DR1P hybrid by the variation of key parameters such as:

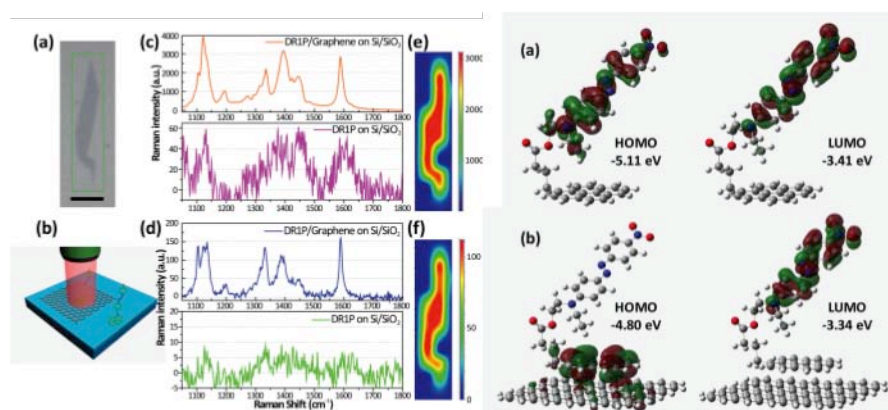


Figure 2: Left hand side panel shows (a) The representative optical microscope image of SLG (scale bar = 5 μm). (b) Schematic illustration of Raman experimental setup for the molecules on graphene and on SiO_2/Si substrate. Raman spectra of DR1P/SLG and DR1P samples obtained (c) at 532 nm excitation (orange trace: DR1P on SLG, magenta trace: DR1P on SiO_2/Si), and (d) at 633 nm excitation (blue trace: DR1P on SLG, green trace: DR1P on SiO_2/Si). Raman intensity mapping results at (e) 1398 cm^{-1} with laser excitation wavelength of 532 nm and at (f) 1388 cm^{-1} with laser excitation wavelength of 633 nm. Right hand side Panel shows the Orbital energy levels and densities obtained from TD-DFT for (a) an isolated DR1P molecule and (b) DR1P/graphene

excitation wavelengths, the surface coverage of DR1P (from sub-monolayer to multilayer), and the number of layers in graphene substrate from (single layer graphene (SLG) to graphite). DR1P was deposited homogeneously onto graphene/ SiO_2/Si and bare SiO_2/Si substrates by spin-coating, and the Raman signals were compared. In this study we are predominantly exploring the GERS for the trans

form of DR1P. In our previous report, we presented Raman spectra of both cis and trans forms of DR1P. The extent of Raman signal enhancement was similar in both cases. Quantitative analysis of Raman scattering cross-section, the saturation of Raman intensity at high DR1P concentration and the shifts in G band and 2D band, as well as TD-DFT calculations on the electronic structure of DR1P/graphene hybrid, all strongly suggest electronic coupling between the highly polarizable molecule and graphene leading to Raman enhancement (Figure 2).

Upon comparison of the Raman signal of DR1P on SLG with that on bare SiO_2/Si substrate, an enhancement factor of 29 ~ 69 at 532 nm excitation was measured. To gain mechanistic insight on the enhancement, we performed quantitative analysis of actual Raman scattering cross-section of the molecule on graphene. Calculated Raman scattering cross-section values were one to two orders of magnitude higher than that in solution at both 532 nm and 633 nm excitations, which correlates well with the observed Raman enhancement. TD-DFT studies showed that the electronic structure of DR1P/SLG is significantly modified, resulting in a lower band gap. This in turn could lead to resonance Raman scattering at both the wavelengths tested. Furthermore, HOMO levels contributing to the first allowed optical excitation are modified significantly by the hybridization.

3) Photo-induced Phase and Surface Gratings in Functionalized Nanocarbon Solid Film

It is apparent from the SHG measurements that there is considerable orientational flexibility in the pyrene tether that links the chromophore to the nanotube. Therefore, upon illuminating DR1P-SWNT with linearly polarized light, *trans-cis-trans* isomerization eventually rotates the *trans* isomer perpendicular to the field vector of the polarized light, as shown schematically in Figure 3. The net effect is manifested as an isotropic to anisotropic transition in linear optical properties, easily detected through photoinduced birefringence experiments. There is

considerable interest in this phenomenon, as light-induced manipulation of chromophore order is central to holographic applications in which dynamic diffraction gratings are optically written with intensity and/or polarization gratings. More recently it has also been observed in the context of photomechanics⁷ in which the reversible shape change of the chromophore upon photoisomerization is exploited to effect surface mass transport. However, neither photoinduced birefringence nor the associated phenomena of surface mass transport have been observed in non-polymeric, nanocarbon solid films. We have recently discovered reversible, photoinduced birefringence in a 200 nm thick DR1P-SWNTs films. The maximum birefringence of $\Delta n \approx 0.01$ at 650 nm was reached using low intensity 480 nm light and followed biexponential dynamics, with characteristic rise times as fast as 0.12 s. Furthermore, upon illuminating the films with 480 nm intensity and polarization grating resulted in dynamic phase diffraction gratings. At longer irradiation times, a permanent periodic surface modulation of the film occurred, with AFM scans showing ± 40 nm modulation in a 220 nm film. This provides direct evidence that azobenzene photomechanical effects can be used to spatially redistribute SWNTs. Independent of photonics applications linked to photoinduced birefringence, the observed coupling of azobenzene photomechanics directly to the SWNT potentially offers an optical means to spatially address and manipulate SWNTs.

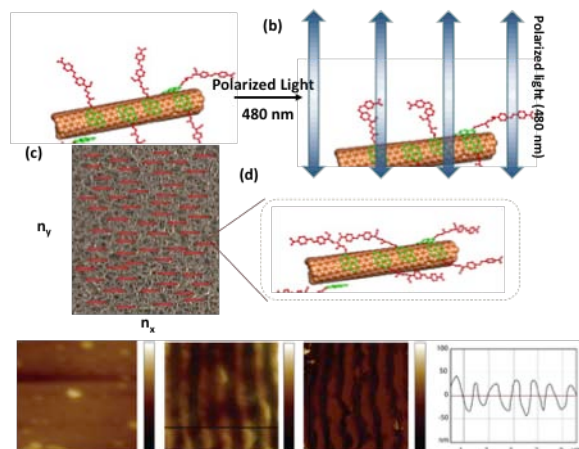


Figure 3 (a) SWNT functionalized with DR1P. In dark, DR1P is predominantly in *trans* conformation, and assumes an isotropic orientation. (b) Linearly polarized 480 nm light induces repeated *trans-cis-trans* isomerization, eventually rotating DR1P perpendicular to 480 nm field vector. (c) Bulk DR1P-SWNT film after illumination exhibits optical anisotropy due to aligned DR1P, resulting in two unique refractive indices (i.e. birefringence), $n_x \neq n_y$. (d) AFM image taken at the surface of a 220 nm thick DR1P-SWNT film where two counter-rotating circularly polarized 480 nm beams intersected. The surface is modulated ± 40 nm with a periodicity of approximately 1.8 μm , in good agreement with the predicted grating spacing of 2.0 μm .

photronics applications linked to photoinduced birefringence, the observed coupling of azobenzene photomechanics directly to the SWNT potentially offers an optical means to spatially address and manipulate SWNTs.

Future Plans: Our focus for future work is develop a mechanistic understanding for the formation of these surface relief gratings in these non-polymeric films through spectroscopic and surface characterization tools, as well as modeling. We will continue to focus on developing new chromophores to tune the flexibility of linker in the dipolar molecule, and expand the absorption window of the chromophore to near-IR range for dual wavelength detection, and to examine the Raman enhancement effect in a series of chromophores.

References:

- (1) Gourdon, P.; Alfredsson, A.; Pedersen, A.; Mahnerberg, E.; Nyblom, M.; Widell, M.; Berntsson, R.; Pinhassi, J.; Braiman, M.; Hansson, O.; Bonander, N.; Karlsson, G.; Neutze, R. *Protein Express Purif* **2008**, *58*, 103.
- (2) Simmons, J. M.; In, I.; Campbell, V. E.; Mark, T. J.; Léonard, F.; Gopalan, P.; Eriksson, M. A. *Physical Review Letters* **2007**, *98*, 086802.
- (3) Zhou, X.; Zifer, T.; Wong, B. M.; Krafcik, K. L.; Léonard, F.; Vance, A. L. *Nano Lett.* **2009**, *9*, 1028.
- (4) Kim, M.; Huang, C. S.; Safron, N. S.; Arnold, M. S.; Gopalan, P. *Abstr Pap Am Chem S* **2013**, 246.
- (5) Johnson, P. S.; Huang, C. S.; Kim, M.; Safron, N. S.; Arnold, M. S.; Wong, B. M.; Gopalan, P.; Himpfel, F. J. *Langmuir* **2014**, *30*, 2559.
- (6) Zhao, Y. C.; Huang, C. S.; Kim, M.; Wong, B. M.; Leonard, F.; Gopalan, P.; Eriksson, M. A. *Acs Appl Mater Inter* **2013**, *5*, 9355.
- (7) Barrett, C. J.; Mamiya, J. I.; Yager, K. G.; Ikeda, T. *Soft Matter* **2007**, *3*, 1249.

Publications Supported by BES in the last two years: 1) Functionalization of Single-Wall Carbon Nanotubes with Chromophores of Opposite Internal Dipole Orientation. Zhao, Y.; Huang, C.; Kim, M.; Wong, B. M.; Léonard, F.; Gopalan, P.; Eriksson, M. A. *ACS Appl. Mater. Interfaces* **2013**, *5*, 9355-9361. 2) Raman Enhancement of a Dipolar Molecule on Graphene. Huang, C; Kim, M.; Wong, B.M.; Safron, N.; Arnold, M.S.; Gopalan, P.; *J. Phys. Chem. C* **2014**, *118(4)*, 2077-2084. 3) Orientation of a Monolayer of Dipolar Molecules on Graphene from X-ray Absorption Spectroscopy. Phillip, J.; Haung, C.; Kim, M.; Safron, N.; Arnold, M.; Wong, B.; Gopalan, P.; Himpsel, F.; *Langmuir* **2014**, *30(9)*, 2559-2565. 4) Photo-induced phase and surface gratings in functionalized nanocarbon solid film David J. McGee, John Ferrie, Aljoscha Plachy, Yongho Joo, Jonathan Choi, Catherine Kanimozhi, and Padma Gopalan, Submitted to APL July 2015.

Program Title: Strong Autonomous Self-healing Materials via Dynamic Chemical Interactions

Principle Investigator: Zhibin Guan, Ph.D.

Mailing Address: 1102 Natural Sciences II, Irvine, CA 92697

Email: zguan@uci.edu

Program Scope

The objective of this project is to investigate new strategies for designing strong, autonomous self-healing materials for potential energy relevant applications. During the previous grant period, our lab has successfully developed a few new strategies for designing autonomously self-healing polymers using both supramolecular and dynamic covalent interactions. A key concept we have pioneered is the multiphase self-healing material design that can combine high modulus, toughness, and autonomous self-healing capability. Built upon these successes, in the current program we further explore new designs toward strong, autonomous self-healing polymeric materials. In one approach, dynamic metal-ligand interactions are used as the healing mechanism in a hard-soft two-phase polymer system, to afford strong, while dynamic, self-healing polymers. In another approach, we combine the advantages of our supramolecular and dynamic covalent self-healing designs to design a two-tiered self-healing system. In this system, the supramolecular interaction provides fast initial healing to bring damaged parts together so that new covalent bonds can be formed for more permanent, quantitative healing. Finally, inspired by the strength and toughness of many natural nanocomposite materials, we propose to develop dynamic, self-healing inorganic-organic nanocomposites that are strong, tough, and self-healable. Self-healing materials are expected to have a huge impact on energy production, environmental impact, energy security, and energy saving.

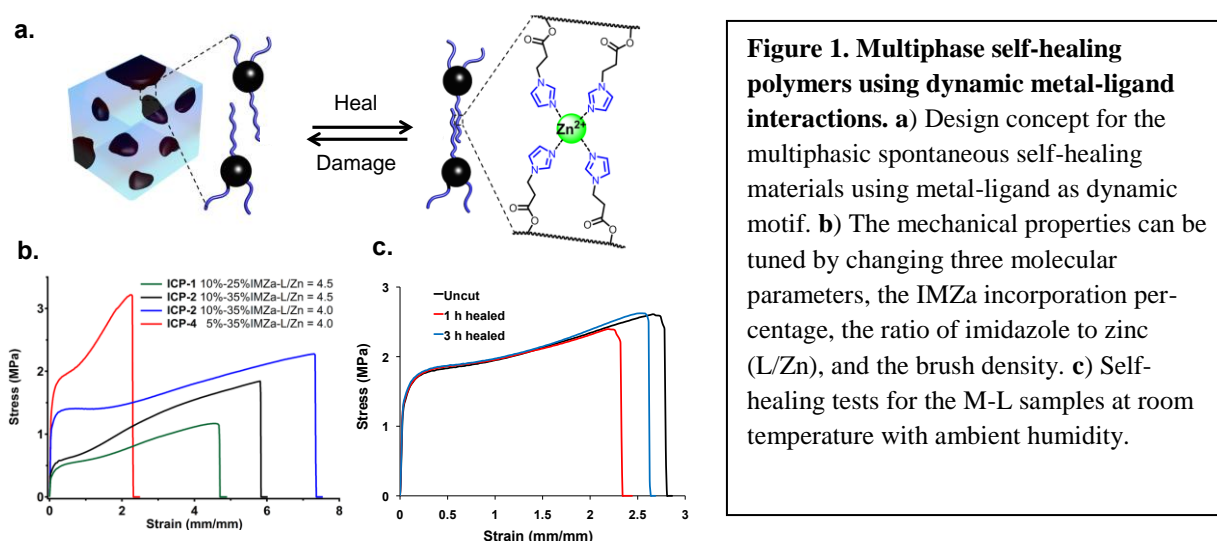
Recent Progress

1. Dynamic Metal-ligand Interactions for Self-Healing Polymers

Metal-ligand (M-L) complexes are promising candidates as dynamic healing motifs because the thermodynamic and kinetic parameters of M-L complexes are tunable over a broad range, which could potentially yield materials with highly tunable mechanical properties. For self-healing solid materials, the most commonly utilized M-L systems involve multidentate nitrogen based aromatic ligands, such as terpyridines.^{1, 2} Due to the high association constants and the fact that the M-L complexes microphase separate into the hard, non-dynamic domains, external energy such as heat² or light¹ must be required to reversibly dissociate the M-L complexes to induce self-healing.

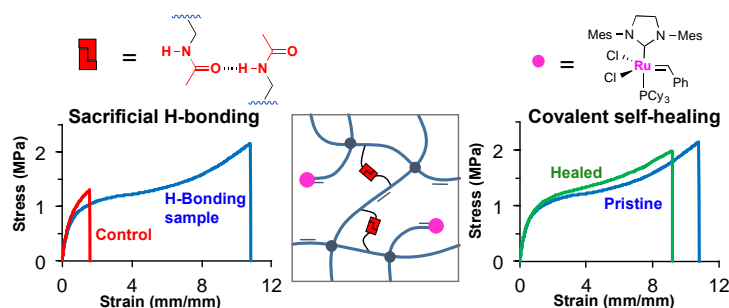
To realize a spontaneous self-healing M-L polymer, we decided to choose a highly dynamic M-L system, Zn²⁺-imidazole, as the healing motif. In addition, to combine good mechanical properties with spontaneous self-healing capability under ambient conditions, we

designed a microphase-separated soft/hard two-phase polymer system with the *M-L complexes strategically embedded in the soft matrix* having low glass transition temperature (T_g) (Fig. 1a). The mechanical and dynamic properties of the materials can be conveniently tuned by varying several molecular parameters (such as the backbone composition and degree of polymerization, the brush density, and the ligand density) as well as the L/M ratio (Fig. 1b). Our multiphase M-L polymers show excellent self-healing property under ambient conditions with minimal intervention (Fig. 1c). Compared to hydrogen-bonding based self-healing systems, the M-L system may offer advantages of being less moisture sensitive and having a broad range of tunability of thermodynamics and kinetics. Several other molecular parameters, such as the identity of the metal ion, counter-ions, and ligand, will be varied to further improve the mechanical and self-healing properties of this new class of materials.



2. Two-tiered Self-healing Polymers for Enhanced Properties

A major goal in the field of self-healing materials is to combine robust mechanical and efficient healing properties. In one approach, we show that combination of supramolecular and dynamic covalent interactions dramatically improves the overall mechanical properties. Specifically, we use simple secondary amide side chains to create dynamic energy dissipative hydrogen bonds in a covalently cross-linked polymer network, which can self-heal via olefin cross-metathesis. By incorporating ~ 20 mol% of a H-bonding monomer into an olefin containing network, the



strain-at-break was increased from 150% for the control network to ~950%, and the toughness of the network was enhanced by more than 7-fold. Rheological and cyclic tensile experiments were used to further probe the energy dissipation and reversible recovery of the sacrificial hydrogen bonds in our bulk system. Mediated by the Grubbs Gen-2 catalyst, the olefin-containing network displays efficient healing under relatively mild conditions. The attained robust mechanical properties combined with the efficient self-healing capability are highly desirable for many practical applications. We anticipate that this straightforward sacrificial bonding strategy can be employed to improve mechanical properties of many other self-healing systems.

3. Mechanically Robust and Self-healable Superlattice Nanocomposites by Self-assembly

For many technological applications, it is critical to develop practical and scalable methods to assemble nano-building blocks into functional materials possessing both high structural order *and* robust mechanical properties. While several methods have been reported using small molecules, DNA, and polymer ligands to facilitate the assembly of nanoparticles into various 2- or 3-dimensional ordered nanostructures, there is a lack of scalable synthesis of ordered 3-dimensional superlattice nanocomposites with robust and dynamic mechanical properties. In this study, we developed a simple, scalable synthesis to introduce multivalent hydrogen bonding polymer grafts onto nanoparticles, which self-assemble into three-dimensional superlattice nanocomposites.

The multivalent H-bonding interactions between nanoparticles provide strong cohesive energy to bind nanoparticles into strong and tough materials. Importantly, facilitated by the strong enthalpic interactions, mechanically robust nanocomposites can be achieved with relatively short polymer grafts without relying on chain entanglement; therefore, the superlattice order can be maintained. Furthermore, the dynamic hydrogen bonding interactions afford the formation of highly dynamic, self-healing, and mechanochromic nanocomposite materials in bulk. We envision this single-component “sticky” polymer-grafted nanoparticle approach could be a simple and general method for assembling various functional nanoparticles into robust and dynamic functional materials.

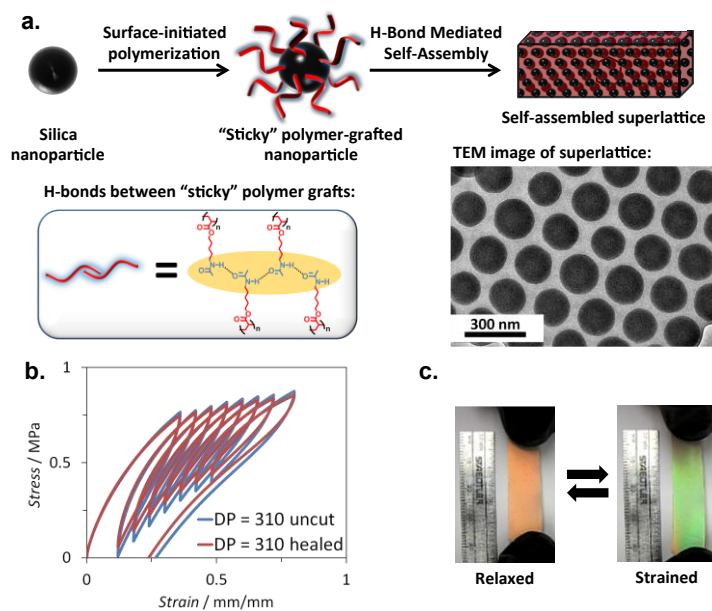


Figure 3. Dynamic and self-healing superlattice nanocomposites. a) Design concept and preparation of self-healing superlattices. b) Fracture toughness test for pristine and self-healed samples shows complete recovery of original mechanical properties. c) Mechanochromic properties of superlattice nanocomposite films.

Future Plans

(1) Further Investigation of Dynamic Metal-ligand Interactions for Self-Healing Polymers

Multiple variables, such as the metal ion, valence of the metal ion, counter anions, and the polymer composition and architecture (brush vs. block) will be systematically varied to further improve the mechanical and self-healing properties.

(2) Further Exploration of Two-tier Self-healing Designs

Various two-tier designs, including H-bonding/dynamic covalent bonds, H-bonding/metal-ligand interactions, and dual metal-ligand interactions, will be investigated.

(3) Further Investigation of Functional Self-assembled Superlattice Nanocomposites

We will synthesize various functional nanoparticles functionalized with supramolecular or dynamic covalent motifs. Furthermore, we will self-assemble them into bulk nanocomposites and investigate both their self-healing and emerging functional properties.

References:

1. Burnworth M, Tang L, Kumpfer JR, et al. Optically healable supramolecular polymers. *Nature* 2011;472(7343):334-37.
2. Bode S, Zedler L, Schacher FH, et al. Self-Healing Polymer Coatings Based on Crosslinked Metallosupramolecular Copolymers. *Adv Mater* 2013;25(11):1634-38.

Publications in year 2013-2015 (which acknowledge DOE support):

1. Cromwell, O. R.; Chung, J.; Guan, Z. "Malleable and Self-Healing Covalent Polymer Networks through Tunable Dynamic Boronic Ester Bonds" *J. Am. Chem. Soc.*, **2015**, *137*, 6492.
2. Williams, G. A.; Ishige, R.; Chung, J.; Takahara, A.; Guan, Z. "Mechanically robust and self-healable superlattice nanocomposites by self-assembly of "sticky" nanoparticles" *Adv. Mater. In press*.
3. Hosono, N.; Kushner, A. M.; Palmans, A. R. A.; Guan, Z.; Meijer, E. W. "Forced Unfolding of Single-Chain Polymeric Nanoparticles" *J. Am. Chem. Soc.*, **2015**, *137*, 6880.
4. Wang, Z. K.; Jiang, F.; Zhang, Y. Q.; Wang, Z. G.; Guan, Z. "Bioinspired design of multiphase polymers to mimic mechanical properties of human skin" *ACS Nano*, **2015**, *9*, 271.
5. Chen, Y.; Guan, Z. "Self-healing thermoplastic elastomer brush copolymers having a glassy polymethylmeth-acrylate backbone and rubbery polyacrylate-amide brushes" *Polymer* 2015, *in press*.
6. Chung, J.; Kushner, A. M.; Weisman, A. C.; Guan, Z. "Direct correlation of single-molecule properties with bulk mechanical performance for the biomimetic design of polymers" *Nature Mater.* **2014**, *13*, 1055.
7. Mozhdghi, D.; Ayala, S.; Cromwell, O. R.; Guan, Z. "Autonomous Self-Healing Multiphase Polymers via Dynamic Metal-Ligand Interactions" *J. Am. Chem. Soc.*, **2014**, *136*, 16128.
8. Chen, Y.; Guan, Z. "Multivalent hydrogen bonding block copolymers self-assemble into strong and tough self-healing materials" *Chem. Commun.* **2014**, *50*, 10868.
9. Mozhdghi, D.; Guan, Z. "Design of Supramolecular Amino Acids to Template Peptide Folding" *Chem. Comm.* **2013**, *49*, 9950.
10. Chen, Y.; Guan, Z. "Self-assembly of core-shell nanoparticles for self-healing materials" *Polym. Chem.* **2013**, *4*, 4885.

Development of Smart, Responsive Communicating and Motile Microcapsules

Daniel A. Hammer and Daeyeon Lee, Department of Chemical and Biomolecular Engineering, University of Pennsylvania, Philadelphia, PA 19104.

Program Scope

The goal of this project is to design motile systems using responsive and adhesive microcapsules that can respond to changes in environmental stimuli and induce collective, smart behavior on length-scales well beyond that of the capsule itself. The general principle that will be employed is particle taxis – or directed motion – in response to nanoparticles, enzymes or analytes that are released from a source capsule in response to light, change in pH, or enzymatic activity. Much of the theory for interparticle communication and collective response has been developed by a DOE-funded effort by Dr. Anna Balazs (University of Pittsburgh); our goal is to test these predictions experimentally. Central to our design are vesicles of various designer chemistries, such as polymersomes – vesicles whose outer membrane is assembled from block-co-polymers. We have shown that we can make large, uniform populations of polymersomes and have designed these capsules to encapsulate and release active agents such as nanoparticles or molecules in response to stimulation such as light. In these proposed experiments, we will release encapsulated nanoparticles from source particles, and induce the motion of target particles through haptokinesis (by making a gradient of particles on a surface) or chemokinesis (making a gradient of particles in solution). We have developed methods for making spatial, ordered arrays of microcapsules using micro-contact printing. Within these ordered arrays, using nanoparticles and surfaces with tailored adhesiveness, we will directly test of the principles of collective smart particle motion. Furthermore, we include principles of self-propulsion from either thermal or biochemical interactions to make capsules that are motile. The long-term impact of this work will be to develop autonomous, self-regulating motion of microcapsules that mimicking biological activity and convert light to motion.

Aims of the project are:

- 1. To use enzymatic activity to engineer release from capsules.** Using polymersomes in which catalase is entrapped, or protein vesicles in which protease cleavable domains have been introduced into chains, we will devise capsules that can be induced to release contents in response to enzymatic activity or light.
- 2. To use specific and weak adhesion and micro-contact printing to make specific spatial arrays of polymersomes and microparticles.** We will place adhesive ligands in specific patterns using microcontact printing, and adhere both signaling particles (polymersomes, polymer microspheres, protein vesicles) and sentinel particles (polystyrene microparticles, polymersomes, and vesicles) to printed arrays. Patterns will be motivated by published theoretical predictions of inter-particle spacing that give rise to collective motion.
- 3. To demonstrate of collective motion of micron-sized particles in response to light and pH.** We will adhere particles weakly on printed arrays, and we will combine photoresponsive, pH sensitive or enzyme sensitive capsules, equipped with nanoparticles as signaling particles, and vary the density and spacing of sentinel particles. Upon change in stimulus, we will use video microscopy to observe the collective motion of particles on the surface. Collective motion will be catalogued as a function of interparticle spacing, nanoparticle density, and particle size.

4. To synthesize spontaneously motile systems, based on floppy vesicles that interact with spatial arrays of proteins. We will make vesicles by microfluidics, and then make them floppy by storing them in hyperosmotic media. Through thermal fluctuation of the vesicles with a surface, and tuning the adhesion to be weak, so that contacts can be both made and broken, we endeavor to make spontaneously motile systems. We have already demonstrated thermal motility on a weakly adherent surface and now we will engineer motility on a substrate through punctate spots of adhesion. We can drive the directional motion using enzymatic activity through patches of enzyme on vesicles, and further drive directionality through haptokinetic or chemokinetic fields, as pursued in aims 3 for rigid particles.

Recent Progress

Secretion from vesicles using an enzymatic cascade. In aim 1, the goal is to use entrapped enzymes to secrete material from vesicle in response to external stimuli. In the present study, a series of two enzymatic reactions, one inside and the other outside of a polymersome, were

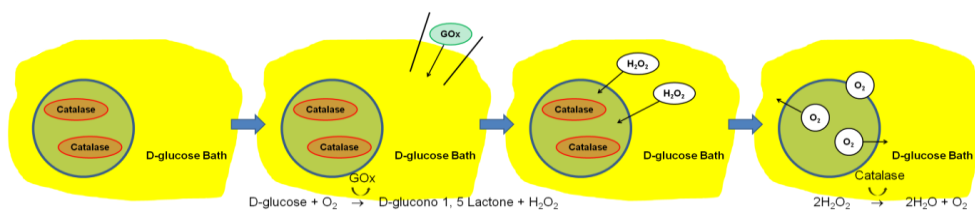


Figure 1. Schematic illustration for using catalase and glucose oxidase to trigger the rupture of polymersomes. Catalase is entrapped inside the polymersomes and glucose oxidase is added outside. H_2O_2 is generated outside and diffuses across the membrane, causing vesicle bursting.

designed to give rise to controlled rupture of polymersomes. We encapsulated the enzyme catalase within the polymersomes.

es, by assembling vesicles using microfluidic technology, and dispersed these polymersomes into a solution containing D-glucose. When the enzyme glucose oxidase was added to the exterior solution, D-glucose was converted to D-glucono 1, 5 lactone and hydrogen peroxide. Hydrogen peroxide is a small, neutral molecule that can pass readily through membranes. The second enzymatic reaction, catalyzed by catalase, generates oxygen radical from hydrogen peroxide that entered the interior of the vesicle; the generation of oxygen radical leads to the triggered rupture of polymersomes. We measured how the kinetics of rupture is affected by altering enzyme concentration.

A schematic illustration of enzyme reaction-triggered rupture of polymersomes is shown in **Figure 1**. The design of our experiments is based on the hypothesis that H_2O_2 generated from GOx catalysis of D-glucose will penetrate the polymersome membrane and interact with encapsulated catalase within the polymersome, generating free oxygen and causing release. Catalase-loaded polymersomes were prepared with microfluidic water-in-oil-in-water (W/O/W) double emulsions. Subsequently, three different weight percents of a GOx solution - 0.2, 1, and 2 wt. % - were added to the outer solution. In the second enzymatic reaction, catalase catalyzes the conversion of H_2O_2 to water and oxygen (O_2), which subsequently induces the failure of polymersomes.

To confirm the effect of enzymatic reactions on polymersome rupture, we compared the survivability (S_V) of polymersomes for a system with all the chemical components, to that seen in three controls in which one critical component is missing. $S_V(t)$ is defined as $N(t)/N_0$ where $N(t)$ is the number of polymersomes in the field of view (FOV) at time t and N_0 is the initial number of polymersomes in FOV. In the absence of GOx or of catalase, there was no disruption

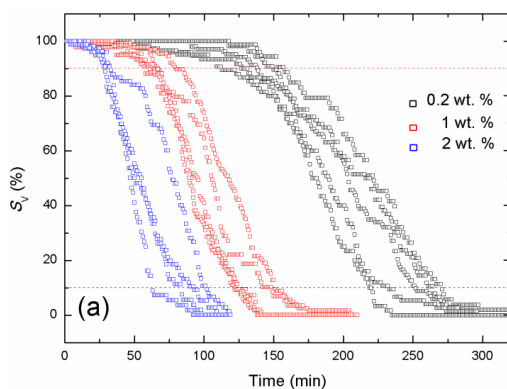


Figure 2. Failure dynamics (survivability S_v) of catalase-loaded polymersomes with under different exterior GOx concentrations. Initial numbers of polymersomes were 73.4 ± 19.2 , 90.6 ± 37.8 , and 65.2 ± 11.9 for 0.2, 1, and 2 wt. %, GO_x concentration respectively.

as a function of time. The onset and termination points for S_v are defined as: $S_v(t_{onset}) = 90\%$ and $S_v(t_{termination}) = 10\%$. Figure 2 shows that the onset and termination times decrease with increasing GOx concentration. Both the onset and termination time decrease with increasing GOx concentration, obviously the kinetics of failure can be controlled by the variation of enzyme (GOx) concentration. Furthermore, we can also tune the release rate of the encapsulated materials by altering the enzyme concentration because the slopes of the curves in Figure 2 increase with GOx concentration. A paper on this work has been submitted to *Small*.

Displacement of capsules from positions on arrays. We have also made progress on Aim 2. We previously showed that we could position biotinylated-vesicles onto avidin-coated arrays (Kamat et al., 2013). The vesicles are uniform in size and made by microfluidics, and the ability to position capsules on arrays is essential to the goal of developing systems with autonomous motion and testing the theories of Balazs. Our strategy for displacing particles is to use small particles that are secreted from a vesicle during rupture, which can then displace neighboring particles through competing with their substrate adhesion. We have a variety of chemistries among which to choose for positioning the capsules, but in this period we showed that even using strong biotin-avidin chemistry, we can displace the particles.

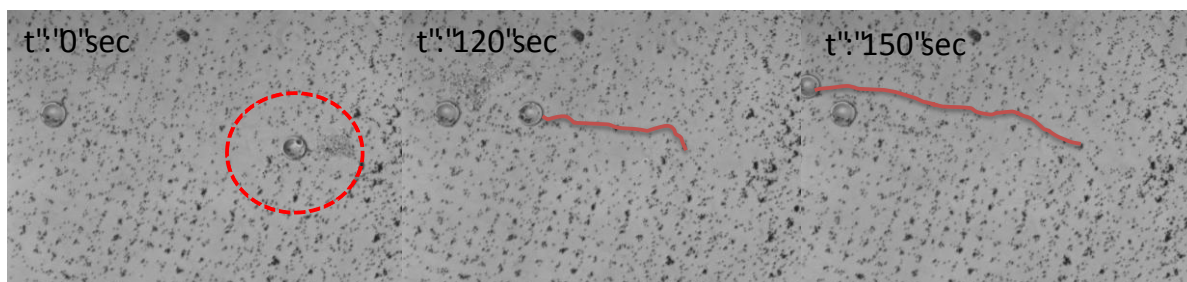


Figure 3. Displacement of 150 micron diameter biotinylated capsules by 6.8 micron biotinylated particles, with a path shown in the orange line. The small particles ultimately take up residence on the spots on the array.

of the vesicles. For the H₂O₂ (+) control, we eliminated both enzymatic reactions: catalase-free polymersomes were dispersed in the D-glucose solution and 2 wt. % H₂O₂ was added in place of GOx solution. This control confirms that polymersome membranes are stable in the presence of H₂O₂, a known oxidizing agent. When all components were present, it took 288.0 ± 31.6 minutes to achieve complete failure ($S_v = 0$). However, the survivability S_v at 300 minutes for GOx(-), catalase(-), and H₂O₂(+) controls were 98.3 ± 1.4 , 96.3 ± 3.3 , and $96.6 \pm 3.8\%$, respectively. These control experiments indicate that both enzymatic reactions are necessary to induce polymersome rupture.

We also measured the effect of GOx concentration on the dynamics of failure by monitoring the number of ruptured polymersomes

We positioned biotinylated vesicles of diameter 150 microns and used 6.8 micron biotinylated particles on arrays in which 50 micron avidin spots separated by 100 microns are printed with a low density of avidin (1 $\mu\text{M}/\text{ml}$). The key to this problem we making the adhesion of the vesicles to the avidin spots as weak as possible by using the lowest possible density of avidin. In these experiments, the 6.8 micron particles were injected in solution to displace the large particles. Figure 3 illustrates the progressive displacement of a larger particle (in a path outlined in orange) by dark nanoparticles that take their position on the arrays. These experiments illustrate the feasibility of our strategy for the displacement of particles using the secretion of nanoparticles.

Incorporation of oleosin into polymersome membranes. Oleosin is a plant protein that acts as a surfactant. Previously, we showed that oleosin can be expressed, modified, and self-assembled into numerous soft-matter structures, such as vesicles (Vargo et al., 2012). Furthermore, we have shown that a variant of oleosin in which the internal hydrophobic core has



Figure 4. Incorporation of a fluorescent oleosin into a polymersome leads to patches of oleosin (and therefore a Janus particle; see white arrow). This affords us the opportunity to append a specific chemistry to the oleosin to drive motion.

been reduced to 30 amino acids assembles into spherical micelles assembles at a critical micellar concentration of 4.1 μM (Vargo et al., 2014). Our current goal is to use oleosin to make vesicles with autonomous motility, driven by H_2O_2 . The idea is to drive the motion using platinum-binding oleosin proteins that are integrated into a polymersome membrane in patches. During this period, we showed that we can incorporate oleosin into a polymersome membrane in a patch by mixing oleosin and the polyethylene oxide – polybutadiene polymer (OB29) at an oleosin concentration below the CMC. Because of lateral interactions of the protein, the protein, which is fluorescently labeled, assembles in a patch (Figure 4). Such patchiness will enable the assembly of Janus particles in which the oleosin bears a

specific chemistry, such as a platinum binding peptide, that can catalyze the reduction of H_2O_2 and drive autonomous motion as a microswimmer.

Future Plans

1) Use light and enzymatic activity to release biotinylated nanoparticles from vesicles, to displace neighboring particles. 2) To position vesicles on arrays using weaker adhesion chemistry, including selectin/carbohydrate adhesion. 3) To integrate the platinum binding peptide PTSTGQA into oleosin, incorporate the oleosin into polymer vesicles, and make vesicles that display autonomous motion in response to H_2O_2 .

References

- Woo-Sik Jang, S.C. Park, K.P. Dooley, S. F. Wheeler, D. Lee, D. A. Hammer, (2015), “Enzymatic Reaction-Triggered Rupture of Polymersomes,” submitted, *Small*.
 N. P. Kamat, St.J. Henry, D. Lee, and D. A. Hammer (2013). *Small*, 9(13); 2272–2276.
 K.B. Vargo, N. Sood, T. D. Moeller, P. A. Heiney, and D. A. Hammer, (2014) *Langmuir* 30(38): 11292-11300.

K.B. Vargo, R. Parthasarathy and D.A. Hammer, (2012), Proceedings of the National Academy of Sciences USA 109 (29) 11657-11662

Two-year Publications

Woo-Sik Jang, Seung Chul Park, Kevin P. Dooley, Samuel F. Wheeler, Daeyeon Lee, Daniel A. Hammer, (2015), “Enzymatic Reaction-Triggered Rupture of Polymersomes,” submitted, Small.

Neha P. Kamat, Steven J. Henry, Daeyeon Lee, and Daniel A. Hammer (2013). “Single vesicle patterning of uniform, giant polymersomes into microarrays,” Small, 9(13); 2272–2276.

Wei Qi, Guizhi Li, P. Peter Ghoroghchian, Daniel A. Hammer, and Michael J. Therien, (2013). “Nano- and Meso-Scale Polymersomes Based on Biodegradable Poly(ethylene oxide)-block-Polycaprolactone (PEO-*b*-PCL) Copolymers”, Nanoscale 5: 10908-10915; doi: 10.1039/C3NR03250G.

Julianne C. Gripenburg, Nimil Sood, Kevin Vargo, Dewight Williams, Jeff Rawson, Michael J. Therien, Daniel A. Hammer and Ivan J. Dmochowski, (2015), “Caging metal ions with light-responsive nano-polymersomes,” Langmuir 31(2):799–807, doi: 10.1021/la5036689.

Woo-Sik Jang, Seungchul Park, Miju Kim, Junsang Joh, Daeyeon Lee, and Daniel A. Hammer, (2015) “The Effect of Stabilizer on the Mechanical Response of Double-Emulsion Templated Polymersomes,” Macromolecular Research Communications, 36 (4):378–384, doi: 10.1002/marc.201400472doi: 10.1002/marc.201400472.

Surface Mechanical Properties of Bio-Inspired Architectures

Anand Jagota* (anj6@lehigh.edu) and Chung-Yuen Hui& (ch45@cornell.edu)

*D331 Iacocca Hall, Chemical Engineering, Lehigh University, Bethlehem PA 18015.

&Sibley School of Mechanical and Aerospace Engineering, Cornell University, Ithaca.

Program Scope

The overall goal of our work is to design bioinspired meso-scale surface architectures resulting in controllable surface mechanical properties such as adhesion, and to understand the surface mechanical properties of compliant/soft materials, especially where they differ from conventional stiff materials. We draw inspiration from materials in nature that have evolved to form remarkable surfaces with unique surface mechanical properties.

In our current project, we have a focus on two problems:

(a) *What is the role of surface-tension or solid capillarity in soft materials?* Biomaterials and synthetic biomimetic materials are usually “soft” or compliant compared to conventional engineering materials (e.g., metals and ceramics). Although the role of surface energy is well-known in determining surface mechanical properties such as adhesion and friction, the role of the equally fundamental surface mechanical property, solid surface tension, has generally been ignored. By experimental and theoretical studies we have shown that solid capillarity can play an important and sometimes dominant role in surface mechanical properties, e.g., shape change due to surface tension, wetting, contact mechanics, and fracture.

(b) *How does one endow a surface with highly selective adhesion using shape complementarity?* There are many examples in nature, ranging from the molecular (shape and charge recognition between folded proteins) to millimeter-scale attachment devices (contacting and attachment surfaces in insects and lizards), of architectures that obtain highly selective and enhanced adhesion using shape-complementarity. We have studied simple designs of shape-complementary surfaces made by ridges and channels that can strongly enhance adhesion. We discovered that interfacial dislocations appear spontaneously, permitting interlocking even in the presence of misorientation.

Recent Progress

1. **Flattening of Features on a Compliant Material by Surface Tension.**

Nearly all works on creating biomimetic structures for enhanced and controlled surface mechanical properties rely on creating structured surfaces. In many cases, this is accomplished by some form of molding technique. We have shown how, by exerting forces that flatten and round-off surfaces, solid surface tension limits our ability to replicate master shapes by molding. To analyze such deformations, we have developed both analytical models as well as computational techniques (special surface tension finite elements). Figure 1 shows measured 3D profiles of a PDMS master (the higher and sharper features) and a gel replica (flattened and rounded features). The gel (Gelatin in a 70/30 glycerol/water mixture) is much more compliant

than the PDMS (Young's modulus of 32.5 kPa versus ~ 3 MPa, respectively) and its profile is flattened and rounded immediately upon removal of the replica from its mold. We modeled the shape change as being due to elastic deformation driven by solid surface tension, which can be brought into excellent agreement with experimental profiles using a single fitting parameter, the solid surface tension[1]. Thus, this experimental set up can serve as a technique to measure solid surface tension.

2. Shapes of Wetting Drops on Compliant Solids.

Wetting of a solid is important as a basic phenomenon and as a surface characterization method. The basic relations governing the shape of liquid drops on surfaces are altered when surface tension begins to play a significant role. For example, the well-known Young's equation relating contact angle of a drop to surface energies is no longer valid for highly compliant solids. For example, for a drop suspended on a thin elastomeric film, Figure 2, we showed that the shape is governed by balance of surface tensions [2, 3] (Neumann's Triangle [4]). In general, we showed that there are two separate conditions, force and configurational energy balance, that need to be satisfied at the contact line [4]. In the conventional limit of a liquid drop on a stiff substrate, only the latter matters and leads to Young's equation. In the case of a highly compliant solid, on the other hand, force equilibrium can dominate, governed by force balance (Neumann's triangle, Figure 2). This experiment can be used to measure surface tension of relatively stiff materials.

3. Effect of Surface Tension on Adhesive Contact Mechanics of Soft Materials and Fracture.

Contact between a rigid particle and a deformable substrate is a canonical problem of central importance in the mechanics of soft or compliant materials. It underlies important

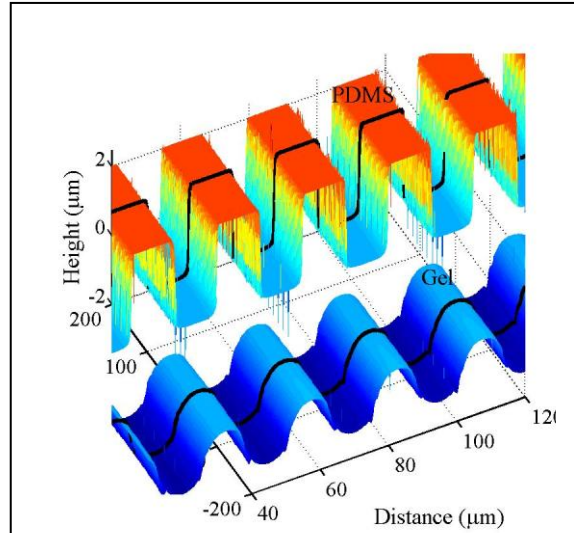


Figure 1 Surface profile of a periodic ridge geometry showing PDMS master (higher and sharper features) and its gel replica (flattened and rounded profile) for gel Young's modulus $E = 32.5$ kPa, wavelength $\lambda \sim 25$ μm and initial height $h \sim 2.7$ μm .

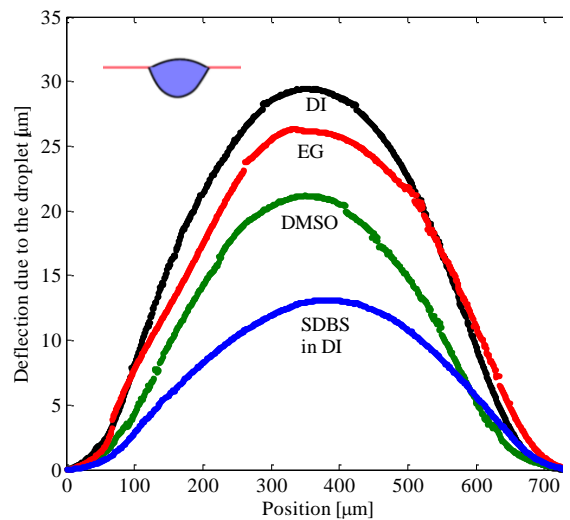


Figure 2 Film bulge measured interferometrically using different liquids. Analysis of the deformed shape reveals that solid surface tension plays an important role in determining the shape of the wetting drop. (Inset drawing shows schematically how capillary forces due to a drop placed under a thin elastomeric film cause it to bulge.)

physical phenomena such as adhesion and friction between surfaces. Conventionally, it is has been thought of as an interplay between two factors, reduction in interfacial energy W_{ad} (that drives contact growth) and increase in elastic energy (which resists contact growth); balance between the two determines equilibrium configurations. We have shown that for sufficiently compliant materials [5-7] (small modulus E) or small particles, the surface tension of the substrate (σ) can play an important and sometimes dominant role in resisting contact growth [5-7]. Our results are in good agreement with experiments conducted by the group of Eric Dufresne at Yale University. For soft materials to be use in bio-medical applications, they have to be highly resistant to fracture. Conventional fracture theory does not account for the resistance to crack growth due to surface tension. We have developed a new theory which shows energy to drive crack growth in soft materials can be significantly reduced by surface tension[8].

4. Ridge-channel, shape-complementary, surface structuring results in strongly enhanced and highly selective adhesion.

We have investigated biomimetic shape-complementary surfaces. We showed that ridge-channel surfaces have highly enhanced adhesion (upto a factor of 40) against shape-complementary surfaces and highly attenuated adhesion against others [9,10]. Interestingly, we found that misorientation is accommodated by interfacial screw dislocations. This finding connects the subject of structured soft materials to the well-developed materials science of defects. We have also investigated the use of shape-complementarity to strengthen the interface between a strongly hydrophilic (a gel) and a strongly hydrophobic (PDMS) material. Figure 3(a) shows an example of the subsequent separation of such an interface. We notice strong crack trapping by the fibrils around which the gel has molded. Figure 3(b) shows that there is very significant enhancement of adhesion.

Future Plans

- *Role of Surface Tension in the Surface Mechanical Behavior of Compliant Solids.*

We will continue our work on understanding the role of surface tension in the surface mechanical properties of compliant materials and structures. We will focus on adhesive contact problems, wetting, and interfacial fracture. We will also work to refine our techniques for measurement of solid surface tension, which has previously been difficult to do.

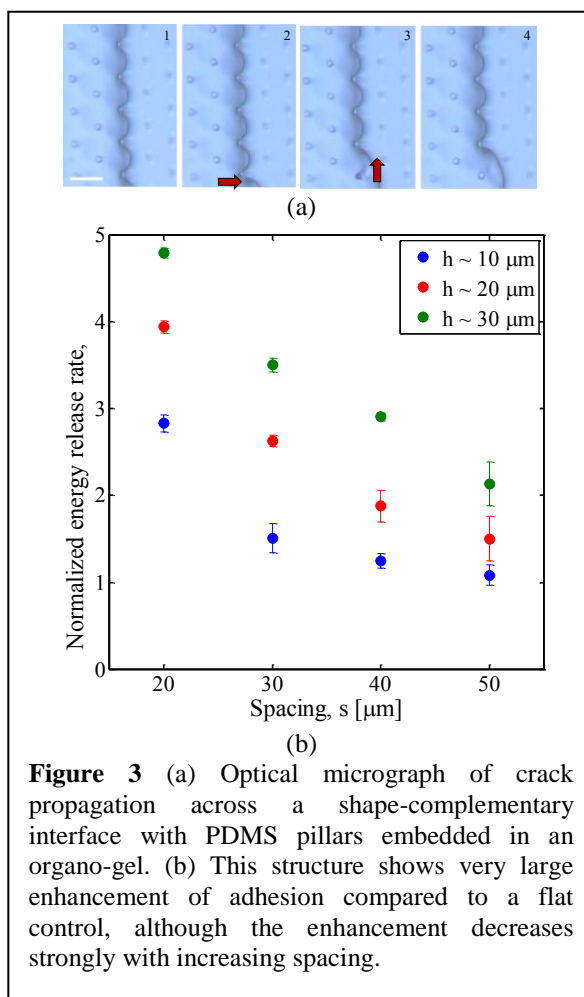


Figure 3 (a) Optical micrograph of crack propagation across a shape-complementary interface with PDMS pillars embedded in an organo-gel. (b) This structure shows very large enhancement of adhesion compared to a flat control, although the enhancement decreases strongly with increasing spacing.

- *Shape Complementary Structures.*

We will continue our study of shape complementary hetero-interfaces between elastomers and gels to include novel self-healing gels, thus to use the shape-complementary mechanism to provide adhesion to otherwise “slippery” interfaces. We will expand our investigation to samples structured with features having different symmetries and with an intentional difference in periodic spacing to establish what types of misfit defects can appear at a structured interface. For example, we hypothesize that a combination of misorientation and lattice mismatch will lead to dislocations with mixed screw and edge character.

- *Continue Work on Techniques.*

As we find important technique-related issues, whether experimental or theoretical, whose solution will aid the entire community, we will pursue them on a selective basis. Specifically, our work on the role of solid surface tension in soft materials is resulting in techniques for the measurement of solid surface tension.

References

1. Paretkar, D., X. Xu, C.-Y. Hui, and A. Jagota, *Flattening of a patterned compliant solid by surface stress*. *Soft Matter*, 2014. **10**(23): p. 4084-4090.
2. Nadermann, N., C.-Y. Hui, and A. Jagota, *Solid surface tension measured by a liquid drop under a solid film*. *Proceedings of the National Academy of Sciences*, 2013. **110**(26): p. 10541-10545.
3. Hui, C.-Y., A. Jagota, N. Nadermann, and X. Xu, *Deformation of a Solid Film with Surface Tension by a Liquid Drop*. *Proceedia IUTAM*, 2015. **12**: p. 116-123.
4. Hui, C.-Y. and A. Jagota, *Deformation Near a Liquid Contact Line on an Elastic Substrate*. *Proceedings of the Royal Society A: Mathematical, Physical and Engineering Science*, 2014. **470**: p. 20140085.
5. Hui, C.-Y., T. Liu, T. Salez, E. Raphael, and A. Jagota, *Indentation of a rigid sphere into an elastic substrate with surface tension and adhesion*. *Proceedings of the Royal Society of London A: Mathematical, Physical and Engineering Sciences*, 2015. **471**: p. 20140727.
6. Xu, X., A. Jagota, and C.-Y. Hui, *Effects of surface tension on the adhesive contact of a rigid sphere to a compliant substrate*. *Soft Matter*, 2014. **10**(26): p. 4625-4632.
7. Liu, T., A. Jagota, and C.-Y. Hui, *Adhesive contact of a rigid circular cylinder to a soft elastic substrate—the role of surface tension*. *Soft Matter*, 2015. **11**(19): p. 3844-3851.
8. Liu, T., R. Long, and C.-Y. Hui, *The energy release rate of a pressurized crack in soft elastic materials: effects of surface tension and large deformation*. *Soft Matter*, 2014. **10**(39): p. 7723-7729.
9. Singh, A.K., Y. Bai, N. Nadermann, A. Jagota, and C.-Y. Hui, *Adhesion of Micro-channel Based Complementary Surfaces*. *Langmuir*, 2012. **28**(9): p. 4313-4222.
10. Jin, Congrui, Anand Jagota, Chung-Yuen Hui, *Structure and Energetics of Dislocations at Micro-Structured Complementary Interfaces Govern Adhesion*, *Advanced Functional Materials* 23 (27) 3453-3462 (2013).

Publications

1. Paretkar, D., X. Xu, C.-Y. Hui, and A. Jagota, *Flattening of a patterned compliant solid by surface stress*. *Soft Matter*, 2014. **10**(23): p. 4084-4090.
2. Nadermann, N., C.-Y. Hui, and A. Jagota, *Solid surface tension measured by a liquid drop under a solid film*. *Proceedings of the National Academy of Sciences*, 2013. **110**(26): p. 10541-10545.
3. Hui, C.-Y., A. Jagota, N. Nadermann, and X. Xu, *Deformation of a Solid Film with Surface Tension by a Liquid Drop*. *Procedia IUTAM*, 2015. **12**: p. 116-123.
4. Hui, C.-Y. and A. Jagota, *Deformation Near a Liquid Contact Line on an Elastic Substrate*. *Proceedings of the Royal Society A: Mathematical, Physical and Engineering Science*, 2014. **470**: p. 20140085.
5. Hui, C.-Y., T. Liu, T. Salez, E. Raphael, and A. Jagota, *Indentation of a rigid sphere into an elastic substrate with surface tension and adhesion*. *Proceedings of the Royal Society of London A: Mathematical, Physical and Engineering Sciences*, 2015. **471**: p. 20140727.
6. Xu, X., A. Jagota, and C.-Y. Hui, *Effects of surface tension on the adhesive contact of a rigid sphere to a compliant substrate*. *Soft Matter*, 2014. **10**(26): p. 4625-4632.
7. Liu, T., A. Jagota, and C.-Y. Hui, *Adhesive contact of a rigid circular cylinder to a soft elastic substrate—the role of surface tension*. *Soft Matter*, 2015. **11**(19): p. 3844-3851.
8. Liu, T., R. Long, and C.-Y. Hui, *The energy release rate of a pressurized crack in soft elastic materials: effects of surface tension and large deformation*. *Soft Matter*, 2014. **10**(39): p. 7723-7729.
9. Jin, Congrui, Anand Jagota, Chung-Yuen Hui, *Structure and Energetics of Dislocations at Micro-Structured Complementary Interfaces Govern Adhesion*, *Advanced Functional Materials* 23 (27) 3453-3462 (2013).
10. Srivastava, A. and C.-Y. Hui, *Nonlinear viscoelastic contact mechanics of long rectangular membranes*. *Proceedings of the Royal Society of London A: Mathematical, Physical and Engineering Sciences*, 2014. **470**: p. 20140528.
11. Long, R., K. Mayumi, C. Creton, T. Narita, and C.-Y. Hui, *Time Dependent Behavior of a Dual Cross-Link Self-Healing Gel: Theory and Experiments*. *Macromolecules*, 2014. **47**(20): p. 7243-7250.

Program Title: Enzyme-Controlled Mineralization in Biomimetic Microenvironments Formed by Aqueous Phase Separation and Lipid Vesicles

Principal Investigator: C. D. Keating

Department of Chemistry, Pennsylvania State University, University Park, PA 16802.

E-mail: keating@chem.psu.edu

Program Scope

The goal of the program is to develop a fundamental understanding of the mechanisms by which biological organisms control the structure and properties of materials during synthesis. Living cells perform mineralization at ambient temperature and pressure, in specially controlled microenvironments often smaller than a single cell. This crucial aspect of how living organisms control the process and outcome of reactions has received little emphasis in the biomimetic mineralization literature, perhaps because experimental systems for generating microcompartments were lacking. The program will perform studies of mineralization in biomimetic microcompartments. Such studies will provide new insight into how organisms control materials growth on the microscale, ultimately leading to nonbiogenic materials synthesis strategies with extraordinary structural and compositional control, for potential applications ranging from low-power electronics to solar cells.

A particular focus of the program is materials synthesis in macromolecularly crowded microcompartments provided by aqueous phase – separated systems and bounded by lipid vesicles. Aqueous two-phase systems (ATPS) form when two or more polymers are present in water at several weight percent [2]. They provide a spatially heterogeneous and biocompatible solvent system that models the macromolecular crowding observed in vivo, in which local concentrations, partitioning, and diffusion-limited reaction fronts can be controlled and symmetry-breaking can be achieved [3]. Molecular partitioning of solutes between the two phases of an ATPS provides a means of control over local concentrations of enzyme catalysts, metal cations, and other molecules that participate in the reactions [4]. By encapsulating aqueous phase systems within semipermeable microscale reaction vessels, artificial mineralizing vesicles will be produced to perform materials synthesis. It is anticipated that the approach should be quite general and will be applicable to many materials systems including but not limited to those traditionally formed by living systems. The program initially focuses on the well-characterized biogenic material CaCO_3 to determine what advantages synthesis in aqueous phase systems and mineralizing vesicles can offer over existing methods. The goal is to both understand and emulate the exquisite control that living systems routinely exert over mineral deposition.

Recent Progress

(1) *Liposome-stabilized, all-aqueous microemulsion droplets as bioreactors.* A key challenge in designing artificial bioreactors is maintaining a favorable internal environment while allowing substrate entry and product departure. We have developed semipermeable, size-controlled bioreactors with macromolecularly crowded interiors by assembling ~130 nm liposomes around all-aqueous emulsion droplets [5]. Dextran-rich aqueous droplets are dispersed in a continuous polyethylene glycol (PEG)-rich aqueous phase, with coalescence inhibited by adsorbed liposomes (Figure 1). Fluorescence recovery after photobleaching and dynamic light scattering data indicate that the liposomes, which are PEGylated and negatively charged, remain intact at

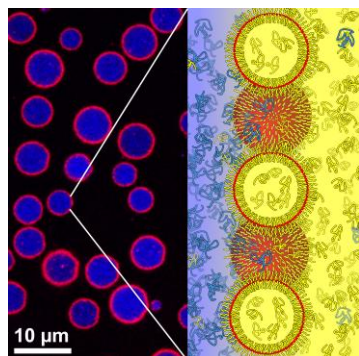


Figure 1. All-aqueous emulsions stabilized by liposomes. (*left*) Fluorescence image showing a population of droplets (blue) stabilized by liposomes (red). (*right*) illustration of interface.

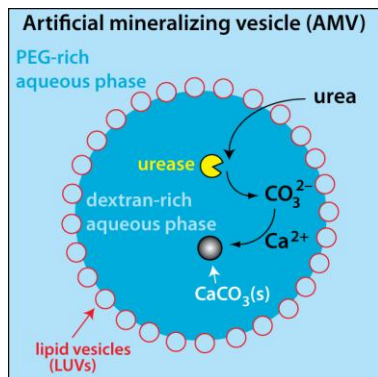


Figure 2. Illustration of AMVs, which are based on the structures in Fig.1, and equipped for mineralization by including urease, Ca^{2+} , and a Ca^{2+} chelator.

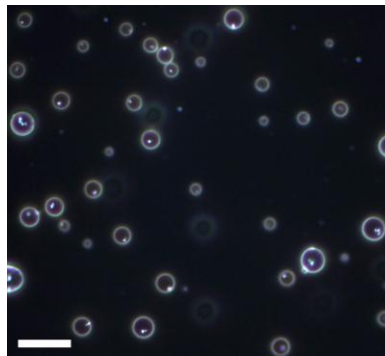


Figure 3. Darkfield optical microscopy image showing CaCO_3 deposition in a population of AMVs. Bright dots inside each structure are $\text{CaCO}_3(\text{s})$. Scale bar = 20 μm .

the interface for extended time. Inter-droplet repulsion provides electrostatic stabilization of the emulsion, with droplet coalescence prevented even for submonolayer interfacial coatings. Molecules such as RNA and DNA oligonucleotides can enter and exit aqueous droplets by diffusion, with final concentrations much higher inside, as dictated by partitioning.

(2) *Enzyme-loaded all-aqueous emulsion droplets as artificial mineralizing vesicles (AMVs).*

Biomimetic mineralization in self-assembled lipid vesicles is an attractive means of studying the mineralization process, but has proven challenging due to vesicle heterogeneity across a population, difficulties encapsulating high and uniform precursor concentrations, and the need to transport reagents across an intact lipid bilayer membrane. We have adapted the liposome-stabilized all-aqueous emulsion droplets described above as simple artificial mineralizing vesicles (AMVs, Figure 2). These biomimetic microreactors allow entry of precursors while retaining a protein catalyst by equilibrium partitioning between internal and external polymer-rich phases. Small molecule chelators with intermediate binding affinity are employed to control Ca^{2+} availability during CaCO_3 mineralization, providing protection against liposome aggregation while allowing CaCO_3 formation. Mineral deposition is limited to the AMV interior, due to localized production of CO_3^{2-} by compartmentalized urease. Particle formation is uniform across the entire population of AMVs, with CaCO_3 particles produced in each one (Figure 3). CaCO_3 products were collected, washed to remove polymers and liposomes, and analyzed by scanning electron microscopy (SEM), powder x-ray diffraction (XRD) and infrared spectroscopy. The mineral formed in AMVs is primarily nanoparticulate amorphous CaCO_3 (ACC). Although it does not appear to be associated with the liposomes in our optical microscopy images, the presence of lipids does lead to formation of a small amount of calcite observable by powder x-ray diffraction. We anticipate that this all-aqueous emulsion-based approach to biomimetic giant mineral deposition vesicles can be used to explore lipid headgroup effects in CaCO_3 deposition and furthermore should be adaptable for enzyme-catalyzed synthesis of other materials, by varying the metal ion, enzyme, and/or chelator.

(3) *Mineralization in multiphase AMVs.* We are incorporating additional phase separation events in our experimental system to exert additional control over the deposition process. This approach is inspired, in part, by computational literature that predicts repeated phase separation events can

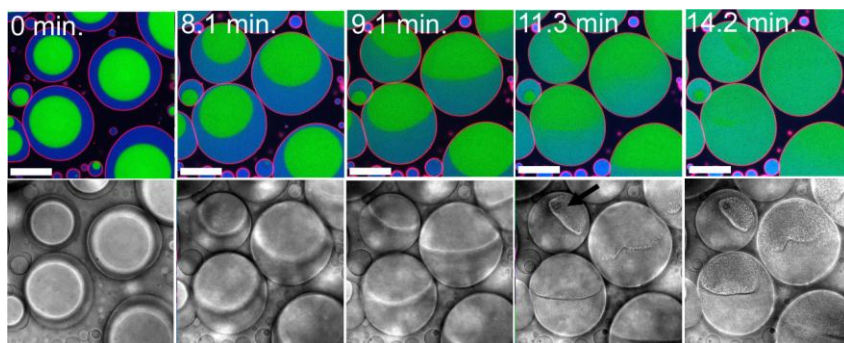


Figure 4. Optical microscopy of PILP-mediated mineralization in AMVs. (*top panels*) Confocal fluorescence images during CaCO_3 deposition. Reaction was initiated by addition of urea at $t = 0$. Red indicates Rhodamine-labeled liposomes that make up the AMV corona; green indicates Alexa 488-labeled PAA; blue indicates Alexa 647-labeled dextran. (*bottom panels*) Transmitted light images show the mineral, appearing around 11 min (see arrow). Scale bars = 20 μm .

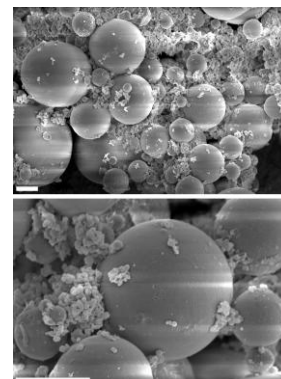


Figure 5. Scanning electron microscopy of CaCO_3 isolated from PILP-containing AMVs. Scale bars = 5 μm .

give rise to a reaction-diffusion system that generates hierarchical morphologies reminiscent of biogenic minerals [6]. When polycarboxylates are present, polymer-induced liquid precursors (PILPs)[7] can be observed inside AMVs. These structures are enriched in polycarboxylate and Ca^{2+} , and are the site of CaCO_3 formation. We first employed poly(aspartic acid), PAA as our PILP-forming additive. Images collected during mineral formation in PAA-containing AMVs are shown in Figure 4. The Ca^{2+} and PAA-rich PILP phase (green) is initially centered in the AMVs, surrounded by the dextran-rich phase. After addition of urea, the PILP phase is in contact with the liposome corona of the AMV, and fluorescence images show a decrease in PAA partitioning. This is consistent with release of some Ca^{2+} from coordination with the PAA: only Ca^{2+} -coordinated PAA is capable of forming a PILP. The Ca^{2+} may be freed due simply to the increase in pH as NH_3 and CO_3^{2-} are produced, or it may be forming soluble CaCO_3 precursors not yet visible by optical microscopy. By 11 min., it is clear that insoluble CaCO_3 is present, which nearly coincides with the complete loss of the phase boundary between the dextran-rich phase and the (formerly) PAA-rich phase. This material appears to be entirely ACC, consisting of submicrometer particles similar to those produced without PAA mixed with microspheres of ACC varying in size from a few microns to several tens of microns (Figure 5).

We have also formed PILPs and subsequently CaCO_3 in poly(glutamic acid) [PGA]-containing AMVs and in AMVs that contained mixtures of both polycarboxylates. PILPs formed with PAA and PGA have different wetting properties with the dextran-rich phase and the liposomes that make up the AMV corona, enabling some degree of control over their shape and location. Additionally, CaCO_3 formation occurs more readily from PGA than PAA systems, and the material produced in PGA-rich phases converts more readily to calcite. These differences presumably arise due to differences in Ca^{2+} binding affinity and PILP phase behavior between the polycarboxylates. We have observed separate mineralization processes occur in different locations within individual AMVs (Figure 7); it is anticipated that the organic content and polymorph of these materials may differ in accordance with their microenvironment.

Future Plans

We are particularly interested in the multi-polycarboxylate AMV systems that allow for sequential mineralization events in distinct microenvironments. We hypothesize that different

amounts and identities of organics or other additives (e.g., Mg^{2+}) can be incorporated within the mineral as a function of the local environment during deposition. These types of additives are known to impact the properties of biogenic $CaCO_3$, for example leading to greatly enhanced mechanical properties. The AMV mineralization platform offers control over local conditions during mineral formation reminiscent of the control exerted by organisms. We are also interested in controlling the morphology of ACC by changing contact angles/wetting between adjacent liquid phases. An exciting aspect of this mineralization system is that, as in vivo, the properties of the mineralizing microcompartments are changing during the course of the mineralization reactions.

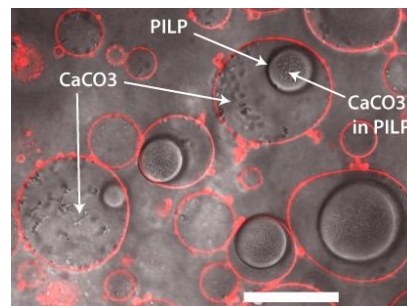


Figure 6. Mineralization in AMVs that contain both PAA and PGA occurs both inside PILPs and free in the AMV interior. Red (lipid fluorescence) indicates AMV corona; this has been overlaid on transmitted light image. Scale bar = 25 microns.

References

1. Biocatalyzed mineralization in an aqueous two-phase system: Effect of background polymers and enzyme partitioning. Cacace, D. N.; Keating, C. D. *J. Mater. Chem. B* **2013**, *1*, 1794-1803.
2. Albertsson, P. *Partition of Cell Particles and Macromolecules* John Wiley & Sons, New York, 2nd ed, 1960.
3. Aqueous phase separation as a possible route to compartmentalization of biological molecules. Keating, C. D. *Accounts of Chemical Research* **2012**, *45*, 2114-2124.
4. RNA catalysis through compartmentalization. Strulson, C. A.; Molden, R. C.; Keating, C. D.; Bevilacqua, P. C. *Nature Chem.* **2012**, *4*, 941-946.
5. Bioreactor droplets from liposome-stabilized all-aqueous emulsions. Dewey, D. C.; Strulson, C. A.; Cacace, D. N.; Bevilacqua, P. C.; Keating, C. D. *Nature Commun.* **2014**, *5*, 4670 (doi: 10.1038/ncomms5670).
6. Lenoci, L.; Camp, P. J. Diatom Structures Templated by Phase-Separated Fluids. *Langmuir* **2008**, *24*, 217-223.
7. Gower, L. B. Biomimetic model systems for investigating the amorphous precursor pathway and its role in biomineralization. *Chem. Rev.* **2008**, *108*, 4551-4627.

Publications

1. Bioreactor droplets from liposome-stabilized all-aqueous emulsions. Dewey, D. C.; Strulson, C. A.; Cacace, D. N.; Bevilacqua, P. C.; Keating, C. D. *Nature Commun.* **2014**, *5*, 4670 (doi: 10.1038/ncomms5670).
2. Aqueous emulsion droplets stabilized by lipid vesicles as microcompartments for biomimetic mineralization. Cacace, D. N.; Rowland, A. T.; Stapleton, J. J.; Dewey, D. C. and Keating, C. D. **2015** (*submitted*).

Program Title: DNA-Grafted Building Blocks Designed to Self-Assemble into Desired Nanostructures

Principle Investigator: S. Kumar; Co-PIs: V. Venkatasubramanian and O. Gang

Department of Chemical Engineering, Columbia University

Mailing Address: 500 W. 120th St. Mudd 510, New York, NY 10027

E-mail: sk2794@columbia.edu

Program Scope

Over the past several decades, there has been increasing interest in programmable self-assemblies for materials fabrication^[1-3]. While the traditional Edisonian approach have led to the development of several new theories and interesting simulation results^[4-8], it is limited in that it does not allow for design of the building blocks to form desirable structures. Such an *a priori* approach involves determining the correct set of parameters with which to construct the initial building block so that they will preferentially self-assemble into any pre-defined target architecture. In order to address this issue, we propose a novel design framework that couples an inverse genetic algorithm (GA) optimization protocol to the pre-existing forward model (Fig. 1). Previous studies performed by Venkatasubramanian^[9-10] et al. indicate that the GA is particularly suited for our unique optimization requirements as it can quickly converge to a solution despite the presence of non-linear relationships of self-assembly modeling and the large space of possible crystal structures. As a result, our goal will be to develop an effective lattice prediction model while also adapting the genetic algorithm into an overall design framework for bottom-up self-assembly for materials fabrication.

Recent Progress

Theory and Experiments:

Repulsion and Effective Interactions: The current contact model (CCM) for lattice prediction assumes DNA-mediated self-assembly is enthalpically driven and ignores all repulsion. Thus, the CCM defines the interaction layer as the one closest to the reference particle that contains colloids with complementary DNA strands. This ignores any potential shorter distance non-complimentary colloids that that could provide enough repulsion to destabilize the predicted lattice. To correct for this, we perform a scaling of all possible interacting particles to the central reference particle into a single interaction shell. This is performed consistently. That is, the number of interacting particles is reduced such that they retain the same solid angle to the central particle as in the unscaled analog. This allows us to redefine an effective interaction layer of the form: $NN_{ij,eff} = \alpha_j^2 NN_{ij}$ where NN_{ij} indicates the number of nearest neighbor ij pairs in the unshifted case. α_j is a scaling factor that is purely defined by the ratio of the ij crystallographic distance from its original to its rescaled value.

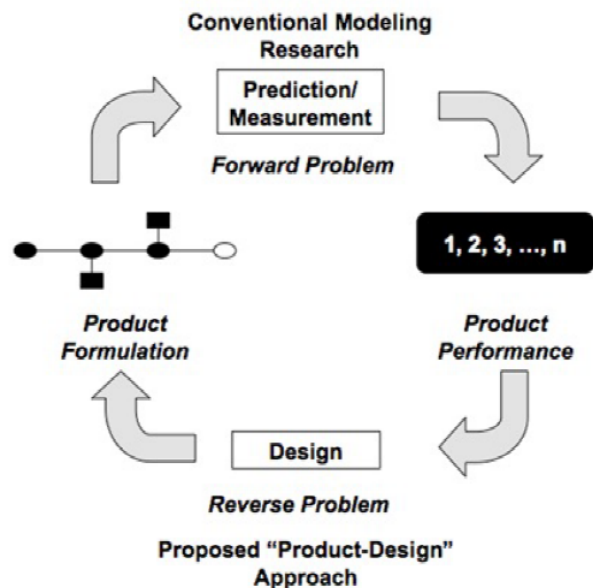


Figure 1. Design framework coupling the forward predictive and inverse optimization protocol

Stoichiometric Control of Self-Assembly:

Previous experimental and simulation results seem to suggest the initial stoichiometric mix of the particles can also be used to directly control the equilibrium lattice structure. However, its exact role on self-assembly remains an open question. Through an equilibrium kinetics analysis, we show that the effect of stoichiometry comes in as a multiplicative correction to the standard state free energy of lattice formation. A scaling analysis also reveals direct relations between the free energy of lattice formation and the relevant size, linker, and stoichiometric ratios of the form: $\mu_{i,eff} \sim \frac{R_L R_N}{R_S^2 a_i}$ where R_L , R_N , and R_S are the linker, stoichiometric, and size ratio, respectively and a_i is the crystal lattice stoichiometric ratio. Furthermore, an excess free energy analysis indicates that stoichiometry serves as an entropic driving force for phase transition between different lattices. These results provide better agreements with experimental observations while also relaxing the need for precise control of the size of the particles as variations in sizes can be corrected for by mixing different ratios of the molecular building blocks (Fig. 2).

Extension to Anisotropic Particles: DNA-grafting on spherical particles seems to be limited to the formation of CsCl, AlB₂, Cr₃Si, and Cs₆C₆₀. Our recent sets of experiments have shown that by grafting DNA to non-spherical particles, several interesting new structures were observed (Fig. 3). These experiments motivated us to build a theoretical model for shape dependent interactions, we utilize the equation for a superellipsoid within the framework of the contact model. The superellipsoid is of particular interest because it can morph between different types of shapes simply by changing control parameters embedded within its governing equation. Through a combination of various machine learning algorithms, we have developed a method to calculate the interaction area between superellipsoids given any arbitrary orientation that provide the same predictions as the original CCM when parameters defining spheres were used for

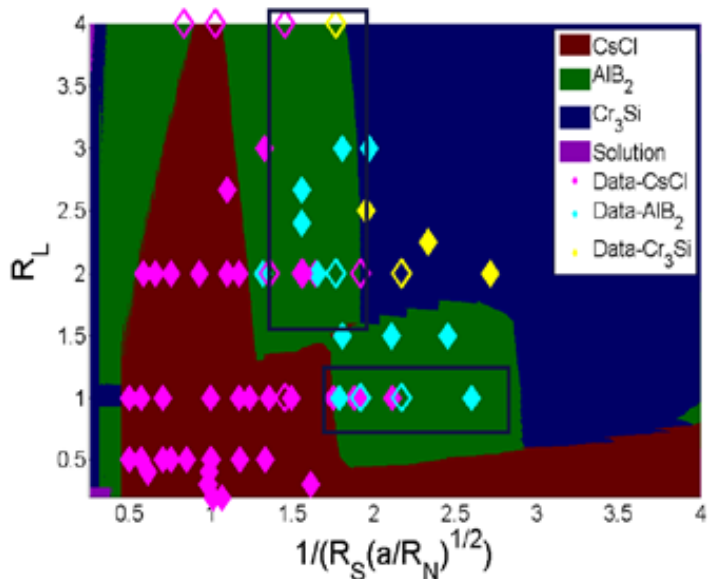


Figure 2. Generalized Phase Diagram. Scatter point represents experimental data – filled: pure, open: disordered. Region within blue boxes show experimental confusion between CsCl and AlB₂, possibly suggestion phase coexistence. General agreement with experimental data observed across various stoichiometric, size and linker ratios.

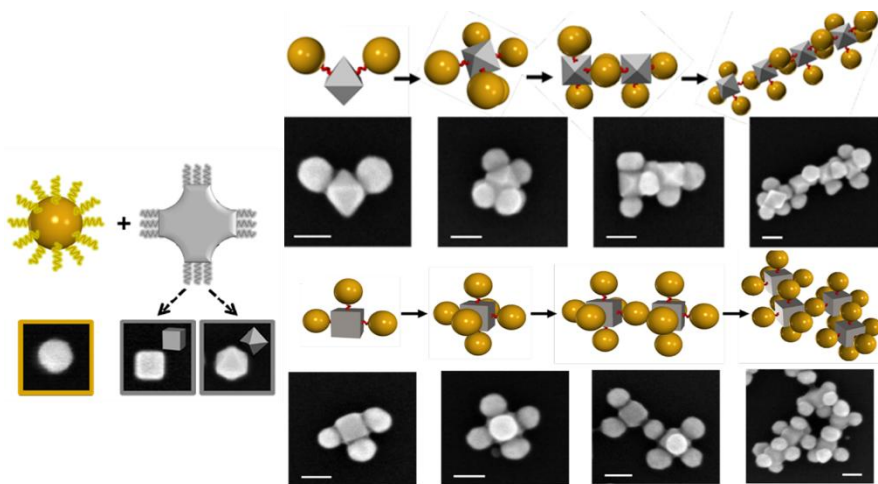


Figure 3. Shape-induced directional bonding. Schematic (left). SEM of tetrahedron-sphere packing (top right). SEM of cube-sphere packing (bottom right). Different architecture observed from sphere-sphere packing.

calculations.

Selective Transformation via Reprogramming of DNA-mediated interactions: The structure of a three-dimensional lattice of DNA-grafted colloid can also be switched from an initial phase into one of multiple mutated phases by introducing different types of interactions, namely blending, stapling, and repelling (Fig. 4). The introduction of different types of reprogramming DNA strands modifies the DNA shells of the nanoparticles within the superlattice, thus shifting interparticle interactions to drive the transformation into a new lattice. These transformation have enabled us to direct the transition of a CsCl lattice to CuAu (blending), face-centered cubic (stapling), and cluster formation (repelling).

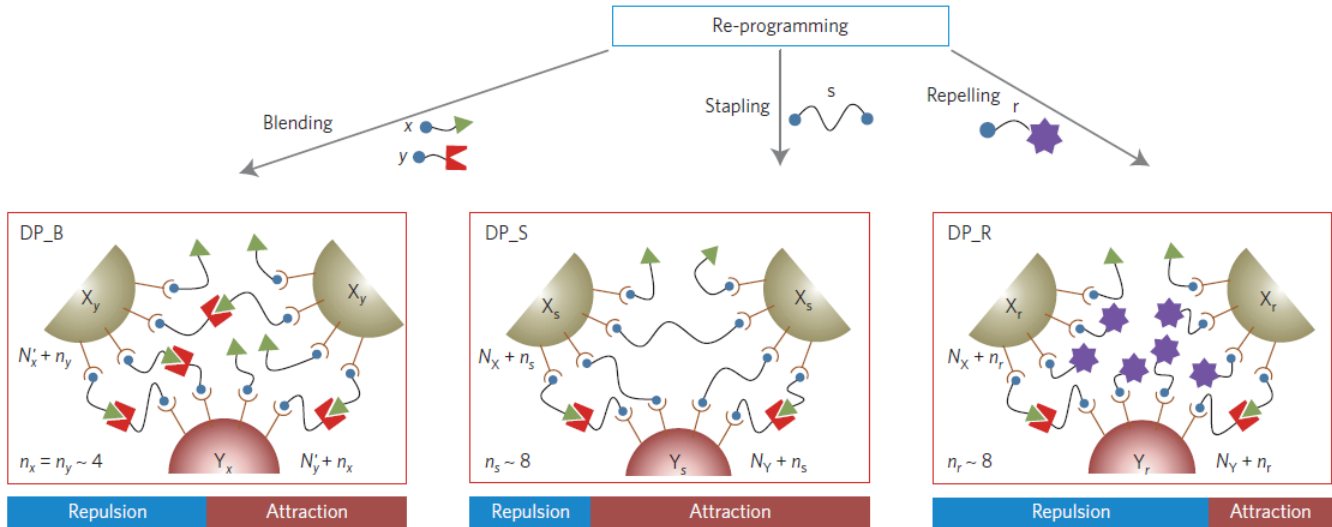


Figure 4. Illustration of experimental design for inducing phase transformations in DNA–NP superlattices via selective reprogramming of interparticle interactions, achieved by inputting different types of strand that modify the DNA shells of NPs in a lattice, causing a shift in the relative attraction and repulsion between complementary particles.

Machine Learning:

Genetic Algorithm: As a consistency check, a revised objective function was defined for the GA inverse optimization of the form

$$f_i = (E_i - E_t)^2 + \sum_j (NP_{i,j} - NP_t)^2 + \sum_{n,m} (NN_{i,nm} - NN_{t,nm})^2$$

where f is the fitness value, NP is the number of particles of each type in the lattice, and NN is the effective number of nearest neighbors for the lattice. Subscripts i and t indicate the test lattice and target lattice, respectively. Subscript j indicates the type of particle in the lattice. Subscripts n and m represent the number of nearest neighbor of type m to particle n . The revised framework is able to predict a phase space density of states distribution for the regimes of feasible lattice formation that matches locations where the lattices have been observed experimentally. Of particular interest is the selection of a new structure called Bi_2O_3 that occurs in the region of experimental confusion between CsCl and AlB_2 as highlighted

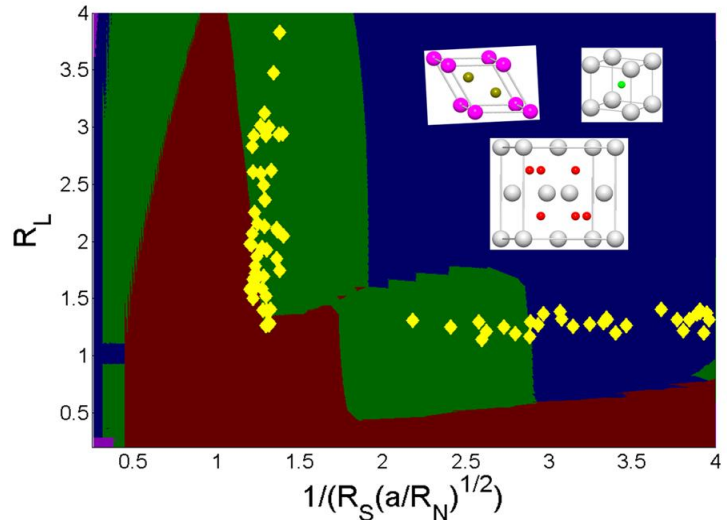


Figure 5. Inverse Design Framework Bi_2O_3 Prediction. Density of states distribution for Bi_2O_3 falls within the same bands of lattice confusion observed in Fig. 3. Inset: AlB_2 (top left), CsCl (top right), Bi_2O_3 (bottom) unit cell structures

in Fig. 2. Closer inspection of the Bi_2O_3 structure reveals that it is a superlattice consisting of an alternating packing of entities that closely resemble CsCl and AlB_2 (Fig. 5). This could suggest that, in addition to phase coexistence, the system seeks to form Bi_2O_3 but lacks precise control over the alternating packing of the sub-lattices making up the structure, thus resulting a lattice of mixed entities observed experimentally. This raises the issue of kinetic traps on lattice formation and should be further explored.

Semi-Supervised Learning: In addition to theory driven lattice prediction, we also seek to develop a data driven model that utilizes existing experimental data as a way to predict the equilibrium lattice structure. The new approach utilizes a dynamic label propagation (DLP) technique. The advantage here comes from bypassing the need to model the underlying physics of self-assembly. Here, we classify unknown points within the phase space purely based on known experimental data. DLP determines a labelling probability matrix P for points distributed within the parameters phase space. The P matrix is then used to label previously uncategorized points generated within the phase space – not all unlabeled points will get labeled. The new set of labeled points will be used to generate a new P matrix and the process is repeated until the change in the labelling matrix drops below a cutoff tolerance value. This dynamic labeling approach allows for classification of parameters within the phase space based purely on their relative distances away from previously known/classified locations.

Future Plans

Grafting to Anisotropic Particles: Recent experimental results seem to indicate that there exists some preferential attachment of DNA with the usage of anisotropic particles that was not observed with spherical nanoparticle cores. This can result in local regions of overlap between particles with higher concentration of interacting linkers and will affect free energy calculations. Molecular dynamics simulations will be performed to constraint the motions of the grafting points to the surface of the core particles. This will allow the DNA-grafts to move along the surface and equilibrate to their final positions. Simulation results will give us a molecular understanding of this preferential attachment process, which we will map into a functional form that can be readily applied to the contact model for lattice predictions.

Genetic Algorithm: The addition of the superellipsoid to the contact model adds an additional set of 8 parameters that must be incorporated into the inverse GA framework – 2 for shape, 3 for stretching in each of the X, Y, and Z directions, and 3 for rotation in each of the θ , ψ , and φ Euler angles. Thus, the GA must be modified such that it can efficiently search through this multidimensional phase space and make the framework computationally feasible.

Semi-Supervised Machine Learning Modeling: The dynamic label propagation approach to building a data-driven database relies on the abundance of a large repository of categorized data. One current limitation of such an approach is that current data for DNA-mediated self-assembly tend to be noisy and limited. Thus, our future works will also focus on adapting the DLP to account for noisy and smaller sets of experimental data.

References

- [1] Mirkin, C. A.; Letsinger, R. L.; Mucic, R. C.; Storhoff, J. J. *Nature* 1996, 382, 607-609.
- [2] Rogers, W. B.; Crocker, J. C. *P. Natl. Acad. Sci. USA* 2011, 108, 15687-15692.
- [3] Macfarlane, R. J.; Lee, B.; Jones, M. R.; Harris, N.; Schatz, G. C.; Mirkin, C. A. *Science* 2011, 334, 204-208.
- [4] Varilly, P.; Angioletti-Uberti, S.; Mognetti, B. M.; Frenkel, D. *J. Chem. Phys* 2012, 137, 094108.
- [5] Leunissen, M. E.; Frenkel, D. *J. Chem. Phys* 2011, 134, 084702.
- [6] Knorowski, C.; Burleigh, S.; Travesset, A. *Phys. Rev. Lett* 2011, 106, 215501.
- [7] Li, T.; Sknepnek, R.; Macfarlane, R. J.; Mirkin, C. A.; Olvera de la Cruz, M. *Nano Lett* 2012, 12, 2509-2514.
- [8] Li, T. I. N. G.; Sknepnek, R.; Olvera de la Cruz, O. *J. Am. Chem. Soc* 2013, 135, 8535-8541.
- [9] Venkatasubramanian, V.; Chan, V.; Caruthers, J. *Comput. Chem. Eng* 1994, 18.

[10] Venkatasubramanian, V.; Chan, V.; Caruthers, J. J. *Chem. Inf. Comp. Sci* 1995, 35.

Publications

[1]. B. Srinivasan, T. Vo, Y. Zhang, O. Gang, S. K. Kumar, and V. Venkatasubramanian. “Designing DNA-grafted particles that self-assemble into desired crystalline structures using the genetic algorithm.” *P. Natl. Acad. Sci. USA* **2013**, 110: 46, 18431-18435.

[2]. T. Vo, V. Venkatasubramanian, S. K. Kumar, B. Srinivasan, S. Pal, Y. Zhang, and O. Gang. “Stoichiometric Control of DNA-grafted Colloid Self-Assembly.” *P. Natl. Acad. Sci. USA* **2015**, 112:16, 4982-4987.

[3]. F. Lu, K. G. Yager, Y. Zhang, H. Xin, and O. Gang. “Superlattices assembled through shape induced directional binding.” *Nature Communications* **2015**, 6, 6912.

[4]. Y. Zhang, S. Pal, B. Srinivasan, T. Vo, S. K. Kumar, and O. Gang. “Selective transformations between nanoparticle superlattices via the reprogramming of DNA-mediated interactions.” *Nature Materials* (accepted) **2015**.

Biomolecular assembly processes in the design of novel functional materials

Jeetain Mittal, Department of Chemical and Biomolecular Engineering, Lehigh University, Bethlehem, PA 18015, jeetain@lehigh.edu

Program Scope. Nature admits innumerable examples where efficient, remarkably parallelized, and precise organization of modular building blocks (e.g., molecules, particles) leads to diverse, complex, and functional structures. Unraveling such processes in order to mimic Nature's design strategies remains the Holy Grail in establishing a multiscale paradigm for programmable materials production. Success in this endeavor would revolutionize the efficiency and precision with which complex materials are designed and synthesized, and would spawn novel, functional structures tailored precisely for applications. Among promising approaches to this bottom-up strategy is the use of particle-tethered, complementary single-stranded DNA (ssDNA) for programming particle assembly mediated by DNA hybridization into complex structures. This program will use a comprehensive computational and theoretical strategy aimed at overcoming current barriers in self-assembly of DNA-functionalized particles (DFPs).

Recent Progress. We have used a binary mixture of multiflavored DFPs (A and B) that can bind complementary unlike as well as like particles with varying attraction strength (E_{AA} , E_{BB} , E_{AB}) to tune interparticle interactions in a simple manner. The precise control over relative attraction strengths (E_{AA}/E_{AB} , E_{BB}/E_{AB}) allows us to create diverse two-dimensional crystalline structures by self-assembly. We are able to program the particle assembly in square, pentagonal, and hexagonal lattices. In addition, the different particle types can be compositionally ordered in checkerboard (square), alternating stripe (hexagonal), honeycomb (hexagonal), and Kagome (hexagonal) arrangements in simulation and experiment. Our approach is flexible that can be further extended to program more exotic two-dimensional as well as three-dimensional crystalline lattices and compositional order.

Future Plans. Our goals are: (i) to bridge various scales involved in the assembly process starting from the standard and non-standard base pairing interactions to interactions between two complementary DFPs to multi-particle assembly (Fig. 1), (ii) to calculate thermodynamic phase diagrams to assess relative stability of various crystal structures as a function of important thermodynamic parameters such as packing density, temperature and system parameters such as DNA grafting density, length and strength of the DNA sticky end, spacer flexibility, etc. (iii) to measure the particle binding dynamics and kinetic rate parameters and elucidate the assembly mechanism, and (iv) to assess the utility of applied external shear in addition to temperature annealing. The proposed work will be done in conjunction with experiment to test and validate our approach as well as to tune the parameters of our model. This will also allow us to focus on issues most relevant for experimental conditions and variables.

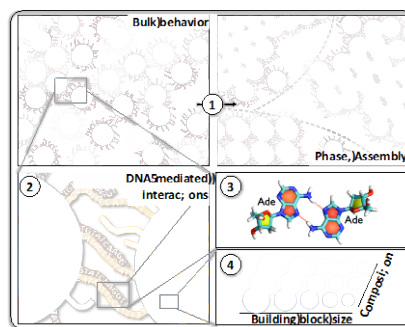


Figure 1. Multiple scales involved in the assembly of DCPs.

Biological and Biomimetic Low-Temperature Routes to Materials for Energy Applications

Daniel E. Morse

California NanoSystems Institute, University of California, Santa Barbara, CA 93106-5100

I. Program Scope:

The overall objectives of our research have been: (1) to attain a deep mechanistic understanding of the kinetically controlled, low-temperature, catalytic synthesis and structural control of silica that we originally discovered in sponges, and (2) from that understanding, develop a rational, biologically inspired methodology for the low-temperature, kinetically controlled catalytic synthesis and nanostructural control of high-performance materials for energy applications.

II. Recent Progress:

Using Biologically Inspired, Kinetically Controlled Catalytic Synthesis to Synthesize More Efficient, High Power Nanocomposite Electrodes for Fuel Cells:

We previously reported our use of the biologically inspired, kinetically controlled catalytic synthesis method that we developed to inexpensively grow nanocomposite anodes and cathodes for high-power lithium ion batteries (Zhang and Morse, 2009, 2012; Zhang et al., 2010; von Bulow et al., 2012; Somodi et al; 2015). We also developed the first high-throughput scale-up and continuous synthesis of high quality nanocrystals using this method (Ould-Ely et al., 2013).

We now demonstrate that this bio-inspired, low-temperature catalytic synthesis process can be extended to catalysis chemistries *beyond hydrolysis*, and that using this approach to kinetically control catalytic metathesis, we can grow very small platinum nanocrystals (Pt, ≤ 3 nm diam.) *in situ* in the interstices of very high surface area, microwave-expanded graphene oxide (MEGO), carbon nanotubes (CNTs), carbon black, graphite, and controlled mixtures of these conductors to obtain high performance fuel cell electrodes (**Figure 1**). The resulting nanocomposites yield hydrogen fuel cells with power and energy identical to those of commercial cells, *but require 70% less Pt than present commercial cells* (Kong et al., 2013, 2015).

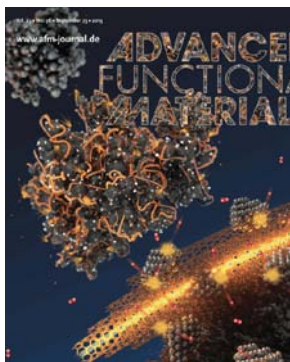


Figure 1. Cover figure from Kong et al., 2013, for the issue of this journal focused on “New Materials through Bioinspiration and Nanoscience.” Artist’s depiction of the catalytically grown nanocrystals of Pt in matrices of carbon nanotubes (CNTs) and carbon nanoparticles. The Pt nanocrystals are shown catalyzing the production of electrons and transfer of the electrons to a CNT conductor in a hydrogen fuel cell electrode.

When transferred by the decal method to a Nafion[®] membrane and assembled into a standard hydrogen-PEM (proton exchange membrane) fuel cell, the Pt-carbon black nanocomposite made by this method gave electrochemical performance (as anode) illustrated in **Figure 2**.

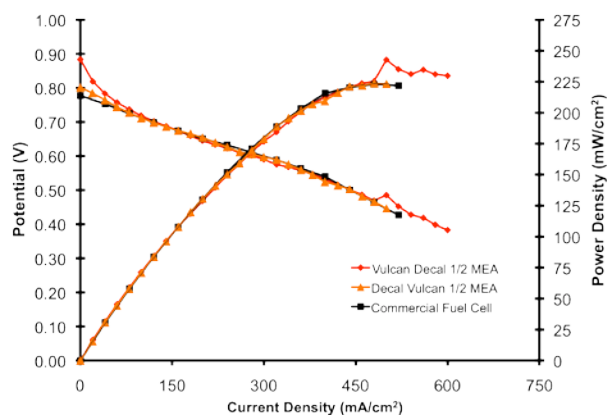


Figure 2. Comparison of electrochemical performance of two fuel cells with nano-Pt@Vulcan[®] carbon black anodes made by our biologically inspired, kinetically controlled, low-temperature catalytic synthesis of nanocrystalline Pt *in situ* in Vulcan[®] carbon black (red and orange symbols) with a standard commercial cell of comparable dimensions (black). Hydrogen-oxygen fuel cells employ Nafion[®] proton exchange membranes; the commercial cell was an ETEK ELAT A-6 cell with 20 wt% Pt on Vulcan XC-72; our anode was paired with an identical ETEK A-6 cathode.

Extending these results to the high surface area conductive matrix afforded by microwave-expanded graphene oxide (“MEGO”) developed by our collaborator Rod Ruoff and his students (Zhu et al., 2011), we found that the greater surface area and open nanoporosity of this material allow us to grow a more uniform distribution of Pt nanocrystals *in situ* within the MEGO matrix than in the carbon black or CNT conductive matrices (Kong et al., 2015; **Figure 3**).

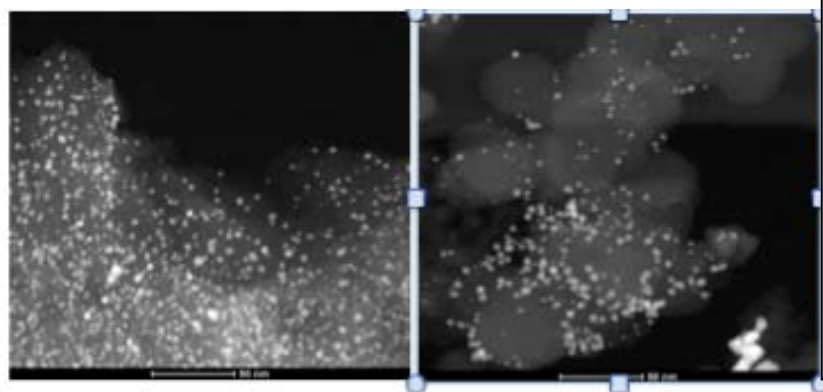


Figure 3. More uniform distribution of Pt nanocrystals grown in MEGO (left) than in Vulcan[®] carbon black (right). The Pt nanocrystals average 3-4 nm diameter. MEGO has BET surface area of 1,623 m²/g and mesopores 2-8 nm diam. vs. 243 m²/g area and macropores 50-300 nm diam. of Vulcan[®]. (From Kong et al., 2015).

Analyses by X-ray diffraction, electron diffraction and high-resolution transmission electron microscopy show that the Pt nanocrystals synthesized in the MEGO matrix by our bio-inspired, kinetically controlled catalytic method are highly faceted, face-centered cubic (fcc) nanocrystals optimal for catalytic activity as fuel-cell cathodes (Kong et al., 2015; **Figure 4**).

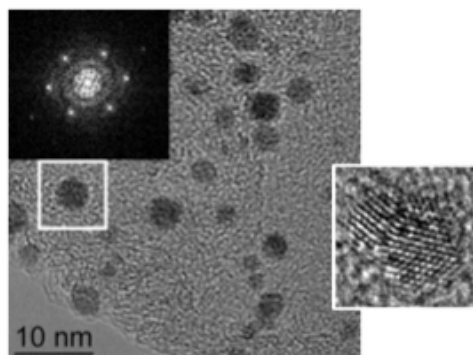


Figure 4. High-resolution TEM and electron-diffraction analyses of the nanocrystals of Pt catalytically grown in the MEGO matrix. (From Kong et al., 2015).

Superior fuel cell performance of the Pt@MEGO nanocomposite relative to that of the Pt@Vulcan[®] carbon black nanocomposite is seen in **Figure 5**, comparing the activities of the two nanocomposites as cathodes in standard hydrogen-oxygen fuel cells at equal loadings of Pt (0.2 mg/cm²) in the two PEM assemblies.

Results show a higher catalytic performance of the Pt@aMEGO cathode, with a current density of 1,020 mA/cm² at 0.6 V compared to 890 mA/cm² of Pt@Vulcan. The better performance over the large voltage range from 0.2 to 0.7 V indicates a **15 % higher power density**, likely attributable to both the faster cathode reaction kinetics and the enhanced mass transport through the expanded graphene conductive matrix.

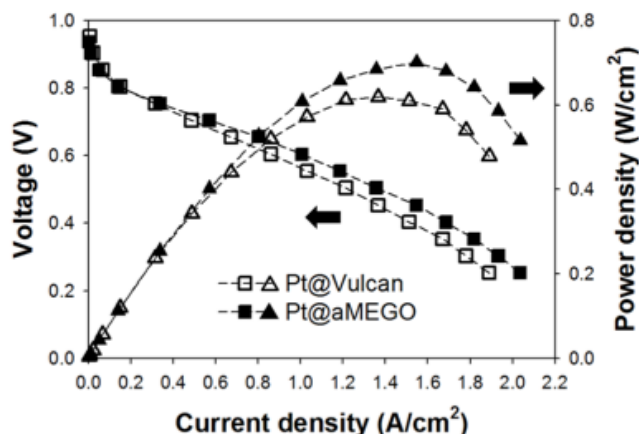


Figure 5. Superior performance of the Pt@aMEGO nanocomposite relative to that of Pt@Vulcan[®] carbon black, when both are evaluated as cathodes in hydrogen-oxygen fuel cells at equal loadings of Pt in the PEM assemblies.

Cells included commercial fuel cell anodes (0.2 mg/cm² Pt@20 wt.% Vulcan[®] carbon black; operation was at 75 °C at flow rates of H₂/O₂ = 150/250 sccm with no back pressure.

(From Kong et al., 2015).

In summary, we have demonstrated that:

(1) The biologically inspired, kinetically controlled catalytic synthesis method (that we developed from our discovery of the mechanism of silica biosynthesis in sponges) can be extended to *non-hydrolytic chemistries*, such as the kinetically controlled catalytic metathesis that we have used for the synthesis of small Pt nanocrystals grown *in situ* in various carbon matrices, with unique advantages for fuel cell applications (Kong et al., 2013, 2015).

(2) Combining the advantage of that bio-inspired, kinetically controlled catalytic synthesis with the exceptionally high surface area of microwave-expanded graphene oxide (MEGO), we can produce uniform nanocomposites of small fcc-Pt grown *in situ* in MEGO with superior performance as fuel cell electrodes.

(3) Further extensions of this research (not described above) demonstrate that functionalization of the carbon matrix with 4-aminomethylpyridine leads to further reduction in the size of the nanocrystalline Pt grown catalytically on the functionalized matrix, with even higher activities of the resulting nanocomposite as fuel cell electrode (Rich et al, 2014).

III. Future Plans:

We plan to extend our investigation of bio-inspired, kinetically controlled catalytic nanofabrication to explore the complete replacement of platinum with cheaper non-noble metals.

IV. References cited:

- Kong, C.S., H.-L. Zhang, F. Somodi and D. E. Morse, 2014. Bio-inspired synthesis of high-performance nanocomposite catalysts for hydrogen oxidation. *Adv. Func. Matr.* 23: 4389- plus cover; DOI: 10.1002/adfm.201370180
- Kong, C.S., T.Y. Kim and D.E. Morse. 2015. Low-temperature catalytic synthesis of high-efficiency fuel cell cathode of nanocrystalline Pt uniformly dispersed in high surface area, microwave-expanded graphene. (In preparation for *Advanced Energy Materials*).
- Ould-Ely, T., L. Kaplan Reinig and D.E. Morse. 2014. High rate continuous synthesis of

- nanocrystalline perovskites and metal oxides in a colliding vapor stream of microdroplets. Adv. Func. Matrils. 2014, DOI: 10.1002/adfm.201301916
- Rich, S. J. J. Burk,[†] C.S. Kong, C. D. Cooper, D.E. Morse, and S.K. Buratto. 2014. Nitrogen functionalized carbon black: A support for Pt nanoparticle catalysts with narrow size dispersion and high surface area. Carbon 81: 115-123.
- Somodi, F., C.S. Kong, J.C. Santos and D.E. Morse 2015. Vesicular hydrogen silsesquioxane-mediated synthesis of nanocrystalline silicon dispersed in a mesoporous silica/suboxide matrix, with potential for electrochemical applications. New J. Chem. 39: 621-630. DOI: 10.1039/C4NJ01762E.
- von Bulow, J.F., H.-L. Zhang and D.E. Morse. 2012. Hydrothermal realization of high-power nanocomposite cathodes for lithium ion batteries. Adv. Energy. Mater. 2: 277-389.
- Zhang, H.-L. and D.E. Morse. 2009. Vapor-diffusion catalysis and *in situ* carbothermal reduction yields high performance Sn@C anode materials for lithium ion batteries. J. Mater. Chem. 19: 9006 – 9011. (DOI: 10.1039/b914554k)
- Zhang H.L., J. R. Neilson and D. E. Morse. 2010. Kinetically controlled sol-gel synthesis of flaky lithium vanadium oxide and its electrochemical behavior. J. Phys. Chem. C 114 (45), 19550–19555,
- Zhang, H.-L. and D.E. Morse. 2012. Transforming large-scale industrially produced carbon nanotubes to high-performance electrode materials for lithium ion batteries. J. Mater. Res. 27: 410-416.
- Zhu, Y., S. Murali, M.D. Stoller, K.J. Ganesh, W. Cai, P.J. Ferreira, A. Pirle, R.M. Wallace, K.A. Cychosz, M. Thommes, D. Su, E.A. Stach and R.S. Ruoff. 2011. Carbon-based supercapacitors produced by activation of graphene. Science, 332: 1537-1541.

V. Publications from work supported by the DOE project over the last two years:

- Kong, C.S., H.-L. Zhang, F. Somodi and D. E. Morse, 2014. Bio-inspired synthesis of high-performance nanocomposite catalysts for hydrogen oxidation. Adv. Func. Matrils. 23: 4389- plus cover; DOI: 10.1002/adfm.201370180
- Ould-Ely, T., L. Kaplan Reinig and D.E. Morse. 2014. High rate continuous synthesis of nanocrystalline perovskites and metal oxides in a colliding vapor stream of microdroplets. Adv. Func. Matrils. 2014, DOI: 10.1002/adfm.201301916
- Bawazer, L. A.M. Newman, Q. Gu, A. Ibish, M. Arcila, J.B. Cooper, F.C. Meldrum and D.E. Morse, 2014. Efficient selection of biomineralizing DNA aptamers using next-generation sequencing and population clustering. ACS Nano <http://dx.doi.org/10.1021/nn404448s>
- Neilson, J.R., N. C. George, M. M. Murr, R. Seshadri and D. E. Morse, 2014. Mesostructure from hydration gradients in demosponge biosilica. Chemistry - A European Journal [doi.org/10.1002/chem.201304704](http://dx.doi.org/10.1002/chem.201304704)><http://dx.doi.org/10.1002/chem.201304704>
- Rich, S. J. J. Burk,[†] C.S. Kong, C. D. Cooper, D.E. Morse, and S.K. Buratto. 2014. Nitrogen functionalized carbon black: A support for Pt nanoparticle catalysts with narrow size dispersion and high surface area. Carbon 81: 115-123.
- Somodi, F., C.S. Kong, J.C. Santos and D.E. Morse 2015. Vesicular hydrogen silsesquioxane-mediated synthesis of nanocrystalline silicon dispersed in a mesoporous silica/suboxide matrix, with potential for electrochemical applications. New J. Chem. 39: 621-630.
- Kong, C.S., T.Y. Kim and D.E. Morse. 2015. Low-temperature catalytic synthesis of high-efficiency fuel cell cathode of nanocrystalline Pt uniformly dispersed in high surface area, microwave-expanded graphene. (In preparation for Advanced Energy Materials).

Electrostatic Driven Self-Assembly Design of Functional Nanostructures

PI: Monica Olvera de la Cruz*

Co-PIs: Michael J. Bedzyk

(*) Department of Materials Science and Engineering, Northwestern University, 2220 Campus Drive, Evanston, IL 60208.

Email: m-olvera@northwestern.edu

Program Scope

The program seeks to design nanostructures and manipulate self-assembly to facilitate improvements in functionality of the structures by using biomolecules as building blocks. Since most biomolecules are charged, it is crucial to understand the role of electrostatic interactions in the self-assembly process. This program shows how electrostatic interactions offer the possibility of generating structures that can be controlled by systematically changing the ionic conditions, as well as the preparation path. Here, we study the influence of electrostatics in the structure of closed vesicles and on the morphology of charged nanofibers, and design dynamic routes of assembly to increase the phase space of structures and functions of vesicles.

Recent Progress

The spontaneous formation of closed vesicles from microscopic units in aqueous solutions is a fundamental process in biology and materials science. Understanding and controlling the shape and properties of vesicle underlies a host of problems in materials geometry and biology from assembly of virus [1] to fabrication of closed structures in materials design [2]. The equilibrium structure of fluid and crystalline vesicles has been extensively studied. The equilibrium vesicle shape space is significantly expanded via external inputs.

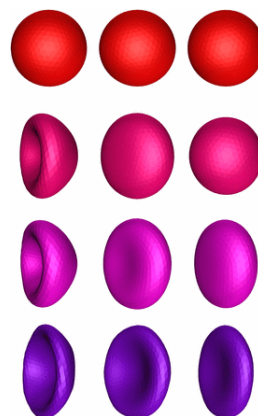
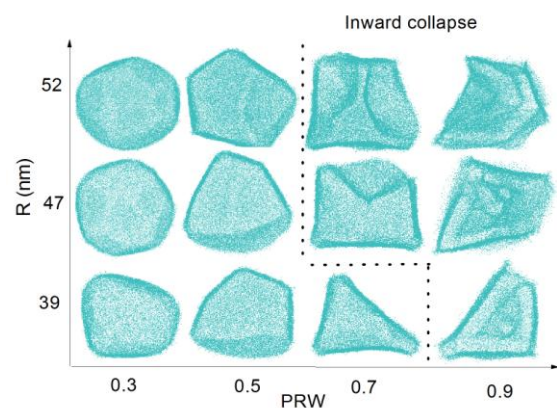


Fig. 1: (a) Shape evolution of ionic crystalline vesicles with different sizes. The deformation of the vesicles follows a pattern with the increase of the percentage of removed water (PRW). (b) Snapshots of conformations of elastic nanoshells with different bending rigidities (soft to rigid from left to right columns) and electrolyte concentration (low to high from top to bottom).

We designed dynamic routes to enlarge the shape space of both fluid and crystalline vesicles beyond the equilibrium zone [3]. By removing water inside cationic and anionic vesicle at different rates, we numerically obtain a series of dynamically trapped stable vesicle shapes in a highly controllable fashion for both liquid and crystalline vesicles. In crystalline ionic vesicles, simulations showed the initial appearance of small flat portions over the crystalline vesicles that ultimately merge to form few flat faces with the continuous removal of water; the vesicle therefore transforms from a fullerene-like shape to various faceted polyhedrons (see Fig. 1.a).

We performed analytical elasticity analysis and show that these salient features are attributed to the crystalline nature of the vesicle. The potential of using dynamic routines to engineer the vesicle shape transformation as revealed in this study opens new possibilities to exploit the richness of vesicle geometries for desired applications

We have also recently showed that when a crystalline shell is charged, it is possible to compensate for the increase in elastic energy associated with the shape deformation if the latter is accompanied with a significant lowering of the electrostatic free energy [4]. We discovered that a uniformly charged, spherical elastic shell, when constrained to maintain the enclosed volume, can lower its free energy by deforming into smooth structures shown in Fig. 1.b.

One of the key aspects of our research is to carefully design experiments to deduce how the molecular geometry, charge and concentration are coupled to the molecular packing within the assembly and the mesoscopic morphology of the assembly. Two distinct experimental designs are being employed: 1) the equilibrium structures of assembly in bulk solutions are investigated by systematically tuning the inter-molecular interactions. Small and wide angle X-ray scattering (SAXS/WAXS) along with cryo-transmission electron microscopy is utilized for structural characterization over Å- μ m length scales. 2) Bilayers are replicated onto solid/liquid interfaces for detailed structural analysis of the molecular packing in the membrane-normal direction and the membrane-ion interactions by X-ray reflectivity and X-ray standing waves (XSW), respectively. For bulk solutions, we showed how temperature and molecular concentration could be used to control the electrostatic-repulsion driven assembly of highly charged nanofibers. For substrate-supported bilayers, we provide a tentative phase diagram delineating the conditions where bilayers onto solid substrates can be formed from faceted vesicles in bulk solutions.

Long range ordering in highly charged nanofibers. The SAXS-derived structural phase behavior of the assembly of nano-filaments of positively charged (+1) azobenzene-based amphiphiles is shown in Fig. 2. Briefly, these highly charged nano-filaments order into two-dimensional hexagonal crystals at temperatures less than 50 °C and for concentrations greater than 4 mM. At lower concentrations or higher temperatures, the assembly is liquid-like. For crystalline arrays, these fibers of ~ 5.6 nm diameter arrange with remarkably large inter-fiber spacing of up to 130 nm, clearly demonstrating that the electrostatic repulsions drives the 2D crystallization. Screening the electrostatic repulsions via salt addition destroyed the crystal packing. Our findings show how electrostatic repulsions in conjunction with confinement can induce crystallization of highly charged nano-objects [5].

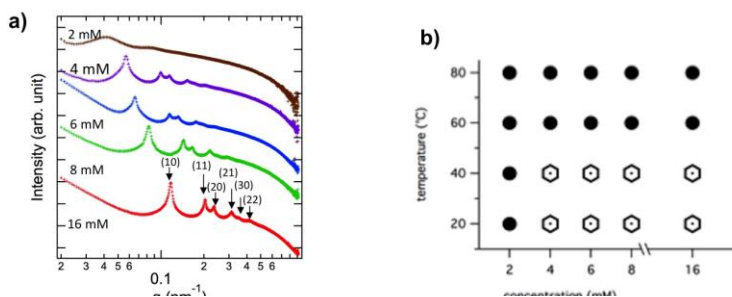


Fig 2. (a) SAXS intensity profiles vs q for different amphiphile concentrations at $T = 20$ °C. (b) SAXS-derived structural phase diagram depicting the hexagonal crystalline and liquid-like (filled circles) ordering of nanofibers as a function of temperature and concentration

Assembled substrate of cationic bilayers. This work focuses on substrate-supported bilayers comprised of cationic peptide-amphiphiles and fatty acids (cationic membranes). This substrate assembly offers the possibility of generating charged patterns at the nanoscale with biocompatible groups. The cationic amphiphile is a C_{16} aliphatic tail coupled to three lysine groups ($C_{16}-K_3^{3+}$). The anionic amphiphile is a fatty acid ($C_{15}-COO^-$). Our previous solution X-

ray scattering and cryo-transmission electron microscopy studies [6,7] probed the co-assembly of these lipids as a function of solution pH, which controlled the strength of inter-molecular electrostatic interactions. Depending on pH, amphiphiles co-assembled into faceted vesicles or nanoribbons, which comprised of lipid bilayers. Important questions remained regarding the lipid packing in the bilayer-normal direction, the interactions between the membranes and their ionic environment and bilayer lipid composition. Cationic bilayers on planar solid/liquid (s/l) interfaces are expected to yield a significantly higher degree of structural and compositional sensitivity. We explored the formation and the structure of the bilayers deposited *via* the vesicle fusion method, and found that bilayer formation depended upon the substrate temperature (T_s) and the solution pH. Uniform bilayers were observed only when the substrate temperature was nearly equal to or greater than the alkyl chain melting transition temperature T_m ($= 57$ °C). Further, bilayers were observed in the regime of pH = 6-8, where both the cationic and the anionic amphiphiles are expected to be predominantly charged. Thus, we have been able to produce a tentative phase diagram for the cationic bilayer formation in a limited pH- T_s parameter space (Fig. 3).

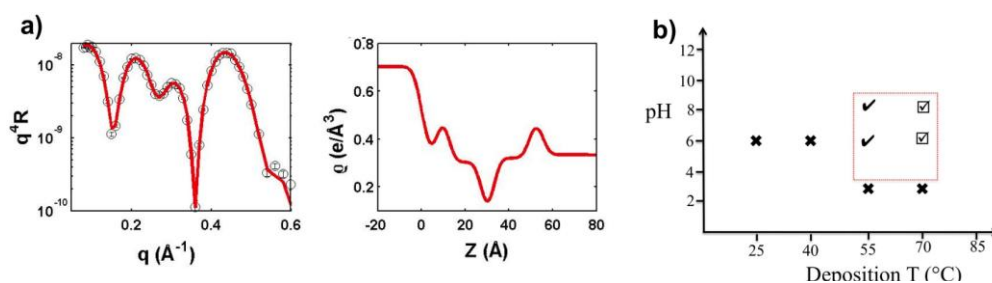


Fig. 3. (a) XRR-data for cationic film deposited at $T_s = 55$ °C and pH = 6 along with best-fit (left) based on a bilayer model

and corresponding best-fit electron density profile (right). (b) The XRR-derived phase diagram for the formation of cationic bilayers at Si/water interface. Crosses indicate regions where uniform bilayers were not observed. Check marks and “check marks in boxes” indicate thick “crystalline-like” and thin “fluid-like” bilayers.

Future Plans

The coupling between molecular geometry and charge leads to distinct inter-molecular interactions, which in turn affect the morphology and the functionality of the assembly. For example, subtle changes in steric and electrostatic interactions can lead to different supramolecular assemblies such as spherical or cylindrical micelles, vesicles or lamellae. The pH-driven micelle to vesicle transition in simple fatty acids has been suggested as the pathway for the formation of the earliest known cellular structures (protocells). We will study a modular series of amphiphilic peptides with 3, 2 or 1 lysine groups conjugated to a C_{16} -carbon tail (C_{16} -K₃, C_{16} -K₂, and C_{16} -K₁). The supramolecular assembly will be studied as a function of solution pH, which continuously tunes the charge on the lysine groups. Via systematic SAXS/WAXS and TEM analysis, we want to elucidate how the coupling between the headgroup size and charge affects the mesoscopic morphology of the assembly.

A key component of the program is to investigate interactions among charged shells and nanostructures. It is well-known that solutions of proteins, nanoparticles or colloids are destabilized by the addition of large amounts of salt, a phenomenon commonly referred to as ‘salting out’. This phenomenon is generally believed to result from ionic screening; salt screens the charge of solutes and lowers the electrostatic barrier that prevents aggregation caused by attractive forces (such as Van der Waals forces). Recently, however, we derived by theoretical analysis that the salt ions themselves can induce attractive forces between like-charged solutes, at

sufficient salt concentrations. The strength of these forces is found to be significant for the ionic conditions of the intra-cellular environment, which indirectly implies that these forces support biological mechanisms. These findings were recently corroborated by experiments on model systems of strongly charged functionalized nanoparticles. The scattering functions obtained by X-ray spectroscopy revealed that the nanoparticles formed aggregates at increased salt concentrations, despite purely repulsive interactions between the nanoparticles themselves. We will quantify ion-induced attractions with theoretical and experimental methods and show that ‘salting out’-effects can actually be used for controlled self-assembly.

The theoretical methods rely on liquid-state theories. We will derive an effective potential between charged nanoparticles by integrating out the degrees of freedom of the salt ions. The result depends on the ion entropy, which causes a depletion potential, and the ion-ion correlations that induce cohesion and salt bridges between the charged sites of the nanoparticles. We will apply this model to study the organization of ionic nano-shells.

References

1. O. Pornillos, B. K. Ganser-Pornillos, B. N. Kelly, Y. Z. Hua, F. G. Whitby, D. C. Stout, W. I. Sundquist, C. P. Hill, and M. Yeager, X-ray structures of the hexameric building block of the HIV capsid, *Cell*, 137, 1282-1292 (2009).
2. A. D. Dinsmore, M. F. Hsu, M. G. Nikolaides, M. Marquez, A. R. Bausch and D. A. Weitz, Colloidosomes: selectively permeable capsules composed of colloidal particles, *Science*, 298, 1006-1009 (2002).
3. Jiaye Su, Zhenwei Yao and Monica Olvera de la Cruz "Fluid and crystalline vesicle geometries enriched by dynamically trapped states" preprint (2015).
4. Vikram Jadhao, Creighton K. Thomas and Monica Olvera de la Cruz "Electrostatics-driven shape transitions in soft shells" *Proc. Natl. Acad. Sci.* 111, 12673–12678 (2014).
5. L. C. Palmer, C.-Y. Leung, S. Kewalramani, R. Kumthekar, C. J. Newcomb, M. Olvera de la Cruz, M. J. Bedzyk and S. I. Stupp. *J. Am. Chem. Soc.* 2014, 136, 14377-14380.
6. Leung, C. Y., Palmer, L. C., Qiao, B. F., Kewalramani, S., Sknepnek, R., Newcomb, C. J., Greenfield, M. A., Vernizzi, G., Stupp, S. I., Bedzyk, M. J., and de la Cruz, M. O. *ACS Nano* 2012, 6, 10901-10909.
7. Leung, C. Y., Palmer, L. C., Kewalramani, S., Qiao, B. F., Stupp, S. I., de la Cruz, M. O., and Bedzyk, M. J. *Proc. Natl. Acad. Sci. U.S.A.* 2013, 110, 16309-16314.

Publications (supported by DOE over last two years; 3 to 7 above and the following 8-10)

8. Topological defects in the buckling of elastic membranes; C.M. Funkhouser, R. Sknepnek, M. Olvera de la Cruz, *Soft Matter* 9: 60-68 (2013).
9. Vikram Jadhao, Zhenwei W. Yao, Creighton K. Thomas, Monica Olvera de la Cruz, “Coulomb energy of uniformly charged spheroidal shell systems” *Physical review E*, 91, 032305 (2015).
10. Niels Boon, Guillermo I. Guerrero-Garcia, Rene van Roij and M. Olvera de la Cruz “Effective charges and virial pressure of concentrated macroion solutions” published on line July 13, 2015. doi: 10.1073/pnas.1511798112

Dynamical Self-Assembly: Constrained Phase and Mesoscale Dynamics in Lipid Membranes

Atul N. Parikh, Biomedical Engineering, Chemical Engineering & Materials Science Departments, University of California, Davis, CA 95616

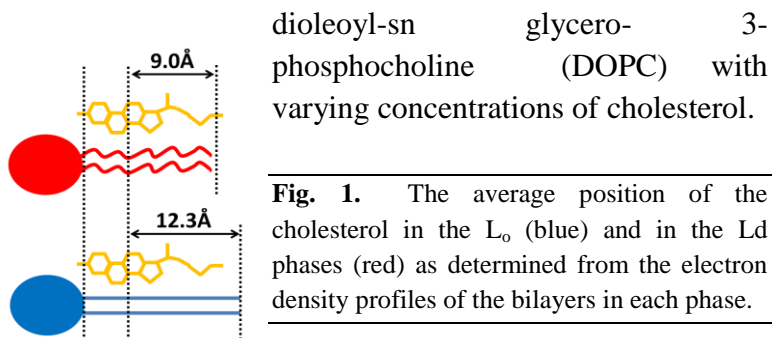
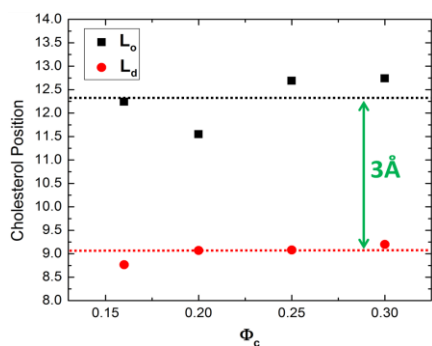
Sunil K. Sinha, Physics Department, University of California, San Diego, CA

Program Scope

This project seeks to abstract a physical science based understanding of spatial organization and dynamic reorganization of amphiphilic molecules within the two-dimensional membrane milieu. Our longer-term objective is to translate these physical principles into quantitative design rules for the development of new classes of membrane-based complex materials that exhibit cooperative and/or adaptive responses. Our approach is primarily experimental; we employ well-defined model of bilayer lipid membranes including multilamellae, supported membranes, and giant vesicles, and probe their dynamics in response to selected environmental perturbations. We are currently focus on the roles of (1) interfacial (including interbilayer) interactions and hydration repulsion; (2) imposed shapes and curvatures; and (3) mechano-chemical perturbations such as induced by osmotic stress and lipid-specific chemistries in membrane spatial organization and dynamics using a combination of spatially- and temporally resolved microscopy and spectroscopy techniques (fluorescence, ellipsometric, infrared vibrational, and x-ray scattering).

Recent Progress

1. Membrane Multilayers. We have now completed a detailed characterization of the partitioning behaviour of cholesterol between saturated and unsaturated lipids using X-ray lamellar diffraction data and analyses using membrane multilayers. Specifically, we examined the cholesterol partitioning and condensing effect in the co-existing liquid ordered (L_o) and liquid disordered (L_d) phases of lipid bilayers. For study, we used three-component lipid multilayers consisting of 1:1 1,2-dipalmitoyl-sn-glycero-3-phosphocholine (DPPC) and 1,2-



dioleoyl-sn glycerol-3-phosphocholine (DOPC) with varying concentrations of cholesterol.

Fig. 1. The average position of the cholesterol in the L_o (blue) and in the L_d phases (red) as determined from the electron density profiles of the bilayers in each phase.

We used X-ray lamellar diffraction to deduce the electron density profiles (EDP) of each phase. The cholesterol concentration in each phase was quantified by fitting the EDP with a newly invented the Basic Lipid Profile scaling

method, which minimizes the number of fitting parameters. The condensing effect of cholesterol in ternary lipid mixtures was evaluated in terms of phosphate-to-phosphate distances (PtP), which together with the estimated cholesterol concentration in each phase was converted into an average area per molecule. In addition, the cholesterol position was determined with precision and an increase of disorder in the lipid packing in the L_0 phase was observed for total cholesterol concentration of 20% and above. This work is currently in revision at the **Biophysical Journal**.

In a previous work¹, we showed that multilayer membranes of mixed lipids and cholesterol phase separated laterally into L_0 and L_d domains, as well as stack along the direction normal to the membrane, thus creating two coexisting but incommensurate bilayer repeat distances.

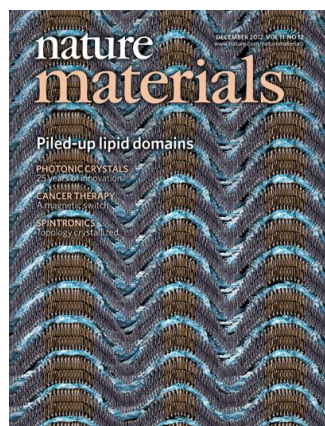


Fig. 2. A schematic depiction of mesoscale ordering of liquid-ordered domains in liquid-disordered surroundings in co-existing lipid phases in membrane multilayers.

This leads to a large energy cost due to hydrophobic mismatch at the domain boundaries. We have recently found, by studying the same system as a function of increasing relative humidity up to 100% in our specially designed humidity cell, that at higher humidity levels the bilayer repeat distance of the L_d phase starts to rapidly increase, thereby increasing the water thickness between the bilayers in the L_d domains, in order to try to equalize the repeat distance in the 2 phases

and thus to lower the mismatch energy at the domain boundaries. This work is currently under review by **JACS**.

2. Using giant lipid vesicles, we studies the effects of osmotic stress on lateral organization of membrane components. When subjected to hypotonic stress, we confirmed previously reported findings that the osmotically swelled vesicles exhibit swell-burst cycles characterized by oscillation in size and periodic pore formation.

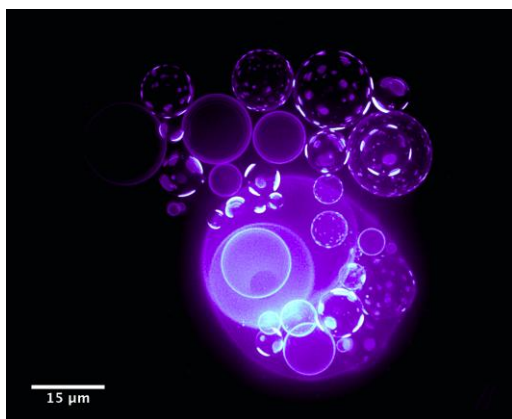


Fig. 3. Coupling of osmotic activity of water (out-of-plane) with the membranes compositional degrees of freedom (in-plane) results in oscillatory domain dynamics.

In domain-forming ternary mixtures (see 1 above), we found that the swell-burst cycles become coupled with the membrane's compositional degrees of freedom, producing a long-lived transient response characterized by damped oscillations in demixing behavior at the membrane surface. This oscillatory phase separation

occurs isothermally and it is driven by a sequence of elementary biophysical processes involving cyclical changes in osmotic pressure, membrane tension, and poration, which attend swell-burst cycles. Moreover, this cyclical pattern exhibits systematic damping: a step-wise diminution of

the osmotic pressure differential, because of the solute leakage during burst events, gradually dampens the oscillations ultimately equilibrating the GUV to the residual osmotic differential. This isothermal phase transition – resulting from a well-coordinated sequence of mechanochemical events – suggests an emergent quasi-homeostatic behavior allowing synthetic vesicles produced from simple components, namely, water, osmolytes, and lipids to sense and regulate their micro-environment in a negative feedback loop. This work appeared in **eLife**.

Future Plans

The work of the previous years has set the stage for extending dynamic membrane reorganization using all three model membrane systems above. Some key activities planned are listed below.

1. **Lipid Multilayer system.** We will address three key questions including (1) characterization of the membrane-water interface; (2) effects of ions; and (3) effects of osmotic stress on the three-dimensional domain stacking we reported during the last PI meeting. *First*, we have previously shown that the thicknesses of the adsorbed water layers intercalated between the lipid bilayers in the phase separated system are significantly different in the two Lo and Ld phases, as are the roughnesses of the lipid-water interfaces. We speculate that this could be due to different states of hydrogen bonding of water in the two phases, which may play a role in stacking up the minority domains in registry in the multilayers. To address these issues, we will combine x-ray scattering and fluorescence measurements under poly(ethylene)glycol imposed osmotic stress. *Second*, we have recently completed several reflectivity studies of the effect of ions on the conformation of cushioned lipid bilayers of DPPC. We plan to extend these studies to off-specular x-ray diffuse scattering studies to quantitatively extract the effect of these ions on the elastic moduli of the bilayers. We plan to conduct parallel experiments using time-lapse spinning disc confocal fluorescence microscopy and pursue parallel measurements of bending moduli of single bilayers using giant vesicles in presence of ions.

2. **Giant Vesicles.** Compartmental morphology of giant vesicles afford introduction of transmembrane concentration gradients, such as we demonstrated in our eLife paper. (See 3 above). Prompted by the quasi-homeostatic osmoregulatory response exhibited by simple synthetic vesicles to osmotic swelling in that study, we now plan to study how (1) intravesicular macromolecular crowding such as occurs in cell affect the osmotic regulation and (2) how membrane compositional degrees of freedom (and corresponding lateral variations in membrane elasticity) influence osmotic deflation, such as occurs during vesicle immersion into hypertonic media. For (2), preliminary results show dramatic shape transformations, which map onto well-known theoretical models based on spontaneous curvature and bilayer-couple hypotheses for single component vesicles but exhibit significant departures not predicted by the models.

3. **Reconstituting cell shapes in synthetic vesicular models.** A major limitation of giant vesicle configuration is that lower symmetry and complex topographies of living cells can not be

stably recapitulated. In an exciting partnership with B. Kaehr and C. J. Brinker Labs (Sandia), we have begun addressing this challenge by employing the so-called silica-cell replica, they pioneered. Here, glass replica of living cells are used as templates to reconstitute lipid bilayers in three-dimensional cell shapes. In addition to conferring stability and reconstituting cell surface topography, replicas provide means to introduce intravesicular macromolecular crowding.

References

1. L. Tayebi, Y. Ma, D. Vashaee, G. Chen, S.K. Sinha, A. N. Parikh, *Nat. Mater.* 11, 1074-1080 (2012).

Publications (2-Year List Supported by BES)

1. Medium Matters: Order through fluctuations?, A. N. Parikh *Biophys. J.* 108, 2751 (2015).
2. Cholesterol Partition and Condensing Effect in Phase Separated Ternary Mixture Lipid Multilayers, Y. Ma, S. K. Ghosh, D. A. DiLena, S. Bera, Laurence B. Lurio, A. N. Parikh, S. K. Sinha, **Biophys. J.** In review (March 2015).
3. Oscillatory phase separation in giant lipid vesicles induced by transmembrane osmotic differentials, K. Oglęcka, P. Rangamani, B. Liedberg, R. S. Kraut & A. N. Parikh **eLife** 3, e03695, **2014 [eCover]**
4. Observation of stripe superstructure in the beta-two-phase co-existence region of cholesterol-phospholipid mixtures in supported membranes, S. R. Tabaei, J. A. Jackman, B. Liedberg, A. N. Parikh*, Nam-Joon Cho*, **J. Amer. Chem. Soc.** 136, 16962–16965, **2014**
5. Reconstituting ring-rafts in bud-mimicking topography of model membranes," Y. Ryu, i. Lee, J.-H. Suh, S. C. Park, S. Oh, L. R. Jordan, N. J. Wittenberg, S.-H. Oh, N. L. Jeon, B. Lee, A. N. Parikh* & S.-D. Lee*, **Nature Communications** 5, Art. No. 4507, **2014**
6. Mixing, diffusion, and percolation in binary supported membranes containing mixtures of lipids and amphiphilic block copolymers, D. L. Gettel, J. Sanborn, M. Patel, H.-P. de Hoog, B. Liedberg, M. Nallani, and A. N. Parikh, **J. Amer. Chem. Soc.** 136, 10186–10189, **2014**.
7. Thermal annealing triggers collapse of biphasic supported lipid bilayers into multilayer islands," S. F. Gilmore, D. Y. Sasaki, and A. N. Parikh **Langmuir** 17, 4962-4969 **2014**.
8. Demonstration of Feasibility of X-Ray Free Electron Laser Studies of Dynamics of Nanoparticles in Entangled Polymer Melts, J. Carnis, W. Cha, J. Wingert, J. Kang, Zhang Jiang, S. Song, M. Sikorski, R. Aymeric, C. Gutt, San-Wen Chen, Y. Dai, Y. Ma, H. Guo, L. B. Lurio, O. Shpyrko, S. Narayanan, M. Cui, I. Kosif, T. Emrick, T.P.Russell, H. C. Lee, C.J. Yu, G. Gruebel, S.K. Sinha, Hyunjung Kim, **Scientific Reports** 4, 6017 (2014)
9. On-Demand Self-Assembly of Supported Membranes Using Sacrificial, Anhydrobiotic Sugar Coats. T. E. Wilkop, J. Sanborn, A.E. Oliver, J. M. Hanson, A. N. Parikh. **J. Amer. Chem. Soc.** 136, 60-63, 2014.
10. Highly resolved structure of a floating lipid bilayer: Effect of Ca²⁺ ions and temperature, S. K. Ghosh, Y. Ma, Curt M. DeCaro, S. Bera, L. B. Lurio, Z. Jiang, S. K Sinha, accepted for publication in **Biophys. J.**, 2014.
11. Lithographically Defined Macroscale Modulation of Lateral Fluidity and Phase Separation Realized via Patterned Nanoporous Silica-Supported Phospholipid Bilayers, E. L. Kendall, V. N. Ngassam, S.F. Gilmore, C.J. Brinker, A. N. Parikh, **J. Amer. Chem. Soc.** 135, 15718-15721, 2013.

Long Range van der Waals-London Dispersion Interactions for Biomolecular and Inorganic Nanoscale Assembly: Design and Anisotropy

Principal Investigators: V.A. Parsegian*, W. Y. Ching[†],
in collaboration with R. H. French[‡], N.F. Steinmetz[§]

Sen. Res. Assoc.: R. Podgornik*, Postdoc: S.Aryal; Ph.D. students: J. C. Hopkins*, Y. Ma[‡], D. M. Dryden[‡], L. Poudel[‡], J. Eifler[‡]; Undergrads: Ka. Nagendra[‡], R. Tai[‡].

Mailing Addresses: *Physics Dept., Univ. of Mass., Amherst, MA, 01003; [†]Dept. of Physics and Astronomy, Univ. of Missouri, Kansas City, MO, 64110; [‡]Materials Science, [§]Biomedical Engineering, Case Western Reserve Univ., Cleveland, Ohio, 44106.

Emails: parsegian@physics.umass.edu, chingw@umkc.edu, rxfl31@case.edu, nfs11@case.edu

Program Scope

The goal of this program is to provide long-overdue practical access to the rigorous modern theory of vdW dispersion, polar and electrostatic long-range interactions and to use the theory of these organizing LRIs in the assembly of organic/inorganic materials, such as filamentous molecules of the duplex DNA type, or globular molecules of the BSA protein type. This is the starting point to investigate also inorganic and metallic materials and (virus-like) nanoparticles that are parts of organic-inorganic material composites.

In the past year, we continued developing our vdW expertise in materials and interaction morphologies where anisotropy of the shape/interaction geometry and the anisotropic spectral properties of materials can be disentangled. We developed theory and implementation of open-science Gecko Hamaker LRI tools for diverse meso-scale architectures, interaction geometries and optically and morphologically anisotropic elements. We added charge regulation, i.e. response of the charge on macromolecular surfaces to the solution conditions, and tested its importance in the charge state of proteinaceous virus shells. We assessed the role of substrate surface energy and roughness for vdW shear adhesion occurring in non-air media in order to understand the ability of geckos to stick to PTFE that is wet.

Recent Progress

Disentangling the Effects of Shape and Dielectric Response in van der Waals Interactions¹ (UMass, CWRU, UMKC): Anisotropic effects contributing to the full Lifshitz formulation of van der Waals

interactions between nanoscale bodies generally result from two system properties- anisotropy of the materials' bulk dielectric

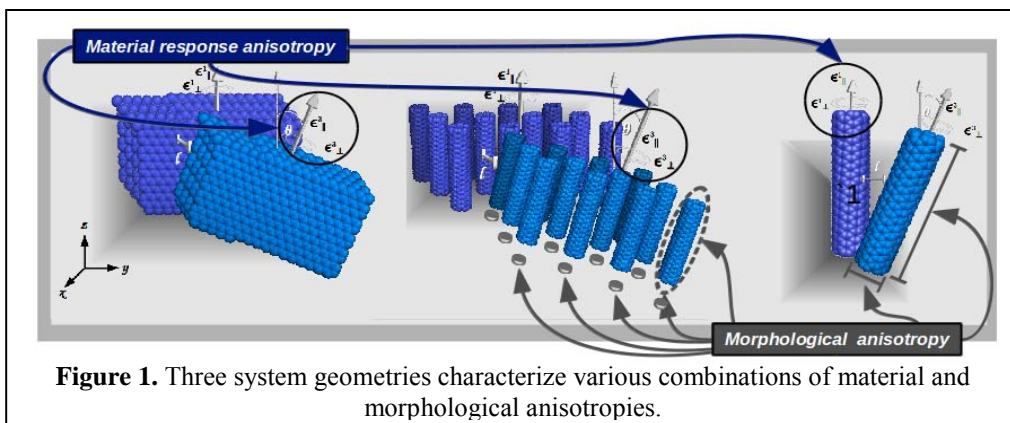
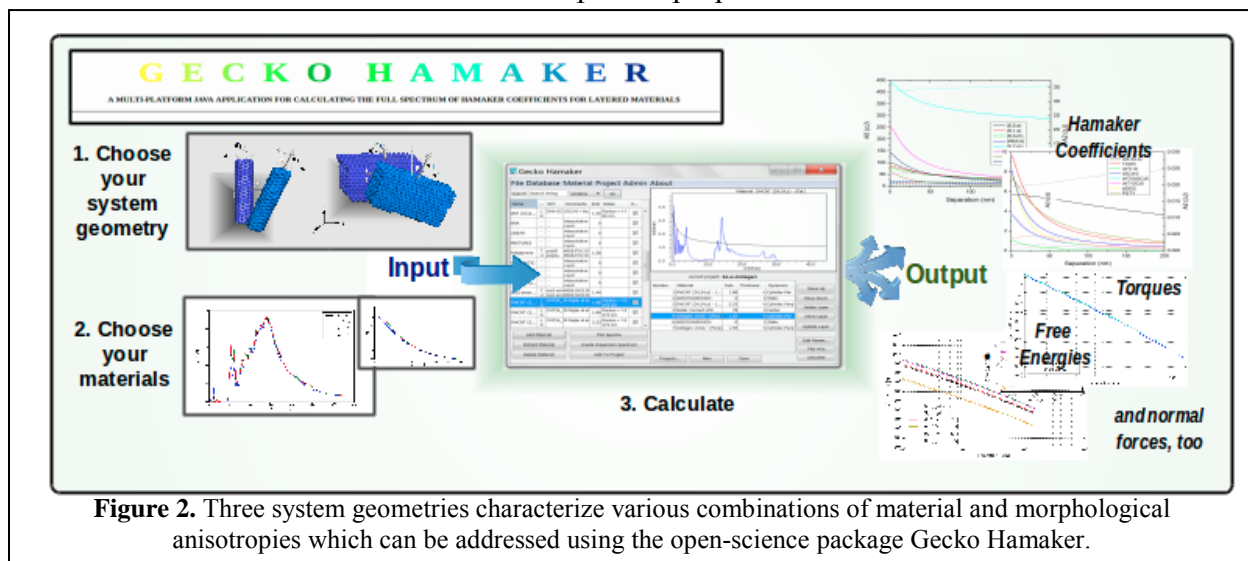


Figure 1. Three system geometries characterize various combinations of material and morphological anisotropies.

responses, and/or anisotropic morphology of the bodies or anisotropic inclusions they may contain. The effects of these properties are isolated through analysis of three interaction geometries- planes, composite planes, and a cylinder pair- each of which characterizes different dependencies on material and/or morphological anisotropies (see Fig.). Surprisingly, the effect of shape on interactions in the retarded regime results in stronger torques between arrays comprising anisotropic shapes, such as carbon nanotubes in an aqueous medium, than torques between thick planes composed entirely of the same material.

Gecko Hamaker Open-Science implementation² (UMass, CWRU,UMKC): The self-assembly of heterogeneous mesoscale systems is mediated by long-range interactions, including vdW. Diverse mesoscale architectures, built of optically and morphologically anisotropic elements such as DNA, collagen, single-walled carbon nanotubes, and inorganic materials, require a tool to calculate the forces, torques, interaction energies, and Hamaker coefficients that govern assembly in such systems. The mesoscale Lifshitz theory of vdW interactions can accurately describe solvent and temperature effects, retardation, and optically and morphologically anisotropic materials for cylindrical and planar interaction geometries. The Gecko Hamaker open-science software enables new and sophisticated insights into the interaction properties of important organic/ inorganic systems: interactions show an extended range of magnitudes and retardation rates, DNA interactions show an imprint of base pair composition, certain SWCNT interactions display retardation-dependent nonmonotonicity, and interactions are mapped across a range of material systems in order to facilitate rational mesoscale design (see Fig.). The Gecko Hamaker project, its source code, and its open spectral optical properties data are distributed freely on Sourceforge under the GNU General Public License (GPL 1991). The latest version 2.1 was released in July 2014, encompassing full retarded cylinder interaction potentials. Gecko Hamaker has been downloaded more than 1250 times since the start of this DOE research project. The machine-readable spectral optical property database is available for download or as a web service and makes available the full spectral properties of over 150 materials from both ab



initio calculations and experiments, including inorganic as well as organic materials such as Type I collagen and (GC)₁₀ duplex DNA.

Virus Charge Distribution and Electrostatics³

(UMass): We have combined electrostatic interactions with the acid-base and surface charging equilibria of a viral proteinaceous shell to analyze the effect of polar acid-base interactions on the charge state of the proteinaceous capsid. We investigated the extremely important and substantial effects of pH and salt concentration on charge regulation of the bacteriophage PP7 capsid. These effects arise as a consequence of a complicated balance of the chemical dissociation of the amino acids, the electrostatic interaction between them, and the counterion release. We show that to properly describe and predict the charging equilibrium of viral capsids in general, one needs to include molecular details as exemplified by the acid-base equilibrium of the detailed distribution of amino acids in the proteinaceous capsid shell. We conclusively demonstrate that to understand the nature and magnitude of the capsid charge, one needs to consider molecular details such as the acid-base equilibrium of the amino acids and their exact distribution across the capsid wall to properly understand the charge state of the virus capsid (see Fig.). These conclusions are also completely vindicated by recent experiments on electrophoretic mobilities of cowpea chlorotic mottle viruses viral capsids and their capsid proteins.

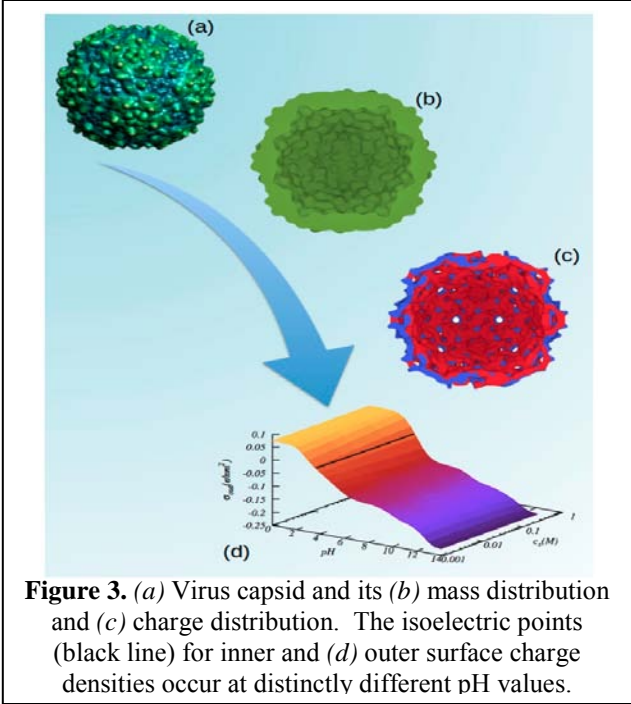


Figure 3. (a) Virus capsid and its (b) mass distribution and (c) charge distribution. The isoelectric points (black line) for inner and (d) outer surface charge densities occur at distinctly different pH values.

Interactions of geckos with wet and dry fluoropolymer substrates⁴

(CWRU). Even geckos, which can stick to most surfaces under a wide variety of conditions, slip on dry PTFE but can stick reasonably well to PTFE if it is wet. To explain this effect, we investigated the role of substrate surface energy and roughness when shear adhesion occurs in media other than air (see Fig. 4). We removed the

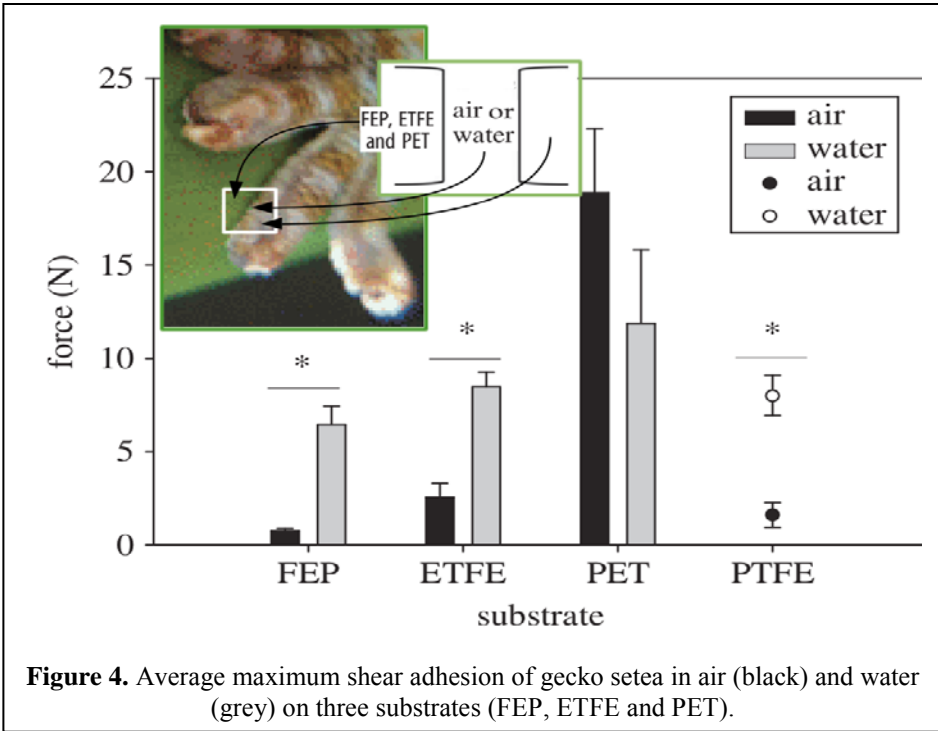


Figure 4. Average maximum shear adhesion of gecko setae in air (black) and water (grey) on three substrates (FEP, ETFE and PET).

roughness inherent to commercially available PTFE and tested geckos on relatively smooth wet and dry fluoropolymer substrates. Roughness had very little effect on shear adhesion in air or in water and the level of fluorination was most important for shear adhesion, particularly in air. Surface energy calculations using the Tabor–Winterton approximation and the Young–Dupré equation were used to determine the interfacial energy of the substrates and the ratio of wet and dry normal adhesion for geckos clinging to the three substrates. Consistent with the results for rough PTFE, our predictions show a qualitative trend in shear adhesion based on fluorination, and the quantitative experimental differences highlight the unusually low shear adhesion of geckos on dry smooth fluorinated substrates, which is not captured by surface energy calculations. Our work has implications for bioinspired design of synthetics that can preferentially stick in water but not in air.

Future Plans

Analyze the effects of monopolar vdW fluctuation forces on LRI when charge fluctuations in nano-circuits with capacitor components give rise to a novel type of long-ranged interaction, which co-exist with the regular Casimir/van der Waals force.

Extend the analysis of charge regulated macromolecules to virus assembly in solution and at surfaces and calculate the second virial coefficient of capsids in electrolyte solutions.

References

1. J. C. Hopkins, R. Podgornik, W.-Y. Ching, R. H. French, V. A. Parsegian: Disentangling the Effects of Shape and Dielectric Response in van der Waals Interactions between Anisotropic Bodies, **J. Phys. Chem.** (2015) submitted.
2. D. M. Dryden, J. C. Hopkins, L. Denoyer, L. Poudel, N. F. Steinmetz, W.-Y. Ching, R. Podgornik, V. A. Parsegian, R. H. French: van der Waals Interactions at the Mesoscale: Open-Science Implementation, Anisotropy, Retardation, and Solvent Effects, **Langmuir** (2015) DOI: 10.1021/acs.langmuir.5b00106.
3. R. J. Nap, A. L. Božič, I. Szleifer, and R. Podgornik: The Role of Solution Conditions in the Bacteriophage PP7 Capsid Charge Regulation, **Biophys. J.** 107, 1970 (2014).
4. A. Y. Stark, D. M. Dryden, J. Olderman, K. A. Peterson, P. H. Niewiarowski, R. H. French and A. Dhinojwala: Adhesive Interactions of Geckos with Wet and Dry Fluoropolymer Substrates, **J. R. Soc. Interface** 12, 20150464 (2015).

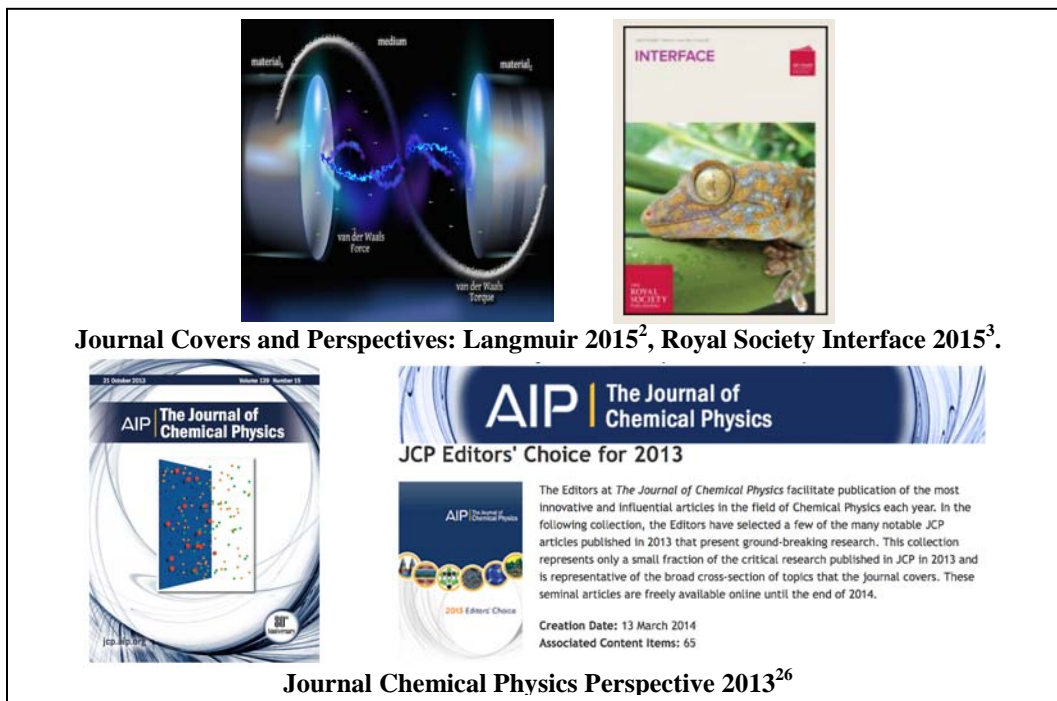
Publications

1. J. C. Hopkins, R. Podgornik, W.-Y. Ching, R. H. French, and V. A. Parsegian: Disentangling the Effects of Shape and Dielectric Response in Van Der Waals Interactions Between Anisotropic Bodies, **J. Colloid and Interface Sci.**, submitted.
2. A. Y. Stark, D. M. Dryden, J. Olderman, K. A. Peterson, P. H. Niewiarowski, R. H. French, and A. Dhinojwala: Adhesive Interactions of Geckos with Wet and Dry Fluoropolymer Substrates,” **J. The Royal Society Interface** 12, 108, 20150464 (2015).
3. D. M. Dryden, J. C. Hopkins, L. K. Denoyer, L. Poudel, N. F. Steinmetz, W.-Y. Ching, R. Podgornik, V. A. Parsegian, and R. H. French: Van Der Waals Interactions on the Mesoscale: Open-Science Implementation, Anisotropy, Retardation, and Solvent Effects, **Langmuir** (2015). doi:10.1021/acs.langmuir.5b00106.
4. J. B. Schimelman, D. M. Dryden, L. Poudel, K. E. Krawiec, Y. Ma, R. Podgornik, V. A. Parsegian, L. K. Denoyer, W.-Y. Ching, N. F. Steinmetz, and R. H. French: Optical properties and electronic transitions of DNA oligonucleotides as a function of composition and stacking sequence, **Phys. Chem. Chem. Phys.** 17, 6, 4589-4599, (2015). Doi: 10.1039/C4CP03395G
5. A. M. Wen, R. Podgornik, G. Strangi, and N. F. Steinmetz: Photonics and Plasmonics Go Viral: Self-Assembly of Hierarchical Metamaterials, **Rendiconti Lincei**, 1-13, March 5th 2015. doi:10.1007/s12210-015-0396-3.
6. L. Poudel, A. M. Wen, R. H. French, V. A. Parsegian, R. Podgornik, N. F. Steinmetz, and W.-Y. Ching: Electronic Structure and Partial Charge Distribution of Doxorubicin in Different Molecular Environments, **Chem. Phys. Chem.**, 16, 7, 1451-60, (2015). doi: 10.1002/cphc.201402893.
7. D. Dean, R. Podgornik, V. A. Parsegian: Fluctuation mediated interactions due to rigidity mismatch and their effect on miscibility of lipid mixtures in multicomponent membranes, **J. Phys.: Condens. Matter** 27, 21, 214004 (2015). Doi: 10.1088/0953-8984/27/21/214004
8. D. M. Dryden, G. L. Tan, and R. H. French: Optical Properties and van der Waals–London Dispersion Interactions in Berlinite Aluminum Phosphate from Vacuum Ultraviolet Spectroscopy, **J. Am. Ceram. Soc.** 97, 4, 1143-50, (2014). Doi: 10.1111/jace.12757
9. S. Yasar, R. Podgornik, and V. A. Parsegian: Continuity of States in Cholesteric - Line Hexatic Transition in Univalent and Polyvalent Salt DNA Solutions, **MRS Proceedings** 1619 (2014). doi:10.1557/opl.2014.358.
10. Y. Ma, D. M. Acosta, J. R. Whitney, R. Podgornik, N. F. Steinmetz, R. H. French, and V. A. Parsegian: Determination of the second virial coefficient of bovine serum albumin under varying pH and ionic strength by composition-gradient multi-angle static light scattering, **J Biol Phys**, 1-13, Jan. 2015. Doi: 10.1007/s10867-014-9367-7

11. L. Poudel, P. Rulis, L. Liang, and W. Y. Ching: Electronic structure, stacking energy, partial charge, and hydrogen bonding in four periodic B-DNA models, **Phys. Rev. E**, 90, 2, 022705 (2014). Doi: 10.1103/PhysRevE.90.022705
12. R. J. Nap, A. L. Božič, I. Szleifer, and R. Podgornik: The Role of Solution Conditions in the Bacteriophage PP7 Capsid Charge Regulation, **Biophysical Journal**, 107,8, 1970-79 (2014). Doi: 10.1016/j.bpj.2014.08.032
13. M. D. Glidden, J. F. Edelbrock, A. M. Wen, S. Shukla, Y. Ma, R. H. French, J. K. Pokorski, and N. F. Steinmetz: Application of engineered viral nanoparticles in materials and medicine, in **Chemoselective and Bioorthogonal Ligation Reactions: Concepts and Applications**, Wiley-VCH, 2014.
14. N. Li and W.-Y. Ching: Structural, electronic and optical properties of a large random network model of amorphous SiO₂ glass, **J. Non-Crystalline Solids** 383. 28-32, (2014). Doi: 10.1016/j.jnoncrysol.2013.04.049
15. S. Yasar, R. Podgornik, J. Valle-Orero, M. R. Johnson, and V. A. Parsegian: Continuity of states between the cholesteric → line hexatic transition and the condensation transition in DNA solutions, **Scientific Reports** 4, 6877 (2014). Doi: 10.1038/srep06877
16. D. S. Dean and R. Podgornik: Relaxation of the thermal Casimir force between net neutral plates containing Brownian charges, **Phys. Rev. E** 89, 3, 032117, (2014). Doi: 10.1103/PhysRevE.89.032117
17. J. C. Hopkins, D. M. Dryden, W.-Y. Ching, R. H. French, V. A. Parsegian and R. Podgornik: Dependence of the Strength of van Der Waals Interactions on the Details of the Dielectric Response Variation, In **MRS Proceedings** 1648 (2014). doi:10.1557/opl.2014.426.
18. D. M. Dryden, Y. Ma, J. Schimelman, D. Acosta, L. Liu, O. Akkus, M. Younesi: Optical Properties and van Der Waals-London Dispersion Interactions in Inorganic and Biomolecular Assemblies, **MRS Proceedings** 1619 (2014). doi:10.1557/opl.2014.301.
19. J. Eifler, P. Rulis, R. Tai, and W.-Y. Ching: Computational Study of a Heterostructural Model of Type I Collagen and Implementation of an Amino Acid Potential Method Applicable to Large Proteins, **Polymers**, 6, 2, 491-514, (2014). Doi: 10.3390/polym6020491
20. P. Adhikari, A. M. Wen, V. A. Parsegian, N. Steinmetz, R. Podgornik, W.-Y. Ching: Electronic Structure, Dielectric Response, and Surface Charge Distribution of RGD (1FUV) Peptide, **Scientific Reports** 4, 5605 (2014). Doi: 10.1038/srep05605
21. J. C. Hopkins, D. M. Dryden, W.-Y. Ching, R. H. French, V. A. Parsegian, and R. Podgornik: Dielectric response variation and the strength of van der Waals interactions, **J. of Colloid and Interface Sci.** 417, 278-84 (2014). Doi: 10.1016/j.jcis.2013.10.040
22. A. M. Wen, P. H. Rambhia, R. H. French, and N. F. Steinmetz: Design rules for nanomedical engineering: from physical virology to the applications of virus-based materials in medicine, **J. Biol. Phys.**, 39, 1-25, (2013). Doi: 10.1007/s10867-013-9314-z

23. A. Naji, M. Kanduč, J. Forsman, and R. Podgornik: Perspective: Coulomb fluids—Weak coupling, strong coupling, in between and beyond, **J. Chem. Phys.**, 139, 15, 150901, (2013). Doi: 10.1063/1.4824681
24. N. Li, R. Sakidja, S. Aryal, and W.-Y. Ching: Densification of a continuous random network model of amorphous SiO₂ glass, **Phys. Chem. Chem. Phys.**, 16, 4, 1500-14, (2013). Doi: 10.1039/C3CP53192A

Other References:



The image displays four journal covers and a perspective article. At the top left is the cover of *Langmuir* (October 2015) featuring a blue and white abstract design with the text 'material, medium, material' and 'van der Waals Force'. To its right is the cover of *Royal Society Interface* (2015) showing a colorful gecko on a green leaf. Below these is the cover of *AIP The Journal of Chemical Physics* (October 2013) with a blue and white abstract design. To the right of the AIP cover is a 'JCP Editors' Choice for 2013' banner and a collection of article covers. The banner includes the AIP logo and the text 'The Journal of Chemical Physics' and 'JCP Editors' Choice for 2013'. Below the banner is a paragraph of text: 'The Editors at *The Journal of Chemical Physics* facilitate publication of the most innovative and influential articles in the field of Chemical Physics each year. In the following collection, the Editors have selected a few of the many notable JCP articles published in 2013 that present ground-breaking research. This collection represents only a small fraction of the critical research published in JCP in 2013 and is representative of the broad cross-section of topics that the Journal covers. These seminal articles are freely available online until the end of 2014.' Below this text are the dates 'Creation Date: 13 March 2014' and 'Associated Content Items: 65'. At the bottom center of the image is the text 'Journal Chemical Physics Perspective 2013²⁶'.

Journal Covers and Perspectives: Langmuir 2015², Royal Society Interface 2015³.

Journal Chemical Physics Perspective 2013²⁶

INTEGRATING RHODOPSINS IN H⁺-FETS FOR BIOINSPIRED ENERGY CONVERSION

Marco Rolandi, Dept. of Materials Science and Engineering

Francois Baneyx, Dept. of Chemical Engineering

University of Washington, Seattle, WA

Program Scope

Energy transduction at the nanoscale is key for developing ever smaller self-powered biotic-abiotic circuitry. In biological systems, chemical, mechanical, and electromagnetic energy is converted from one form to another using ubiquitous proton gradients.^{1, 2} Here, Prof. Rolandi and Prof. Baneyx develop materials and proton (H⁺)-based devices to modulate proton gradients for understanding and exploiting bioinspired energy conversion. This research is enabled by the ability to control proton currents in H⁺-FETs (Rolandi)³⁻⁵ and express membrane proteins in large quantities in optimized *E. coli* strains (Baneyx). The project scope is as follows: (1) Express proton-pumping rhodopsins and proteorhodopsins in large quantities in optimized *E. coli* strains and engineer these proteins to selectively bind to proton contacts. (2) Integrate these proteins in solid-state proton conducting transistors with lipid bilayer contacts. (3) Perform proton transport measurements in the resulting devices to evaluate proton-pumping characteristics (e.g., voltage, current, ΔpH) as a function of light intensity, wavelength, solution pH, and contact protochemical potential (Fig. 1).

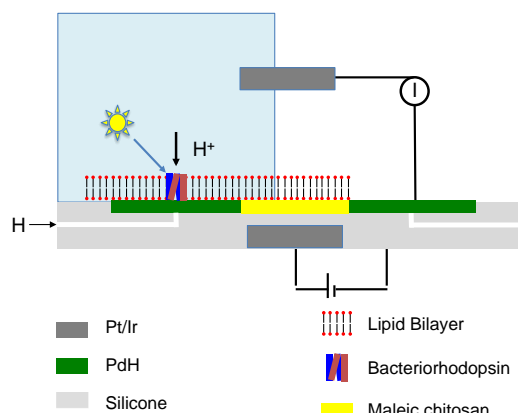


Fig. 1 Schematic of H⁺-FET with integrated lipid bilayer and rhodopsin.

Recent Progress

1. Electrochemical transfer of H⁺ across Pd water interface and Pd/PdH_x formation

In order to integrate rhodopsins with proton conducting PdH_x contacts³, we need to characterize the dynamics of the PdH_x proton-conducting interface. We measure the electrochemical behavior of a Pd/PdH_x reversible electrode in solution (Fig 2a). This reversible reaction depends on H⁺ activity,

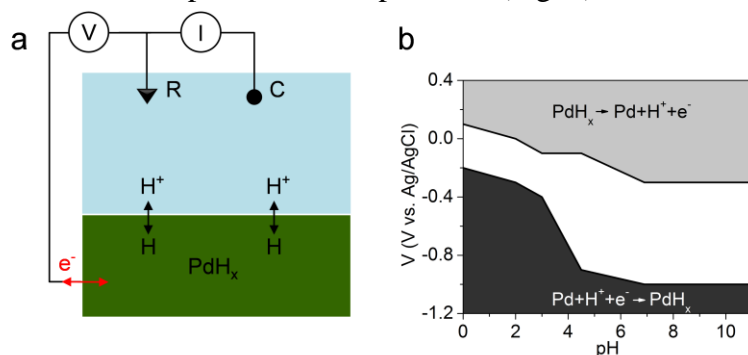


Fig. 2 (a) Schematic of a PdH_x electrochemical cell: Electrons and protons travel into the Pd/PdH_x during formation and out during depletion, according to the electrochemical potential. Ag/AgCl is the reference electrode, Pt is the counter electrode and PdH_x is the working electrode. (b) Pd-PdH Process Map: Formation and depletion of PdH_x dependence on the solution pH and V.

electrochemical potential and applied potential (V). As solution pH increases, the threshold values of formation voltage and depletion voltage decrease due to the influence of pH on the proton chemical potential in solution (Fig. 1b). In a particular range of pH and V (white area), the solution and the PdHx are in equilibrium, and no H⁺ exchange occurs across the interface. This data will be used to estimate how change in pH and Voltage affect proton transfer between the rhodopsins and the PdHx contacts through the water interface.

2. Integration of polypeptide proton channel with bioprotonic device

To understand the interactions of biofunctional proton channels with our bioprotonic device, we incorporate gramicidin A in single lipid bilayer (SLB) coated Pd microelectrode. Gramicidin A is a short helical polypeptide from *Bacillus brevis*, which can dimerize in the lipid membrane to form a transmembrane channel. This channel allows the passage of small monovalent cations, while being impermeable to anions. Gramicidin A is reconstituted into the DOPC vesicles by drying and rehydration. We prepare stock solutions of 5 mg/mL of gramicidin A in ethanol and 10 mg/mL of DOPC in chloroform and mix to get 1:100 gramicidin A to DOPC molar ratio. We flow nitrogen gas over the mixture for 45 minutes to dry completely, then add degassed 50 mM MES buffer solution to make final solution of 0.5 mg/mL DOPC.

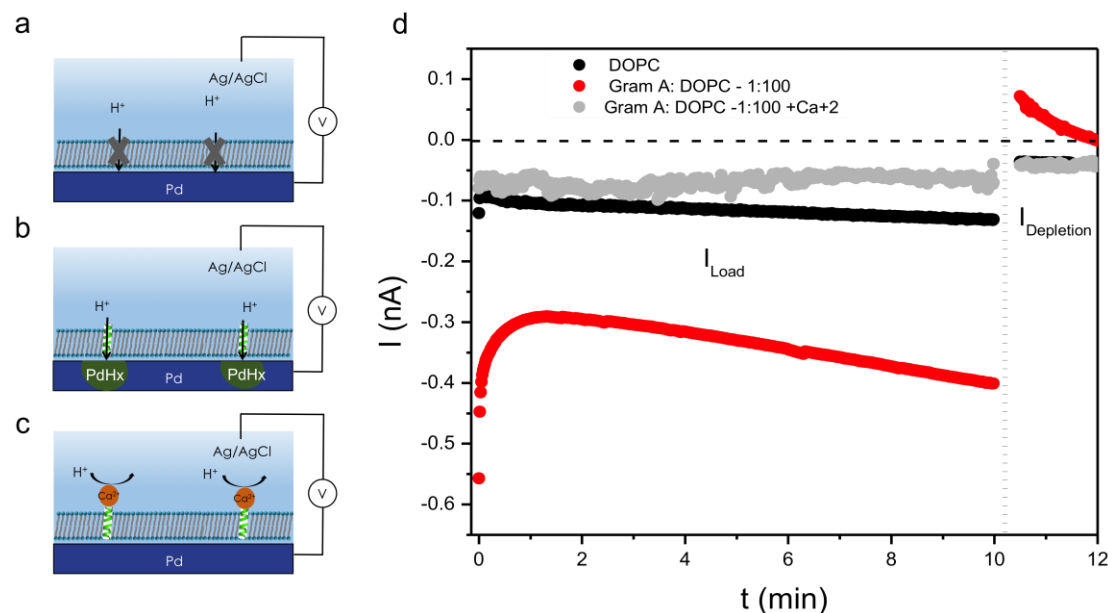


Fig. 3 The operation of a bioprotonic device incorporating gramicidin A pores. (a) (b) (c) Schematics of proton transfer between solution and PdH(d) No proton loading occurs from the bulk solution into the Pd substrate due to the SBL as an isolated layer (black curve), proton loading from the bulk solution into the Pd substrate and depleting of PdHx for a SLB device with gramicidin A pores as a transmembrane (red curve), and SLB device with gramicidin A pores in the presence of Ca²⁺ ions (gray curve). Dash vertical line partitions the loading currents at -200mV for 10 min and depletion currents at 0mV for 2 min.

Our device characterization shows that SLB as an isolated layer prevents the proton transfer from the bulk solution to the interface of Pd substrate (Fig 3a, 3d, black curve) as expected. However, our device confirms the proton transfer from the bulk solution through gramicidin A ion channels

to the interface of Pd substrate which can lead the formation of PdH_x at -200mV (Fig 3b, 3d, red curve). Moreover, addition of 1 mM Ca²⁺ to the solution dramatically decreases the steady-state response of the device, and no formation of PdH_x occurs in the presence of Ca²⁺ (Fig 7c, 7d, gray curve). This phenomenon indicates that with Ca²⁺ blocking the Gramicidin channel no proton transfer occurs across the lipid bilayer. This characterization demonstrates that our device platform amplifies the effective potential driving the reduction of protons at the Pd interface due to a pH gradient across the SLB.

3. Membrane-associated Pd4-HtdR-His binds to Palladium

Haloterrigena turkmenica deltarhodopsin (HtdR) is a retinal-containing member of the rhodopsin family that supports the light-activated and outwards transport of protons. We have produced a Pd-binding variant of His-tagged HtdR called Pd4-HtdR-His for integration in the H⁺-FET (Fig. 4).

7. Purification of Pd4-HtdR-His

In order to purify enough material for liposome reconstitution experiments, 500 mL cultures of *E. coli* KtD101 cells harboring plasmids encoding the HtdR-His control protein or Pd4-HtdR-His were grown to mid-exponential phase in LB medium at 37°C. Cultures were supplemented with all-*trans* retinal to a 10 μM final concentration and protein synthesis was induced by addition of 0.2% L-arabinose. Cells were harvested 3h post-induction and disrupted with a French press operated at 10,000 psi. Aggregated material was removed by centrifugation at 14,000g for 15 min at 4°C and the supernatant was centrifuged at 150,000g for 1h at 4°C to harvest membrane fractions. The resulting material was incubated with buffer supplemented 1.0% of the non-ionic detergent n-dodecyl β-*D*-maltoside (DDM) overnight and at 4°C with shaking. This procedure produces detergent-solubilized proteins, detergent micelles and mixed micelles consisting of detergents and phospholipids. Solubilized membranes were loaded onto a Ni-NTA chromatography column equilibrated in DDM-containing buffer and washed extensively. The protein was eluted with 250 mM imidazole. Protein purity was determined by SDS-PAGE. Fig. 5A shows the presence of a possible Pd4-HtdR-His degradation product (lower band in lanes E1 and E2) that we intend to eliminate in the future by addition of a protease inhibitor cocktail and a subsequent gel filtration chromatography step. The UV/visible spectrum of the purified proteins show the characteristic peak at 550 nm of functional HtdR, indicating

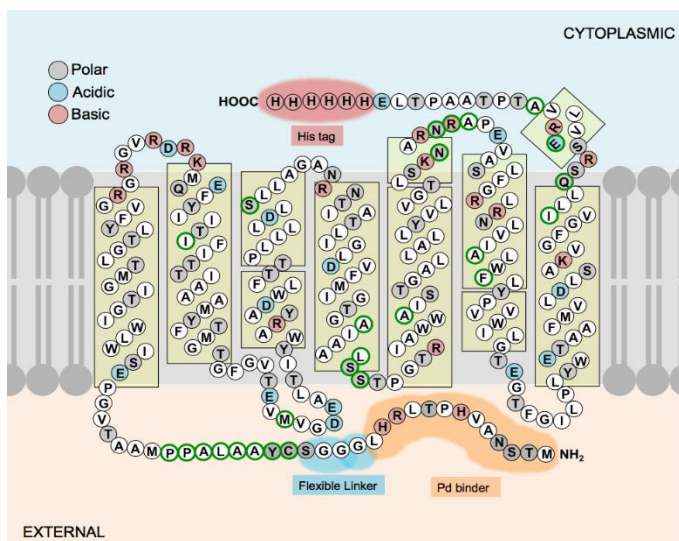


Fig. 4. Organization of Pd4-HtdR-His in the membrane of *E. coli* based on the topology of dR3 (1). The Pd4 binding sequence is in orange and the hexahistidine tag in pink. Transmembrane segments are boxed and polar, acidic and basic amino acids are color-coded.

that the detergent-extracted material remains properly folded (Fig. 5B).

Future Plans

In year two we finalized the development of devices with integrated microfluidic architecture and lipid bilayer as well as expression and purification of HtdR. We are now in a position to integrate HtdR

with the protonic devices and conduct the studies planned for year 3. These studies will lead to a precise characterization and understanding of H^+ transfer driven by HtdR to and from PdH. Specifically, in year 3 we will: (1) Deposit SLB with HtdR proton pumping channels onto Pd microfluidic devices, (2) Investigate energetics of protonic gradient across SLB, (2) Improve purification of Pd4-HtdR for higher yield proteoliposomes, (2) Orient HtdR in liposomes prior to deposition on Pd microfluidic device, (2) Test light response of SLB devices with HtdR proton pump

References

1. Morowitz HJ. Proton Semiconductors and Energy Transduction in Biological-Systems. *Am J Physiol.* 1978;235(3):R99-R114.
2. Decoursey TE. Voltage-gated proton channels and other proton transfer pathways. *Physiol Rev.* 2003;83(2):475-579.
3. Zhong C, Deng Y, Roudsari AF, Kapetanovic A, Anantram MP, Rolandi M. A polysaccharide bioprotonic field-effect transistor. *Nat Commun.* 2011;2:476.
4. Deng Y, Josberger E, Jin J, Roudsari AF, Helms BA, Zhong C, Anantram MP, Rolandi M. H^+ -type and OH^- -type biological protonic semiconductors and complementary devices. *Sci Rep.* 2013;3:2481.
5. Wunsche J, Deng YX, Kumar P, Di Mauro E, Josberger E, Sayago J, Pezzella A, Soavi F, Cicoira F, Rolandi M, Santato C. Protonic and Electronic Transport in Hydrated Thin Films of the Pigment Eumelanin. *Chemistry of Materials.* 2015;27(2):436-442.

Publications

1. E. Josberger, Y. Deng, W. Sun, R. Kautz, M. Rolandi, Two-terminal protonic devices with synaptic-like short term depression and device memory, *Advanced Materials* **26**, 4986 (2014)
2. T. Miyake, E. E. Josberger, S. Keene, Y. Deng and M. Rolandi “An enzyme logic bioprotonic transducer”, *APL Materials* **3**, 014906 (2015).
3. Z. Hemmatian, T. Miyake, Y. Deng, E. Josberger, S. Keene, R. Kautz, C. Zhong, J. Jin, M. Rolandi “Taking Electrons out of Bioelectronics: Bioprotonic Memories, Transistors, and Enzyme Logic”, *J. Materials Chemistry C* **2**, 6407 (2015).(Cover Article)
4. Z. Hemmatian, S. Keene, T. Miyake, J. Soto Rodriguez, E. E. Josberger, F. Baneyx, M. Rolandi “Integrating ion channels with microfluidic bioprotonic devices”, In preparation.

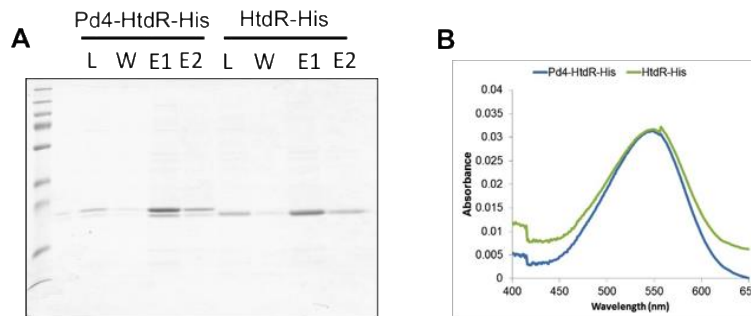


Fig. 5. (A) SDS-PAGE of DDM-solubilized Pd4-HtdR-His and HtdR-His following their affinity purification. (B) Absorbance spectra of the purified proteins

Project Title: Miniaturized Hybrid Materials Inspired by Nature

Principle Investigator (PI): C. R. Safinya

Co-PIs: Y. Li and K. Ewert

**Materials Department, University of California at Santa Barbara
Santa Barbara, CA 93111**

E-mail: safinya@mrl.ucsb.edu

Program Scope

The objectives of our research program is to develop a scientific understanding of higher-order-assembly in charged biomolecular material systems (proteins, charged membranes, nucleic acids), which may be near equilibrium, in kinetically trapped states, or out-of-equilibrium. One current focus is on biological polyampholyte directed assembly of filamentous proteins. The biological polyampholytes belong to a group of “intrinsically disordered proteins” with structure-function relations distinct from globular proteins where interactions are mediated through non-specific forces (not complementary shapes). Another focus involves developing an understanding of the influence of biomolecule shape (e.g. in environmentally-responsive biomolecular materials), on dynamical assembly. Both the building blocks and their directed assembly may contribute important functional properties to the biomimetic materials on different length scales (e.g. biomimetic hydrogels with slow and fast water-release properties [1]).

A strategy that we use to achieve our aims is to design biomimetic materials [1, 2] inspired by complex cellular assemblies [3], which operate under dissipative conditions. Bio-macromolecules studied in this program include neurofilaments [4, 5] and microtubules (MTs) assembled with multivalent counterions or associated unstructured proteins, where electrostatic forces play an essential role in the directed assembly [6-9]. Our very recent study, describes the discovery of a highly charged molecular switch (the polyamine spermine 4+) triggering the disassembly of a bundle of paclitaxel-stabilized MTs followed by re-assembly into inverted tubulin tubules, which expose the inner surface of the original MTs [10]. Synchrotron small-angle X-ray scattering and electron microscopy uncovered the pathway of the tubule inversion process revealing a straight-to-curved shape transition of protofilaments comprising the precursor MT wall. The finding opens the path for a new paradigm for self-assembly where the use of encoded building blocks enables trigger-ready structures, which disassemble on demand and reassemble shape-remodeled building blocks into a new form of matter with a new property. Potential applications in a synthetic mimic include encapsulation of molecules and release upon triggered disassembly. In ongoing related work we are studying the effect of multivalent ions on the structure and dynamics of active microtubule assemblies in buffer containing GTP in the absence of paclitaxel. This has led to an unexpected finding that the transition from the bundled phase of MTs to inverted tubules occurs through a new “intermediate” state.

The projects utilize the broad spectrum of expertise of the PI and the two co-PIs in biomolecular self-assembling methods, synchrotron x-ray scattering, electron and optical microscopy, small-angle x-ray scattering-osmotic pressure technique for direct force measurements, and custom organic/polymer synthesis and purification of biological molecules.

Recent Progress

(I) Protein Tubule Inversion Triggered by a Molecular Switch: A New Paradigm for Assembly

Proteins often undergo abrupt structural transitions, which enables their functions. These discrete conformational changes underlie the exquisite control and sensitivity of biological organisms. Examples include pH sensitive flagella and molecular motor ATPases such as kinesin and myosin motors undergoing conformational changes during ATP hydrolysis [3]. In our studies we used proteins, which harness discrete shape remodeling specificity (to enable their function in cells) as self-assembling building blocks. The building block enzymes in our study were $\alpha\beta$ -tubulin heterodimers, which exist in either a straight or curved conformation with the transition between these two states controlled by GTP hydrolysis (see cartoons in Fig. 1). Microtubules shown in Fig. 1a consist of paclitaxel-stabilized polymerized tubulin. Tubulin's distinct conformations underlie the broad range of cellular activities of tubulin and polymerized tubulin (i.e. microtubules), which include imparting cell shape, as tracks for organelle transport, and as building blocks of dynamical spindles [3].

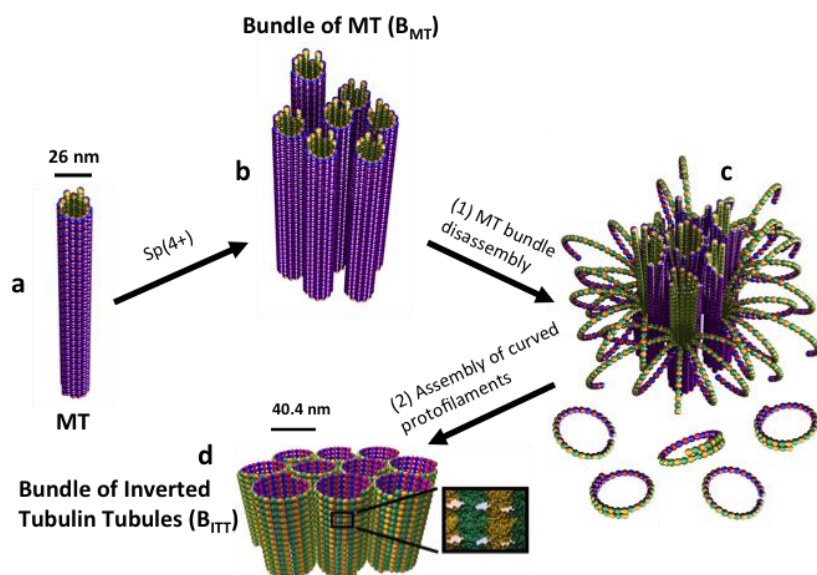


Figure 1 Schematic of a polyamine spermine (4+) induced inversion process from bundles of paclitaxel-stabilized microtubules (B_{MT}) to bundles of inverted tubulin tubules (B_{ITT}). (a and b) paclitaxel-stabilized microtubules (MTs, a) may be induced to form MT bundles above a critical concentration of spermine (4+) counterions (B_{MT} , b). The bundles result from the nonspecific electrostatic attraction between spermine coated MTs. (c and d) For concentrations several times larger than the critical bundling concentration a specific spermine-triggered straight-to-curved conformation transition in protofilaments, leads to MT

disassembly into curved protofilaments (c-PFs) within the bundles (c). Concurrent to MT disassembly spermine counterions induce non-specific assembly of c-PFs into the B_{ITT} phase (d). Both phases are hierarchically ordered, liquid crystalline nanotubes, but the tubes are inverted: the tubulin surface, which is on the inside of the tubes in the B_{MT} phase is on the outside in the B_{ITT} phase. Adapted from [10].

Our paper describes the discovery that tetravalent spermine controls the straight to curved transition rate in paclitaxel-stabilized tubulin. This has led to the creation of microtubule bundles (Fig. 1b), which upon a spermine trigger, undergo a dynamical transformation involving (i) an inside-out curving of tubulin oligomers during the depolymerization peeling process (Fig. 1c) and (ii) concurrent re-assembly of curved tubulin building blocks into an array of inverted tubulin tubules (Fig. 1d).

Significance of the findings The work described here shows that polyamine spermine controls the straight to curved transition rate in paclitaxel-stabilized GDP-*protofilaments*. This has led to the creation of microtubule bundles, which upon a spermine trigger, undergo a dynamical

transformation to an assembly of inverted tubulin tubules. The creation of such robust assemblies where the “inner lumen” of MTs is stably exposed allows for a convenient platform for future experiments addressing interactions of biomolecules with the inner surface of MTs.

(II) Patterned Thread-like Lipidic-Micelles and DNA-Tethered Nanoparticles: Self-Assembly of PEGylated Cationic Liposome–DNA Complexes. There is currently very large research activity in the area of self-assembly driven by the promise of designable nanomaterials. At the molecular level, objects interact through a combination of forces. Thus, an understanding of inter-particle forces and structures is required for nanomaterials to achieve their full potential in applications.

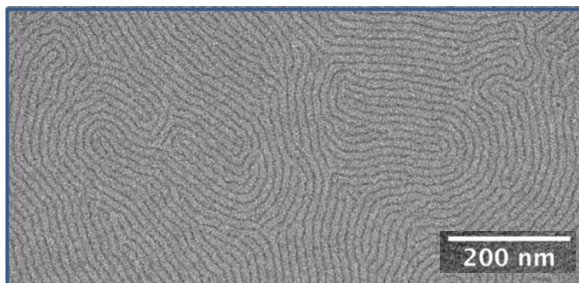


Figure 2 Cryogenic TEM of lipid-based patterned cylindrical micelles resulting from PEGylated cationic liposomes (PEG-CLs) mixed with linear DNA. The image shows the center of the carbon hole where the thinly hydrated film shows remarkable ordered and patterned thread-like micelles with uniform spacing of order 14 nm. The ends of the thread-like lipid-based micelles are clearly visible. Near the edge of the carbon hole, PEG-CL–DNA nanoparticles, liposomes, and small spherical micelles coexist with the cylindrical micelles (not shown). These

well-ordered lipid-based thread-like micelles (with inter-micellar spacing tunable by changes in the length of the PEG-chain) may have applications as masks in nanoscale lithography. Adapted from [11, 18] (*Langmuir*, in press).

The system studied here involves complexation of PEGylated cationic liposomes and DNA (PEG-CL–DNA), with distinct length (short 11 bp and long 48k bp) and topology (linear and circular), resulting from the release of counter-ions (i.e. self-assembly stabilized by entropic considerations). PEGylated-CL–DNA complexes spontaneously form nanometer scale particles. Unexpectedly, we found distinct novel phases that appear away from the isoelectric point. Overall positive PEG-CL–DNA NPs coexist with spherical liposomes, spherical micelles and thread-like micelles. Interestingly, long thread-like micelles can be induced to form a layered morphology with fingerprint like patterns (Fig. 2).

Significance of Findings The 1D ordered thread-like micelles with controllable nanometer scale inter-micellar spacing may have applications in nanolithography (Fig. 2). Generally, nanoparticles formed via self-assembly of oppositely charged macromolecules (and the release of counterions) have a range of potential applications and a more detailed picture of their stability and structure will aid future design.

Future Plans

Biological polyampholyte-induced assembly in an active matter system. In our most recent work we studied microtubule-associated-protein tau directed assembly of microtubules (MTs) under equilibrium conditions [6]. In the next set of studies we will remove the fixing molecule paclitaxel and probe the “active matter system” consisting of tubulin, the fuel molecule GTP, and protein tau. In the absence of tau, MTs exhibit dynamical instability (i.e. cycles of MT growth and shrinkage). Tau appears to modulate MT dynamic instability by promoting assembly while suppressing the shrinkage state. Tau isoforms are inherently unstructured polyampholytes (polymers containing both positive and negative charged groups) and belong to a group of

recently recognized intrinsically disordered proteins (IDPs) where non-specific interactions determine inter-protein interactions. The role of IDPs in modulating inter-protein interactions is a nascent field of high interest in biomolecular materials. (This contrasts with the standard dogma in molecular biology where protein-protein interactions are mediated by shape specific lock and key interactions.) The experiments promise to reveal a fundamentally new type of assembly resulting from macromolecular ion correlations in an active matter system.

References

1. Safinya, C. R.; Deek, J.; Beck, R.; Jones, J. B.; Li, Y.: Assembly of Biological Nanostructures: Isotropic and Liquid Crystalline Phases of Neurofilament Hydrogels. *Ann. Rev. Cond. Matter Phys.* **2015**, *6*, 113-136.2
2. Safinya, C. R.; Raviv, U.; Needleman, D. J.; Zidovska, A.; et al.: Nanoscale Assembly in Biological Systems: From Neuronal Cytoskeletal Proteins to Curvature Stabilizing Lipids. *Adv. Mater.* **2011**, *23*, 2260-2270.
3. Pollard TD, Earnshaw WC, Lippincott-Schwartz J. 2007. *Cell Biology*. New York: Elsevier. 2nd ed.
4. Deek, J.; Chung, P. J.; Kayser, J.; Bausch, A. R.; Safinya, C. R.: Neurofilament sidearms modulate parallel and crossed-filament orientations inducing nematic to isotropic and re-entrant birefringent hydrogels. *Nature Communications* **2013**, *4*, 2224.
5. Beck, R.; Deek, J.; Jones, J. B.; Safinya, C. R.: Gel Expanded-Gel Condensed Transition in Neurofilament Networks Revealed by Direct Force Measurements. *Nature Materials*. **2010**, *9*, 40-46.
6. Chung, P. J.; Choi, M. C.; Miller, H. P.; Feinstein, H. E.; et al.: Direct force measurements reveal microtubule-associated-protein tau confers short-range attractions and isoform-dependent steric stabilization to microtubules. *Submitted*.
7. Needleman, D. J.; Ojeda-Lopez, M. A.; Raviv, U.; Miller, H. P.; Li, Y.; Song, C.; Feinstein, S. C.; Wilson, L.; Choi, M. C.; Safinya, C. R.: Ion specific effects in bundling and depolymerization of taxol-stabilized microtubules. *Faraday Discussions* **2013**, *166*, 31-45.
8. Choi, M.C.; Raviv, U.; Miller, H.P.; Gaylord, M.R.; Kiris, E.; Ventimiglia, D.; Needleman, D.J.; Kim, M.W.; Wilson, L.; Feinstein, S.C.; Safinya, C.R.: Human Microtubule-Associated-Protein Tau Regulates the Number of Protofilaments in Microtubules: A Synchrotron X-ray Scattering Study. *Biophys. J.* **2009**, *97*, 519-527
9. Needleman, D. J.; Ojeda-Lopez, M. A.; Raviv, U.; Miller, H. P.; et al.: Higher-order assembly of microtubules by counterions: From hexagonal bundles to living necklaces. *Proc. Natl. Acad. Sci. U.S.A.* **2004**, *101*, 16099-16103
10. Ojeda-Lopez, M. A.; Needleman, D. J.; Song, C.; Ginsburg, A.; Kohl, P.; Li, Y.; Miller, H. P.; Wilson, L.; Raviv, U.; Choi, M. C.; Safinya, C. R.: Transformation of taxol-stabilized microtubules into inverted tubulin tubules triggered by a tubulin conformation switch. *Nature Materials* **2014**, *13*, 195-203.
11. Majzoub, R. N.; et al.: Patterned Thread-like Micelles and DNA-Tethered Nanoparticles: A structural study of PEGylated Cationic Liposome–DNA Assemblies. (*Langmuir*, in press).

Publications (BES-supported, last 24 months, **only in print and accepted papers**)

12. Deek, J.; Chung, P. J.; Kayser, J.; Bausch, A. R.; Safinya, C. R.: Neurofilament sidearms modulate parallel and crossed-filament orientations inducing nematic to isotropic and re-entrant birefringent hydrogels. *Nature Communications* 2013, 4, 2224. DOI: [10.1038/ncomms3224](https://doi.org/10.1038/ncomms3224).
13. Needleman, D. J.; Ojeda-Lopez, M. A.; Raviv, U.; Miller, H. P.; Li, Y.; Song, C.; Feinstein, S. C.; Wilson, L.; Choi, M. C.; Safinya, C. R.: Ion specific effects in bundling and depolymerization of taxol-stabilized microtubules. *Faraday Discussions* 2013, 166, 31-45. DOI: [10.1039/C3FD00063J](https://doi.org/10.1039/C3FD00063J)
14. Safinya, C. R.; Deek, J.; Beck, R.; Jones, J. B.; Leal, C.; Ewert, K. K.; Li, Y.: Liquid crystal assemblies in biologically inspired systems. *Liquid Crystal* 2013, 40, 1748-1758. DOI: [10.1080/02678292.2013.846422](https://doi.org/10.1080/02678292.2013.846422)
15. Silva, B. F. B.; Majzoub, R. N.; Chan, C.-L.; Li, Y.; Olsson, U.; Safinya C. R.: PEGylated Cationic Liposome–DNA Complexation in Brine is Pathway-Dependent. *Biochim. Biophys. Acta – Biomembranes* 2014, 1838, 398-412. DOI: [10.1016/j.bbamem.2013.09.008](https://doi.org/10.1016/j.bbamem.2013.09.008).
16. Ojeda-Lopez, M. A.; Needleman, D. J.; Song, C.; Ginsburg, A.; Kohl, P.; Li, Y.; Miller, H. P.; Wilson, L.; Raviv, U.; Choi, M. C.; Safinya, C. R.: Transformation of taxol-stabilized microtubules into inverted tubulin tubules triggered by a tubulin conformation switch. *Nature Materials* 2014, 13, 195-203. DOI: [10.1038/NMAT3858](https://doi.org/10.1038/NMAT3858).
17. Silva, B. F. B.; Zepeda-Rosales, M.; Venkateswaran, N.; Fletcher, B. J.; Carter, L. G.; Matsui, T.; Weiss, T. M.; Han, J.; Li, Y.; Olsson, U.; Safinya, C. R.: Nematic Director Reorientation at Solid and Liquid Interfaces under Flow: SAXS Studies in a Microfluidic Device. *Langmuir* 2015, 31, 4361-4371. DOI: [10.1021/la5034614](https://doi.org/10.1021/la5034614)
18. Safinya, C. R.; Deek, J.; Beck, R.; Jones, J. B.; Li, Y.: Assembly of Biological Nanostructures: Isotropic and Liquid Crystalline Phases of Neurofilament Hydrogels. *Annual Review Condensed Matter Physics* 2015, 6, 113-136. DOI: [10.1146/annurev-conmatphys-031214-014623](https://doi.org/10.1146/annurev-conmatphys-031214-014623).
19. Ramsey N. Majzoub, R. N.; Ewert, K. K.; Jacovetty, E. L.; Carragher, B.; Potter, C. S.; Li, Y.; Safinya, C. R.: Patterned Thread-like Micelles and DNA-Tethered Nanoparticles: A structural study of PEGylated Cationic Liposome–DNA Assemblies. (*Langmuir*, in press).

Assembling microorganisms into energy converting materials

PI: Ozgur Sahin

Department of Biology Sciences and of Physics, Columbia University

Program Scope

Our current efforts focus on investigating hydration driven energy conversion kinetics within spore nanopores and scaling up this process by assembling these microorganisms into functional materials. We have built an experimental setup to probe nanoscale water dynamics with millisecond time resolution. So far, we found that hydration-dehydration kinetics depend strongly on the relative humidity and temperature of the environment and appear unique to the spore when compared against other hygroscopic materials. To explore mechanisms that enhance water transport kinetics in materials with macroscopic dimensions, we have followed a hierarchical design strategy. We developed hygroscopy driven artificial muscles (HYDRAs) that exhibit fast speed and high strain actuation in response to changing humidity. These HYDRAs, prepared by periodically coating alternating sides of polyimide tapes with bacterial spores, can quadruple their length and lift 50 times their own weight while exchanging less than 5% water by weight. We validated the functionality these materials by demonstrating evaporation driven engines that generate sustained linear oscillatory motion (piston-like) in the presence of evaporation. These engines are able to start autonomously when placed at an air-water interface. In addition, we have demonstrated an electricity generator that rests on water, harvesting evaporation, to power a light source as the water evaporates.

Recent Progress

Kinetics of Spore Water

We developed an experimental setup (Fig. 1a), in which a heat source LED periodically perturbs the equilibrium state of spores, causing them to contract and bend the AFM cantilever to which they are adhered. Using this setup, we have measured the recovery speed of spores as they re-absorb water under various humidity conditions (see

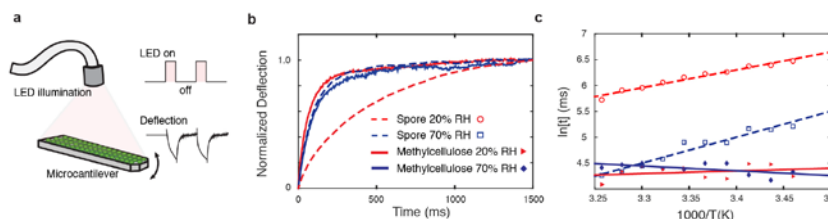


Figure 1 (a) Experimental design whereby the spore equilibrium state is perturbed through periodically heating of the a spore-coated cantilever, forcing momentary evaporation, while resultant deflection is measured (b) Normalized deflection is shown for spores (dashed line) versus traditional hygroscopic material, methylcellulose (solid), in high humidity (RH 70%) versus low (RH 20%). (c) Natural log of relaxation times from heat pulsing are shown plotted against Inverse temperature, wherein the slope of the linear regression is directly proportional to water activity.

Fig. 1a). Fig. 1b show that partially hydrated spores (70% RH) recovered rapidly after the LED was turned off at room temperature. This relatively fast response, comparable in speed to a traditional hygroscopic substance (methylcellulose), can be attributed to the small thickness of the water responsive layer in the spore, complying with the classical Washburn law of diffusion ($t \approx h^2/D$, where t is the diffusion time, h is the thickness of the water responsive layer, and D is the diffusivity). However, when we examine the spore in its desiccated state (20% RH), we observed extended relaxation not typical of water-responsive materials. This finding implicates

humidity dependent transport kinetics of water in the spore as the rate-limiting factor in spore size change. The observed kinetics could be explained by the state-dependent variations in spore pore size as well as the physical state of the water within spores.

To further investigate our hypothesis that the local environment may be able to change the physical property of water inside spores, we referred to the temperature-dependent behavior of a viscous flow in amorphous materials. To describe this behavior, we considered the Arrhenius-type viscosity equation of the form $\mu = A \cdot e^{Q/RT}$, where μ is dynamic viscosity (cantilever relaxation times from heat pulse). By using this equation, we can experimentally measure the activation energy (Q) of water inside of spores, which will quantitatively indicate the state of water anywhere between bulk phase (~5 kCal/mol*K) and completely immobilized (~14 kCal/mol*K). To obtain this activation energy parameter, relaxation times are measured across a range of temperatures while the LED is pulsed. We have measured the relaxation speed of spores at both low relative humidity and high relative humidity at temperatures from 16 °C to 34 °C. To fit these experimental results to the Arrhenius-type viscosity equation properly, we plot the natural log of the relaxation times versus inverse temperature and consider the slope of the linear regression (Fig. 1c). We have initially observed that the spore displays increased water activation energy which is comparable to an amorphous solid (~7-10 kCal/mol*K). In contrast, a methylcellulose coated control cantilever, while producing similar cantilever deflection, results in a monotonic regression reflective of bulk water activity for the temperature range considered. This spore-specific effect persists in both the wet and dry conditions indicating that some other geometric constraint of the spore's structure, rather than differential water activity within the spore, is responsible for physically limiting transport in the compacted dry spore state.

Through studying the behavior of the water within the spores we will be able to determine whether the spore as a biomaterial can be optimized synthetically. Further investigation into these findings will help us to improve the energy and power density of water-responsive materials and simultaneously illuminate the important mechanical roles of water transportation in at the nanoscale in biological organisms. We are currently refining the experimental setup to improve the stability of temperature and relative humidity so that activation energies can be measured more precisely while expanding our examinations to include diverse non-spore materials for reference. Further understanding of the phase states of water in nano-confined spaces can have an impact on our understanding of a wide range of technologies (e.g., nano-filtration membranes, solvent-impregnated anti-fouling surfaces, transport phenomena in zeolites).

Hygroscopy driven artificial muscles

Nanoscale confinement of water in spores provides a means to covert energy from evaporation by generating mechanical force in response to changing relative humidity. Because confinement imposes kinetic limitations, understanding and mitigating this limitation is important for practical applications. Scaling up the dimensions of hygroscopic materials is not expected to increase power, because the time scale of wetting and drying depend on the square of the travel distance of water. We have followed a hierarchical design strategy as illustrated in Figure 3. We have developed hygroscopy driven artificial muscles (HYDRAs) exhibiting a high response speed, large strain, and high-energy output using bacterial spores, while a very small amount of water is exchanged. After bacterial spores (Fig. 2a) are mixed with an adhesive and deposited on micrometer thick plastic films (Fig. 2b), these films change curvature in response to humidity (see Fig. 2c). A net linear movement can be achieved by coating alternating sides of a

long tape with spores (Fig. 2d) thereby scaling up the material in two dimensions without diminishing hydration/dehydration kinetics (Fig. 2e). Moreover, this layered architecture maximizes the surface area for evaporation.

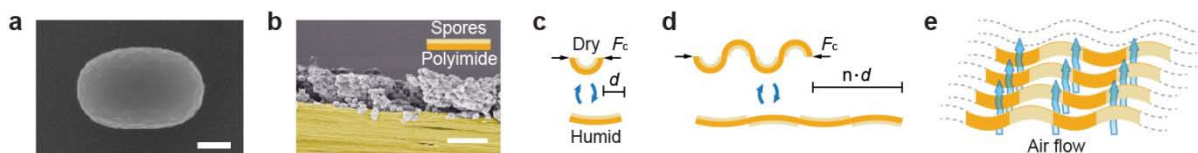


Figure 2 (a) A scanning electron microscopy (SEM) image of a *B. subtilis cotE gerE* spore. (b) A false-colored SEM image of spores deposited on a polyimide tape. (c) The spore-coated films change its curvature in response to changing relative humidity. (d) Linearly expanding and contracting structures are created by patterning equally spaced spore layers on both sides of the plastic tape. (e) Assembling the tapes in (d) with air gaps between them results in a material that can be scaled in two dimensions without affecting hydration/dehydration kinetics. Scale bars: (a) 200 nm, (b) 5 μ m.

We have fabricated these HYDRAs using *Bacillus subtilis* spores genetically altered to lack the unresponsive proteinaceous layers of the spore coat. Figure 3a,b shows HYDRA curvature in humid (90% RH) and dry conditions (10% RH). Composite HYDRAs were created and assembled in parallel by using the design strategy outlined in Fig. 2b-e. The overall length change of the resulting muscles is shown in Fig. 3c,d.

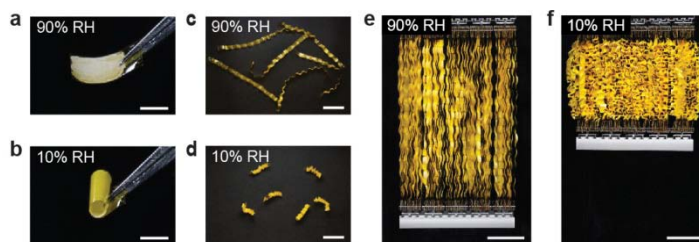


Figure 3 Photos of HYDRAs in humid and dry conditions. (a, b) Photos of individual spore-coated polyimide tapes at low and high relative humidity. (c, d) Linearly expanding and contracting muscles are created by patterning equally spaced spore layers on both sides of a plastic tape. (e, f) HYDRA strips can be packaged in parallel to lift weights. Scale bars: (a, b) 2 mm, (c-f) 2 cm.

Figure 3e and f show these HYDRAs lifting weights when assembled in parallel. By dividing the area enclosed by the curves to the weight of the strip, we estimated the work density of the entire strip to be approximately 17 J/kg, which is close to mammalian skeletal muscles, while yielding greater strain [1]. These characteristics could allow HYDRAs to find application in devices that convert energy from evaporation, as artificial muscles and bio-hybrid cell-based actuators for soft robotic systems.

The evaporation-driven oscillatory engine

HYDRAs primarily respond to changes in relative humidity, but in typical environmental conditions relative humidity changes slowly. Spatial gradients in relative humidity near evaporating water surfaces provide an opportunity to alternate local humidity. For example a small portion of the power generated by HYDRAs can be used to control evaporation rates. Figure 4a illustrates this strategy. Our prototype (Fig. 4) exhibits oscillations and is able to continuously extract energy from evaporation when placed above the air-water interface.

To induce oscillations, we have designed relaxation oscillators that rely on a bi-stable circuit element held under feedback control with which the oscillator circuit repeatedly switches between two internal states (Fig. 4a-c). In our system, HYDRAs are coupled to a beam that is compressed beyond its buckling limit to achieve mechanical bi-stability (Fig. 4a,b). As illustrated in Fig. 4b, this buckled beam controls a shutter mechanism that allows or blocks passage of moist air (feedback). Figure 4c shows four key stages during oscillations: When the shutters are closed (Stage I), the relative humidity of the chamber increases, causing the

HYDRAs to expand rightward until they trigger the buckled beam to switch positions (Stage II). Opening the shutters suppresses incident relative humidity, leading to HYDRA contraction (Stage III). The cycle is completed when contracting HYDRAs pull the buckled beam, triggering it to switch back to the left configuration (Stage IV), which then closes the shutters resets the system. This device is self-starting and generates piston-like oscillatory motion.

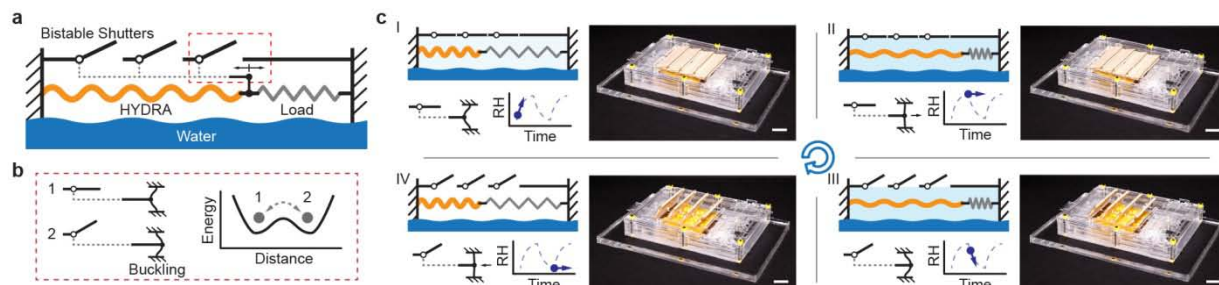


Figure 4 (a) The oscillator is comprised of horizontally placed HYDRAs coupled to a load spring and shutters that control permeation of moisture. (b) Shutters are connected to a beam that is compressed beyond its buckling limit so that it has two stable configurations. As the beam switches its position due to the force exerted by HYDRAs, the shutters open and close to alter the relative humidity of the chamber. (c) Four stages of the oscillatory motion. Scale bars: 2 cm.

To demonstrate an application of the engine, we coupled the device to a generator and provided electricity to LEDs. When water temperature was maintained at 30°C, two oppositely connected LEDs gave light repeatedly in alternating order (Fig. 5b). The electrical power was measured to reach 60 μ W by replacing the LED pair with a 100-k Ω resistor (Fig. 5c,d). Our prototype demonstrates that despite the slow variations in relative humidity found in nature, it is possible to synthesize rapid fluctuations by modifying local evaporation rates at water surfaces, allowing generation of practical work for wide-ranging applications.

Future Plans

Moving forward we plan to study the potential to harvest energy from evaporation by modeling the changes in the mass/energy balance of evaporation due to changes in weather and workload while continuing to develop alternative methods to assemble spores for improved energy conversion efficiency. Additionally we aim to advance our studies of water transport within the spore nanopores using AFM based methods described herein. We also plan to model the mechanical behavior of spore nanostructures mathematically in relation to predicted energy densities to better understand and optimize relevant water-responsive synthetic or genetically altered biomolecular materials.

References:

[1] X. Chen, D. Goodnight, Z. Gao, A.H. Cavusoglu, N. Sabharwal, M. DeLay, A. Driks and O. Sahin. Scaling up nanoscale water-driven energy conversion into evaporation-driven engines and generators. *Nature Communications* 6:7346 (2015).

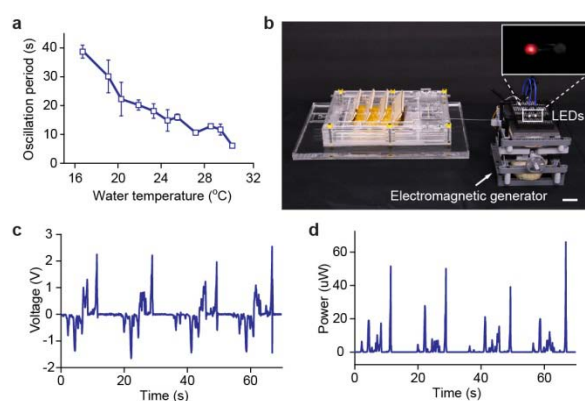


Figure 5 (a) Average oscillation period as a function of water surface temperature. (b) Picture of the oscillator connected to an electromagnetic generator using a thread. The inset photo of the LEDs is taken during operation. (c, d) Voltage and power measured across a load resistor of 100 k Ω . Scale bars: 2 cm.

Publications

1. X. Chen, L Mahadevan, A. Driks and O. Sahin. *Bacillus* spores as building blocks for stimuli-responsive materials and nanogenerators, *Nature Nanotechnology* **9**, 137-141 (2014).
2. X. Chen, D. Goodnight, Z. Gao, A.H. Cavusoglu, N. Sabharwal, M. DeLay, A. Driks and O. Sahin. Scaling up nanoscale water-driven energy conversion into evaporation-driven engines and generators. *Nature Communications* **6**:7346 (2015).

Exploration of Chemically-Tailored, Hierarchically-Patterned 3-D Biogenic and Biomimetic Structures for Control of Infrared Radiation

Kenneth H. Sandhage (PI), School of Materials Science and Engineering, Georgia Institute of Technology, Atlanta, GA 30332

Joseph W. Perry (Co-PI), School of Chemistry and Biochemistry, Georgia Institute of Technology, Atlanta, GA 30332

Program Scope

Nature provides impressive examples of organisms that utilize complex, 3-D, hierarchically-patterned structures to achieve spectacular control of visible light. For example, certain species of diatoms form SiO₂-based frustules, possessing particular overall morphologies decorated with intricate fine features, that exhibit selective transmission, reflection, and/or transmission of light. Certain butterflies form chitin-based scales with intricate 3-D patterns tailored for the reflection of particular wavelengths of light (i.e., to achieve desired color or color patterns). While the control of visible light by biological structures has been a highly-researched topic, the interactions of such structures, and of biomimetic analogues, with IR light has not. The control of IR radiation is important for a number of devices and applications related to energy harvesting (e.g., concentrated solar thermal power; photovoltaic cells; thermoelectric devices) and energy use (e.g., thermal management, ranging from electronic devices to buildings).

The **objectives** of this research effort are: i) To learn how to shift the optical transmission and reflection behaviors of biological structures from the visible into the infrared via chemical conversion of such structures into synthetic IR materials, and ii) To obtain fundamental understanding as to how biological structures may be mimicked and coupled with synthetic inorganic chemistries to enable a new generation of biomimetic materials for controlling IR radiation.

The proposed effort comprises 3 collaborative thrusts:

Thrust I: Chemical conversion of bio-enabled SiO₂-bearing structures into high-refractive index IR materials. SiO₂-based diatom frustules with particular overall frustule shapes and fine features, and oxide replicas (see Thrust II) of the scales of butterflies with particular 3-D reflective structures, will be chemically converted into 3-D replicas comprised of nanostructured materials with high IR refractive indices. Kinetic mechanisms and nanostructural evolution upon such reactive conversion will be evaluated to allow for high-fidelity replication.

Thrust II: Syntheses of structurally-tailorable biomimetic inorganic assemblies. SiO₂ diatom-mimetic structures and oxide replicas of butterfly-mimetic structures (with tailorable morphologies) will be synthesized via coating of transient patterned templates formed by multiphoton lithography and other patterning methods. The influences of surface treatments, oxide precursors,

coating conditions, and drying and pyrolysis kinetics on nanostructural evolution of the oxide coatings will be examined. These structures will then be converted (Thrust I) into IR replicas.

Thrust III: Simulation and measurement of bio-enabled IR transmission and reflection.

Simulations will be used to predict and evaluate: i) how the morphologies of high-index replicas of diatom frustules, and biomimetic analogues, affect IR transmission, and ii) how butterfly scale morphologies, and associated biomimetic structures, comprised of high-index replicas affect IR reflection. Modelling of IR behavior will be used to guide the design and syntheses of new lightweight bio-enabled structures with tailorable IR transmission and/or reflection.

Recent Progress

This project has only just begun (start date of July 1, 2015).

Future Plans

See above.

Publications

None yet.

A Modular Architecture for Dynamic, Environmentally Adaptive DNA Nanostructures

Rebecca Schulman, Departments of Chemical and Biomolecular Engineering and Computer Science, Johns Hopkins University

Program Scope

Within cells, the cytoskeleton orchestrates functions such as motility, the organization of chromatin, and directed cellular transport. A relatively small set of filament components and proteins that organize filaments form a diverse array of structures because different spatiotemporally controlled processes of assembly and disassembly can produce different assembled structures. The decision about which architecture to form within a cell is made by signal transduction programs and gene expression programs that sense chemical and physical input signals and produce outputs that control the abundance and activity of cytoskeletal building materials, thereby controlling what is assembled. These circuits make it possible for the cytoskeleton to respond in complex ways to simple signals and *vice versa*, and to respond to chemical or physical signals that do not directly interact with cytoskeletal components.

The cytoskeleton illustrates how components that can self-assemble into different structures and molecular circuits that control their assembly can together produce a complex material that can take on many programmable

forms that adapt to the environment. The goal of our program, in collaboration with Prof. Elisa Franco, is to develop programmable active materials made from synthetic DNA components using the cytoskeleton as a model. The architectures we build are formed from DNA nanotubes assembled from small tile monomers² (Figure 1), semi-flexible polymer fibers with a persistence length similar to actin fibers³ and a structure similar to microtubules. DNA origami structures⁴ organize nanotubes into functional architectures, and DNA-based molecular circuits that sense inputs and produce outputs that in turn direct the assembly and disassembly of nanotube architectures. The ability to program the architecture of synthetic fibers could make it possible to create a toolkit of components that can form many different structures in different environments and to build materials that self-heal or metamorphose.

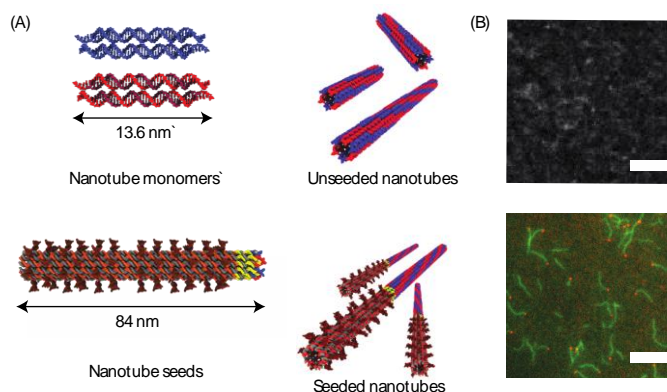


Figure 1: (A) DNA nanotubes assemble from tile monomers. Nanotube seeds present a template that allows nanotubes to form with a minimal nucleation barrier. (B) Few nanotubes form without seeds (top) as compared to when seeds are present (bottom, seeds red, nanotubes green). Scale bars 5 μm .

Recent Progress

1. Tinkertoy materials for assembling nanotube architectures. To build a system in which nanotube filaments can be assembled into architectures, we have designed a set of *nanotube organizing structures* that can control the arrangement of nanotubes. *Organized nanotube growth sites* control how nanotubes are arranged by controlling where nanotubes nucleate to form specific types of junctions, and *nanotube caps* attach to growing nanotube ends, terminating nanotube growth.

Nanotube organizing structures work by directing nanotube assembly: nanotubes can grow from specific sites on organizing structures but tend not to nucleate otherwise (Figure 1). Our

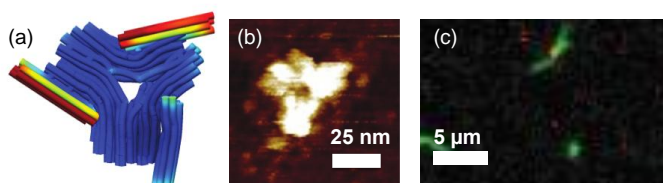


Figure 2: An organized growth site for DNA nanotubes can direct the formation of specific nanotube architectures. (a) a cadNano¹ model of a triangle organizing site. (b) Atomic force micrograph of the organizing site. (c) Fluorescence micrograph of nanotubes (green) grown from organized growth sites (red).

collection of organized nanotube growth sites includes structures that can connect the same or different types of nanotubes with a floppy linker, a structure that can direct the nucleation of two nanotubes at a 90° angle with respect to one another and three nanotubes at angles of 120° (Figure 2). Nanotube organizing structures are assembled using the DNA origami technique; the versatility of this

technique means that it is straightforward to precisely control the number of nanotube nucleation sites and the angles between these sites⁵. We have used fluorescence microscopy, atomic force microscopy and transmission electron microscopy to verify that both the structures of the nanotube organizing structures and the nanotube architectures that grow from them correspond to the designed structures. To verify that nanotube caps bind to nanotubes and stop nanotube growth, we have used time-series fluorescence micrographs, analogous to those in our previous investigations⁶ to show that when nanotube caps are added to a solution of growing nanotubes, nanotubes stop increasing in length.

2. DNA strand-based control of nanotube organizing structure and cap activity. A powerful way to assemble dynamic nanotube architectures is to control the activity of nanotube organizing structures and nanotube caps in space and time. We have developed a flexible mechanism for activating and deactivating nucleation sites on organizing structures and capping sites using short DNA strands with specific sequences. These DNA strands add or remove essential components of these structures *via* strand displacement reactions in order to turn on or off the function of the corresponding nucleation sites. The combinatorial variety of available DNA sequences makes it possible to program the design systems where different DNA strands activate or deactivate different nanotube nucleation or capping sites. We have verified that the addition of specific DNA strands can be used to activate nanotube nucleation and capping using fluorescence microscopy. Autonomously controlling the activation and deactivation of different

sites at different times or in response to particular environmental stimuli will make it possible to build complex, environmentally responsive assembly programs.

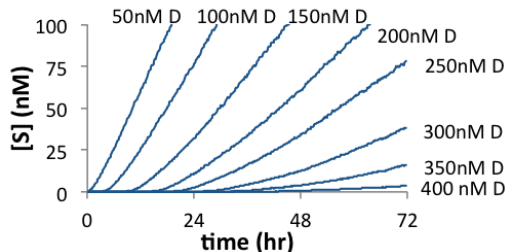


Figure 3: Output of a molecular circuit that produces a signal S after a controlled delay. The concentration of a delay element D controls the delay length. Several such circuits could be used to order a self-assembly process by releasing triggers for different assembly events at different times.

two completely designed DNA strand outputs and a cascade in which a VEGF input controls the free concentration of one of the two outputs for the thrombin cascades. In each case, one-parameter fits enabled quantitative prediction of the DNA strand output concentration as a function of protein input concentration.

4. Programmed control of assembly timing using DNA delay circuits.

An important feature of biological systems for directing the assembly of complex structures is the ability to trigger a complex assembly program in response to a single environmental stimulus. We are working to develop this capacity using DNA strand displacement circuits. We have recently developed a simple DNA strand displacement delay circuit that begins to produce an output after a prescribed delay that can be programmatically controlled by varying the concentrations of the components (Figure 3). Delays from 10-70 hours are possible and

3. Programming responses to disparate environmental inputs.

(1) and (2) describe mechanisms for designing nanotube architectures that can be altered through the addition of specific DNA strands. In order to control DNA nanotube architectures using inputs other than DNA strands, we have developed a modular mechanism called aptamer exchange for translating small molecular or protein inputs into DNA strand outputs. To demonstrate the utility and versatility of this method, we have constructed cascades in which thrombin is an input to two cascades that produce

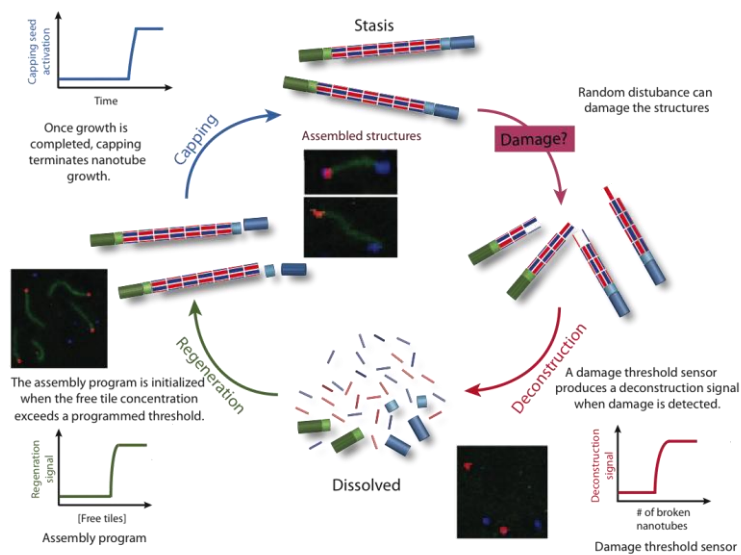


Figure 4: A schematic for self-regenerating nanotube structures, along with fluorescence micrographs of nanotubes in each of the illustrated state. Nucleic acid circuits monitor assembled structures and when they detect damage (by sensing molecules that are usually sequestered in the nanotube interior), initiate a cascade that disassembles damaged structures and reassembles the designed structures.

release rates can be controlled across two orders of magnitude. Further, multiple delays for different outputs can be programmed for different signals in the same test tube.

Future Plans

The development of a toolkit for interpreting environmental signals and using them to programmably control the assembly and disassembly of DNA nanotube architectures will make it possible to build materials with both complex architectures and complex dynamic responses to a variety of input signals. We plan to use the toolkit that we have been developing to build materials that can serve as a proof of concept for these new capacities. One research direction is to develop nanotube architectures that are self-regenerating (Figure 4). This work will require that we integrate the capacity to control the activity of nanotube nucleating sites and caps using DNA strands with circuits that release outputs that change this activity. To make it possible to detect when DNA nanotubes are damaged, we will augment existing tile monomers with sequences that become sequestered during tube assembly, so that increases in the free concentration of these tags will indicate nanotube damage or disassembly.

References

- 1 Castro, C. E. *et al.* A primer to scaffolded DNA origami. *Nat Methods* **8**, 221-229, doi:10.1038/nmeth.1570 (2011).
- 2 Rothmund, P. W. *et al.* Design and characterization of programmable DNA nanotubes. *Journal of the American Chemical Society* **126**, 16344-16352, doi:10.1021/ja044319l (2004).
- 3 Gittes, F., Mickey, B., Nettleton, J. & Howard, J. Flexural rigidity of microtubules and actin filaments measured from thermal fluctuations in shape. *The Journal of cell biology* **120**, 923-934 (1993).
- 4 Rothmund, P. W. Folding DNA to create nanoscale shapes and patterns. *Nature* **440**, 297-302, doi:10.1038/nature04586 (2006).
- 5 Douglas, S. M. *et al.* Rapid prototyping of 3D DNA-origami shapes with caDNAno. *Nucleic acids research* **37**, 5001-5006, doi:10.1093/nar/gkp436 (2009).
- 6 Mohammed, A. M. & Schulman, R. Directing self-assembly of DNA nanotubes using programmable seeds. *Nano letters* **13**, 4006-4013, doi:10.1021/nl400881w (2013).

Publications

1. Deepak Agrawal, Elisa Franco and Rebecca Schulman. A Self-Regulating Biomolecular Comparator for Processing Oscillatory Signals. Proceedings of American Control Conference, 2015. Journal article submitted.
2. Abdul M. Mohammed, John Zenk and Rebecca Schulman. Adaptive Self-Assembly of DNA Nanotube Connections Between Molecular Landmarks. In preparation.
3. Deepak Agrawal and Rebecca Schulman. Universal Aptamer Exchange. In preparation.
4. Dominic Scalise, Angelo Cangialosi, Dylan Howie and Rebecca Schulman. DNA Strand-Displacement Timer Circuits. In preparation.

Biopolymers Containing Unnatural Amino Acids

Peter G. Schultz, The Scripps Research Institute

Program Scope

Control over the composition of polymers remains a challenge – it is difficult to define the sequence of chain elongation when mixtures of monomers are polymerized, and postpolymerization side chain modification is made difficult by polymer effects on side chain reactivity. In contrast, the mRNA templated synthesis of polypeptides on the ribosome affords absolute control over the primary sequence and length of the twenty amino acid monomers. However, whereas synthetic polymers can be synthesized from monomers with a wide range of chemically defined structures, ribosomal biosynthesis is largely limited to the 20 canonical amino acids. To generate biopolymers with novel material properties, ideally one would like the ability to incorporate structurally distinct unnatural building blocks at any number of defined sites in a polymer chain. For example, collagen which is one of the most commonly used biomaterials has regularly repeating hydroxyproline residues as well as lysyl crosslinks. Both are introduced by extensive posttranslational modification which has made recombinant expression of collagen like materials difficult. In previous funding periods we have developed and applied technology that allows one to efficiently genetically encode noncanonical amino acids with novel structures and properties in bacteria. In order to use templated-directed ribosomal synthesis to produce unnatural biopolymers with chemically defined side chain and backbone sequences, we are developing (1) efficient methods to recombinantly introduce multiple distinct building blocks into a single polymer chain; and (2) efficient methods to screen or select for such polypeptides with novel properties. We will then begin to apply these advances to generate novel collagen-like polypeptides recombinantly, and analyze the effects of changes in structure on properties. Taken together these efforts should significantly impact our ability to use Nature's programmable translational machinery to begin to produce a new class of hybrid biopolymers with novel materials properties.

Recent Progress

(1) Ribosomal templated synthesis of novel biopolymers. The ability to use the ribosomal mRNA-templated biosynthetic machinery to synthesize biopolymers from novel building blocks requires: (1) efficient methods to incorporate one or more distinct noncanonical amino acid at multiple sites throughout the biopolymer, and (2) unique codons not assigned to the 20 canonical amino acids. Among the 64 triplet codons, only the three nonsense "stop" codons have been used to encode noncanonical amino acids. Use of quadruplet "frame-shift" suppressor codons provides an abundant alternative but suffers from low suppression efficiency. Deletion of release factor 1 in a genomically recoded strain of *E. coli* (*E. coli* C321) in which all endogenous amber stop codons (UAG) are replaced with UAA abolished UAG mediated

translation termination.¹ We have shown that a *Methanocaldococcus jannaschii*-derived frame-shift suppressor tRNA/aminoacyl-tRNA synthetase pair enhanced UAGA suppression efficiency in this recoded bacterial strain.² We have also developed an enhanced suppression system that enables the expression of proteins incorporating unnatural amino acids (UAA) at up to three sites.³ However, the efficiency of this process needs to be improved to biosynthesize biopolymers that incorporate UAAs throughout their sequence. We are now developing a systematic strategy to evolve *E. coli* strains in which multiple UAAs can be efficiently genetically incorporated into the same polypeptide and can be incorporated in response to all four UAGN codons. An *E. coli* strain library generated by chemical mutagenesis will be subjected to a novel complementation selection system for increased suppression of multiple amber codons within an essential gene. To this end a dual selection plasmid containing a pyrF gene with multiple amber codons or UAGN at permissive sites, a chloramphenicol acetyltransferase gene with the Asp112TAG mutation and an amber suppressor pyrrolysyl-tRNA synthetase (PylRS)/tRNA pair has been constructed. The genomic mutagenesis library with the selection plasmid is being subjected to the selection based on the growth rates of strain variants in the M9-glycose minimal medium with H-Lys(Boc)-OH. To elucidate the mechanism of functional mutations in the genome, genomic sequencing will be performed on the new strains. The above advances will allow us to further increase the number of building blocks that can be used to biosynthesize novel polymers.

(2) Evolving proteins with novel activities using an expanded genetic code. An open question whether organisms with additional amino acids beyond the common twenty might have an evolutionary advantage in the generation of proteins with novel or enhance properties. We have begun to test this notion by asking whether one can enhance the physical properties of proteins, in particular the thermal stability of the enzyme MetA. Specifically, we are making libraries of proteins containing chemically reactive amino acids that can form covalent crosslinks

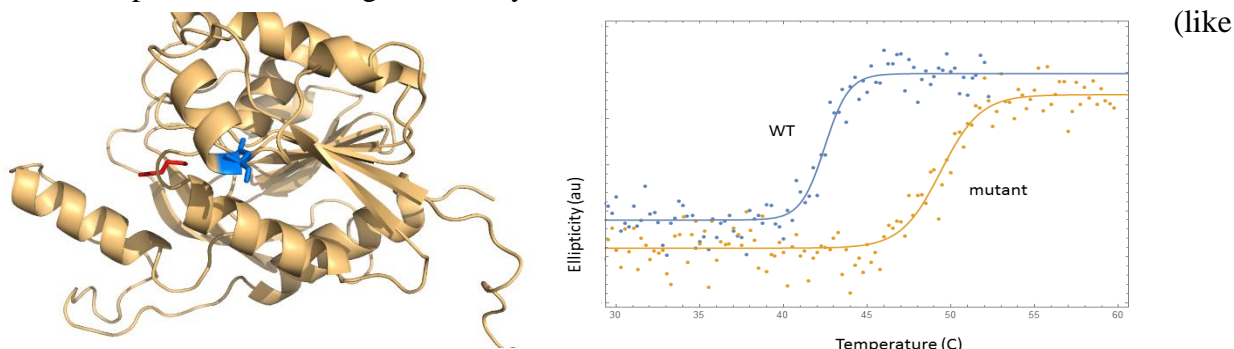


Figure 1. A). *E. coli* metA structure predicted through homology modeling using PDB entry 2VDG (SWISS-MODEL). Position N86 is shown in red. B). CD melt of wild type metA (wt) and N86OtBuY metA (mutant). Melting temperature for wild type and mutant metA wer

collagen) and amino acids that may improve stability through improved packing interactions. In a previous study, it was shown that the growth of *E. coli* is greatly inhibited at elevated temperatures (44 °C) in minimal media due to the thermal instability of a homoserine o-succinyltransferase (metA), which unfolds and aggregates above 40 °C.⁴ It was shown that by moderately increasing metA stability and reducing aggregation, *E. coli* can exhibit greatly enhanced growth at 44°C.^{5,6} To select for metA proteins with improved stability owed to an unnatural amino acid, a metA TAG scanning library was generated using site directed

mutagenesis on 261/309 residues. The library was transformed into *E. coli* strain JW3973 (Δ metA) with a UAA synthetase/tRNA pair and was used for an initial screen with a collection of unnatural amino acids – pAcF, pFACF, pAzF, OMeY, pIF, pBrF, OtBuY, OallyY, and pAcryIF. *E. coli* transformed with this library was grown at 44 °C in liquid culture, such that *E. coli* with more stable metA mutants will outgrow ones with less stable mutants⁶, where a strong consensus (N86TAG) was observed in the presence of UAA OtBuY. (Fig. 1)The recombinant metA N86OtBuY mutant was expressed and purified, and its thermostability compared to WT metA by circular dichroism spectroscopy, where a ~7 °C increase in melting temperature was observed(Fig. 1). Next, a crystal structure of metA variants will be solved to determine the mechanism of this specific UAA in improving enzyme thermostability. We have also identified a p-boronophenylalanine mutant that also appears to have increased stability by forming a covalent dimer. These experiments are beginning to demonstrate that an expanded genetic code will make accessible proteins with new or enhanced properties for a variety of applications.

(3) Engineering orthogonal aminoacyl-tRNA synthetics to encode building blocks for collagen like polymers.

To create novel biopolymers like collagen we need to encode additional building blocks with a range of chemical functionality. Currently the most versatile orthogonal aminoacyl-tRNA synthetases (aaRS) are based on archaea-derived tyrosyl and pyrrolysyl tRNA/aaRS pairs.^{7,8} An engineered seryl-tRNA synthetase might offer the ability to

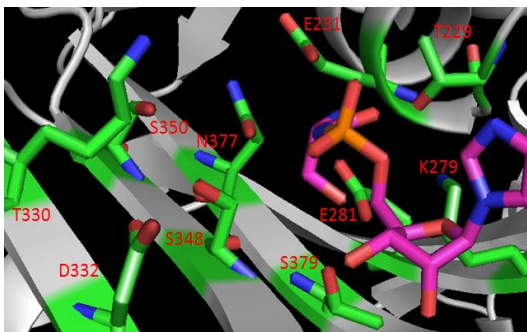


Figure 2. Residues in NNK5 and NNK6 libraries. The labeling is based on MmSerRS.

genetically encode aliphatic amino acids with novel functional groups (amino, cyano, acryl, alkenyl, etc.). To this end we have begun to evolve an orthogonal tRNA/aaRS pairs using AfSer-tRNA (from *Archaeoglobus fulgidus* DSM 4304) and Mm Seryl-tRNA synthetase (from *Methanosarcina mazei*) as the starting points. The anticodon of the AfSertRNA was mutated to 5'-CUA to allow amber suppression, and 5'-CCA was added to the 3'-terminus. A tRNA library was constructed by randomizing the first five base pairs in the acceptor stem, and subjected to a round of negative selection

(barnase TAG suppression) followed by a round of positive selection (chloramphenicol TAG suppression). Colonies surviving much higher (> 60 µg/mL) chloramphenicol were sequenced, and an orthogonal tRNA was identified and validated. To select for aaRS's that incorporate noncanonical amino acids, selection libraries (NNK5 and NNK6) are being constructed on the basis of the crystal structure of a homologous seryl-tRNA synthetase from *Pyrococcus horikoshii*.⁹ In both libraries, S379 is fixed to alanine in order to eliminate the serine loading activity of the wildtype synthetase; the NNK5 library targets T330, D332, S348, S350, N377, and the NNK6 library targets T330, D332, S348, S350, N377 (Fig.2). With these libraries in hand, alternating positive and negative selection will be carried out to evolve synthetases specific for amino acids with novel functional groups

Future Plans. In the next period the will focus on the following: (1)Continue to enhance our ability to simultaneously incorporate multiple noncanonical building blocks into biopolymers by expanding the number of unique codons and improving the efficiency of suppressing multiple

noncoding codons in a single protein. We are characterizing the first round of mutant strains from selections based on (TAG) constructs and are constructing the TAGN selection scheme: (2) Continue studies aimed at using random mutagenesis and selection schemes with an expanded genetic code to improve the stabilities of proteins. We will also carry out detailed structural studies of these proteins to understand the molecular basis for the increased stability: and (3) Evolve orthogonal tRNA/aaRS pairs that accept aliphatic amino acids with novel functional groups in their side chains. We are currently in the panning libraries of the Seryl-tRNA synthetase using a variety of aliphatic amino acids with novel structures and reactivity. Together these advances will allow us to begin to make “unnatural” biopolymers with novel materials properties using the templated biosynthetic machinery of Nature.

References

1. Lajoie, M.J., Rovner, A.J., Goodman, D. B., Aerni, H.-R., Haimovich, A.D., Kuznetsov, G., Mercer, J.A., Wang, H.H., Carr, P.A., Mosberg, J.A., Rohland, N., Schultz, P.G., Jacobson, J.M., Rinehart, J., Church, G.M., Isaacs, F.J. "Genomically recoded organisms expand biological functions" *Science*, 2013, 342, 357–360.
2. Chatterjee, A., Lajoie, M.J., Xiao, H., Church, G.M., Schultz, P.G. "A Bacterial Strain with a Unique Quadruplet Codon Specifying Non-native Amino Acids" *ChemBioChem*, 2014, 15, 1782-1786.
3. Chatterjee, A., Sun, S.B., Furman, J.L., Xiao, H., Schultz, P.G. "A versatile platform for single and multiple unnatural amino acid mutagenesis in Escherichia coli" *Biochemistry*, 52(10):1828-1837, 2013.
4. Gur, E., Biran, D., Gazit, E., Ron, E.Z. "In vivo aggregation of a single enzyme limits growth of Escherichia coli at elevated temperatures" *Molecular Microbiology* (2002) 46(5), 1391-1397
5. Mordukhova, E.A., Lee, H., Pan, J. "Improved Thermostability and Acetic Acid Tolerance of Escherichia coli via Directed Evolution of Homoserine o-Succinyltransferase" *Appl. Environ. Microbiol.* 2008, 74(24), 7660-7668
6. Mordukhova, E.A., Kim, D., Pan, J. "Stabilized homoserine o-succinyltransferases (MetA) or L-methionine partially recovers the growth defect in Escherichia coli lacking ATP-dependent proteases or the DnaK chaperone" *BMC Microbiology*, 2013, 13:179
7. Liu, C.C., Schultz, P.G. "Adding New Chemistries to the Genetic code" *Annual Review of Biochemistry*, 2010, 79, 413-444.
8. Wan, W., Tharp, J.M., Liu, W.R. "Pyrrolysyl-tRNA synthetase: An ordinary enzyme but an outstanding genetic code expansion tool" *Biochimica et Biophysica Acta*, 2014, 1844, 1059–1070.
9. Itoh, Y., Sekine, S., Kuroishi, C., Terada, T., Shirouzu, M., Kuramitsu, S., Yokoyama, S. "Crystallographic and mutational studies of seryl-tRNA synthetase from the archaeon *Pyrococcus horikoshii*" *Rna Biology*, 2008, 5(3), 169-177.

Publications

Xiao, H., Schultz, P.S. "At the Interface of Chemical and Biological Synthesis: An Expanded Genetic Code" *CSH Perspectives*, *submitted*, March 2015.

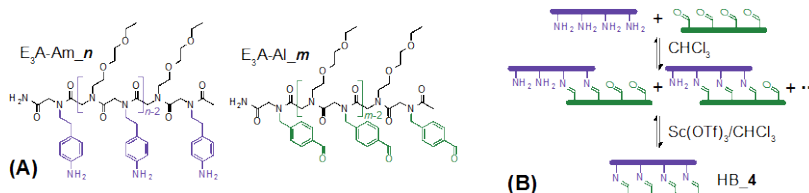
This work was supported by DOE Grant DE-SC0011787 (PGS). This is manuscript number 29056 of The Scripps Research Institute.

Fabrication and Assembly of Robust, Water-Soluble Molecular Interconnects via Encoded Hybridization

Timothy F. Scott, Department of Chemical Engineering, University of Michigan

Program Scope

The dynamic covalent self-assembly of sequence-specific oligomers is employed as a unique approach to the deterministic fabrication of thermally, chemically, and mechanically robust molecular interconnects and nanostructures. In contrast to Watson-Crick base pairing, which is mediated by hydrogen bonds, dynamic covalent base pairs are utilized whose dimerization reactions are orthogonal and reversible by carefully controlling the reaction mixture acidity, such as the boronic acid/vicinal diol and amine/aldehyde condensations. Model peptoid-based oligomers that incorporate alternating pendant functional groups, where the first monomer type is hydrophilic and the second able to participate in dynamic covalent reactions, are synthesized and nuclear magnetic resonance (NMR) spectroscopy, gel permeation chromatography (GPC) and electrospray ionization (ESI) and matrix-assisted laser desorption/ionization (MALDI) mass spectrometry are performed to examine the reaction kinetics and thermodynamic equilibrium of the base pair condensation and oligomer hybridization reactions (Scheme 1). Subsequently, monomers incorporating the most promising hydrophilic groups and dynamic covalent reactants, determined from the model peptoid oligomer reactions, are synthesized and utilized in conventional solid-phase synthesis to generate sequence-specific, water-soluble oligo(phenylene-ethynylene) strands. Upon cleavage from the solid support, mixtures of oligomers bearing the reversible functional groups self-assemble *via* hybridization between strands with complementary sequences. ESI mass spectrometry, GPC, and fluorescence microscopy are performed to determine the hybridization specificity between pairs of complementary, mismatched, and parallel/anti-parallel strands.



Scheme 1. Dynamic covalent assembly of peptoid-based molecular ladders. **a**, Structures of linear oligopeptoids bearing pendant amine (E^3A-Am_n) and aldehyde (E^3A-Al_m) functional groups. **b**, Dimerization of complementary peptoid oligomers with commensurate functionalities (HB_n).

Recent Progress

Oligomeric peptoid sequences incorporating pendant aldehyde, amine, boronic acid, and catechol functional groups were prepared using the ‘submonomer’ solid-phase peptoid synthesis

approach. These peptoid sequences were synthesized as alternating co-oligomers consisting of dynamic covalent monomer residues, utilizing monomers bearing dynamic covalent- reactive functional groups protected with acid-labile groups to prevent unwanted side reactions during solid-phase synthesis, interspersed with inert residues.

Preliminary hybridization experiments of

peptoids incorporating benzylamine or 2-methoxyethylamine as inert spacer residues resulted in rapid formation of a precipitate after complementary oligomer mixing, indicating poor solubility of the assembled structures. However, molecular ladders with up to twelve rungs were successfully fabricated by dynamic covalent dimerization of aldehyde- and amine-based oligopeptoids (see Figure 1) by utilizing 2-(2-ethoxyethoxy)ethylamine (E3A) as the spacer residue to ensure solubility of both the unhybridized oligomers and the subsequent assembled molecular ladders.

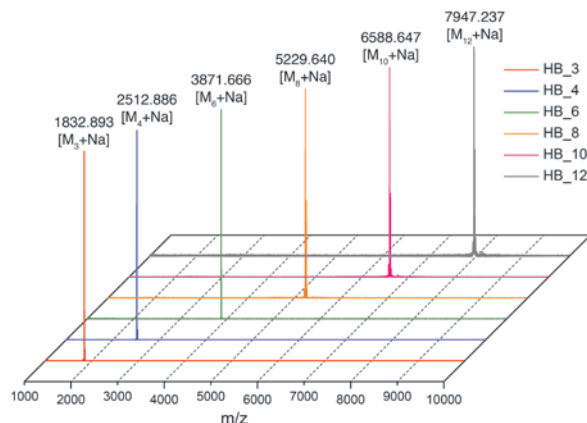
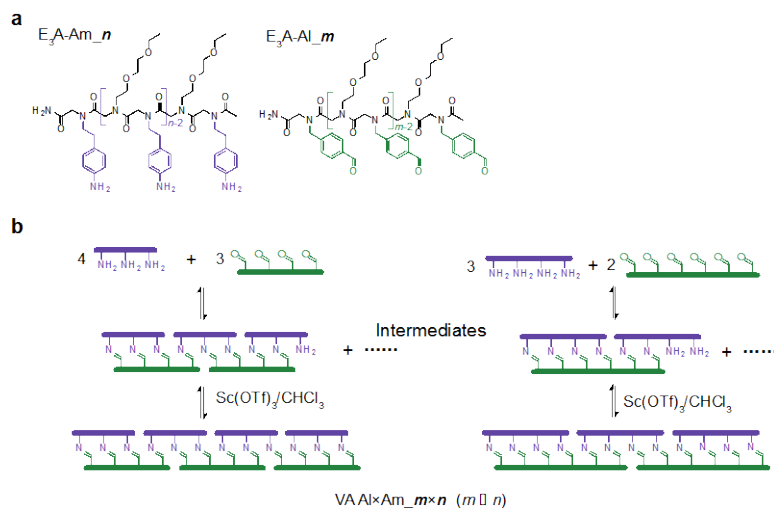


Figure 1. Molecular ladders formed by dynamic covalent oligopeptoid dimerization. **a**, MALDI mass spectra of the crude reaction mixtures. Calculated molecular weights: $[M_{HB_3}+Na]^+ = 1832.927$; $[M_{HB_4}+Na]^+ = 2512.286$; $[M_{HB_6}+Na]^+ = 3871.002$; $[M_{HB_8}+Na]^+ = 5229.718$; $[M_{HB_{10}}+Na]^+ = 6588.434$; $[M_{HB_{12}}+Na]^+ = 7947.150$.

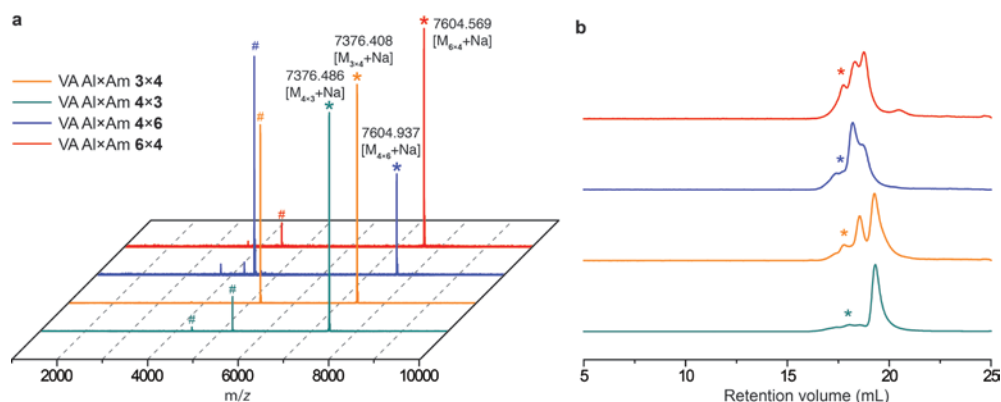


Scheme 2. Vernier-templated assembly of complementary oligopeptoids with non-commensurate functionalities. **a**) Given the structures of linear oligopeptoids bearing pendant amine (E^3A-Am_n) and aldehyde (E^3A-Al_m) functional groups, **b**) the resultant assembled molecular ladders possess the least common multiple of $m \times n$ rungs ($VAAl \times Am_m \times n$).

As thermodynamically disfavored but kinetically trapped products will necessarily be generated for sufficiently long precursor oligomers, and indeed the synthesis and purification of such oligomers is itself challenging, we investigated Vernier templating as an alternative and facile approach to achieve large molecular ladders *via* the dynamic covalent assembly of small oligomeric species (see Scheme 2).

This approach to attain large molecular ladders was successfully demonstrated using

non-commensurate functionality aldehyde- and amine-based oligopeptoids. MALDI mass spectra and gel permeation



chromatography (GPC) traces of the crude hybridization reaction mixtures utilizing non-commensurate length precursor strands shown in Figure 2 a and b, respectively,

Figure 2. Molecular ladders formed by dynamic covalent oligopeptoid dimerization. a) MALDI mass spectra of the crude reaction mixtures. The target ladder structures are labeled with * symbols and the intermediates are labeled with #. Calculated molecular weights for the target ladders: $[M_{3 \times 4} + Na]^+ = [M_{4 \times 3} + Na]^+ = 7376.810$; $[M_{4 \times 6} + Na]^+ = [M_{6 \times 4} + Na]^+ = 7604.946$. Intermediates are identified as $(E^3A-Al_3)_3(E^3A-Am_4)_2$; $(E^3A-Al_4)_2(E^3A-Am_3)_3$, $(E^3A-Al_4)_2(E^3A-Am_3)_2$; $(E^3A-Al_4)_2(E^3A-Am_6)_1$; $(E^3A-Al_6)_1(E^3A-Am_4)_2$. b) GPC traces for crude reaction mixtures (PS standards). The traces are normalized to the height of the largest peak. The target ladder structures are labeled with * symbol. VA_Al x Am_3 x 4, $V_r = 17.783$ mL, $M_n = 7272.692$, PDI = 1.040; VA_Al x Am_4 x 3, $V_r = 17.811$ mL, $M_n = 7124.223$, PDI = 1.045; VA_Al x Am_4 x 6, $V_r = 17.725$ mL, $M_n = 7503.989$, PDI = 1.063; VA_Al x Am_6 x 4, $V_r = 17.726$ mL, $M_n = 7638.854$, PDI = 1.011.

demonstrate major peaks assignable to the desired 12-rung ladder structures with observed molecular weights equivalent to the expected values, demonstrating the success of this dynamic covalent approach to Vernier-templated self-assembly. Notably, in addition to the desired product, both the mass spectra and chromatograms also indicate the presence of partially-assembled intermediates. For example, mass spectra of the trimer and tetramer peptoid co-reactions revealed peaks corresponding to partially-assembled intermediates of $(E^3A-Al_3)_3(E^3A-Am_4)_2$ for the trialdehyde/tetraamine system, and $(E^3A-Al_4)_2(E^3A-Am_3)_3$ and $(E^3A-Al_4)_2(E^3A-Am_3)_2$ for the tetraaldehyde/triamine system. Similarly, for the tetramer and hexamer peptoid co-reactions, additional peaks in the mass spectra are assignable to the intermediate $(E^3A-Al_4)_2(E^3A-Am_6)_1$ for the tetraaldehyde/hexamine system, and $(E^3A-Al_6)_1(E^3A-Am_4)_2$ for the hexaaldehyde/tetraamine system. We believe that the attained mixtures, composed of the desired Vernier ladders and partially-assembled intermediates, may in part be attributable to the respective reactions having yet to achieve equilibrium or, more likely given the extended reaction times, be an artifact of the functional group stoichiometric ratios for each reaction not being precisely 1:1, resulting in the molecular ladder mixtures observed.

Future Plans

Having determined appropriate hybridization conditions for the aldehyde/amine dynamic covalent reactant pair and examined the reaction kinetics of this system, we will continue refining reaction conditions necessary for boronic acid/catechol oligomer hybridization. As the

backbone of the model peptoid oligomers currently under examination is achiral and does not afford directional hybridization selectivity, we will also synthesize dynamic covalent peptide oligomers to induce selective anti-parallel hybridization between complementary oligomers and afford double helicity in the resultant structure. Subsequently, we will determine the conditions to afford quantitative *in situ* protecting group cleavage and examine the hybridization of oligomers bearing the four dynamic covalent reactants. Finally, π -conjugated, sequence specific phenylene-ethynylene oligomers bearing dynamic covalent pendant groups will be synthesized and their dynamic covalent self-assembly examined.

Publications

T. Wei, J.-H. Jung, T. F. Scott, Dynamic Covalent Assembly of Peptoid-Based Ladder Oligomers by Vernier Templating, (submitted).

Self-assembly for colloidal crystallization and biomimetic structural color

Michael J. Solomon and Sharon C. Glotzer, University of Michigan Ann Arbor

Program Scope

The focus of this research program is to understand the self- and field-assisted assembly of anisotropic particles into colloidal crystals with iridescent structural color by measuring their phase behavior, assembled unit cell symmetry, defect structure, and spectral response due to diffraction. Colloidal crystals produce structural color because their periodic physical structure diffracts light at Bragg resonances. The complex structural color response of living systems is linked to the presence of structural morphologies more complex than simple close-packed arrays; we seek these more complex symmetries by assembly of anisotropic building blocks. The objectives of our work are to: (1) Describe the fundamental relationship between colloidal particle anisotropy, in both shape and pair potential interactions, and the symmetry of unit cells that can be assembled at high volume fraction and under the effect of applied fields; (2) Understand how colloidal building block anisotropy and the characteristics of applied fields mediate the crystal quality of assembled structures, as quantified by measures such as crystal fraction, crystal size, and dislocation density; (3) Measure the spectral and light diffraction response of colloidal crystals of anisotropic particles and model the response in terms of the project's real space characterization and simulation of phase diagrams, unit cell symmetries, and crystal quality.

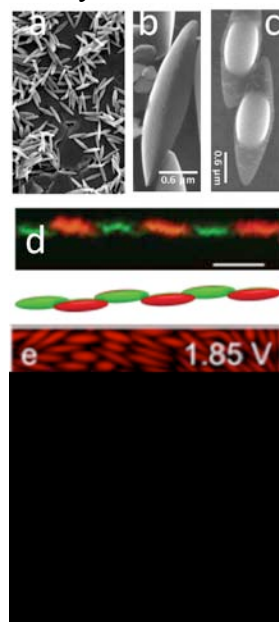


Figure 1. Synthesis (a-c), confocal microscopy (d), assembly (e), and simulation methods (f) for structural color from crystals of anisotropic colloids.

Recent Progress

The scientific approach we have developed exploits abilities to synthesize colloidal particles with homologous variations in anisotropy, use real space imaging methods involving 3D confocal microscopy, apply assembly methods based on direct and alternating current electric fields, and perform free energy analyses of equilibrium phase behavior and defect structure that can guide experiments. Figure 1 shows particles, imaging, assemblies, and effective interactions of anisotropic colloids.¹⁻⁵

Future Plans

- Measure, simulate and understand the effect of variable anisotropy on phase diagrams of anisotropic colloids. Crystals of Janus colloids are our initial target structure.
- Adapt bond order parameter formulations previously used for simulation to anisotropic colloidal assembly experiments so as to characterize defect densities and structures.

- Measure spectral and diffraction response of equilibrium assemblies produced from anisotropic colloids. Our first target is the optical response of ellipsoidal rods with nematic order, as assembled by means of steady electric fields.

References

1. Harper, E. S., Marson, R. L., Anderson, J. A., van Anders, G. & Glotzer, S. C. Shape allophiles improve entropic assembly. *Soft Matter* (2015). doi:10.1039/c5sm01351h
2. Mohraz, A. & Solomon, M. J. Direct visualization of colloidal rod assembly by confocal microscopy. *Langmuir* **21**, 5298–5306 (2005).
3. Shah, A. A., Schultz, B., Kohlstedt, K. L., Glotzer, S. C. & Solomon, M. J. Synthesis, Assembly, and Image Analysis of Spheroidal Patchy Particles. *Langmuir* **29**, 4688–4696 (2013).
4. Shah, A. A., Schultz, B., Zhang, W., Glotzer, S. C. & Solomon, M. J. Actuation of shape-memory colloidal fibres of Janus ellipsoids. *Nat. Mater.* **14**, 117–24 (2015).
5. Shah, A. A. *et al.* Liquid crystal order in colloidal suspensions of spheroidal particles by direct current electric field assembly. *Small* **8**, 1551–1562 (2012).

PROJECT TITLE: Carbon nanotubes for solar energy harvesting in plants

Michael S. Strano
Carbon P. Dubbs Professor of Chemical Engineering
Massachusetts Institute of Technology

Program Scope

Our laboratory has been interested in how we can learn from mechanisms of self-assembly and repair displayed by living plants to create human-synthesized analogs that benefit from these higher functions. This program in our laboratory is supported exclusively by the Department of Energy and has led to several important and novel areas of inquiry and technology. Nature continually develops and maintains an infrastructure for light harvesting and energy storage using the self-assembly of photosynthetic protein complexes coupled with mechanisms of repair and replacement of active components (Boghossian et al., 2011).[1] Our laboratory at MIT has produced the first such analogs in the human engineering realm, where synthesis and maintenance costs are generally recognized as prohibitive barriers to the widespread use of solar energy technologies. This area of scientific inquiry has directed us into new areas of investigation. Our work over the previous project period lead to several important discoveries relating to the interfacing of nanomaterials directly with living plants, and also in the first successful nanoparticle based engineering of the extracted chloroplast (Giraldo et al., 2014).[2] In photoenergy generation, we have extensively modelled single-walled nanotube photovoltaic efficiency to understand and optimize solar cell design by employing physical theory and chemical engineering models (Bellisario et al. 2014).[3] Both discoveries build upon our previous success with nanocarbon based photoelectrochemical cells (Ham et al., 2010) and all-carbon PV cells for near infrared solar harvesting (Jain et al., 2012) – now a rapidly growing application in this area of nanotechnology.[4,5]

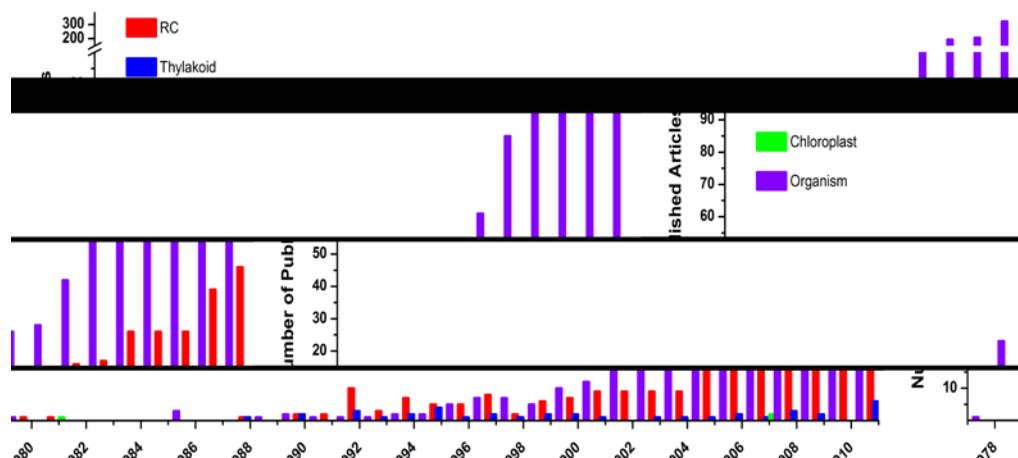


Figure 1. There has been a surge in publications using reaction centers and organisms for solar energy capture and conversion. However, the use of isolated chloroplasts is relatively unexplored.

Our success in mimicking plant self-repair directed our attention to the prospect of direct incorporation of higher level plant systems into synthetic devices, or the reverse of synthetic nanoparticles into living plants for new attributes. We argue that the chloroplast – a plant organelle organized for photosynthesis and self-repair of photosynthetic proteins – is greatly under explored as an engineering material (Figure 1). Responsible for CO₂ reduction to valuable and energy rich sugars and sugar precursors, these non-living machines perform an important chemistry given the circumstances of today with respect to atmospheric carbon and a desired for solar energy harvesting. In recent work for this DOE project, we have explored the use of nanoparticles and specific nanomaterials to ‘engineer’ new features and functions in extracted chloroplasts (Giraldo et al., 2014). We then extended these findings to living

plants themselves, outlining a new field that we tentatively call ‘plant nanobionics’. This unexplored area of materials science and nanotechnology can yield valuable contributions to technology and energy science.

The interface between plants and non-biological nanostructures has recently imparted photosynthetic organelles with new and enhanced functions. In our 2014 Nature Materials paper “Plant nanobionics approach to augment photosynthesis and biochemical sensing” (Giraldo et al., 2014), we show that single-walled carbon nanotubes (SWNT) passively transport through the lipid envelope and irreversibly localize into extracted chloroplasts. Internalized SWNT then promote over three times higher photosynthetic activity in plant tissues, and enhance maximum electron transport rates.

Recent Progress

We have built upon this work and developed design principles and a general mechanistic model for the transport of nanoparticles into chloroplasts. Significant interest lies in understanding the uptake of biological molecules such as DNA into chloroplasts due to the potential for applications including gene transfer [6] and plant synthetic biology. For instance, the forced uptake of DNA into chloroplast plastids by biolistic means involving have been studied extensively [7,8] but remains poorly understood [9], although mechanisms such as DNA penetration of the chloroplast envelop [9], transient alteration of envelop permeability, or the formation of temporal holes in membrane structures [10] have been suggested. Surprisingly, it was observed that the uptake of nanoparticles into chloroplasts were correlated to the magnitude of surface charges. This was true of both positively and negatively charged nanoparticles. Highly charged nanoparticles such as (AT)₁₅-SWNCT nanoparticles which entered the chloroplasts were further found to be irreversibly trapped, remaining within the chloroplast interior over many multiples of the time scale of entry. This is consistent with a mechanistic model which we have termed as the Lipid Exchange and Envelop Penetration (LEEP) mechanism.

Establishing design principles for the delivery of nanoparticles into chloroplasts has enabled the development a wide variety of promising applications. For instance, our lab have recently demonstrated the first nanobionic chemiluminescent plant (Figure 1). Through the delivery of silica nanoparticles functionalized with luciferase-luciferin into plant tissues, we utilize the plants own ATP to generate visible light. This enables us to indirectly utilize the energy stored by the plant photosynthetic machinery and channel it towards powering silica nanoparticles conjugated with enzymes that make plants luminescent in visible wavelengths in the dark. Having ambient background lighting generated from plants own ATP might establish new paradigms of scaled illumination, where less energy is needed to bring our environment to an adequate brightness. Here, we have essentially demonstrated the use of a plant as an engineering material to produce plant-powered illumination.

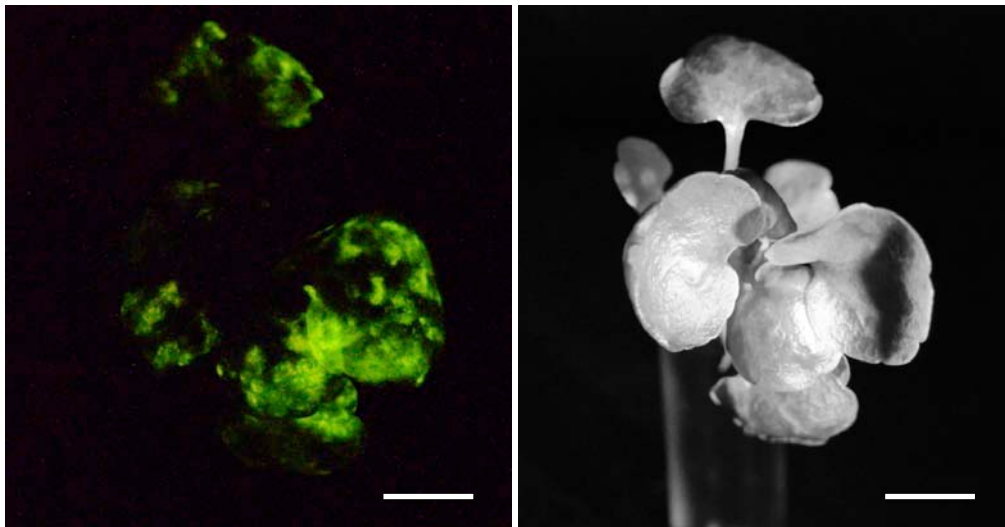


Figure 2. Chemiluminescent Plant. Watercress (3 week-old, lab grown) Photo was taken by Nikon D5300, 1 min exposure, ISO 6400, f/4.5.

In solar energy conversion with carbon nanotubes, photovoltaics using single-walled carbon nanotubes (SWNTs) as near-infrared photo-absorbers experienced high initial interest, [5,11,12] but efficiency growth slowed without an understanding of how to improve solar cell design. To address that shortcoming and improve our understanding of SWNT photo-conversion for plant applications, we derived a deterministic model of CNT photovoltaic steady-state operation directly from single- and aggregate-nanotube photophysics. We optimized that model, first solving it numerically and then analytically, to extract design principles for solar cell design and connect device efficiency to the nanotube network's intrinsic physical properties. We find that nanotube networks are most efficient when the charge collection axis is aligned with the nanotube lengths, due to high exciton diffusivity along the nanotube axis (5 orders of magnitude higher than between nanotubes). Further, we discovered that the maximum photoconversion efficiency of a nanotube network and its optimal thickness are determined by a single grouping of parameters, α , the product of the network density and the exciton diffusion length, reflecting a cooperativity between the rate of exciton generation and the rate of exciton transport. That generates a master plot mapping the EQE-maximizing film thickness to α , allowing device-makers to identify their target device thickness simply by measuring their material's α . Furthermore, the maximum EQE is locally tolerant to film thickness variations, providing a robust rule of thumb that film thickness should equal the exciton diffusion length.

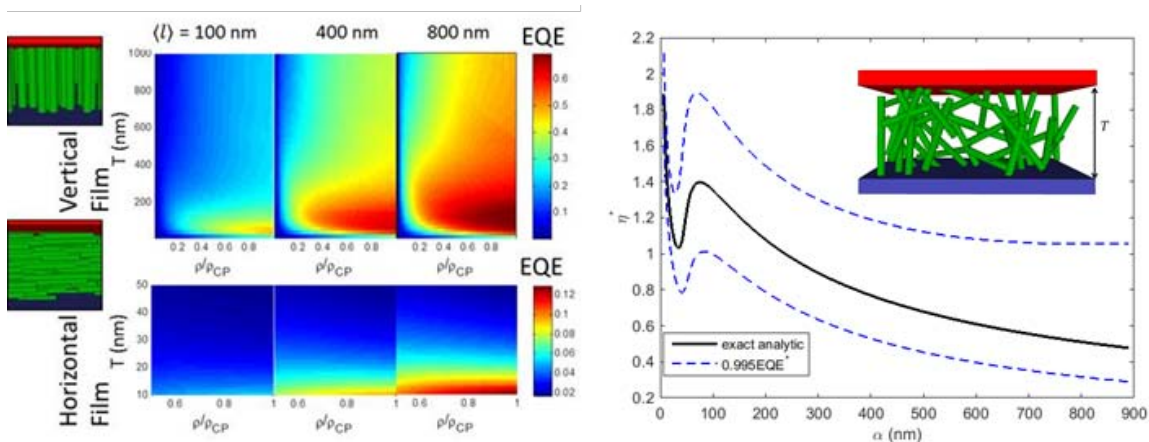


Figure 3. Results of modelling carbon nanotube films. On the left, plots of film efficiency (EQE) versus density (ρ/ρ_{CP}), network thickness (T), and mean nanotube length ($\langle l \rangle$), with the latter effecting exciton quenching. On

the right, optimal device thickness normalized to exciton diffusion length in the charge collecting axis, η^* , versus the governing design parameter for SWNT films, α , see text.

Future Plans:

Interfacing nanomaterials with plants – self powered sentinels of chemicals in the environment We will further undertake work to explore the use of novel SWNT-based plant-imbedded sensors to replace sensors in habitable spaces. As pre-concentrators of their immediate environment, SWNT-plant hybrids could essentially act as self-powered chemical/biological sensors utilizing natural mechanisms of preconcentration and bioaccumulations, ground water filtration, and processing. Detection of pollutants, war chemicals and nitroaromatics can also be accomplished in this manner. Plant pre-concentration of these compounds will enable us to detect very small quantities that are present in the plant's immediate environment, and nIR hand-held devices can be used to monitor SWNT-sensor infiltrated plants in the field. Mold and other fungal toxins, and other pathogens are also health hazards that our sensors could detect before the infection becomes widespread. Current methods of pathogen detection rely on identifying affected subsections of crops due to visual monitoring. We envision that our SWNT-plant imbedded sensors could provide real-time remote information on the state of hazards in the environment.

2-year BES Publications:

1. AA Boghossian, F Sen, BM Gibbons, S Sen, SM Faltermeier, JP Giraldo, CT Zhang, J Zhang, DA Heller, MS Strano. Application of Nanoparticle Antioxidants to Enable Hyperstable Chloroplasts for Solar Energy Harvesting *Advanced Energy Materials* 2013 3, 7, 881-893
2. JP Giraldo, MP Landry, SM Faltermeier, TP McNicholas, NM Iverson, AA Boghossian, NF Reuel, AJ Hilmer, F Sen, JA Brew, MS Strano. Plant nanobionics approach to augment photosynthesis and biochemical sensing *Nature Materials* 2014 13, 400-408
3. RM Jain, K Tvrdy, R Han, Z Ulissi, MS Strano. Quantitative Theory of Adsorptive Separation for the Electronic Sorting of Single-Walled Carbon Nanotubes *ACS Nano* 2014 8, 4, 3367-3379
4. K Tvrdy, RM Jain, R Han, AJ Hilmer, TP McNicholas, MS Strano. A Kinetic Model for the Deterministic Prediction of Gel-Based Single-Chirality Single-Walled Carbon Nanotube Separation *ACS Nano* 2013 7, 2, 1779-1789

References:

- [1] A. A. Boghossian, M.-H. Ham, J. H. Choi, and M. S. Strano, *Energy & Environmental Science* **4**, 3834 (2011).
- [2] J. P. Giraldo *et al.*, *Nat Mater* **13**, 400 (2014).
- [3] D. O. Bellisario, R. M. Jain, Z. Ulissi, and M. S. Strano, *Energy & Environmental Science* (2014).
- [4] M.-H. Ham *et al.*, *Nat Chem* **2**, 929 (2010).
- [5] R. M. Jain, R. Howden, K. Tvrdy, S. Shimizu, A. J. Hilmer, T. P. McNicholas, K. K. Gleason, and M. S. Strano, *Adv Mater* **24**, 4436 (2012).
- [6] R. Bock, Greiner, S., Keuthe, M., Stegemann, S., *Proc Natl Acad Sci* **109**, 2434 (2012).
- [7] Z. H. Svab, P., Maliga, P., *Proc Natl Acad Sci* **87**, 8526 (1990).
- [8] G. Ye, Daniell, H., Sanford, J., *Plant Mol. Biol.* **15**, 809 (1990).
- [9] H. Cerutti, Jagendorf, A., *Photosynth. Res.* **46**, 329 (1995).
- [10] G. Weber, Monajembashi, S., Greulich, K., Wolfrum, J., *Eur. J Cell Biol.* **49**, 73 (1989).
- [11] M. Bernardi, J. Lohrman, P. V. Kumar, A. Kirkemide, N. Ferralis, J. C. Grossman, and S. Q. Ren, *Acs Nano* **6**, 8896 (2012).
- [12] M. J. Shea and M. S. Arnold, *Applied Physics Letters* **102**, 243101 (2013).

Nanoengineering of Complex Materials

Principal Investigator: Samuel I. Stupp

Departments of Chemistry and Materials Science and Engineering, Northwestern University

2220 Campus Drive, Evanston, IL 60208-3108

Program Scope

The goal of this of program is to use self-assembly and molecular design to direct the formation of materials on the nanoscale. One of the strategies used is supramolecular chemistry integrated with other forces in order to learn how to program molecules for self-assembly of soft matter across scales, especially hierarchical structures. A second strategy of interest in the program is the use of biomimetic templating to create unique structures and functions, for example inorganic structures templated by organics or the use of organic templates to create complex nanostructures.

Recent Progress

Self-Assembling Tripodal Small-Molecule Donors for Bulk Heterojunction Solar Cells

Supramolecular self-assembly is an attractive strategy to combine the beneficial properties of polymeric donors, such as a well-controlled morphology, with the homogeneous composition of small molecule donors for organic solar cells (OSCs). We report here on two tripodal ‘star-shaped’ small-molecule donor compounds based on diketopyrrolopyrrole (DPP) side chains for solution-processed bulk heterojunction (BHJ) OSCs. C₃-symmetric tripodal molecules to direct the assembly of molecules along the π -surface to form nanowires. The two molecules have comparable optoelectronic properties in solution and neat films, but respond differently to the addition of solvent additives. This generates significantly different film morphologies and device performances. The tripod molecules were found not to aggregate in solution or form crystalline domains in thin films when a branched alkyl chain (2-ethylhexyl) substituent was used, whereas linear (dodecyl) alkyl chains promote the formation of one-dimensional (1D) nanowires and more crystalline domains in the solid state. Devices made from dodecyl show a 50% increase

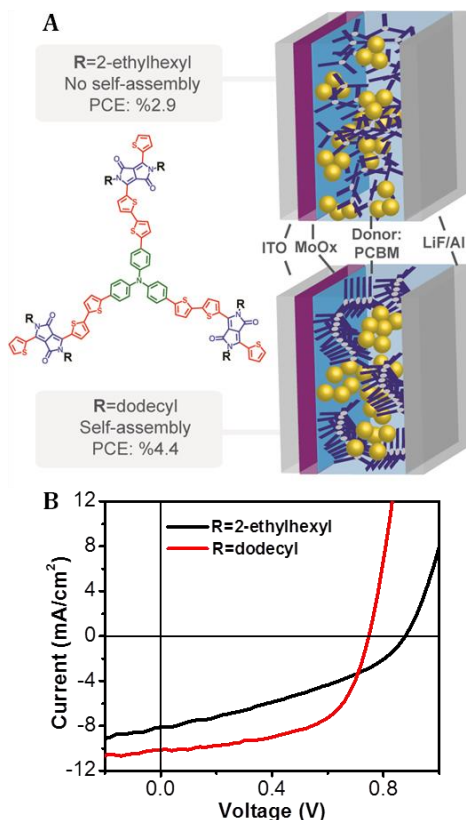


Fig. 1. (A) Chemical structure of tripodal donor molecules with 2-ethylhexyl (no self-assembly) and dodecyl (self-assembly) solubilizing groups (B) J-V curves of the organic solar cell devices from these molecules.

in efficiency (4.4% vs. 2.9%) relative to 2-ethylhexyl owing to a significant gain in fill factor. We attribute the improvement in performance to the nanowires reducing trap states in the active layer, which is supported by impedance spectroscopy.

2D Ferroelectricity

Crystalline organic intermolecular charge-transfer complexes, consisting of complementary pairs of aromatic donor and acceptor molecules, offer great promise in electronic, optical and magnetic applications. We recently developed a design motif that allows for the growth of solvent-free co-crystals of aromatic donor and acceptor molecules. While these crystals typically form 1D structures, we discovered the assembly of an unusual 2D supramolecular charge transfer network. The solid-state structure revealed that a 2:1 ratio of acceptor and donor molecules organized into layers of nearly orthogonal and crystallographically unique face-to-face and edge-to-face charge transfer stacks, stabilized by an extended network of hydrogen bonds (Fig. 2a). While a centrosymmetric $P\bar{1}$ space group was assigned to the co-crystal, we observed strong non-linear optical behavior by two-photon confocal microscopy as well as second harmonic generation spectroscopy.

This supports the hypothesis that there is a source of non-centrosymmetry in these 2D co-crystals, perhaps due to local distortions that are not observable by conventional X-ray crystallographic techniques. Furthermore, we observed ferroelectric behavior across both the face-to-face and edge-to-face axes at cryogenic and room temperatures (Fig. 2b). This is the first example of room temperature ferroelectric behavior in an organic co-crystal across two crystallographically independent axes, which is potentially valuable for high density and non-volatile information storage applications with low energy requirements. In addition to information storage, these ferroelectric systems could be utilized to create highly dynamic behaviors in soft matter utilizing external electric fields.

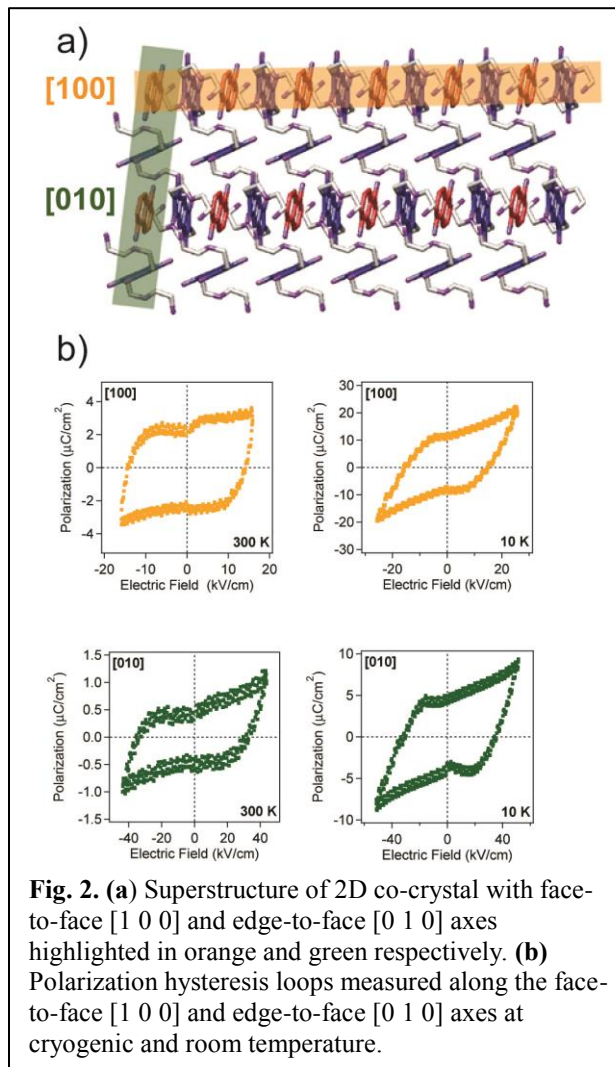


Fig. 2. (a) Superstructure of 2D co-crystal with face-to-face [1 0 0] and edge-to-face [0 1 0] axes highlighted in orange and green respectively. (b) Polarization hysteresis loops measured along the face-to-face [1 0 0] and edge-to-face [0 1 0] axes at cryogenic and room temperature.

Synthesis of Peptide–DNA Hybrids

We have recently developed DNA-peptide hybrid materials that form hierarchical structures and reversible hydrogels, programmed by DNA base pairing. DNA acts as a “glue” to link the peptide components to each other, as well as a handle to anchor important bio-functional components. DNA-peptide amphiphiles (DNA-PAs) were synthesized using copper-free click chemistry, which allows for rapid and selective conjugation of the two components. Co-assembling this DNA-PA conjugate at 10-20% with a DNA-free PA results in nanofibers with the appended DNA handles.

These nanostructures were organized into hierarchical gels using DNA as a cross-linker. Adding a displacement strand or a nuclease enzyme breaks the cross-links and renders these gels reversible. We have discovered that the resulting DNA-PA gels phase separate to include dense tangles of fibers that form DNA-rich hierarchical structures, as shown by SEM in Fig. 3C.

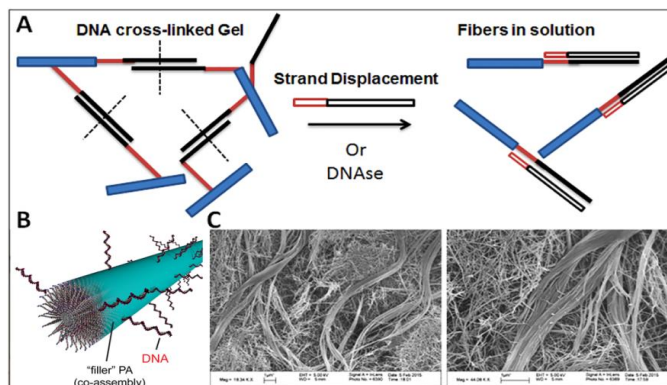


Fig. 3. Characterization of cross-linked DNA-PA gels. (A) Mixing two PAs with complementary DNA results in a gel due to the DNA hybridization. Subsequent displacement of the cross-link results in dissolution of the gel. (B) Schematics of the DNA-PA co-assembled with the filler, DNA-free, PA. (C) Scanning electron micrographs of the cross-linked DNA-PA gels.

Accessing and controlling dynamics within self-assembled nanostructures

Using electron paramagnetic resonance (EPR) spectroscopy, we have been able to map out experimentally for time internal dynamics in a supramolecular nanostructure ranging from liquid-like to solid-like behavior. Very recently we have extended this work to water dynamics in supramolecular assemblies. Inspired by the importance of solvent in native biological systems, we expect the motion of water molecules on sub-nanometer length scales to be just as important as conformational dynamics in functional supramolecular assemblies. Water dynamics, however, are very difficult to probe experimentally.

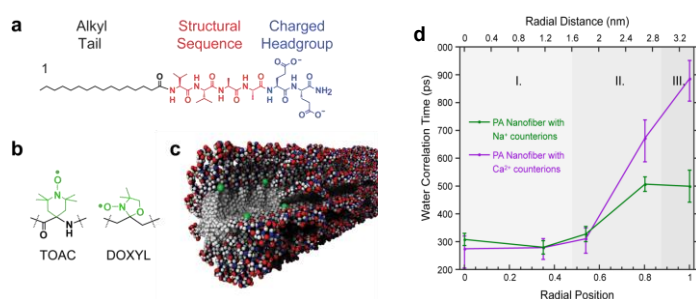


Fig. 4. (a) Peptide amphiphile structure; (b) Radical electron moieties such as TOAC and DOXYL can be included in the molecular structure to yield (c) self-assembled peptide amphiphile nanofibers containing spin labels. (d) Water dynamics measured by Overhauser dynamic nuclear polarization enhanced NMR spectroscopy (ODNP) show differences in the water dynamics through the cross-section of the nanofiber in the presence of Na^+ versus Ca^{2+} counterions. In both cases, water moves faster in the hydrophobic core and slower near the charged residues at the nanofiber surface.

Using Overhauser dynamic nuclear polarization spectroscopy (ODNP) (collaboration with Songi Han), we measured water dynamics through the cross-section of a self-assembled nanofiber. As shown in Fig. 4, the water close to the hydrophobic core of the PA nanofiber exhibits short (~300 ps) correlation times (corresponding to fast moving water), whereas the water dynamics at the surface are slow (~900 ps). We also show that the surface water is strongly affected by counterion valency. These data provide the first experimental measure of water dynamics on length scales relevant to the design of functional supramolecular nanostructures. This information can be used to optimize binding events or the use of these structures to template to template hybrid materials.

Future Plans

Our future plans for this program include: exploring ferroelectric behavior in hydrated materials and solutions to determine if switching under external fields can be used to induce dynamic behavior in soft matter; precisely controlling hierarchical organization within DNA-peptide supramolecular assemblies; developing hybrid systems containing perovskite chemistry and organic components; investigating adaptive behavior in supramolecular assemblies using stochastic optical reconstruction microscopy.

Publications Supported By BES (2013–2015)

- (1) Aytun, T.; Barreda, L.; Ruiz-Carretero, A.; Lehrman, J. A.; Stupp, S. I. "Improving Solar Cell Efficiency through Hydrogen Bonding: A Method for Tuning Active Layer Morphology" *Chem. Mater.* **2015**, *27*, 1201–1209.
- (2) Barnes, J. C.; Dale, E. J.; Prokofjevs, A.; Narayanan, A.; Gibbs-Hall, I. C.; Juricek, M.; Stern, C. L.; Sarjeant, A. A.; Botros, Y. Y.; Stupp, S. I.; Stoddart, J. F. "Semiconducting Single Crystals Comprising Segregated Arrays of Complexes of C₆₀" *J. Am. Chem. Soc.* **2015**, *137*, 2392-2399.
- (3) Matson, J. B.; Navon, Y.; Bitton, R.; Stupp, S. I. "Light-Controlled Hierarchical Self-Assembly of Polyelectrolytes and Supramolecular Polymers" *ACS Macro Lett.* **2015**, *4*, 43-47.
- (4) Blackburn, A. K.; Sue, A. C.-H.; Shveyd, A. K.; Cao, D.; Tayi, A.; Narayanan, A.; Rolczynski, B. S.; Szarko, J. M.; Bozdemir, O. A.; Wakabayashi, R.; Lehrman, J. A.; Kahr, B.; Chen, L. X.; Nassar, M. S.; Stupp, S. I.; Stoddart, J. F. "Lock-Arm Supramolecular Ordering: A Molecular Construction Set for Cocrystallizing Organic Charge Transfer Complexes" *J. Am. Chem. Soc.* **2014**, *136*, 17224-17235. N/A
- (5) Palmer, L. C.; Leung, C.-Y.; Kewalramani, S.; Kumthekar, R.; Newcomb, C. J.; Olvera de la Cruz, M.; Bedzyk, M. J.; Stupp, S. I.; "Long-Range Ordering of Highly Charged Self-Assembled Nanofilaments" *J. Am. Chem. Soc.* **2014**, *136*, 14377-14380.
- (6) Korevaar, P. A.; Newcomb, C. J.; Meijer, E. W.; Stupp, S. I. "Pathway Selection in Peptide Amphiphile Assembly" *J. Am. Chem. Soc.* **2014**, *136*, 8540-8543.
- (7) Ortony, J. H.; Newcomb, C.; Matson, J. B.; Palmer, L. C.; Doan, P. E.; Hoffman, B. M.; Stupp, S. I. "Internal Dynamics of a Supramolecular Nanofiber" *Nature Mater.* **2014**, *13*, 812-816.
- (8) Stupp, S. I.; Palmer, L. C. "Supramolecular Chemistry and Self-Assembly in Organic Materials Design" *Chem. Mater.* **2014**, *16*, 507-518.
- (9) Sampath, S.; Basuray, A. N.; Hartlieb, K. J.; Aytun, T.; Stupp, S. I.; Stoddart, J. F. "Direct Exfoliation of Graphite to Graphene in Aqueous Media with Diazaperopyrenium Dications" *Adv. Mater.* **2013**, *25*, 2740-2745.
- (10) Ruiz-Carretero, A.; Aytun, T.; Bruns, C.; Newcomb, C. J.; Tsai, W.-W.; Stupp, S. I. "Stepwise Self-Assembly to Improve Solar Cell Morphology" *J. Mater. Chem. A* **2013**, *1*, 11674-11681.
- (11) Bruns, C. J.; Herman, D. J.; Minuzzo, J. B.; Lehrman, J. A.; Stupp, S. I. "Rationalizing Molecular Design in the Electrodeposition of Anisotropic Lamellar Nanostructures" *Chem. Mater.* **2013**, *25*, 4330-4339.
- (12) Stupp, S. I.; Zha, R. H.; Palmer, L. C.; Cui, H.; Bitton, R. "Self-Assembly of Biomolecular Soft Matter" *Faraday Disc.* **2013**, *166*, 9-30.

Chemically Directed Self-Assembly of Protein Superstructures

F. Akif Tezcan, University of California, San Diego

Program Scope

Our research aims to develop chemical design strategies to control protein self-assembly and to construct protein-based materials with new chemical, physical and dynamic properties. Proteins represent the most versatile building blocks available to living organisms for constructing functional materials and molecular devices. Underlying this versatility is an immense structural and chemical heterogeneity that renders the programmable self-assembly of protein an extremely challenging design task. To circumvent the challenge of designing extensive non-covalent interfaces for controlling protein self-assembly, we have endeavored to use other types of chemical bonding interactions (metal coordination, disulfide linkages) that are simultaneously strong, reversible and externally tunable. Under our DOE-funded program, we established design strategies that led to the construction of a diverse array of discrete (*i.e.*, closed) or 0-, 1-, 2- and 3-dimensional (*i.e.*, infinite) protein assemblies with crystalline order over the entire nm to μm range.^{1,2} These novel protein-based materials possess emergent physical and functional properties including photoredox-controlled/templated mineralization,³ hyperstability³ and coherent dynamics. At the same time, the process of bottom-up protein design resulted in the development of new experimental platforms that allowed us to study and provide insights into the self-assembly of natural protein assemblies.⁴

Recent Progress

We summarize here four distinct, recently developed (unpublished) chemical design approaches that led to different classes of self-assembled protein materials.

Metal-Directed Assembly of 1D Protein Nanotubes with Tunable Widths: Helical, 1D protein architectures fulfill key biomechanical roles, including the formation of the cytoskeleton (microtubules),⁵ movement (flagella),⁶ and compartmentalization (tubular virus capsids).⁷ A defining characteristic of these nano/microscale architectures is their dynamicity and reconfigurability. Owing to their structural and mechanical properties, self-assembled 1D protein nanoarchitectures are highly appealing targets for protein design. Yet, past successes in the design of tubular protein assemblies have been limited to the use of physical methods,⁸ or of natively ring-shaped protein assemblies which can be manipulated to stack into tubes.⁹ In previous work, we showed that 2D protein arrays could fold into 1D helical tubular architectures.¹ We thus envisioned that if we could construct a 2D protein array from a building block that is anisotropic in terms of its metal binding (*i.e.*, it presents different metal binding motifs on its different facets), we could modulate the relative dimensions of the 2D array (and thereby the diameter of the tubes) through metal coordination. Toward this end, we designed a D_2 symmetric tetrameric assembly of cytochrome cb562 (^{H59/C96}RIDC3₄) with two sets of distinct metal binding motifs on its facets. ^{H59/C96}RIDC3₄ formed crystalline nanotubular architectures whose widths could be reproducibly tuned by varying solution conditions to modulate metal-protein interactions (Fig. 1a-c). These architectures have persistence lengths (9-

20 μm) that are similar to actin filaments (18 μm) and Young's moduli (0.3-25 MPa) that compare with soft protein fibers such as fibrin (1-10 MPa) or elastin (1 MPa).¹⁰ This study presents the first example of nanotubular protein assemblies with chemically controllable dimensions, constructed from a single protein building block under kinetic control.

Porous, 3D “metal-organic-protein” crystal frameworks with tunable lattices:

3D protein lattices not only form the basis of protein crystallography, but they have also been proposed as stable, porous platforms for carrying out catalytic reactions under harsh, non-biological conditions.¹¹ However, 3D crystallization of proteins is largely carried out in an *ad hoc* fashion and not by design. In contrast, there have been considerable progress in using interactions between organic building blocks (connectors) and metal ions/clusters (nodes) to form porous 3D crystals, termed Metal Organic Frameworks (MOFs). We asked whether the design principles for MOFs can be applied to 3D protein crystallization, where proteins are utilized as nodes and their self-assembly is guided by tunable organic linkers.

In proof-of-principle experiments, we used human H ferritin as a protein “metal node”, as it is a pseudo-spherical architecture with O_h symmetry, resembling many metal nodes in MOFs. Owing its octahedral symmetry, ferritin possesses several symmetry axes (4-, 3- and 2-fold), which can be used for anchoring stable metal coordination sites. We first used the 3-fold symmetric pores of ferritin to engineer stable, 3-coordinate metal ions with open coordination sites available to interact with a ditopic (C_2 symmetric) linkers (Fig. 2a). Upon binding a linker with high Zn(II) affinity (1,4-benzenedihydroxamate), Zn-bound ferritin self-assembled into 3D crystals that possessed the desired *bcc* morphology that was previously not observed for human ferritin (Fig 2b). The structure of the *bcc* ferritin crystals was determined at 3.5 Å resolution, which revealed that the

ferritin molecules essentially make no surface contact with one another and that they are solely held together by benzene-1,4-dihydroxamate linkers that bridge the ferritin-anchored Zn ions (Fig. 2c,d). This first “metal-protein-organic framework” demonstrates

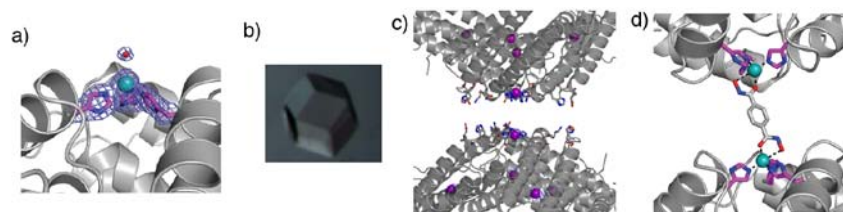


Figure 2. (a) Zn coordination sites engineered in ferritin 3-fold symmetric pores. (b) *bcc* morphology obtained through the benzene-1,4-dihydroxamate-mediated assembly of Zn-^{H122}ferritin. (c-d) Neighboring ferritin molecules in the lattice are held together by organic linkers bridging the anchored Zn ions.

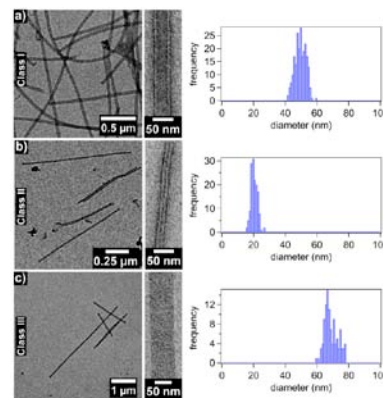


Figure 1. Three classes of metal/pH tunable 1D nanotubes formed through the self-assembly of ^{H59/C96}RIDC3, and their width distributions.

the possibility of directing the self-assembly of large macromolecules through synthetically addressable and interchangeable chemical functionalities.

Coherently Dynamic, Defect-Free 2D Protein Crystals by Expedient Design (*invention disclosure filed*): 2D crystalline materials exhibit unique mechanical and electronic attributes, possess high surface area-to-volume ratios, offer a uniform display of atomic/molecular entities as well as pores, and provide structural access to 0-, 1, and 3D materials.¹² These properties have rendered synthetic 2D materials immensely attractive in applications including electronics, sensing, coating, filtration and catalysis. Nevertheless, the rational design of self-assembling 2D crystals remains a considerable challenge and a very active area of development.¹³

The most straightforward route to obtaining self-assembled 2D protein lattices would be the tiling of C_3 , C_4 or C_6 symmetric building blocks through appropriately positioned C_2 symmetric linkages. Given that both metal coordination and disulfide bonds simultaneously provide bond strength and reversibility, we exploited them for the 2D self-assembly of a C_4 symmetric protein RhuA. Following a quick inspection of the RhuA architecture, we created two variants (C^{98} RhuA and H^{63}/H^{98} RhuA) with four conditionally self-associating corners for forming square lattices (Fig.3a). We readily found conditions under which that both variants formed monolayered 2D crystalline lattices, whose sizes exceeded several microns in some cases (Fig.3b). Importantly, both types of 2D RhuA

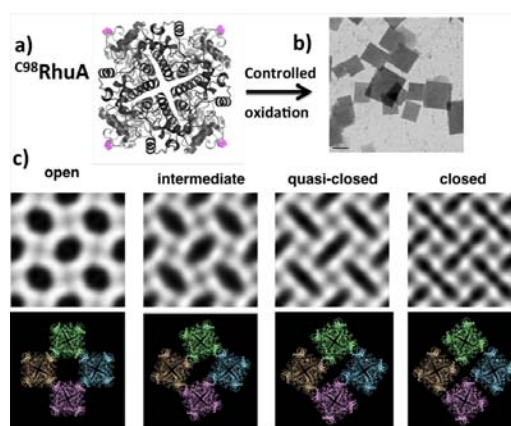


Fig. 3. (a) Structure of C^{98} RhuA, (b) disulfide-directed, 2D C^{98} RhuA crystals, (c) EM snapshots of C^{98} RhuA lattice in different conformations.

crystals are formed in an unsupported fashion, their formation is readily controllable by solution conditions and their mode of assembly is unambiguous. Uniquely, C^{98} RhuA crystals exhibit coherent dynamics in the 2D plane thanks to the “semi-rigidity” of the disulfide linkages (Fig.3c) and they are essentially defect-free. These attributes of RhuA make it an exciting and easily accessible platform to create new, functional 2D materials, to study protein self-assembly and crystallization, and to explore—for the first time—the properties of flexible protein crystals.

2D Crystals Assembled Through the Cooperativity of Different Types of Biological Interactions:

The energy landscape for metal-protein interactions is rather shallow with many minima of similar energies, which ultimately is responsible for the tunability/responsiveness of metal-directed protein assemblies.^{1,2} We surmised that metal-directed protein self-assembly could be rendered more specific if the protein building blocks could be decorated with complementary DNA sequences. Toward this end, we modified a metal-binding cyt cb_{562} variant (C^{21} RIDC3) with DNA single strands (Fig.4a). DNA-RIDC3 chimeras could be prepared in high purity, and their metal/DNA-directed self-assembly was studied under various conditions (Zn and protein concentration, pH, ionic strength, and mixtures of variants). Crystalline, 2D lattices were obtained only when the solutions contained two complementary DNA-RIDC3 chimeras and

3-4 fold excess Zn(II) at pH 4.5-5.0 and ~10 °C (Fig.4b). When one type of protein-DNA conjugate was present or two conjugates with mismatching DNA sequences, no ordered assemblies formed. CryoEM analysis suggested that the 2D protein framework was formed

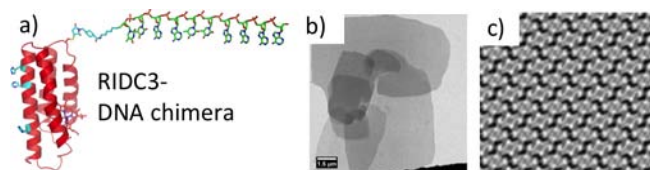


Fig. 4. (a) Model of the C21 RIDC3-DNA (10mer) chimera, (b) 2D crystals of C21 RIDC3-DNA chimeras, (c) and their 8-Å cryoEM reconstruction.

through metal-protein and protein-protein interactions, which appear to be “stapled” above and below the 2D plane by double stranded DNA linkages (Fig. 4c). The highly specific conditions under which these crystals are formed are noteworthy: at pH 4.5-5.0 metal-protein and protein-protein interactions are considerably weakened, while 10 °C is close to the melting temperature of the 10meric DNA duplex. Thus, crystalline self-assembly is enabled only when the three different types of operative interactions (metal-protein, protein-protein, DNA-DNA) are metastable in isolation, but stable when acting cooperatively. This novel, synthetic system recapitulates how molecular specificity arises from a combination of multiple, weak(ened) interactions, and demonstrates our ability to fabricate increasingly more complex biological architectures through rational design.

Future Plans

Our continuing goal is to refine and develop new chemical design approaches to fabricate increasingly more complex, functional protein materials that not only emulate but also extend what natural evolution has produced. Our immediate objectives are: 1) development of a library of functional linkers to direct the formation of tunable, stimuli-responsive 3D protein lattices; 2) development of inorganic chemical strategies for the assembly of heteromeric protein assemblies consisting of multiple different building blocks; 3) to fabricate scalable, functionalized, patterned 2D protein crystals and to explore their mechanical/functional properties; 4) to elucidate the molecular basis of defect-free self-assembly of 2D RhuA crystals through advanced imaging techniques; 5) to understand and exploit the molecular basis of the coherent dynamicity of 2D RhuA crystals toward the generation of responsive/adaptable protein devices.

References

- (1) Brodin, J. D.; Ambroggio, X. I.; Tang, C. Y.; Parent, K. N.; Baker, T. S.; Tezcan, F. A. *Nat. Chem.* 2012, 4, 375.
- (2) Salgado, E. N.; Radford, R. J.; Tezcan, F. A. *Acc. Chem. Res.* 2010, 43, 661.
- (3) Brodin, J. D.; Carr, J. R.; Sontz, P. A.; Tezcan, F. A. *Proc. Natl. Acad. Sci. USA* 2014, 111, 2897.
- (4) Huard, D. J. E.; Kane, K. M.; Tezcan, F. A. *Nat Chem Biol* 2013, 9, 169.
- (5) Nogales, E. *Annu. Rev. Biophys. Biomol. Struct.* 2001, 30, 397.
- (6) Terashima, H.; Kojima, S.; Homma, M. *Int. Rev. Cell Mol. Biol.* 2008, 270, 39.
- (7) Stubbs, G.; Kendall, A. *Adv. Exp. Med. Biol.* 2012, 726, 631.
- (8) Lu, G.; Komatsu, T.; Tsuchida, E. *Chem. Commun.* 2007, 2980.
- (9) Ballister, E. R.; Lai, A. H.; Zuckermann, R. N.; Cheng, Y.; Mougous, J. D. *Proc. Natl. Acad. Sci. USA* 2008, 105, 3733.
- (10) Guthold, M.; Liu, W.; Sparks, E. A.; Jawerth, L. M.; Peng, L.; Falvo, M.; Superfine, R.; Hantgan, R. R.; Lord, S. T. *Cell Biochem. Biophys.* 2007, 49, 165.
- (11) Margolin, A. L.; Navia, M. A. *Angew Chem Int Edit* 2001, 40, 2205.
- (12) Butler, S. Z.; Hollen, S. M.; Cao, L.; Cui, Y.; Gupta, J. A.; Gutierrez, H. R.; Heinz, T. F.; Hong, S. S.; Huang, J.;

Ismach, A. F. *ACS Nano* 2013, 7, 2898. (13) Colson, J. W.; Dichtel, W. R. *Nat. Chem.* 2013, 5, 453.

Publications

- 1) S. J. Smith, K. Du., R. J. Radford, F. A. Tezcan, “Functional, metal-based crosslinkers for α -helix induction in short peptides”, **Chem. Sci.**, 4, 3740-3747 (2013).
- 2) D. J. E. Huard, K. M. Kane, F. A. Tezcan., “Re-engineering protein interfaces yields copper-inducible ferritin cage assembly” **Nat. Chem. Biol.**, 9, 169-176 (2013).
- 3) A. Medina Morales, A. Perez, J. D. Brodin, F. A. Tezcan, “In Vitro and Cellular Self-Assembly of a Zn-Binding Protein Cryptand via Templated Disulfide Bonds”, **J. Am. Chem. Soc.**, 135, 12013–12022 (2013).
- 4) J. D. Brodin, J. R. Carr, P. A. Sontz, F. A. Tezcan, “Exceptionally Stable, Redox-Active Supramolecular Protein Assemblies with Emergent Properties”, **Proc. Natl. Acad. Sci. USA**, 111, 2897-2902 (2014)
- 5) W. Song, P. A. Sontz, X. I. Ambroggio, F. A. Tezcan, “Metals in Protein-Protein Interfaces”, **Ann. Rev. Biophys.**, 43, 409-431 (2014)
- 6) P. A. Sontz, W. Song, F. A. Tezcan, “Interfacial Metal Coordination in Engineered Protein and Peptide Assemblies”, **Curr. Opin. Chem. Biol.**, 19, 42-49 (2014)

Submitted/In Preparation:

- 7) L. A. Churchfield, A. Medina-Morales, J. D. Brodin, A. Perez, F. A. Tezcan, “Effects of macromolecular rigidity and strain on metal coordination and thermostability in synthetic metalloprotein assemblies”, **J. Am. Chem. Soc.** (2015), *in revision*.
- 8) J. D. Brodin, S. J. Smith, J. R. Carr, F. A. Tezcan, “Designed, Helical Protein Nanotubes with Variable Diameters from a Single Building Block”, **J. Am. Chem. Soc.** (2015), *under review*.
- 9) P. A. Sontz, J. B. Bailey, S. Ahn, F. A. Tezcan, “A Porous Metal-Protein Framework Directed by Bifunctional Linkers”, (2015), *to be submitted*.
- 10) Y. Suzuki, G. Cardone, T. S. Baker, F. A. Tezcan, “Coherently Dynamic, Defect-Free 2D Protein Crystals by Expeditious Design”, *to be submitted*.
- 11) S. J. Smith, G. Cardone, L. Suominen, T. S. Baker, F. A. Tezcan, “Two-Dimensional Crystals Assembled Through Three Different Types of Biological Interactions”, (2015), *to be submitted*.

Self-Assembly of Pi-Conjugated Peptides in Aqueous Environments Leading to Energy-Transporting Bioelectronic Nanostructures

PI: John D. Tovar. Johns Hopkins University, Department of Chemistry, Department of Materials Science and Engineering, and Institute for NanoBioTechnology, Baltimore, MD 21218

Co-PI: Howard E. Katz. Johns Hopkins University, Department of Materials Science and Engineering, Department of Chemistry, and Institute for NanoBioTechnology, Baltimore, MD 21218

Co-PI: Andrew L. Ferguson. University of Illinois at Urbana-Champaign, Department of Materials Science and Engineering, Urbana, IL 61801

Program Scope: The realization of new supramolecular pi-conjugated organic structures as driven by peptide-based self-assembly will offer a new approach to interface with the biotic environment. Previously, we developed pi-conjugated peptides that undergo supramolecular self-assembly into one-dimensional (1-D) organic electronic nanomaterials under benign aqueous conditions. The intermolecular interactions among the pi-conjugated organic segments within these nanomaterials lead to defined perturbations of their optoelectronic properties and yield nanoscale conduits that support energy transport within individual nanostructures and throughout bulk macroscopic collections of nanomaterials (Figure 1). These materials were characterized photophysically using steady-state and time-resolved UV-vis, photoluminescence and circular dichroism. Nanomaterial morphologies were visualized using atomic force, scanning electron and transmission electron microscopies. The resulting nanostructures are under 10 nm in diameter and extend microns in length. This ability to fashion pi-conjugated structures from aqueous environments at this length scale is unprecedented and opens up many possibilities for future research as discussed below. Our current objectives entail (1) **synthesis** of new pi-electron units to embed within self assembling peptides and **detailed characterization** and **molecular modeling** of the resulting nanomaterial aggregates, (2) **exploration of the surface chemistry** presented by these nanostructures as relevant for the development of optoelectronic interaction with cells or other biotic systems and (3) development of new assembly paradigms leading to **heterogeneous electronic properties** (*i.e.* gradients and localized electric fields) within the nanomaterials. This research will lead to the continued development of a powerful materials set capable of making connections between nanoscale electronic materials and macroscopic bulk interfaces, be they those of a cell, a protein or a device.

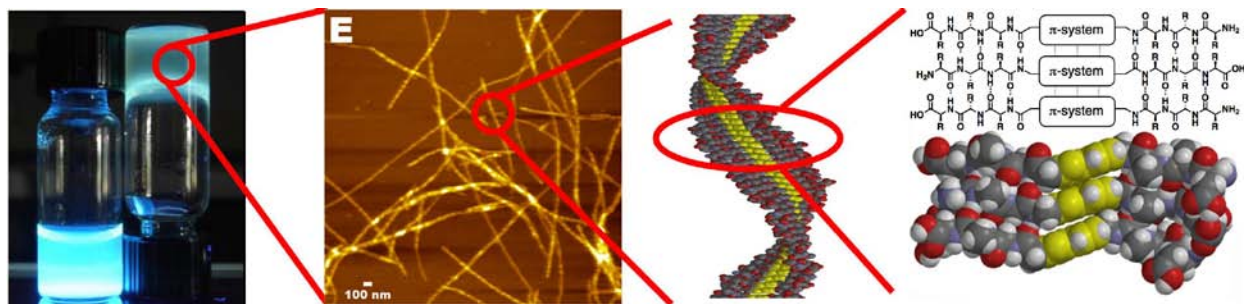


Figure 1: A solution of pi-conjugated (bithiophene) peptides (fluorescent at far left) is triggered to assemble resulting in a macroscopic self-supporting hydrogel comprised of random networks of 1-D nanostructures (center left) that form as molecular components (far right) self-associate into pi-stacked aggregates (center right).

Recent progress. The primary research activities over the past two years have involved (1) chemical synthesis of pi-electron peptides: of known entities or subtle variations thereof in support of spectroscopic investigations, of more complex molecules capable of exciton and electron transfer within nanomaterials, (2) continued investigations of how peptide sequence variation impacts the photophysical properties, and new to this project period, the energetics and the early stages of the molecular self-assembly events, and the electrical conductivities and carrier mobilities and (3) new studies of exciton and electron migration in assembled nanomaterials with donor and acceptor chromophores. Nine papers arising from DOE-BES support have been published or accepted over this period, and two others or will very shortly be submitted for review. These publications include four invited review/feature article manuscripts.

(1) Chemical synthesis of pi-electron peptides. The majority of the synthetic efforts have been to prepare materials in support of the characterization tasks of this project. We published previously on oligothiophene and oligophenylene vinylene-based peptides, and over the past two years, we have made systematic variations to the peptide architecture in order to understand and conceive predictive design rules. For example, a series of peptides with varying amino acid sequence were studied to understand how controlled variation would impact excitonic character or electrical transport properties. Most of these syntheses take advantage of the cross-coupling methods developed previously with this DOE-BES support. We have furthered the synthetic development of graphene-based peptides. Although reported in prior progress reports, achieving these very insoluble molecules at analytical purity has been very challenging. Using longer and more ionizable peptide side chains, we have finally achieved acceptable purity levels and are now completing spectroscopic and morphological evaluation of the nanomaterials that form from these graphene-peptides. Finally, we have designed peptides with internal electron pathways as the first step to photon-driven electric field generation (e.g. “exciton splitting”) and are characterizing the dynamics associated with this process.

(2) Experimental and computational impacts of “supramolecular polymorphism”. Continuing from the last meeting, we published two exhaustive papers (and an invited review summary) documenting how subtle changes in peptide sequence can rationally influence electronic coupling within the 1-D nanomaterials. For example, we found very clear progressions between classical H-aggregate exciton coupling and excimer-like structures as the steric bulk and/or the hydrophobicity of the amino acid residues are altered at controlled positions along the peptide backbone in molecules of the form HO-DXXX-OPV-XXXD-OH, where X denotes a possible site of variation and OPV is the central embedded oligophenylene vinylene chromophore. This “polymorphism” arises from the fact that the molecular design can accommodate several variations in intermolecular electronic coupling among the same chromophore unit just by varying the primary amino acid sequence. In parallel, we have initiated electrical measurements to show how sequence variation impacts electrical

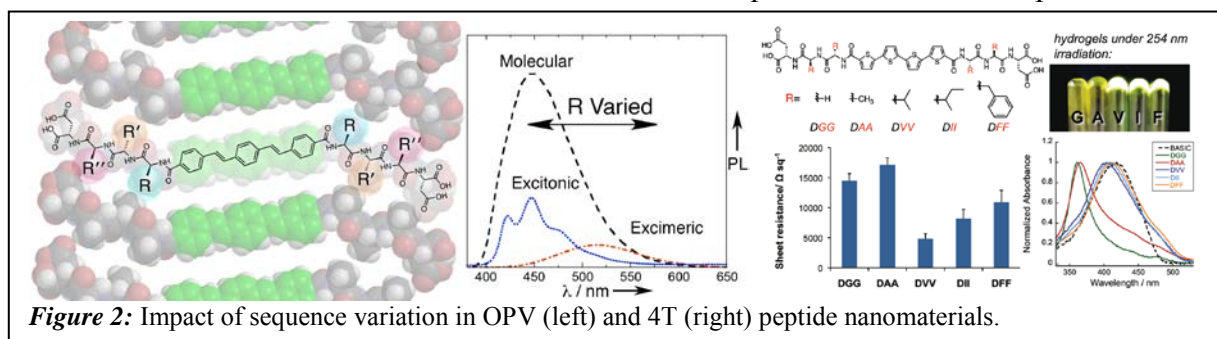


Figure 2: Impact of sequence variation in OPV (left) and 4T (right) peptide nanomaterials.

conductivities and hole mobilities on quaterthiophene (4T) peptides of the form HO-DXX-4T-XXD-OH. The trends suggest that the roughness of a peptide film appears to play a more crucial role in determining the bulk resistivity value rather than the geometry or persistence length of each nanostructure, and the final surface roughness of the films can be correlated to the gelation properties of each peptide. The conductivity of these nanowire films was sufficient for them to transmit gating voltages from a probe to a field effect transistor gate dielectric, thus allowing us to use these nanomaterials as gate electrodes themselves. Mobilities were correlated with stronger intermolecular pi-electron interactions indicated by absorbance blue-shifts. These experimental findings were strongly corroborated through detailed atomistic molecular dynamics simulations in order to ascertain the inter-peptide spacing and ribbon morphology as a function of peptide sequence, and accelerated sampling techniques were employed to compute the free energy of dimerization for symmetric and non-symmetric peptide monomers in parallel and anti-parallel arrangements. These simulations provided immense insight about the relative degrees of local order (and ensemble disorder) in these materials. We have developed an implicit solvent model for peptide aggregation permitting direct molecular simulation of the early stages of peptide self-assembly on μs time scales in molecular detail.

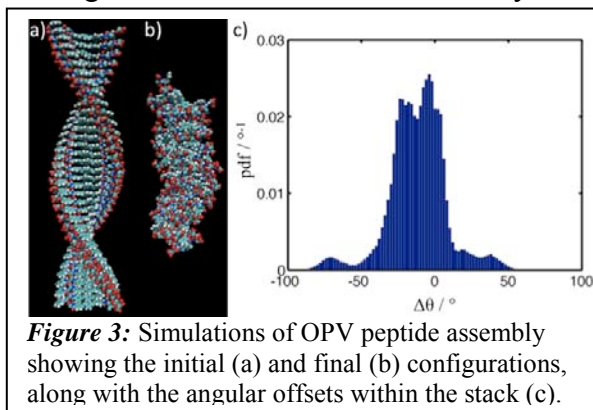


Figure 3: Simulations of OPV peptide assembly showing the initial (a) and final (b) configurations, along with the angular offsets within the stack (c).

(3) Electric field generation. We demonstrated that two peptides with different chromophore units can be intimately co-mixed, and that excitation of the high-energy unit can be transferred to the low energy “dopant” leading to energy transfer. Specifically, we add in varying amounts of a 4T peptide (the photonic acceptor) into a majority OPV3 (photonic donor) assembly. Because the absorption maxima of the 4T and the OPV are “orthogonal”, we can selectively excite the OPV channel without meaningful excitation of the 4T. However, we observe excited states suggestive of energy transfer to the 4T core structures diluted within the nanomaterial matrices, both through steady-state and time-resolved photoluminescence spectroscopies. In unpublished work, we have shown that similar schemes can be designed for *electron transfer* whereby an excited state electron donor can transfer an electron to a suitable acceptor thus using photons to create a transient electric field within the biomaterial matrix. This approach stands to offer an exciting new way to attenuate material properties in an externally controlled manner with spatial and temporal control.

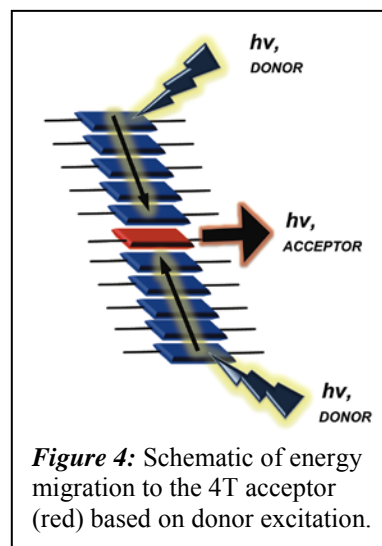


Figure 4: Schematic of energy migration to the 4T acceptor (red) based on donor excitation.

Future plans. Ad hoc synthesis activities will remain ongoing as required to support the other active tasks of the project. We will examine the ionic and electrical contributions to observed conductivities and will attempt to quantify the nature of the exciton delocalization within photo-excited nanostructures. We will use the innovative transistor design developed over the last

funding period to probe the electrical observables associated with photoexcitation. Now that we have validated the ability to mix different peptides within self-assembled nanostructures, activities over the next period will examine the self-sorting capabilities of different peptides as a way to engineer band-gap differences along the length of a self-assembled structure. We shall conduct implicit solvent simulations of different peptide sequences and conjugated cores to resolve the impact of monomer chemistry upon the morphology, thermodynamics, and kinetics of the early stages of self-assembly. We will attempt to simulate larger and longer nanostructures and use this to make direct contact with experimental measurements, such as attempting to observe temporal variation of excited state lifetimes that would be expected as monomeric peptides self-associate into excimeric or excitonic states.

Publications supported by DOE-BES support (2013-2015)

- [1] J. D. Tovar, "Supramolecular construction of optoelectronic biomaterials," invited by *Accounts of Chemical Research*, 2013, (46) 1527-1537. (DOI: 10.1021/ar3002969)
- [2] S. R. Diegelmann and J. D. Tovar, "Polydiacetylene-peptide one-dimensional nanomaterials," invited as a Feature Article by *Macromolecular Rapid Communications*, 2013 (34) 1343-1350. (DOI: 10.1002/marc.201300423)
- [3] A. B. Marciel, M. Tanyeri, B. D. Wall, J. D. Tovar, C. M. Schroeder, W. L. Wilson, "Fluidic-directed assembly of aligned oligopeptides with π -conjugated cores," in *Advanced Materials*, 2013 (25) 6398-6404. (DOI: 10.1002/adma.201302496)
- [4] A. M. Sanders and J. D. Tovar, "Solid-phase Pd-catalyzed cross-coupling methods for the construction of pi-conjugated peptide nanomaterials," in *Supramolecular Chemistry*, 2014 (26) 259-266. (DOI: 10.1080/10610278.2013.852675)
- [5] B. D. Wall, A. E. Zacca, A. M. Sanders, W. L. Wilson, A. L. Ferguson and J. D. Tovar, "Supramolecular polymorphism: Tunable electronic interactions within pi-conjugated peptide nanostructures dictated by primary amino acid sequence," in *Langmuir*, 2014 (30) 5946-5956. (DOI: 10.1021/la500222y)
- [6] B. D. Wall, **Y. Zhou**, **S. Mei**, H. A. M. Ardoña, A. L. Ferguson and J. D. Tovar, "Variation of formal hydrogen bonding networks within electronically delocalized pi-conjugated oligopeptide nanostructures," in *Langmuir*, 2014 (30) 11375-11385. (DOI: 10.1021/la501999g)
- [7] H. A. M. Ardoña and J. D. Tovar, "Energy transfer within responsive pi-conjugated peptide-based coassembled nanostructures in aqueous environments," in *Chemical Science*, 2015 (6) 1474-1484 (DOI: 10.1039/C4SC03122A)
- [8] J. D. Tovar, "Peptide nanostructures with pi-ways: photophysical consequences of peptide/pi-electron molecular self-assembly," invited by the *Israel Journal of Chemistry* (special issue on Functional Peptide and Protein Nanostructures), *in press*. (DOI: 10.1002/ijch.201400161)
- [9] H. A. M. Ardoña, K. Besar, **M. Togninalli**, H. E. Katz and J. D. Tovar, "Sequence-dependent mechanical, photophysical and electrical properties of pi-conjugated peptide hydrogelators," in the *Journal of Materials Chemistry C* (2015), *in press* (part of a special web-themed issue on "Bioelectronics"). (DOI: 10.1039/C5TC00100E)
- [10] K. Besar, H. A. M. Ardoña, J. D. Tovar and H. E. Katz, "Demonstration of hole transport and voltage equilibration in self-assembled pi-conjugated peptide nanostructures using field-effect transistor architectures," *in preparation*.
- [11] B. A. Thurston, J. D. Tovar and A. L. Ferguson, "Thermodynamics, morphology and kinetics of early-stage self-assembly of pi-conjugated oligopeptides," *in preparation*.

Dynamic Self-Assembly, Emergence, and Complexity

George M. Whitesides
Department of Chemistry and Chemical Biology
Harvard University
Cambridge MA 02138

Program Scope

This program includes two major components. These programs share the common feature that both deal with dissipative systems, but they are significantly different. The objective of the first is to explore the materials science of systems whose functions depends upon conversion of one form of energy into another, and particularly the conversion of pressure-volume work (in a pneumatic actuator) into another form of mechanical work (e.g. In lifting a weight, or moving). The second is more conceptual, and is concerned with examining the behaviors that emerge when individual dissipative systems interact with one another. Much of this work has concentrated on the behavior of flames (either singly, or in collections).

- 1. Soft Actuators.** The primary objective of our program in soft actuators is to understand how to use a simple energetic input (low-pressure air) to accomplish mechanical work. The work has two specific foci: i) the exploration and demonstration of new types of actuators; ii) the understanding of the mechanisms by which the motion of these actuators occurs, and particularly how the nonlinearities in elastomeric materials subjected to high strains is converted into relatively simple and useful motion, appropriate for an actuator. Our program in soft actuators has been very productive.
- 2. Complex, Dissipative Systems.** As a model, the early focus for our work in dissipative systems is the behavior of small flames (“flamelets”). A flame is an entity that converts chemical free energy into heat, light, and mechanical motion (e.g., convective motion of gases). We have studied in detail the behavior of a strip of burning nitrocellulose, and developed a very attractive system for looking at interacting flamelets (and particularly for emergent behaviors in these systems).

Recent Progress

- 1. Soft Actuators.** This work has produced several important results. i) The development of first – generation ideas for pneumatic actuators (“Pneu-nets”) as the basis for functionally simple grippers, tentacles, and other functionally related systems. These systems have now demonstrated themselves to be mechanically robust through millions of cycles of actuation, and to have the potential for broad application in a range of areas from packaging to search and rescue.(1,2) We have

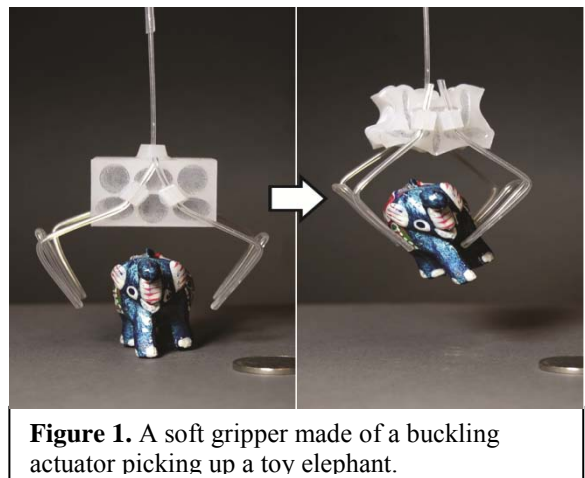


Figure 1. A soft gripper made of a buckling actuator picking up a toy elephant.

largely finished our work in this area, and have moved on to explore other mechanisms for actuation. ii) The work has developed a number of new methods for fabricating three-dimensional elastomeric structures capable of pneumatic actuation. These methods (e.g. “Click-e-Bricks”) substantially simplify the fabrication of complex test structures, by using a fabrication strategy intentionally modeled to resemble children’s toys (e.g., Legos), but using elastomeric “bricks” and “tiles.” (3, 4) iii) The most interesting new development has exploited a complex, nonlinear behavior in elastomeric beams under compression to generate linear actuation. This strategy rests on an unexpected opportunity: that is, buckling. The buckling of structural elements (e.g. I-beams, wings of airplanes, bridge foundations) under stress is commonly regarded as an undesirable mechanism of failure in a material system. Buckling in elastomers has been relatively little explored. Our initial work indicates that this type of buckling is (not unexpectedly) completely reversible, but (unexpectedly) extremely useful as the basis for a fundamentally new class of actuators. In these structures, we use collapse of “cells” consisting of interconnected voids in an elastomeric slab to create a collective motion as the slab buckles under external pressure that can be converted into linear or rotary actuation.

- 2. Complex, Dissipative Systems.** We have explored in detail – as a model system for small, intense, flames – the burning of a strip of nitrocellulose. The behavior of this system is quite remarkable. (5) A single strip can undergo a transition between two states, one characterized by steady, low intensity combustion, and the second by unstable high intensity combustion. We have considered this system as using the conceptual framework of a folded bifurcation, and identified the key feature leading to the transition as the nonlinear coupling between the chemical processes involved in combustion, and the “wind” – that is, convective flow of air reflecting the motion of hot gases-- and the flame. We have argued that this system provides a distant but instructive model for naturally occurring, high – intensity flames such as crown fires in forest fires. The utility of the model for this purpose remains to be seen, but it already provides one of the best – defined models for combustion that is available.

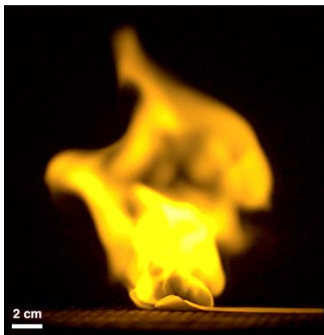


Figure 2. High-speed image of a flame propagating along a strip of nitrocellulose. This rapidly moving, “unstructured” flame represents one of two possible modes of propagation; the other is a slowly moving, “structured” flame.

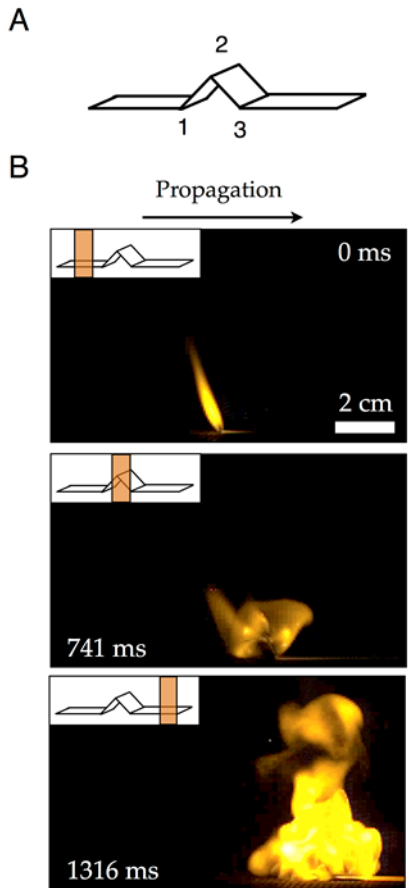


Figure 3. A bistable combustion system. (A) A 1-cm inverted “V” composed of three folds and two sides, each 1 cm in length. (B) Sequential high-speed images of a flame propagating along a strip of nitrocellulose. A slowly moving, “structured flame” (top) encounters the inverted “V” from (A) (middle) and transitions to a rapidly moving, “unstructured flame” (bottom). Under conditions where these transitions were more likely (increased slope of the surface supporting the strip, higher ambient temperatures), structured flames recovered more slowly from perturbations. This phenomenon, termed “critical slowing down” may warn of eruptions in spreading fires.

Future Plans Put the description of future plans here using this font (Times New Roman 12 pt).

- 1. Soft Actuators.** Our future work in soft actuators will continue a program that is presently working well. We will investigate other systems in which large nonlinearities in mechanical behavior of materials systems can (perhaps) be converted into new mechanisms of actuation in soft (e.g., elastomeric) materials. Much of our work to date has focused on silicone elastomers, primarily because we are familiar with their properties and methods of fabricating using them, but also because they are very familiar to the communities beginning to move into soft actuation. We will, however, extend work that we have already begun on elastomeric composites, and on new composite structures involving non-silicone elastomers, to identify new functions and capabilities in soft actuation. The major focus will, however, be on looking for nonlinear phenomena (buckling, “snap through”, and others) that have the potential to be the basis for new mechanisms of actuation and new types of soft actuators. As we proceed with this work, we will demonstrate mechanical (and in principle other) functions, but applications are not the primary focus of the work at this point. We are more interested in exploring the possible space of new types of actuation, and new methods of coupling the properties of materials-- especially nonlinear properties under stress-- to potentially useful-- and necessarily relatively simple-- mechanical work.

- 2. Complex, Dissipative Systems.** We have made a substantial investment in developing model systems based on flames, in configurations designed to allow us to study the fundamental physics of strongly dissipative, strongly coupled, systems. We will continue to work with the combustion of nitrocellulose-based structures, and continue to use model fires to explore for analogies with important, but larger classes of fires (forest fires, brushfires, and perhaps room or building fires). The development of these models will proceed first by trying to design systems that give regular behaviors (for example, cyclic, rotating flames progressing periodically in a ring of flamelets), and then to use these systems to study the influence of external perturbations (fuel type in supply, electrical and magnetic fields, local heating, changes in gas supply).

We also intend to explore systems other than flames. (6) Flames had the advantage that they are highly dissipative, chemically complex, relatively unexplored, and enormously important – both from the point of view of manipulation of energy, and from the vantage of their potential for damage. They have the disadvantage that they are not experimentally trivial to work with, since even small flames involve combustible gases, and have the potential for hazards if not treated carefully. We will, thus, also look for other highly localized, exothermic, systems of reactions (for example, polymerization or heterogeneous catalysis) where it may be experimentally easier to study interacting, dissipative model systems.

References

1. "Soft Actuators and Robots that are Resistant to Mechanical Damage", Martinez, R. V., Glavan, A., Keplinger, C., Oyetibo, A. I. and Whitesides, G. M. *Adv. Func. Mater.*, 2014, 24, 3003-3010.
2. "Soft Actuators and Robots that are Resistant to Mechanical Damage", Martinez, R. V., Glavan, A., Keplinger, C., Oyetibo, A. I. and Whitesides, G. M. *Adv. Func. Mater.*, 2014, 24, 3003-3010.
3. "Elastomeric Tiles for the Fabrication of Inflatable Structures", Morin, S. A., Kwok, S. W., Lessing, J., Ting, J., Shepherd, R. F., Stokes, A. A. and Whitesides, G. M. *Adv. Func. Mater.*, 2014, 24, 5541-5549.
4. "Using "Click-e-Bricks" to Make 3D Elastomeric Structures", Morin, S. A., Shevchenko, Y., Kwok, S. W., Shepherd, R. F., Stokes, A. A., Lessing, J. and Whitesides, G. M. *Adv. Mater.*, 2014, 26, 5991-5999.
5. "Warning Signals for Eruptive Events in Spreading Fires", Fox, J. M. and Whitesides, G. M. *Proc. Natl. Acad. Sci. USA*, 2015, 112, 2378-2383.
6. "Charging of Multiple Interacting Particles by Contact Electrification", Soh, S., Liu, H., Cademartiri, R., Yoon, H. J. and Whitesides, G. M. *J. Amer. Chem. Soc.*, 2014, 136, 13348-13354.

Publications Acknowledging This DoE BES Grant (2014 – 2015)

"Control of Soft Machines Using Actuators Operated by a Braille Display", Mosadegh, B., Mazzeo, A. D., Shepherd, R. F., Morin, S. A., Gupta, U., Sani, I. Z., Lai, D., Takayama, S. and Whitesides, G. M. *Lab on a Chip*, 2014, 14, 189-199.

"Omniphobic "RF Paper" Produced by Silanization of Paper with Fluoroalkyltrichlorosilanes", Glavan, A., Martinez, R. V., Subramaniam, A. B., Yoon, H. J., Nunes, R. M. D., Lange, H., Thuo, M. M. and Whitesides, G. M. *Adv. Funct. Mater.*, 2014, 24, 60-70.

"Magnetic Assembly of Soft Robots with Hard Components", Kwok, S. W., Morin, S. A., Mosadegh, B., So, J.-H., Shepherd, R. F., Martinez, R. V., Smith, B., Simeone, F. C., Stokes, A. A. and Whitesides, G. M. *Adv. Funct. Mater.*, 2014, 24, 2180-2187.

"Pneumatic Networks for Soft Robotics that Actuate Rapidly", Mosadegh, B., Polygerinos, P., Keplinger, C., Wennstedt, S., Shepherd, R. F., Gupta, U., Shim, J., Bertoldi, K., Walsh, C. J. and Whitesides, G. M. *Adv. Funct. Mater.*, 2014, 24, 2163-2170.

"Soft Actuators and Robots that are Resistant to Mechanical Damage", Martinez, R. V., Glavan, A., Keplinger, C., Oyetibo, A. I. and Whitesides, G. M. *Adv. Funct. Mater.*, 2014, 24, 3003-3010.

"Separation and Enrichment of Enantiopure from Racemic Compounds Using Magnetic Levitation", Yang, X., Wong, S. Y., Bwambok, D. K., Atkinson, M. B. J., Zhang, X., Whitesides, G. M. and Myerson, A. S. *Chem. Comm.*, 2014, 50, 7548-7551.

"Elastomeric Tiles for the Fabrication of Inflatable Structures", Morin, S. A., Kwok, S. W., Lessing, J., Ting, J., Shepherd, R. F., Stokes, A. A. and Whitesides, G. M. *Adv. Funct. Mater.*, 2014, 24, 5541-5549.

"Using "Click-e-Bricks" to Make 3D Elastomeric Structures", Morin, S. A., Shevchenko, Y., Kwok, S. W., Shepherd, R. F., Stokes, A. A., Lessing, J. and Whitesides, G. M. *Adv. Mater.*, 2014, 26, 5991-5999.

"Noncontact Orientation of Objects in Three Dimensional Space Using Magnetic Levitation", Subramaniam, A. B., Yang, D., Yu, H.-D., Nemiroski, A., Tricard, S., Ellerbee, A. K., Soh, S. and Whitesides, G. M. *Proc. Natl. Acad. Sci. USA*, 2014, 111, 12980-12985.

"A Resilient, Untethered Soft Robot", Tolley, M. T., Shepherd, R. F., Mosadegh, B., Galloway, K. C., Wehner, M., Karpelson, M., Wood, R. J. and Whitesides, G. M. *Soft Robotics*, 2014, 1, 213-223.

"Charging of Multiple Interacting Particles by Contact Electrification", Soh, S., Liu, H., Cademartiri, R., Yoon, H. J. and Whitesides, G. M. *J. Amer. Chem. Soc.*, 2014, 136, 13348-13354.

"Ionic Skin", Sun, J.-Y., Keplinger, C., Whitesides, G. M. and Suo, Z. *Adv. Mater.*, 2014, 26, 7608-7614.

"Odd-Even Effects in Charge Transport across n-Alkanethiolate-Based SAMs", Baghbanzadeh, M., Simeone, F. C., Bowers, C. M., Liao, K. C., Thuo, M. M., Baghbanzadeh, M., Miller, M., Carmichael, T. B. and Whitesides, G. M. *J. Amer. Chem. Soc.*, 2014, 136, 16919-16925.

"Stretchable Conductive Composites Based on Metal Wools for Use as Electrical Vias in Soft Devices ", Lessing, J., Morin, S. A., Keplinger, C., Tayi, A. and Whitesides, G. M. *Adv. Func. Mater.*, 2015, 25, 1418-1425.

"Mechanical Model of Globular Transition in Polymers", Tricard, S., Shepherd, R. F., Stan, C. A., Snyder, P. W., Cademartiri, R., Zhu, D., Aranson, I. S., Shakhnovich, E. I. and Whitesides, G. M. *ChemPlusChem*, 2015, 80, 37-41.

"Warning Signals for Eruptive Events in Spreading Fires", Fox, J. M. and Whitesides, G. M. *Proc. Natl. Acad. Sci. USA*, 2015, 112, 2378-2383.

"Emergence of Reconfigurable Colloidal Wires and Spinners via Dynamic Self-Assembly", Kokot, G., Piet, D., Whitesides, G. M., Aranson, I. S. and Snezhko, A. *Scientific Reports*, 2015, 5, 1-8.

"Bioinspiration: Something for Everyone", Whitesides, G. M. *Interface Focus*, 2015, 5, 20150031.

DIRECTED ASSEMBLY OF BIO-INSPIRED SUPRAMOLECULAR MATERIALS FOR ENERGY TRANSPORT and CAPTURE: *Mesoscale Construction of Functional Materials in Hydrodynamic Flows*

PI: William L. Wilson^{a,b} and Co-PI: Charles Schroeder^c; Collaborators A. L. Ferguson^a and J.J. Cheng^a; ^aDepartment of Materials Science and Engineering, University of Illinois at Urbana-Champaign, ^bCenter for Nanoscale Systems, Harvard University; ^cDepartment of Chemical and Biomolecular Engineering, University of Illinois at Urbana-Champaign.

PROJECT SCOPE: The directed mesoscale engineering of nanoscale building blocks holds enormous promise to catalyze a revolution in new functional materials for advanced energy technologies. Bio-inspired systems can play a key role in this effort due to their inherent “programmable” function. This research program aims to engineer new classes of mesoscale functional materials using reactive processes mediated by microscale fluid flows. This program has three major thrusts:

(1) **Fluidic-directed assembly and characterization of assembled materials** – development of custom-designed microfluidic devices for the assembly of functional materials, extensive materials characterization using physical, chemical, and optical methods.

(2) **Molecular dynamics simulations and modeling of material assembly** – development of detailed molecular dynamics (MD) simulations of peptide assembly for key molecular-scale insight into the early-time kinetics and molecular structure of self-assembled polypeptides.

(3) **Synthesis of ‘model’ hybrid oligopeptides for self-assembly** – synthesis of new peptide monomer materials with photoactive or functional cores with variable flanking peptide sequences, allowing exploration of a broad chemical space for self-assembly including biomaterials printing.

CURRENT PROGRESS | Microfluidic-based assembly and characterization: Work has been completed on the first studies aimed at characterizing the assembly dynamics in these tailored flows fields[1], both experimentally and theoretically. The peptide precursor reaction kinetics data are extracted from *in situ* dynamic fluorescence imaging of the assembly of peptide monomers as they form nanoscale and larger constructs. Figure 1 illustrates the microfluidics geometry used for flow-directed assembly of synthetic oligopeptides triggered by an acid stream. In this initial work, we are evaluating this general microfluidics setup and exploring the

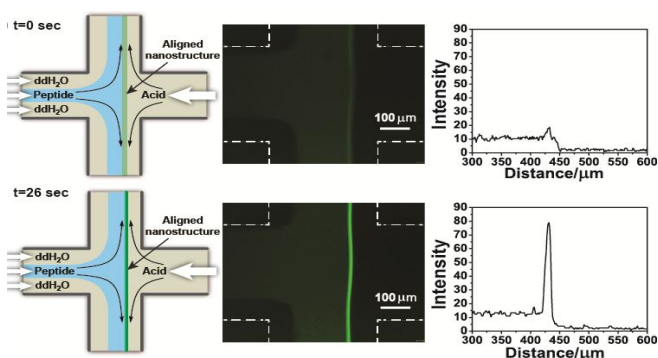
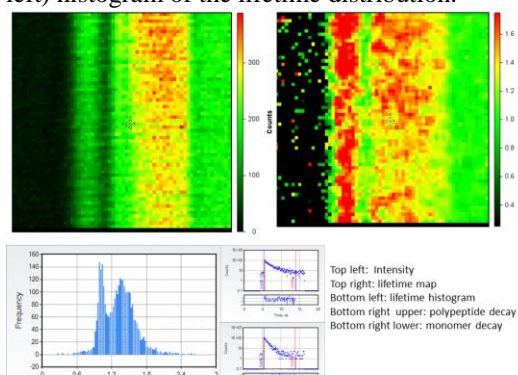


Figure 1: Overview of microfluidic-directed materials assembly platform. **Left panel:** microfluidic flow geometry of the device. **Middle panel:** wide-field fluorescence image of the cross-slot, the green line is the polypeptide assembly front. **Right panel:** Line cuts perpendicular to the flow direction.

assembly of peptides with different chemical structure, (i.e., variable cores and flanking residues). Shown is an aqueous solution of peptide monomer (~1 mg/mL) in basic solution flow-focused in the 2D flow plane and directed toward an opposing acidic stream at a microfluidic cross-slot. At the acid stream, the synthetic oligopeptide self-assembles into nanoscale ribbons and macromolecular ‘bundles’ such that the fibers align in the direction of outflow axis due to the extensional/compressional nature of the flow. The left panel shows a schematic of

the directed flows in the microfluidic reactor. The center panel shows an image of the early (top) and optimal growth of the polypeptide assembly front, with the right panel illustrating line cuts of the cross-section of the channel. The peak intensity as a function of time is determined to map the assembly rate. In related work, we are also characterizing assembled materials using scan-probe microscopy of species collected from the microdevices. The experiment will be used to explore structure and basic photophysics. For assembled DFAG-OPV3-GAFD polypeptide, nanoscale “ribbon-like” filaments are readily observable. Our results suggest the character of the filaments is strongly dependent on steric hindrance driven by the “bulky” nature of the residues. In DFAF polypeptides for example, we hypothesize that the phenyl rings (F), prevent formation of long distinct fibrils, and more ‘nanocrystal-like’ species are formed, (this is also suggested by DFAF AFM images). In all cases, the structural and excited state photophysics of the structural and excited state photo physics of the assembled species is consistent with aligned H-aggregate formation[2, 3]. We are currently re-designing our flow devices and performing a series of new experiments in order to fully probe the assembly kinetics, the goal comparison to continuum models to better capture the details of the assembly process. Recently, we began efforts to implement more sophisticated *in situ* imaging methods to capture excited state dynamics during

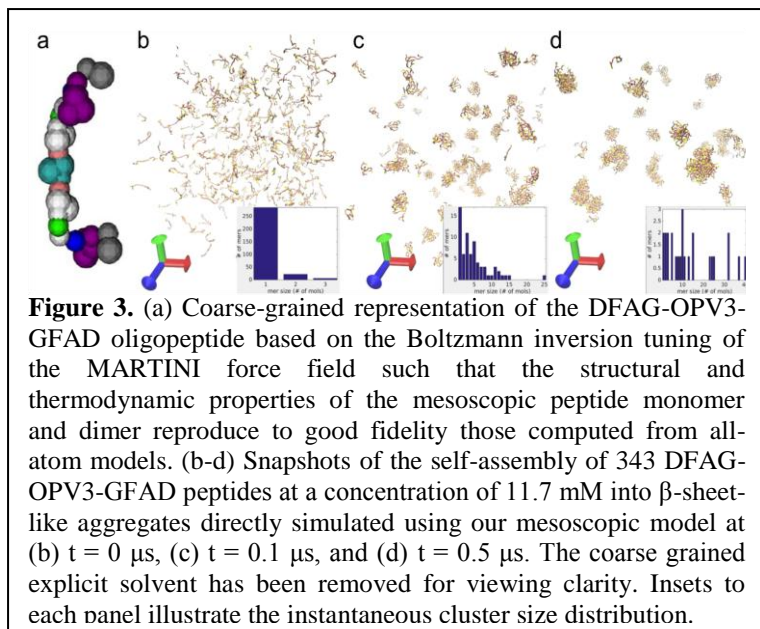
Figure 2: *In situ* confocal imaging of peptide assembly. Fluorescence Intensity (top left) and Excited-state lifetime image (top right); (bot left) histogram of the lifetime distribution.



assembly. In prior work, we performed fluorescence lifetime imaging (FLIM) on collected materials to explore the exciton dynamics of the assembled aggregates. *We are now performing direct confocal imaging of the assembly process in microfluidic reactors, which offers the ability for in situ FLIM.* This allows for observation of the assembled species during formation in flow and gives us the freedom to interrogate processes spatially within the reactor. **Figure 2** illustrates preliminary experimental data obtained using this approach. Results from FLIM/confocal imaging are shown in the top panel, illustrated by a color-coded ($100\mu\text{m}^2$) intensity image (left) and the color-coded excited state lifetime image (right). As expected, the monomer lifetime is typically of order $\sim 1\text{ns}$ (green area). *The expectation is if the polypeptide structure is a pure H-aggregate type formation, the lifetime should increase upon assembly, that is, the effective transition moment would decrease[4-6](the red regions).* A longer lifetime is also expected if the excited state is delocalized across aggregates with some disorder. In this case the defect structure localizes part of exciton wavefunction, again resulting in a longer lifetime. However our results suggest that this simple picture of the excited state dynamics is not correct. Indeed, we observe regions of longer lifetimes, however the distribution of lifetimes is much shorter than expected (1-2ns), given our prior FLIM data on assembled materials (captured from the device and analyzed outside the microfluidic cell), where the lifetimes often ranged from 3-10 ns. The histogram captured, with our in-situ approach (bottom left), shows a bimodal lifetime distribution of the species during assembly. This bimodal behavior may be indicative of both true H and slip stack H-aggregates (which would explain the lifetime shortening). Natural amyloids are known to form “spherulites[7, 8]”, which are wagon wheel-like, radial nematic structures. These which can be easily observed via polarization microscopy, have observe here. Direct aging studies are underway to track their formation here.

Finally, as noted we are fabricating microfluidic devices with chevron patterns in the floors and ceilings, which will generate fluid flows that are focused in the z-plane, thereby spatially separated from the top and bottom surfaces of the microdevice. We are currently fabricating and prototyping these microfluidic devices to enable better controlled flow dynamics.

COARSE-GRAINED SIMULATIONS OF EARLY-STAGE SELF-ASSEMBLY: Collaborator Ferguson and graduate researcher Rachael Mansbach have developed coarse-grained molecular models of DXXX-OPVn-XXXD oligopeptides to enable direct mesoscopic simulation of the self-assembly



of hundreds of peptides over length scales of tens of nm and time scales of μs . Molecular dynamics simulations offer a means to directly probe the molecular details of assembly inaccessible to experiment[3, 9]. The large number of degrees of freedom limits atomistic molecular simulations to time scales of nsec and length scales of $\sim\text{nm}$, which are too short to observe oligopeptide assembly. Coarse-grained molecular simulations sacrifice atomistic resolution to reach long length and time scales[10, 11]. Comparison of existing coarse-grained models to

short atomistic simulations of monomers and dimers demonstrated unsatisfactory agreement of the structural and thermodynamic properties of the oligopeptides. Employing Boltzmann inversion[10] to re-parameterize the MARTINI force field[11] to match the structural and thermodynamic behavior in all-atom simulations, we developed an explicit-solvent mesoscopic model that strikes a balance between atomistic realism and computational efficiency, reproducing the secondary structure and contact matrix of the monomer and dimerization free energy while permitting access to length scales of tens of nm and time scales of μs (**Fig. 3a**). Using this model, we have simulated the early stages of the self-assembly of 343 DFAG-OPV3-GAFD peptides over $0.5 \mu\text{s}$ to directly observe the formation of β -sheet-like aggregates, probe their morphologies, and model the dynamic evolution of the cluster size distribution (**Fig. 3b-d**). We are currently working to extract time constants for the assembly, probe the impact of concentration and peptide chemistry upon assembly, and compute the thermodynamic stability of the various cluster architectures using biased simulations.

SYNTHESIS OF SYNTHETIC PI-CONJUGATED PEPTIDES: An alternative method to synthesize peptides is the ring-opening polymerization (ROP) of α -amino acid *N*-carboxyanhydrides (NCAs) which is useful to prepare peptides with higher molecular weights in larger scale amounts compared to solid phase synthesis of oligo-peptides. The recent development of controlled ROP of NCAs enables the synthesis of polypeptides with predictable molecular weights (MWs) and narrow molecular weight distributions (MWDs). We are utilizing ROP of NCAs to synthesize π -conjugated peptides, and we aim to prepare peptides in large scale

amounts. Using this approach, we will explore the effect of sequence and polydispersity on peptide self-assembly behavior. In preliminary work, we have used the ring-opening polymerization (ROP) of α -amino acid *N*-carboxyanhydrides (NCAs) to prepare peptides, and the resulting peptides were further used for conjugation with different π -cores to obtain the π -conjugated peptides. Compared to solid phase synthesis, NCA polymerization allows for the synthesis of peptides with a much larger scale and much higher yield, albeit with random sequence and broader molecular weight distributions (MWDs). All NCA monomers are polymerized in one step without tedious purification procedures, which greatly simplifies the peptide synthesis process. By selecting different NCA co-monomer ratios and monomer-to-initiator (M/I) ratios during ROP, we are able to tune the chain lengths, hydrophobicity, and hence the secondary structure of peptides. At the same time, we can explore the effect of peptide sequence and polydispersity on the self-assembly behaviors. We are currently synthesizing glutamic acid (Glu)-leucine (Leu) peptides with perylene core; enabling larger material amounts (~ 100 mg scale) of π -conjugated peptides relative to the solid-phase synthesis method. After three-step synthesis (NCA polymerization, π -core conjugation, and deprotection), π -conjugated Leu-Glu peptides were successfully synthesized with pH-dependent water solubility, which is similar with the π -conjugated peptides synthesized by solid phase synthesis. The protonation of Glu residues at acidic conditions changes the peptide charge states and secondary structure, which triggers the assembly of π -conjugated peptides. Moving forward, we will pursue this promising synthesis method to generate a wide variety of synthetic peptides with variable sequences and properties.

FUTURE WORK: We will conduct coarse-grained simulations of the self-assembly of other molecules in the DXXX-OPV_n-XXXD family, and run simulations to probe the impact of peptide sequence, core chemistries, and environmental conditions such as temperature, pressure, and flow upon the morphology, stability and kinetics of peptide assembly. *Focus will be to relate the cluster size distributions and kinetic relaxation rates to experimental measures of assembly progress in microfluidic flow cells, and to relate structural morphology predicted by simulations to experimental in-situ fluorescence measurements.* Synthetically, future work includes further tuning the π -core structures, peptide lengths, Leu/Glu ratios, and the incorporation of other amino acid residues in order to get optimized self-assembly behavior of π -conjugated peptides.

REFERENCES:

1. Marciel, A.B., et al., *Advanced Materials*, 2013. **25**(44): p. 6398-6404.
2. Wall, B.D., et al., *Advanced Materials*, 2011. **23**(43): p. 5009-5014.
3. Wall, B.D., et al., *Langmuir*, 2014. **30**(20): p. 5946-5956.
4. Spano, F.C. and C. Silva, *Annual Review of Physical Chemistry*, Vol 65, 2014. **65**: p. 477-500.
5. Yamagata, H., C.M. Pochas, and F.C. Spano, *Journal of Physical Chemistry B*, 2012. **116**(49): p. 14494-14503.
6. Yamagata, H. and F.C. Spano, *Journal of Physical Chemistry Letters*, 2014. **5**(3): p. 622-632.
7. Krebs, M.R.H., et al., *Proceedings of the National Academy of Sciences of the United States of America*, 2004. **101**(40): p. 14420-14424.
8. Strodel, B., et al., *Journal of Physical Chemistry B*, 2008. **112**(32): p. 9998-10004.
9. Wall, B.D., et al., *Langmuir*, 2014. **30**(38): p. 11375-11385.
10. Noid, W.G., *Journal of Chemical Physics*, 2013. **139**(9).

11. Marrink, S.J., et al., *The MARTINI force field: Coarse grained model for biomolecular simulations*. Journal of Physical Chemistry B, 2007. **111**(27): p. 7812-7824.

PUBLICATIONS: (FIRST YEAR OF PROGRAM) Two manuscripts in preparation

Poster Sessions

Biomolecular Materials Principal Investigators' Meeting

POSTER SESSION I *Monday, August 3, 2015*

- 1) **Biopolymers Containing Unnatural Amino Acids**
Peter Schultz, Scripps Research Institute
- 2) **Fabrication and Assembly of Robust, Water-Soluble Molecular Interconnects via Encoded Hybridization**
Timothy Scott, University of Michigan
- 3) **Active Assembly of Dynamic and Adaptable Materials: Active Protein Assemblies**
George Bachand, Erik Spoerke, Mark Stevens, and Darryl Sasaki, Sandia National Laboratories
- 4) **Active Assembly of Dynamic and Adaptable Materials: Artificial Microtubules**
Erik Spoerke, George Bachand, Mark Stevens, and Darryl Sasaki, Sandia National Laboratories
- 5) **Directed Assembly of Bio-inspired Supramolecular Materials for Energy Transport and Capture: Mesoscale Construction of Functional Materials in Hydrodynamic Flows**
William L. Wilson, Charles Schroeder, Andrew L. Ferguson and J.J. Cheng, University of Illinois/Harvard University
- 6) **DNA-Grafted Building Blocks Designed to Self-Assemble into Desired Nanostructures**
Sanat Kumar, V. Venkatasubramanian and Oleg Gang, Columbia University
- 7) **Chemically Directed Self-Assembly of Protein Superstructures**
F. Akif Tezcan, University of California, San Diego
- 8) **Harnessing Chemo-mechanical Energy Transduction to Create Systems that Selectively Catch and Release Biomolecules**
Joanna Aizenberg, Anna Balazs, and Ximin He, Harvard University
- 9) **Carbon Nanotube Porin: A Biomimetic Material-Based Membrane Nanopore Platform**
Aleksandr Noy, Jim De Yoreo, Tony van Buuren and Chun-Long Chen, Lawrence Livermore National Laboratory and Pacific Northwest National Laboratory
- 10) **Peptoid-Based 2D materials and Porous Networks for Artificial Membranes**
Aleksandr Noy, Jim De Yoreo, Tony van Buuren and Chun-Long Chen, Lawrence Livermore National Laboratory and Pacific Northwest National Laboratory

- 11) Bioinspired Hierarchical Design of Chiral Mesoscale Liquid Crystalline Assemblies**
Nicholas Abbott and Juan de Pablo, University of Wisconsin and University of Chicago
- 12) Dynamics of Active Self-Assembled Materials**
Igor Aronson, Alexey Snezhko, and Andrey Sokolov, Argonne National Laboratory
- 13) Miniaturized Hybrid Materials Inspired by Nature: Protein Tubule Inversion Triggered by a Molecular Switch: A New Paradigm for Assembly**
Cyrus Safinya, University of California, Santa Barbara
- 14) Molecular Nanocomposites—Adaptive and Reconfigurable Nanocomposites**
Dale L. Huber, Darryl Y. Sasaki, Mark J. Stevens, Amalie L. Frischknecht, Hongyou Fan, and Paul Clem, Sandia National Laboratories
- 15) Spinning Liquid Crystal Vortices and Self-Pumping Active Gels**
Zvonimir Dogic, Brandeis University
- 16) Dynamical Self-Assembly: Constrained Phase and Mesoscale Dynamics in Lipid Membranes**
Atul Parikh and Sunil K. Sinha, University of California, Davis
- 17) Carbon Nanotubes for Solar Energy Harvesting in Plants**
Michael Strano, Massachusetts Institute of Technology
- 18) Integrating Rhodopsins in H^+ -FETs For Bioinspired Energy Conversion**
Marco Rolandi and Francois Baneyx, University of Washington
- 19) Optical and Electro-optic Modulation of Biomimetically Functionalized Nanocarbon Materials**
Padma Gopalan, David McGee, Francois Leonard, Bryan Wong, Franz Himpsel, University of Wisconsin
- 20) Dynamic Self-Assembly, Emergence, and Complexity**
George Whitesides, Harvard University
- 21) Experimental Realization of ‘Repair-and-Go’ Using Microencapsulation of Nanomaterials**
Todd Emrick, University of Massachusetts, Amherst
- 22) Development of Smart, Responsive Communicating and Motile Microcapsules**
Daniel Hammer and Daeyeon Lee, University of Pennsylvania
- 23) Bioinspired Materials**
Surya Mallapragada, Mufit Akinc, David Vaknin, Marit Nilsen-Hamilton, Alex Traveset, Wenjie Wang, Ruslan Prozorov, Tanya Prozorov, and Dennis Bazylinski, Ames Laboratory

24) Material Lessons from Biology: Nano-to-Mesoscale Organization of Biominerals by Mollusk Shell Proteins

John Spencer Evans, New York University

25) Emergence of Crystallinity and Magnetism in a Nanoparticle: The In Situ Study

Tanya Prozorov, Ames Laboratory

Biomolecular Materials Principal Investigators' Meeting

POSTER SESSION II

Tuesday, August 4, 2015

- 1) **Dynamic Self-Assembly of DNA Nanotubes**
Elisa Franco and Rebecca Schulman, University of California, Riverside and Johns Hopkins University
- 2) **A Modular Architecture for Dynamic, Environmentally Adaptive DNA Nanostructures**
Rebecca Schulman and Elisa Franco, Johns Hopkins University and University of California, Riverside
- 3) **Self-Assembly and Self-Replication of Novel Materials from Particles with Specific Recognition**
Paul Chaikin, Ned Seeman, Marcus Weck, and David Pine, New York University
- 4) **Design and Anisotropy in Long Range Interactions of Biomolecular Systems**
Adrian Parsegian, Wai Yim Ching, Roger French, and Nicole Steinmetz, University of Massachusetts, Amherst
- 5) **Electronic Structure and Interactions in Duplex to Quadruplex DNA**
Roger French, Nicole Steinmetz, Adrian Parsegian, and Wai Yim Ching, Case Western Reserve University
- 6) **Rigid Biopolymer Nanocrystal Systems for Controlling Multicomponent Nanoparticle Assembly and Orientation in Thin Film Solar Cells**
Jennifer Cha, University of Colorado
- 7) **Electrostatic Driven Self Assembly Design of Functional Nanostructures**
Monica Olvera de la Cruz, Northwestern University
- 8) **Defects, Partial Order, and Thermodynamics in Virus-Like Particles**
Bogdan Dragnea, Indiana University
- 9) **Self-Assembly for Colloidal Crystallization and Biomimetic Structural Color**
Michael Solomon and Sharon Glotzer, University of Michigan
- 10) **Light-Driven Electron Transfer and H₂ Production in Nanocrystal-Hydrogenase Complexes**
Gordana Dukovic, University of Colorado
- 11) **Nanoengineering of Complex Materials**
Samuel I. Stupp, Northwestern University

- 12) Solvent-Assisted Nonequilibrium Directed Self-Assembly of Complex Polymeric Materials**
Juan de Pablo, Matt Tirrell, Paul Nealey, and Wei Chen, Argonne National Laboratory/University of Chicago – Institute for Molecular Engineering
- 13) Design and Synthesis of Structurally Tailored and Engineered Macromolecular (STEM) Gels, Part 1**
Anna C. Balazs and Krzysztof Matyjaszewski, University of Pittsburgh
- 14) Design and Synthesis of Structurally Tailored and Engineered Macromolecular (STEM) Gels, Part 2**
Anna C. Balazs and Krzysztof Matyjaszewski, University of Pittsburgh
- 15) Designing Dual-Functionalized Gels that Move, Morph and Self-Organize in Light**
Anna Balazs, University of Pittsburgh
- 16) Self-Healing and Self-Regulating Bio-inspired Materials**
Sarah Heilshorn, Seb Doniach, Nick Melosh, Andy Spakowitz, SLAC National Accelerator Laboratory
- 17) Strong Autonomous Self-Healing Materials via Dynamic Chemical Interactions**
Zhibin Guan, University of California, Irvine
- 18) Self-Assembly of Pi-Conjugated Peptides in Aqueous Environments Leading to Energy-Transporting Bioelectronic Nanostructures**
John Tovar, Howard E. Katz, and Andrew L. Ferguson, Johns Hopkins University
- 19) Surface Mechanical Properties of Bio-inspired Architectures**
Anand Jagota and Chung-Yuen Hui, Lehigh University
- 20) A Hybrid Biological/Organic Photochemical Half-Cell for Generating H₂**
John Golbeck and Donald Bryant, Pennsylvania State University
- 21) Molecular Nanocomposites – Complex Nanocomposites**
Jeff Brinker, Bryan Kaehr, Hongyou Fan, Frank van Swol, Stanley Chou, and Paul G. Clem, Sandia National Laboratories
- 22) Enzyme-Controlled Mineralization in Biomimetic Microenvironments Formed by Aqueous Phase Separation and Lipid Vesicles**
Christine Keating, Pennsylvania State University
- 23) Controlling Structure Formation Pathways in Functional Bio-hybrid Nanomaterials**
Lara Estroff and Ulrich Wiesner, Cornell University\

24) Assembling Microorganisms into Energy Converting Materials

Ozgur Sahin, Columbia University

25) Biomimetic Templated Self-Assembly of Light Harvesting Nanostructures

Alfredo Alexander-Katz, Massachusetts Institute of Technology

26) Shape, Crowding and Colloidal Alchemy

Sharon Glotzer, University of Michigan

*Author Index
and
List of Participants*

Author Index

Abbott, Nicholas L.	59	Jagota, Anand	148
Aizenberg, Joanna	64	Kaehr, Bryan.....	13
Akinc, Mufit	36	Katz, Howard E.	226
Alexander-Katz, Alfredo.....	69	Keating, C. D.....	153
Aronson, Igor S.	3	Kumar, S.....	157
Bachand, George D.....	9, 51	Lee, Daeyeon.....	143
Balazs, Anna	64, 73, 77	Leonard, Francois	134
Baneyx, Francois	182	Li, Y.	186
Bazylinski, Dennis.....	36	Mallapragada, Surya	36
Bedzyk, Michael J.	167	Matyjaszewski, Krzysztof	73
Brinker, Jeff.....	13	McGee, David.....	134
Bryant, Donald A.....	130	Melosh, Nick	31
Cha, Jennifer N.....	81	Mittal, Jeetain	162
Chaikin, P.....	87	Morse, Daniel E.	163
Chen, Chun-Long	41	Nealey, Paul.....	25
Chen, Wei.....	25	Nilsen-Hamilton, Marit	36
Cheng, J. J.	236	Noy, Aleksandr	41
Ching, W. Y.	123, 175	Olvera de la Cruz, Monica	167
Chou, Stanley	13	Parikh, Atul N.....	171
Clem, Paul G.	13, 20	Parsegian, V. A.	123, 175
de Pablo, Juan J.	25, 59	Perry, Joseph W.....	196
De Yoreo, Jim	41	Pine, D.....	87
Dogic, Zvonimir	91	Prozorov, Ruslan.....	36
Doniach, Seb	31	Prozorov, Tanya.....	36, 47
Dragnea, Bogdan	95	Rolandi, Marco	182
Dukovic, Gordana.....	100	Safinya, C. R.....	186
Emrick, Todd.....	105	Sahin, Ozgur	191
Estroff, Lara A.....	110	Sandhage, Kenneth H.....	196
Evans, John Spencer	114	Sasaki, Darryl Y.....	9, 20, 51
Ewert, K.	186	Schroeder, Charles	236
Fan, Hongyou	13, 20	Schulman, Rebecca	198
Ferguson, Andrew L.	226, 236	Schultz, Peter G.	202
Franco, Elisa.....	119	Scott, Timothy F.	207
French, R. H.	123, 175	Seeman, N.	87
Frischknecht, Amalie L.....	20	Sinha, Sunil K.....	171
Gang, O.	157	Snezhko, Alexey	3
Glotzer, Sharon C.	211	Sokolov, Andrey	3
Golbeck, John H.	130	Solomon, Michael J.	211
Gopalan, Padma.....	134	Spakowitz, Andy.....	31
Guan, Zhibin	139	Spoerke, Erik D.	9, 51
Hammer, Daniel A.....	143	Steinmetz, N. F.	123, 175
Heilshorn, Sarah	31	Stevens, Mark J.....	9, 20, 51
Himpfel, Franz	134	Strano, Michael S.....	213
Huber, Dale L.	20	Stupp, Samuel I.....	217
Hui, Chung-Yuen	148	Tezcan, F. Akif	221

Tirrell, Matt	25
Tovar, John D.	226
Travesset, Alex	36
Vaknin, David	36
Van Buuren, Tony	41
van Swol, Frank.....	13
Venkatasubramanian, V.....	157
Wang, Wenjie.....	36
Weck, M.....	87
Whitesides, George M.	230
Wiesner, Ulrich	110
Wilson, William L.	236
Wong, Bryan	134

Participant List

Name	Organization	E-mail Address
Abbott, Nicholas	University of Wisconsin-Madison	abbott@engr.wisc.edu
Aizenberg, Joanna	Harvard University	jaiz@seas.harvard.edu
Aizenberg, Michael	Harvard University	michael.aizenberg@wyss.harvard.edu
Alexander-Katz, Alfredo	Massachusetts Institute of Technology	aalexand@mit.edu
Aronson, Igor	Argonne National Laboratory	aronson@anl.gov
Bachand, George	Sandia National Laboratories	gdbacha@sandia.gov
Balazs, Anna	University of Pittsburgh	balazs@pitt.edu
Baneyx, François	University of Washington	baneyx@uw.edu
Brinker, C. Jeffrey	Sandia National Laboratories	cjbrink@sandia.gov
Cha, Jennifer	University of Colorado Boulder	Jennifer.Cha@colorado.edu
Chaikin, Paul	New York University	chaikin@nyu.edu
Ching, Wai-Yim	University of Missouri-Kansas City	chingw@umkc.edu
de Pablo, Juan	University of Chicago	depablo@uchicago.edu
De Yoreo, James	Pacific Northwest National Laboratory	james.deyoreo@pnl.gov
Dogic, Zvonimir	Brandeis University	zdogic@brandeis.edu
Dragnea, Bogdan	Indiana University	dragnea@indiana.edu
Dukovic, Gordana	University of Colorado Boulder	gordana.dukovic@colorado.edu
Emrick, Todd	University of Massachusetts Amherst	tsemrick@mail.pse.umass.edu
Estroff, Lara	Cornell University	lae37@cornell.edu
Evans, John	New York University	jse1@nyu.edu
Ferguson, Andrew	University of Illinois at Urbana-Champaign	alf@illinois.edu
Franco, Elisa	University of California, Riverside	efranco@ucr.edu
French, Roger	Case Western Reserve University	roger.french@case.edu
Glotzer, Sharon	University of Michigan	sglotzerkjc@umich.edu
Golbeck, John	Pennsylvania State University	jhg5@psu.edu
Gopalan, Padma	University of Wisconsin-Madison	pgopalan@wisc.edu
Guan, Zhibin	University of California, Irvine	zguan@uci.edu
Hammer, Daniel	University of Pennsylvania	hammer@seas.upenn.edu
He, Ximin	Arizona State University	ximin.he@asu.edu
Huber, Dale	Sandia National Laboratories	dlhuber@sandia.gov
Hui, Chung Yuen	Cornell University	ch45@cornell.edu
Jagota, Anand	Lehigh University	anj6@lehigh.edu
Katz, Howard	Johns Hopkins University	hekat@jhu.edu
Keating, Christine	Pennsylvania State University	keating@chem.psu.edu
Kini, Aravinda	U.S. Department of Energy	a.kini@science.doe.gov
Kumar, Sanat	Columbia University	sk2794@columbia.edu
Mallapragada, Surya	Ames Laboratory	suryakm@iastate.edu
Markowitz, Michael	U.S. Department of Energy	mike.markowitz@science.doe.gov
Matyjaszewski, Krzysztof	Carnegie Mellon University	km3b@andrew.cmu.edu
McGee, David	The College of New Jersey	mcgeed@tcnj.edu

Noy, Aleksandr	Lawrence Livermore National Laboratory	noy1@llnl.gov
Olvera de la Cruz, Monica	Northwestern University	m-olvera@northwestern.edu
Parikh, Atul	University of California, Davis	anparikh@ucdavis.edu
Parsegian, V Adrian	University of Massachusetts Amherst	parsegian@physics.umass.edu
Prozorov, Tanya	Ames Laboratory	tprozoro@ameslab.gov
Rolandi, Marco	University of Washington	rolandi@uw.edu
Safinya, Cyrus	University of California, Santa Barbara	safinya@mrl.ucsb.edu
Sahin, Ozgur	Columbia University	sahin@columbia.edu
Schroeder, Charles	University of Illinois at Urbana-Champaign	cms@illinois.edu
Schulman, Rebecca	Johns Hopkins University	rschulm3@jhu.edu
Schultz, Peter	The Scripps Research Institute	schultz@scripps.edu
Scott, Timothy	University of Michigan	tfscott@umich.edu
Seeman, Nadrian	New York University	ned.seeman@nyu.edu
Severs, Linda	ORISE	Linda.Severs@orau.org
Sinha, Sunil	University of California, San Diego	ssinha@physics.ucsd.edu
Snezhko, Oleksiy	Argonne National Laboratory	snezhko@anl.gov
Solomon, Mike	University of Michigan	mjsolo@umich.edu
Spakowitz, Andrew	SLAC National Accelerator Laboratory & Stanford University	ajspakow@stanford.edu
Spoerke, Erik	Sandia National Laboratories	edspoer@sandia.gov
Steinmetz, Nicole	Case Western Reserve University	nicole.steinmetz@case.edu
Strano, Michael	Massachusetts Institute of Technology	strano@mit.edu
Stupp, Samuel	Northwestern University	s-stupp@northwestern.edu
Tezcan, F. Akif	University of California, San Diego	tezcan@ucsd.edu
Tovar, J. D.	Johns Hopkins University	tovar@jhu.edu
Whitesides, George M.	Harvard University	gwhitesides@gmwgroup.harvard.edu
Wilson, William	Harvard University	wwilson@cns.fas.harvard.edu